Rockfall Trajectory Analysis —

Parameter Determination and Application

A thesis

submitted in partial fulfilment

of the requirements for the degree

of

Master of Science in Engineering Geology

In the

University of Canterbury

By

Baishan Peng

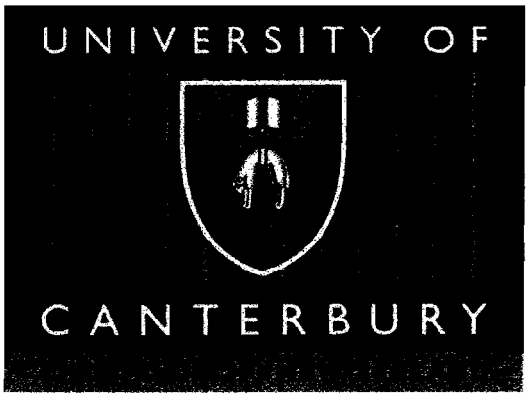

University of Canterbury

June 2000.

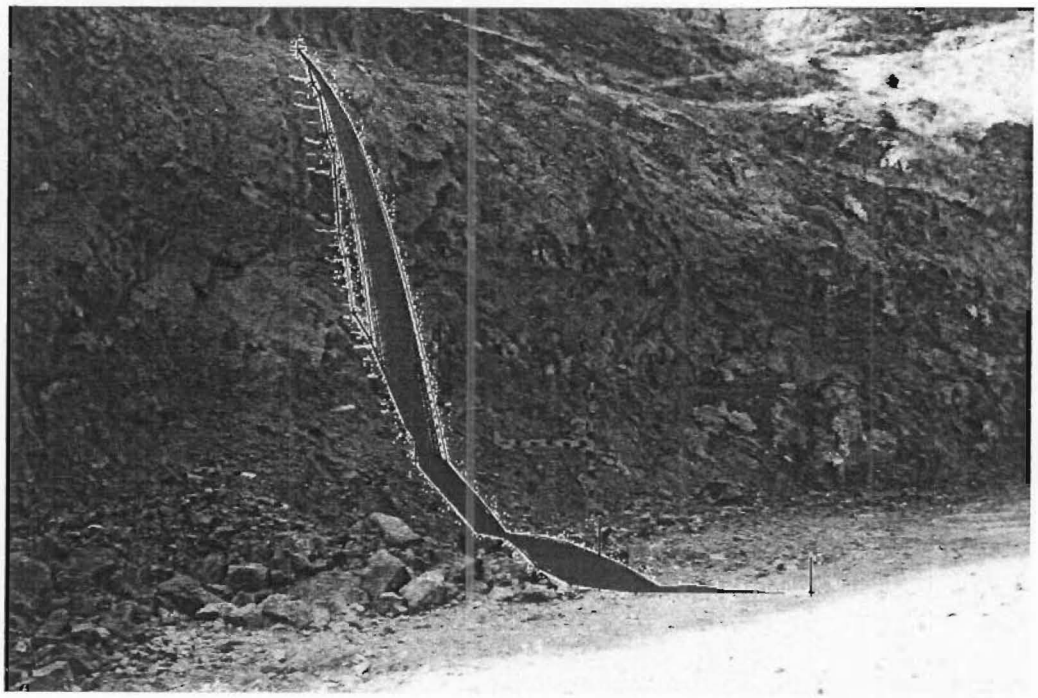

ABSTRACT

Computer simulation of rockfalls has been widely used in rockfall analysis in recent years, and the coefficient of restitution is an important parameter input that is difficult to determine. Aimed at finding an easy solution to this problem, three stages of laboratory and field tests have been carried out. Rockfall trajectory analysis at a specific site has been done as an application to verify the method developed.

In the first stage of laboratory testing, quasi-spherical rock "balls" made from different rock samples were dropped from 1 m onto polished rock slabs that were clamped on a concrete deck, which can be set to different slope angles. A high-speed video camera was used to record the impact processes, and normal and tangential coefficients of restitution were calculated from the video records. The results show a linear relationship between the normal restitution coefficient and the Schmidt hammer numbers of both the rock slabs and the falling rock "balls", and the slope angle. An empirical equation was then established to calculate the normal coefficient of restitution from those three parameters. However, the correlations between the tangential coefficient of restitution and the above parameters are poor, indicating that the tangential coefficient of restitution is not adequately determined by such rock properties.

The second stage of laboratory testing was under more practical conditions. Three different rough rock blocks were used as rock slopes. Angular rock boulders were dropped from different heights onto the rock blocks, and a rock "ball" was also used to make a comparison. The results show that the normal coefficients of restitution from impacts of angular rocks are much smaller than those of rock "balls", and have a linear correlation with those calculated from the empirical equation obtained by the earlier test. Tests on beds of gravel, soil, rock fragments and sand have also been carried out to obtain the coefficients of restitution of those materials.

Finally, field tests have been carried out at a quarry site in Lyttelton. Basalt rock boulders of about 0.3 m in diameter were dropped from about 4 m onto rock and debris slopes using an excavator. The values of restitution coefficients obtained are similar to those from laboratory tests but larger than those calculated from the empirical equations due to the effect of weathering and surface roughness of rocks in the field on the Schmidt hammer measurement. Forty basalt boulders were then rolled down a bench slope of about 16 m, three cameras were used to record the rockfall processes. Two different rockfall simulation programs (CRSP and RocFall) were used to simulate the rockfall processes. The simulated bounce heights and velocities from CRSP are close the field trial, while those from RocFall are smaller than the field results.

Comprehensive rockfall analysis has been carried out for the Marine apartments, Sumner, where a steep cliff of 35–45 m represents potential rockfall hazards to a car park and proposed buildings at the base. Site investigation, rockfall simulation and risk assessment have been carried out for the site. The results show that without any protection measures, a majority of rocks from the cliff face reach the edge of the car park. The probability of an accident at the car park is moderate (1 in 195 years), while the probability of fatality at the car park is low ($8.69*10^{-6}$) and acceptable under the proposed risk criteria for "Major Civil Engineering Projects".

ACKNOWLEDGEMENTS

I am grateful to all those who helped and supported me throughout this project. Special thanks to:

Mr David Bell, for his guidance and enthusiasm on my research, his comments, discussion and carefully reading my draft chapters are greatly appreciated. Dr Laurie Richards, for his initial idea about the possible ways of determining the coefficient of restitution and providing me with the useful reading materials, and for his availability and efforts to discuss, review and guide my progress. The technical staff of the Department of Geological Sciences, Rob Spiers, Arthur Nichols and Cathy Knight, for their assistance and help in the preparation of the laboratory and field tests.

The Natural Resources Engineering Group of Lincoln University, for permitting me to carry out my laboratory tests in the workshop. Professor Tim Davis, for lending me the high-speed camera. Mr Kelvin Nicolle, for his assistance during my laboratory tests and image processing in Lincoln.

The lyttelton Port Company, for providing me the quarry site for field tests.

TABLE OF CONTENTS

LIST OF FIGURES

LIST OF TABLES

Chapter 1

Introduction

1.1 Background of study

Computer simulation of rockfalls has become an easy and economical means of rockfall analysis. Different simulation programs have been developed and applied in practical rockfall prediction during the last two decades. These programs use simplified parameters to simulate rockfall behaviour, calculate trajectories and provide useful statistics for the design of mitigation measures. Parameters required for rockfall simulation include slope geometry, slope material properties and rock characteristics, of which the coefficient of restitution of the slope is a key input and is the most difficult to determine.

The coefficient of restitution is usually determined from in situ tests that are very expensive and risky. Little work has been done to develop an easy method of determining the coefficient of restitution from other rock properties such as strength and modulus of elasticity. A preliminary test has been done by Rayudu (1997) using a steel ball impacting rock slabs, which showed quite good correlation between the coefficient of restitution and the Schmidt number of the rock slab. Further laboratory tests are needed to find the restitution coefficient of rock-rock impact, and its relationship with the Schmidt number of the rock, so that this method can be practically used in the determination of the restitution coefficient of a rock slope in rockfall analysis.

1.2 Objectives

The objectives of this study are:

- To find the coefficients of restitution of different rocks, and to analyse the correlation between the restitution coefficients and the Schmidt number and other properties of rocks with laboratory impact tests in order to find an easy means of determining the coefficient of restitution;

- To carry out in situ rockfall tests at a selected quarry to verify the results from laboratory tests;
- To carry out rockfall field trials at a particular slope and simulate rockfalls at this site with selected computer programs, and compare actual rockfall behaviour with the results of computer simulations;
- To conduct rockfall analysis at the proposed Marine apartments site in Christchurch with appropriate computer programs and assess the level of risk from rockfalls at this site.

1.3 Rockfalls

1.3.1 Rockfall problem

Rockfalls are a major hazard to properties and public transportation networks in mountainous areas and rock cuts. While rockfalls do not pose the same level of economic risk as large-scale failures that can close major transportation routes for days at a time, the number of people killed by rockfalls tends to be of the same order as those killed by other forms of rock slope instability (Hoek 1998). Spang (1987) has reported that rockfalls rather than deep-seated slides are the major causes of interruption to the West German Federal Railway's 28,000 km track network. Martin (1988) stated that rockfalls, small rockslides and ravelling are the most chronic problems on transportation routes in the mountainous areas of North America. Hungr and Evens (1989) noted that there have been 13 rockfall deaths in the past 87 years on the mountain highways of British Columbia in Canada. Lundy (1995) documented 29 historic rockfall events in Bank Peninsula, Christchurch, with one death and significant property loses reported.

1.3.2 Definitions

Varnes (1978) defines a rockfall as a free fall of rocks through the air, with leaping, bouncing or rolling of fragments. Chen and Huang (1994) define rockfalls as abrupt movements of independent blocks or complexes of uninterrupted rocks detached from steep slopes. Lee and Elliot (1998) define rockfall as "the downslope movement of boulders (from natural slopes) or rock blocks (from cut faces) that, if not properly restrained, has the potential to destroy

or damage structures along its path or create an obstacle to public transportation networks".

Spang (1987) suggests that the term "rockfall" be restricted to events which have a maximum energy of 500 kNm, this being equivalent to a 5 tonne block dropping vertically from a height of 5 m. Spang considers that potential rockfalls with greater kinetic energy would require active stabilization since it would not be practical to contain them with passive structures. By comparison, Chan and Au (1986) designed their boulder fences to be able to withstand impact energy of 100 kNm, with boulders liable to attain greater energies required to be stabilised in situ. These definition are somewhat arbitrary, but the classification is helpful in the determination of rockfall mitigation measures.

Richards (1988) summarized the generally accepted characteristics of rockfalls as follows:

- The event involves a single block or group of blocks which become detached from the rock face.
- Each falling block behaves more or less independently of other blocks.
- There is temporary loss of ground contact and high acceleration during the descent.
- The blocks attain significant kinetic energy during their descent.

Rockfall failures differ from sliding failures which form on a slip surface of the rock slope. Individual rock blocks form because of discontinuities in rocks. Rockfalls should be distinguished from rock avalanches which involve huge volume of mass movement, a part of the whole slope (which may consist of facial and bed rock) collapses suddenly, while rockfalls involves individual rock boulders with limited size.

1.3.3 Mechanics of rockfalls

Rockfalls are developed from rock mass discontinuities within rock slopes. Four types of rock slope failure can be identified (Norrish and Wyllie, 1996): planar

failure, wedge failure, toppling failure and circular failure (figure 1-1). Rockfalls are often developed from toppling, buckling (planar failure) and wedge failures.

Rockfalls are generally initiated by climatic or biological events (trees and animals), earthquake or blasting vibration, or external forces such as construction activities. Table 1-1 shows the results of a study of 308 rockfalls on California highways in which 14 different causes of instability were identified. Of the 14 causes, 6 are directly related to water, namely, rain, freeze-thaw, snowmelt, channelled runoff, differential erosion, and springs or seeps (Wyllie and Norrish, 1996).

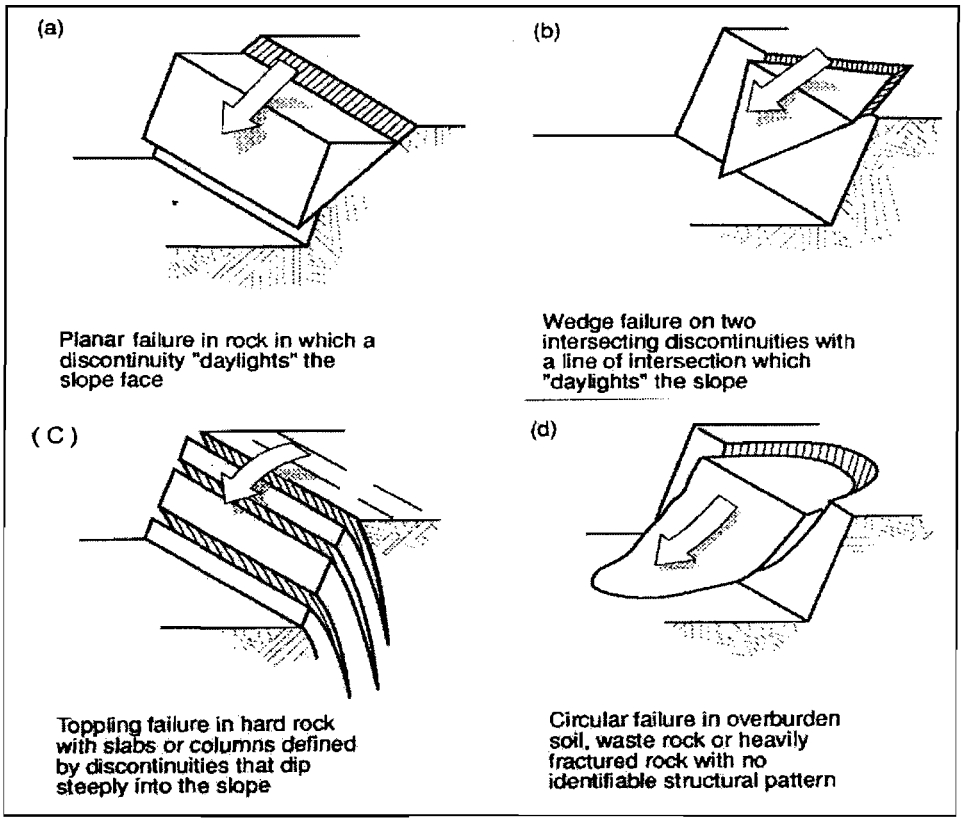

Figure 1-1: Types of rock slope failures (from Norrish and Wyllie, 1996)

A block detached from a rock face may have the following types of motion during flight:

Table 1-1: Causes of Rockfalls on Highways in California (from Wyllie and Norrish, 1996).

Cause	Percentage (%)
Rain	30
Freeze-thaw	21
Fractured rock	12
Wind	12
Snowmelt	8
Channelled runoff	7
Adverse planar fracture	5
Burrowing animals	2
Differential erosion	1
Tree roots	0.6
Springs or seeps	0.6
Wild animals	0.3
Truck vibrations	0.3
Soil decomposition	0.3

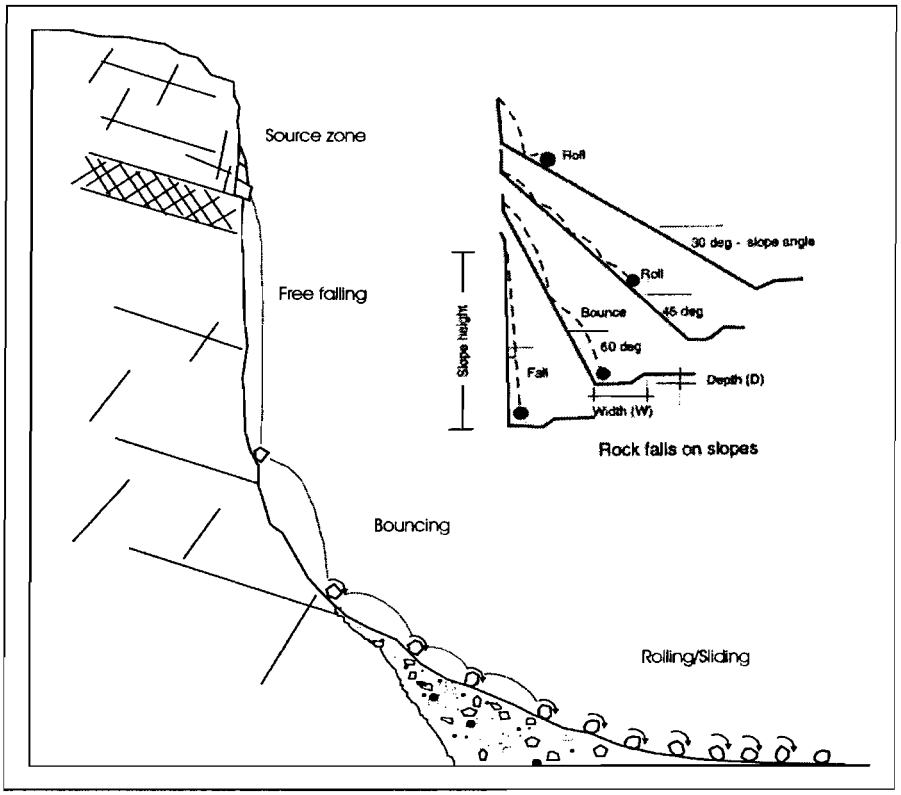

Figure 1-2: Diagram showing a typical rockfall process and the Rockfall design criteria based on the work of Ritchie (1963)

- Free falling: rocks falling down a steep cliff under the influence of gravitational force;
- Bouncing: a movement that occurs when the falling rock impacts with the slope surface, the block bouncing behaviour is governed by the characteristics of the slope;
- Rolling: the block rolls on the slope with an angular velocity;
- Sliding: the block slides on the slope, the sliding velocity is a function of the coefficient of kinetic friction and the slope angle. A combination of rolling and sliding often occurs during rockfall.

A typical rockfall process is shown in figure 1-2. The detached rock starts movement by freefalling, then bounces, rolls and slides, and stops finally. The inset figure is the criteria proposed by Ritchie (1963), showing that the mode of rock movement is determined by the slope angle.

1.3.4 Rockfall parameters

Once movement of a rock perched on the top of a slope has been initiated, its falling behaviour is controlled by slope geometry, slope properties and boulder properties. Slope angle determines the motion of the rock (figure1-2). Clean hard rock slopes with smooth surface and a sphere-shaped boulder represents the greatest rockfall hazard. The following are parameters of slope properties that influence rockfall trajectory:

- **Coefficient of restitution**: the retarding capacity of the slope surface is the most important parameter influencing rockfall behaviour. Normal and tangential coefficients of restitution are used in rockfall analysis. Details of the restitution coefficients will be discussed in the following chapter.
- **Surface roughness**: the irregularities in slope surface, which account for most of the variability observed among rockfalls because they alter the angle at which a rock impacts the surface. The surface roughness of a slope segment is defined as the variation of slope angle from the average angle of this segment, or the maximum perpendicular variation within a slope distance equal to the radius of the boulder (figure 1-3).

- **Rolling friction coefficient**: the resistance of the slope to angular velocity of the boulder, defined as the tangent of the angle at which a boulder initially at rest starts rolling.
- **Coefficient of friction**: the resistance of the slope to sliding of the boulder, defined as the tangent of the angle at which a boulder initially at rest starts sliding.

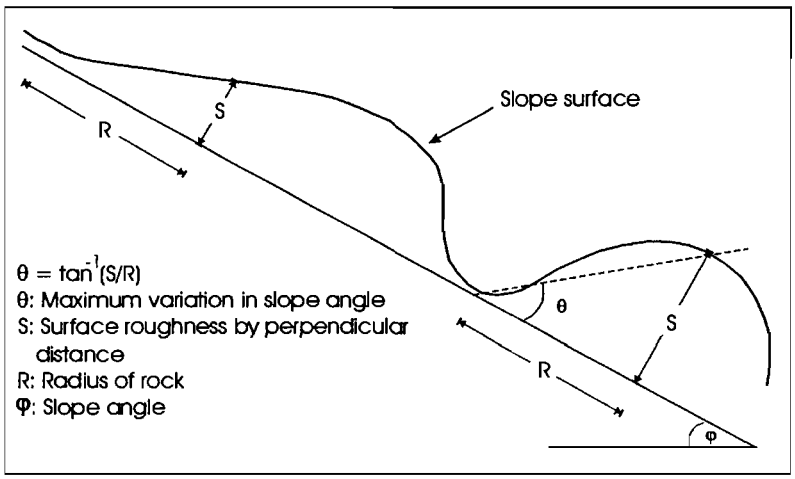

Figure 1-3: Slope roughness (s) established as the perpendicular variation within a slope distance R (Pfeiffer and Bowen, 1989).

Among those parameters the coefficient of restitution is the most sensitive variable in rockfall trajectory analysis, and will be the main topic of this thesis.

1.4 Research on rockfalls

1.4.1 Background

The earliest research into rockfall behaviour was carried out by Ritchie (1963) for the Washington State Highway Commission. Ritchie noted that there is a need for a means of predicting the stability of the material on the surface of a rock cut. By conducting hundreds of full-scale rockfall tests, Ritchie developed criteria for designing cut slopes and ditches (figure1-2) which are still widely used in design of rockfall protection works. Ritchie has also studied the motion and trajectory of boulders and tried to develop an analytical solution of rockfall based on the laws of motion.

Following Ritchie's work, considerable progress has been made in the analysis of rockfall behaviour. Most of the research is related to highway projects. Rockfall

research has been approached by empirical studies, physical modelling and computer simulation. Early research was generally done through empirical methods, while computer simulation has become widely used in last two decades.

1.4.2 Empirical studies

Empirical studies of rockfall are done by means of in situ tests. Ritchie (1963) performed in situ tests using a slow motion camera to determine effective ditch sections and rock fences. Most of his study was done with hard basaltic rocks and natural or excavated slopes of varying ages. Ritchie's study results were used by Fookes and Sweeney (1976) to prepare a rock trap design chart, which was further revised by Whiteside (1986).

Large scale rockfall was analysed by Broili (1974). He described some fundamental observations on the path and behaviour of boulders including relationships between volume, height of rebound and width of trajectories following free falling of several hundred meters. Lied (1977) gave criteria to assess the maximum reach of rockfalls from his experience. John and Spang (1979) gave a systematic review of the conditions under which rockfall occurs, based on field tests.

One of the few detailed rockfall studies in the field has been reported by Mak and Blomfield (1986). The work involved releasing more than 10,000 boulders on pre-split rock faces that had an approximately horizontal base. Angular blocks of 100 to 300 mm size were used. The study showed that the angle and height of the slope have a major influence on boulder trajectory.

Chan, Chan and Au (1986) performed some field tests to study rockfall trajectories for fence design purpose. They rolled around 70 boulders, from 30 kg to over 1 tonne, down two 30^{o} slopes. They compared the field data with the predicted boulder velocity using a mathematical model with octagonal prisms, and found that actual velocities were less than predicted.

The latest and most comprehensive field tests were reported by Azzoni et al (1991). Several experiments were carried out on five different slopes to understand the different types of motion of single rocks, and to study coefficient of restitution, rolling friction coefficient, dispersion of trajectories, effect of block geometry on its fall, and efficiency of ditches. Three or more cameras were placed along each test slope and the images were digitised for analysis. The result was used to calibrate the computer program CADMA for rockfall analysis (Azzoni et al, 1995).

Field tests and field test-obtained parameters are useful in rockfall analysis and rockfall design. However, field tests are site specific, and the results cannot be applied directly to different conditions. Field tests are generally expensive and risky, and there is obviously a need for a convenient and universally applicable method for rockfall analysis.

1.4.3 Physical modelling

Physical modelling of rockfalls is the study of rockfall behaviour through artificially constructed models of the site of interest. The most comprehensive scale modelling of rockfall problem to date is the work carried out by ISMES in Italy (Fumagalli, 1976; Componuovo, 1976). A detailed three-dimensional model of the mountain St.Martino in Italy was constructed to a scale of 1:160, with a model height of about 4.5 m. The main purpose of the study was to understand rockfall behaviour at all the important sections of the mountain. Several model rocks were rolled along the model slope at different sections. The results were calibrated against in situ test results reported by Broili (1977). The results show that good mechanical similitude was possible after some corrections to deformability, compactness and roughness of the slope.

The advantage of physical modelling is a better representational study of rockfalls compared to analytical and computer modelling. The disadvantages are the cost and time, and the difficulty in achieving dynamic similitude, as a low scale has to be used for more accuracy. That is why no further attempt has been made to construct physical models of rockfalls.

1.4.4 Computer simulation

Early research on rockfalls was mostly carried out by in situ tests, which involve high cost and risk. With a better understanding of rockfall behaviour through in situ tests and physical modelling, researchers attempted to develop mathematical models to simulate rockfalls with a computer. Piteau and Clayton (1977) announced the first computer program for rockfall analysis. The program used a slope profile divided into straight-line segments termed cells, and the laws of motion to determine where the rock will impact the ground. A coefficient of restitution and slope roughness were used in their model. The program produces velocity and bounce height distributions for the slope. After Piteau and Clayton, many simulation programs have been developed by different researchers. Now computer simulation is used to produce rockfall statistics for design of protective structures, including boulder height, velocity and the range of kinetic energy. Since the computer is efficient for simulation of both random and repeatable behaviour of rockfalls, the computer simulation has become a preferable method of rockfall analysis for the design of protective measures.

Two methods have been used in computer modelling of rockfalls: the rigorous method and the lumped mass method (Hungr and Evens, 1988).

1) Rigorous method: In this method, actual shape and dimensions of the boulder are assumed and all motions are considered. Both translational and rotational momenta are transferred by an impact according to a very complex set of conditions, depending upon the shape of the contact corner, the precise rotation angle at the point of contact, slope surface roughness, and normal and frictional deformations. This method was first developed by Cundall (1971) and has been extended into three dimensions by Descoeuders and Zimmermann (1987). Because of the difficulties in modelling all the conditions, various simplifying assumptions must be made. Simple boulder shapes such as sphere, cylinder, disk, cube and ellipsoid are used in various programs to calculate the momentum of the boulder.

2) Lumped mass method: In this approach, the boulder is considered as a single point with a certain mass. Normal and tangential coefficients of restitution are used to calculate translational velocity at impact; no attempt is made to keep track of the rotational momentum. Early programs often used this method. Now boulder shape and size are considered by most programs.

1.5 Rockfall Protection measures

Martin (1988) provides a summary of protection methods for slopes with rockfall problems (table 1-2).

Table 1-2: Rockfall protection measures (Martin, 1988)

Stabilisation methods	Protection methods	Warning methods	Monitoring systems
Excavation Scaling Trimming Ground water control and drainage Rock reinforcement and support: • Shotcrete and mortar • Dental treatment • Rock bolt, dowels, anchors • Buttresses and bulk heads • Retaining wall and tie back wall • Anchored beam and strapping • Beam and cable walls • Cable nets, lashing and chains	Relocation Tunnels and sheds Interception ditches and shaped ditches Interception berms and shaped berms Catch walls Draped and pinned mesh Catch fences and catch nets	Patrols and signs Electric fences and wires Warning lights and sirens	Precise surveys Extensometers, inclinometers, tilt meters, load cells. Systems in combination with protection.

Stabilisation methods are used either to permanently reduce the rockfall hazards or to improve the stability of slope. The purpose is to prevent boulders from becoming detached rather than stopping the boulder reaching the road or

any other site. They are called active methods. **Protection methods** are also called passive methods, which involve the control of rockfalls and are generally inexpensive as stabilisation methods, but they require an ongoing commitment to maintenance. The use of warning methods is generally restricted to railways or other controlled access systems (Martin, 1988).

The appropriate stabilisation measures should be selected according to particular site geotechnical, construction and environmental conditions. For example, where the slope is steep and the toe is close to the highway or railway, there will be no space to excavate a catch ditch or construct a fence. Alternative measures may be to remove the loose rock, secure it in place with bolts, or cover the slope with mesh. If the slope is susceptible to weathering, the scaling work may have to be repeated every 3 to 5 years. Alternatively, a more comprehensive program can be carried out using shotcrete and bolting in addition to scaling (Wyllie and Norrish, 1996).

1.6 Rockfall hazards analysis systems

In order to decide whether stabilisation works are needed for a particular site subject to rockfalls, detailed hazard assessment should be carried out to determine the relative risk compared with other sites. That involves detailed site investigation and rating to particular parameters to evaluate the inventory of stability conditions.

Several researchers have developed risk rating systems for slope stability. Hunt (1992) reported risk mapping of slope failure. He proposed two ways of dealing with slope problems: to provide complete stability of all cuts and fills, or to accept some risk of failure by stabilising only those slopes with potential failure. His approach was qualitative with a scale of 1 to 5 for very high to low risk respectively. Romana (1985, 1988, 1991) used Bieniawski's (1976) rock mass rating (RMR) classification of rocks to develop a slope mass rating (SMR) system. Cancelli and Crosta (1993) suggested a risk mapping technique for rockfalls using relative risk rating for different conditions with respect to characteristics of rockfalls.

The most widely accepted method is the Rockfall Hazard Rating System (RHRS) developed by the U.S. Department of Transportation (1993). The first step in the process is to make an inventory of the stability conditions of each slope. The rockfall areas identified in the inventory are ranked by scoring 11 categories representing the significant elements of a rock slope that contribute to the overall hazards. The RHRS system will be used for this project and is discussed in chapter 5.

1.7 Thesis organisation

This thesis includes 6 chapters, covering the results of works from the determination of the coefficient of restitution in laboratory and in the field, rockfall field trial, rockfall analysis and risk assessment of the Marine apartments.

Chapter 2 is a literature review of the coefficient of restitution, covering its origin, definitions and the methods of determining the coefficient of restitution by different authors.

Chapter 3 and chapter 4 cover the main subject of this project. Chapter 3 describes the process of laboratory tests to determine the coefficient of restitution, reports the study on the relationship between the coefficient of restitution and properties of both the slope and the falling rock, and an empirical method to calculate the coefficient of restitution using the Schmidt hammer number and slope angle. Chapter 4 deals with a rockfall field trial at Lyttelton Quarry, including field-tests for the coefficient of restitution, rockfall in situ tests on a slope, computer simulation of rockfalls on the same slope and comparison between the results from field trial and simulation.

Chapter 5 covers the result of site geotechnical investigation, rockfall trajectory analysis and risk evaluation for the proposed Marine Apartments at Sumner, where a steep cliff of 35-45 m high consisting of basaltic lava and volcanic agglomerate poses rockfall hazards to a car park and the proposed buildings at its base.

Chapter 6 concludes the work, with discussions focusing on the overall topic of the coefficient of restitution and rockfall analysis, and suggestions for continued work.

The results of the mechanical property measurements (density, dynamic modulus of elasticity and Schmidt number) of samples for laboratory tests are summarised in Appendix A. The coefficient of restitution calculation results for both laboratory and field tests are presented in Appendix B. Field investigation data (profile survey, Schmidt number and surface roughness measurement) are summarised in Appendix C.

Chapter 2

A Review of the Coefficient of Restitution

2.1 Introduction

The coefficient of restitution is an important parameter in rockfall simulation. It was initially defined in rigid body mechanics to represent the amount of energy loss during rigid body collision, and adapted to rock mechanics to calculate the velocity of bounce in rockfall simulation. In rigid body mechanics, analytical solutions (obtaining post-impact velocity in terms of pre-impact velocity) of rigid body collision problems are formulated in terms of Newton's law of motion and Coulomb's law of friction, and the coefficient of restitution and coefficient of friction are used to deal with impact behaviours in the normal and tangential directions. In rockfall simulation, the definitions of normal and tangential coefficients of restitution are introduced to calculate the normal and tangential components of rebound velocity.

The process of rigid body collision is very complicated. The major characteristics are the very brief duration and the large magnitude of the forces generated. Other phenomena include vibration waves propagating through the bodies, local deformations produced in the vicinity of the contact area, and frictional and plastic dissipation of mechanical energy. In the collision event, a crater is formed on the surfaces of the colliding bodies (involving elastic or permanent deformation), normal and tangential forces act on the crater surface, tangential force is created by the horizontal component of the normal stress and friction. Figure2-1 shows a typical impact process of a sphere impacting on an immobile plane. The deformation history is assumed to consist of two periods: the period of compression and the period of restitution. The compression period extends from the instant of contact to the point of maximum compression, at which the approach velocity becomes zero. The period of restitution then begins, lasting to the instant of separation (Wang and Mason, 1992). In the compression phase elastic loading takes place first, and if the impact velocity exceeds a yield point,

plastic loading then takes places. In the restitution phase, elastic unloading takes place and kinetic energy is recovered as resultant velocity, while plastic loading results in plastic deformation. If there is no plastic deformation, and ignoring energy losses due to elastic waves, the coefficient of restitution is 1, but if there is no elastic recovery, the coefficient of restitution is zero (Thornton, 1997).

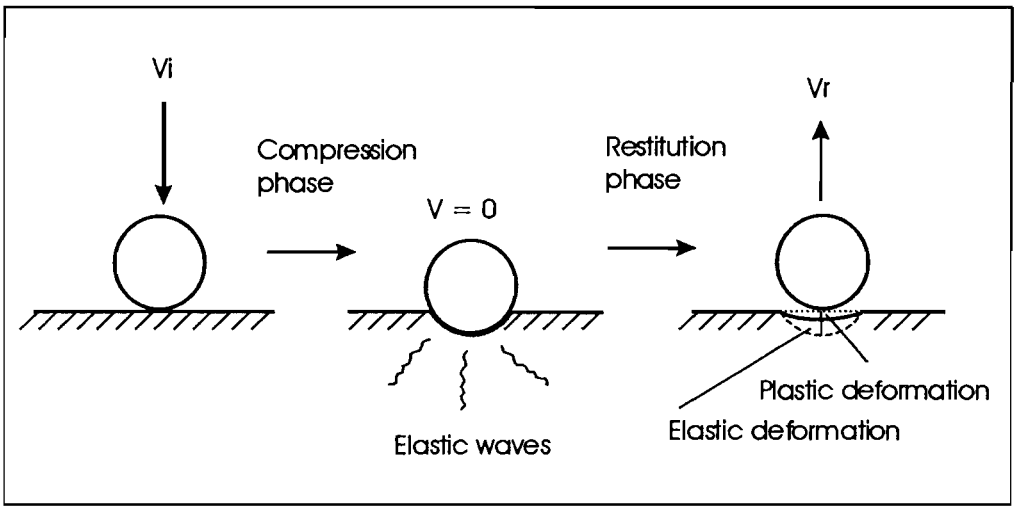

Figure 2-1: A typical impact process showing the deformation history. Note deformation of the sphere is not shown in this figure.

Smotzyk (1983) described the energy transformation in dynamic compaction as:

- Generation of elastic waves;
- Grain displacement under constant volume;
- Compaction (reduction of volume by displacement of grains);
- Destruction of grains;
- Air resistance, rolling and sliding resistance.

2.2 Background to the coefficient of restitution

2.2.1 The kinematic definition of the coefficient of restitution

The original definition of the coefficient of restitution was given by Newton (1686) as the ratio of the rebound and incidence velocities of two colliding particles (or small spheres) in the normal direction:

$$R = \frac{-(V_{1n} - V_{2n})}{v_{1n} - v_{2n}}$$

where V_{1n}/V_{2n} are the normal components of the rebound velocities, and v_{1n}/v_{2n} are the normal components of the initial velocities of the two colliding bodies. This is called the kinematic definition of the coefficient of restitution.

Newton's coefficient has been used for the collinear impact for more than 300 years. Its use has been generalised and extended to three-dimensional collisions by Brach (1991, 1997). However, this coefficient was treated as a material constant, and did not consider cases where there is a relative tangential velocity at the contact point. There exist some problems involving the tangential component of the contact impulse (frequently attributed to friction) and the fact that some solutions violate energy conservation laws (Wang and Mason, 1992, Battle, 1993). But Brach (1997) proved that Newton's approach can be energetically consistent with suitable bounds on the friction coefficient (defined as the ratio of the tangential impulse to the normal impulse).

2.2.2 The kinetic definition of the coefficient of restitution

The kinetic definition of the coefficient of restitution was given by Poisson (1817), who defined the coefficient of restitution as the ratio of the normal restitution impulse to the compression impulse at the contact point:

$$R = \frac{P_{nr}}{P_{nc}}$$

where P_{nr}, P_{nc} are the normal impulses in the periods of restitution and compression.

Poisson pointed out that there were several possible tangential motions that may arise at the contact point during the collision period. With the help of his co-worker (Morin, 1855), he proved that Coulomb's friction could be used to relate the normal and tangential contact forces. Routh (1860) developed a graphical method to solve planar impact problems of rough, inelastic bodies. His method brought solution to collisions where the slip between colliding bodies changes direction during impact. This development led to Whittaker's (1904) method of solution of impact with friction. Whittaker's method combines Newton's definition

of the coefficient of restitution and Poisson's definition of the phases of collision, and yields algebraic equations that can be easily solved for the post-impact velocities. Although this approach does not treat the contact forces properly when the slip direction changes during collision, it has been widely accepted as a standard method. Wang and Mason (1992) compared Newton's law and Poisson's definition to deal with impact as tangential velocity reversal (final tangential velocity opposes initial velocity) and tangential impact (impact with zero normal impulse), and showed that Poisson's method guarantees energy conservation laws while Newton's law of restitution cannot.

2.2.3 The energetic coefficient of restitution

The energetic coefficient of restitution is defined as the ratio of work done by the normal component of the reaction forces at the contact point during the compression phase to that during the restitution phase (Stronge, 1990).

$$R = \sqrt{\frac{W_{nr}}{-W_{nc}}}$$

where W_{nc}, W_{nr} is the work done by normal impulse during compression and restitution, respectively. W_{nc} represents a transformation of kinetic energy to forms associated with deformation during compression, while W_{nr} represents the return of deformation-associated energy to kinetic energy during restitution. Stronge (1990) suggested that in a consistent theory the part of the energy dissipation during restitution cannot be larger than the corresponding part during compression, and he also demands an energetically consistent (normal) coefficient of restitution to be one that is independent of the tangential contact process (friction). This definition resolved the arguable inconsistencies in energy loss predicted by the kinematic definition.

2.2.4 Difference of the three definitions

Smith and Liu (1992) studied the relationships between the coefficients of restitution from the three definitions in planar collision. In general, the three coefficients are expected to differ, however they can be the same under conditions where there is no inertia coupling between the normal and tangential

directions (the tangential impulse doesn't affect the normal impulse), or if the tangential component of the contact forces is zero (figure 2-2). The extent to which these values may differ depends on the amount of friction, direction of approach velocity, and the inertial characteristics of the system. Smith and Liu calculated the effects of those parameters with planar collision under simplified assumptions and by means of a computer code based on a finite element model. The result shows that when the inertia coupling tends to reverse the direction of the tangential velocity (figure 2-2), the normal velocity ratio may be expected to be lower than the other two coefficients, whereas for cases in which α (angle of approach velocity) and θ (angle of the principal direction of the impacting body, see figure 2-2) have the same sign, the normal velocity ratio may be expected to be larger than the two other coefficients.

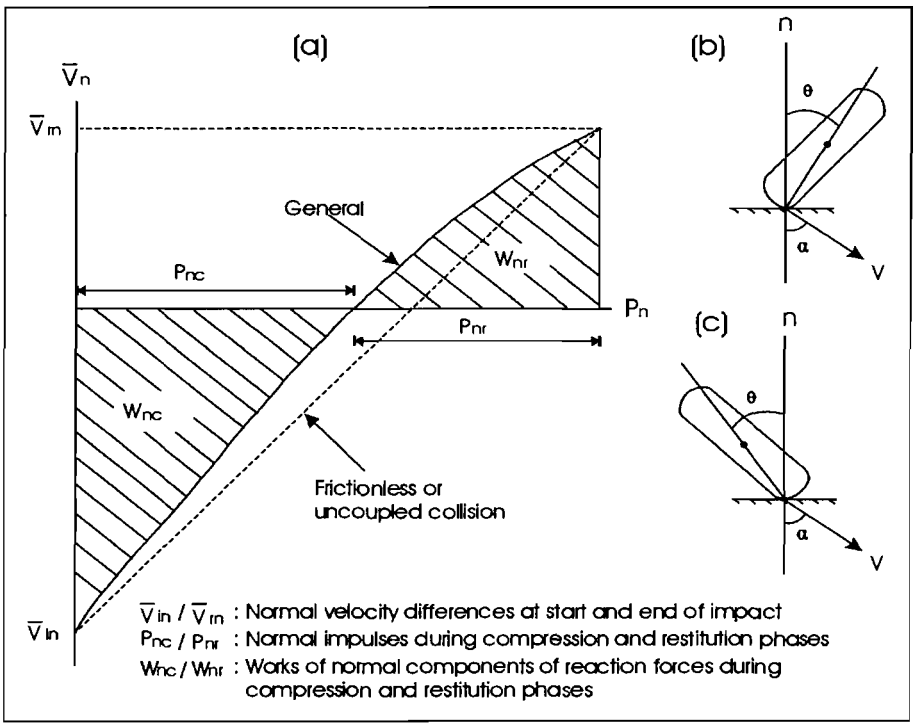

Figure 2-2: Diagram showing the velocity difference, impulse and work during impact (a), and inertial configurations of an unconstrained body impacting on an immobile plane; (b): inertial coupling tends to reverse tangential velocity; (c): α and θ with same sign (from Smith and Liu, 1992).

2.3 Coefficient of restitution in rockfall simulation

The coefficient of restitution was introduced in the past two decades to the area of rockfall simulation to calculate rebound velocity, but different authors used different definitions. For example, Azzoni (1995) used energetic coefficient of restitution, while Wu (1985), Hungr and Evans (1988), Pfeiffer and Bowen (1989), Elliot (1992), Robothan, Wang and Walton (1995) used kinematic (velocity) coefficient of restitution. Although the coefficient of restitution was originally restricted in the normal direction, it is applied in both the normal and the tangential directions in rockfall analysis, and normal and tangential coefficients of restitution are often used separately to determine the rebound velocity components normal and tangential to the slope (Piteau, 1978; Wu, 1985). **The normal coefficient of restitution** (Rn) is a measure of the degree of energy dissipation in the collision normal to the slope, defined as the ratio of normal component of the rebound velocity to the approach normal velocity, which is the same as Newton's coefficient of restitution in rigid-body mechanics. The **tangential coefficient of restitution** (Rt) is a measure of the resistance to movement parallel to the slope, defined as the ratio of tangential component of the rebound velocity to the approach tangential velocity.

The coefficient of restitution is by no means a material constant, but depends on particle velocities, particle geometry, their mass, elastic moduli, radii of curvature at contact point, and their attenuation properties (Goldsmith, 1952). The values of the coefficients of restitution (especially the normal coefficient of restitution) have a great significance in rockfall trajectory analysis. Richards (1988) showed the influence of the coefficients of restitution on the maximum trajectories calculated using the program Rockfall (figure 2-3 and figure 2-4). From figure 2-3 and figure 2-4, it can be seen that small changes in the values of the coefficients of restitution result in totally different trajectories. Values of Rn greater than 0.6 lead to an unrealistically high bouncing mode, which explains the importance of the coefficients of restitution in rockfall simulation. Simulations realistic to site conditions can only be obtained with accurate and site-specific parameters including the coefficients of restitution.

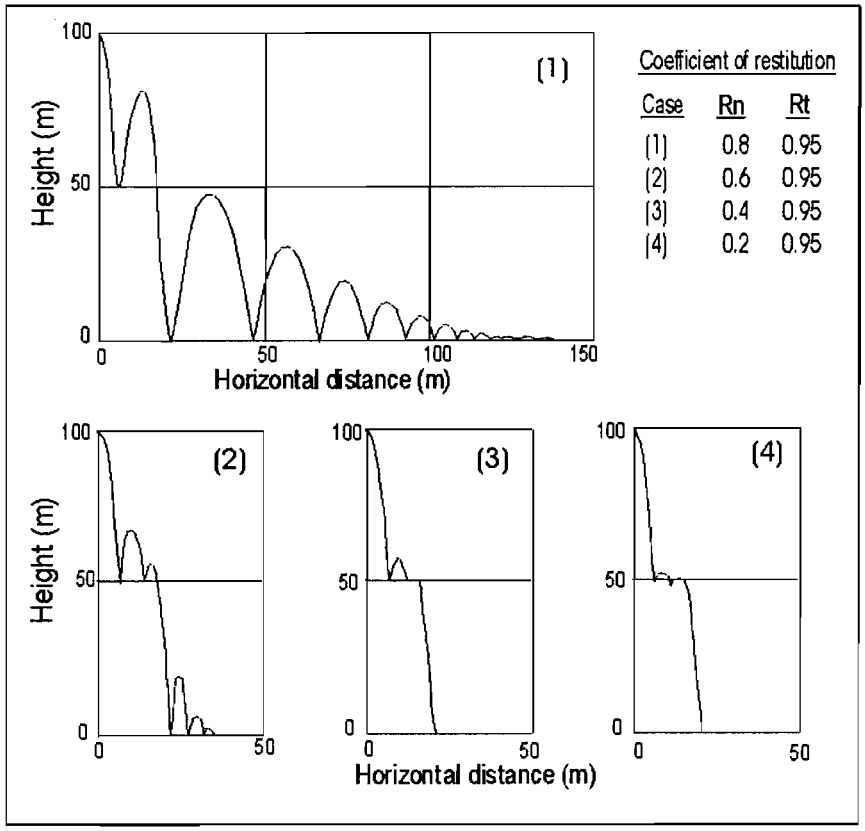

Figure 2-3: Plots showing the effect of normal coefficient of restitution on bounce mode (Richards, 1988)

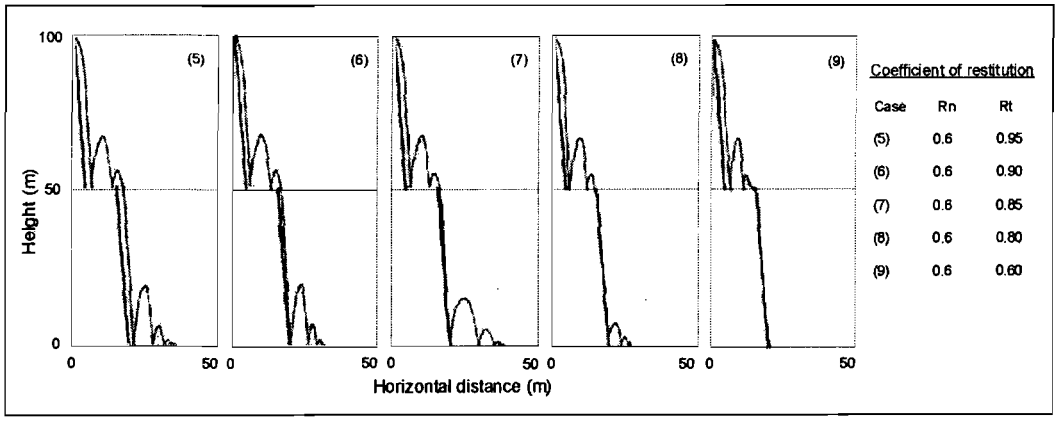

Figure 2-4: Plots showing the effect of tangential coefficient of restitution on rockfall bounce mode (Richards, 1988)

2.4 Determination of the Restitution Coefficient

The coefficient of restitution can be found by field tests (e.g. Wu 1985, Evans and Hunr 1993, Robotham et al 1995, Azzoni *et al* 1995), by back analysis of actual events (e.g. Budetta & Santo 1994, Fornaro *et al.* 1990, Pfeiffer & Bowen 1989), or by laboratory tests (e.g. Auberger & Rinehart 1960, Bowman et al. 1995, Chau et al. 1998, Rayudu 1997). Typical values of the coefficient of restitution reported by different researchers are listed in table 2-1.

Table 2-1: Reported values for coefficient of restitution (modified from Richards, 1988)

Reference & methods	R	R_n	R_t	Slope properties
Habit (1977), based on experience	0.75-0.80 0.50-0.60			Based on experience in Italy Based on experience in Norway.
Descoeudres et Zimmermann (1987)	0.40 0.85			Vineyard slopes Rock slopes
Brioli(from Pasquero,1987)	0.75-0.80 0.20-0.35			Rock on rock Rock on soil/scree
Piteau and Clayton(1987)		0.9-0.8 0.8-0.5 0.5-0.4 0.4-0.2	0.75-0.65 0.65-0.45 0.45-0.35 0.3-0.2	Solid rock Detrital material with large rock boulders Compact detrital material with small boulders Grass covered slopes
Hoek (1987)		0.53 0.40 0.35 0.32 0.30	0.99 0.90 0.85 0.82 0.80	Clean hard bedrock Asphalt roadway Bedrock outcrops with hard surface, large boulders. Talus cover Soft soil, some vegetation
Azzoni et al (1991) Field tests on different slopes		0.45-0.85 0.30 0.62 1.22	0.45-0.75 0.66 0.66 0.80	Rock/thin debris, 30-80° Fine debris, 40° Debris and earth, 25° Coarse debris, 40°
Azzoni and Freitas (1995), field tests	0.51-0.92 0.32-0.65			Rock slope Debris slope
Robotham et al (1995), in situ tests		0.315 0.303 0.315 0.251 0.276 0.271	0.712 0.613 0.712 0.489 0.835 0.596	Limestone face Partially vegetated limestone scree Uncovered limestone blast pile Vegetated covered limestone pile Chalk face Vegetated chalk scree
Rayudu(1997) Laboratary tests		0.33-0.77		Steel ball on different rock slabs
Chau, et al(1998)	0.487	0.197	0.910	Rock slope
Laboratary tests	0.393	0.290	0.567	Soil slope
	0.453	0.263	0.737	Shotcreted slope

2.4.1 Field tests

Wu (1985) conducted an *in situ* test of rockfall impact on an inclined wooden platform (angle 30°, 40°, 45°, 60°) and on rock slopes. Rock blocks of different size (diameter 20–45 cm) were used to drop onto the slopes. Records of the dropping process were taken by a movie camera. Normal and tangential coefficients of restitution (Rn, Rt) were calculated from the recorded rebound distance, height and time interval. Only the first bounce was used in the calculations. Wu found that both the mean values and standard deviation of Rn decrease linearly with the impact angle θ (angle between slope surface and the direction of the incoming boulder), while those of Rt increase with the impact angle (figure 2-5). Wu used the equations to calculate values of mean and standard deviation for a given slope angle, and then to generate a random number for Rn and Rt in his rockfall simulation.

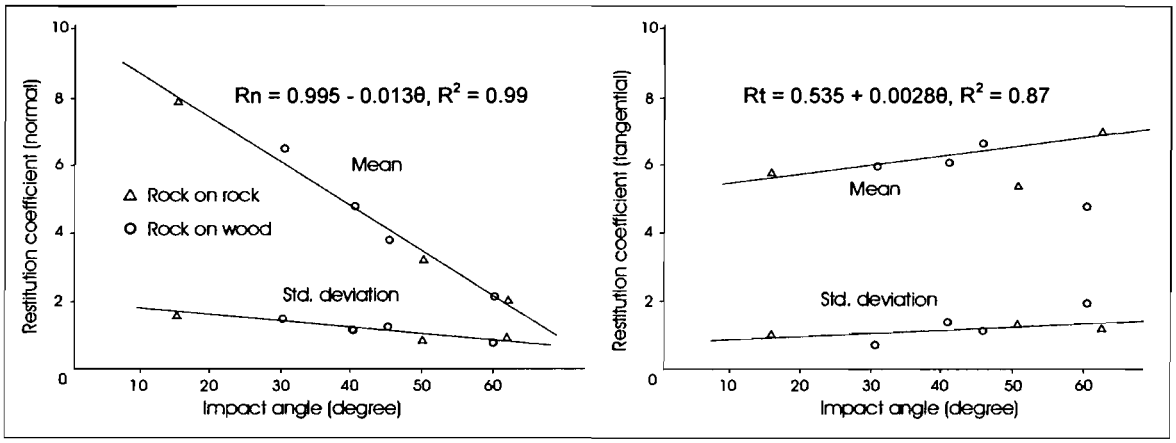

Figure 2-5: Impact angle versus means and standard deviations of restitution coefficient (Wu, 1985)

Azzoni et al (1991) carried out several rockfall experiments on slopes of different geological and geomorphological features. The tests were carried out at five sites: a quartzite quarry, a gneiss quarry, an orthogneiss quarry, a limestone quarry and a natural slope. Slope angle varied from 25°-80°. Tabular to spheroid boulders of different rocks (quartzite, gneiss and limestone) were dropped down the slopes. Boulder sizes ranged between 0.5-3.0 m^3. Three or more cameras were placed along the test slopes to record the rockfall process. Coefficients of restitution for different slopes were then calculated from the records (table 2-1).

2.4.2 Laboratory tests

Auberger and Rinehart (1960) used small steel balls of different diameters (1/2 – 1/64 inch) impacting plexiglas and different rock plates to study the energy loss associated with the impact and the attenuation of elastic waves. It was found that the coefficient of restitution is a function of the striking velocity as well as the sphere diameter. Generally the coefficient of restitution decreases slightly with striking velocity and increases with the diameter. Figure 2-6 shows the variation of the coefficient of restitution with the striking velocity and diameter from impact on plexiglas.

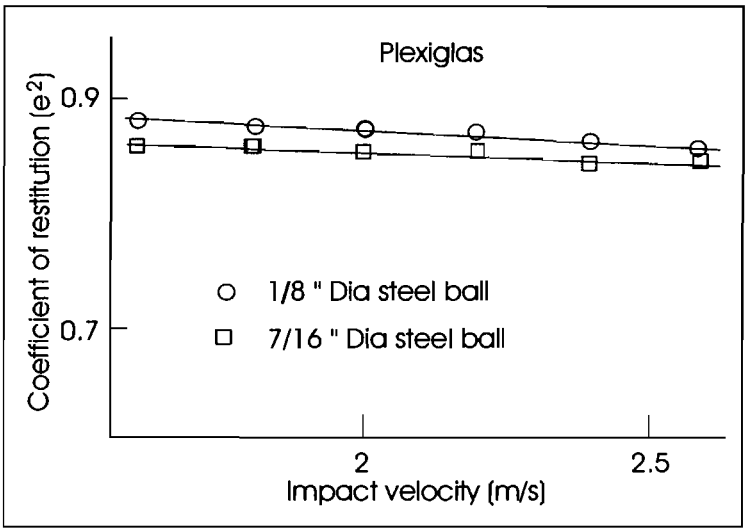

Figure 2-6: Variation of the of the coefficient of restitution (normal) with the impact velocity for steel balls striking plexiglas (Auberger and Rinehart, 1960)

Chau *et al* (1998) carried out a laboratory test with fresh granite boulders impacting different slope surfaces: soil slope, rock slope, shotcreted slope and rock/soil slope. Slope angles varied from 25° to 32°, and the rock pieces were cuboids or angular with diameters from 3 to 5 cm. The rock boulders were dropped from 1.06 m above the slope surface. Results of the test are shown in table 2-1. Recent comprehensive experimental research has been carried out by the same researchers to investigate the effects of impact conditions on the coefficient of restitution (Chau *et al*, 1999). They used both rock and artificially plaster-cast boulders (various shapes and sizes) impacting artificial slope surfaces (plaster-cast slopes). Spheres, cylinders, cubes and hexagonal boulders (diameter 40 – 76 mm) were used to drop from heights of 80 – 160 cm, and slope angles were adjusted to 30°, 45°, 60° and 70°. Records were captured by a high-speed camera, from which parameters were obtained and the coefficient of

restitution calculated. Test results show that the coefficient of restitution increases with the slope angle and decreases with impact energy. For impacts on soil slopes, the normal coefficient of restitution (Rn) increases with the moisture content of soil, especially when the moisture content exceeds an optimum point (about 10.5%), while the tangential coefficient of restitution (Rt) increases with moisture content before the optimum point and decreases after the optimum point. The normal coefficient of restitution increases with the angularity of the boulders, while the tangential restitution coefficient is relatively insensitive to the shape of boulders.

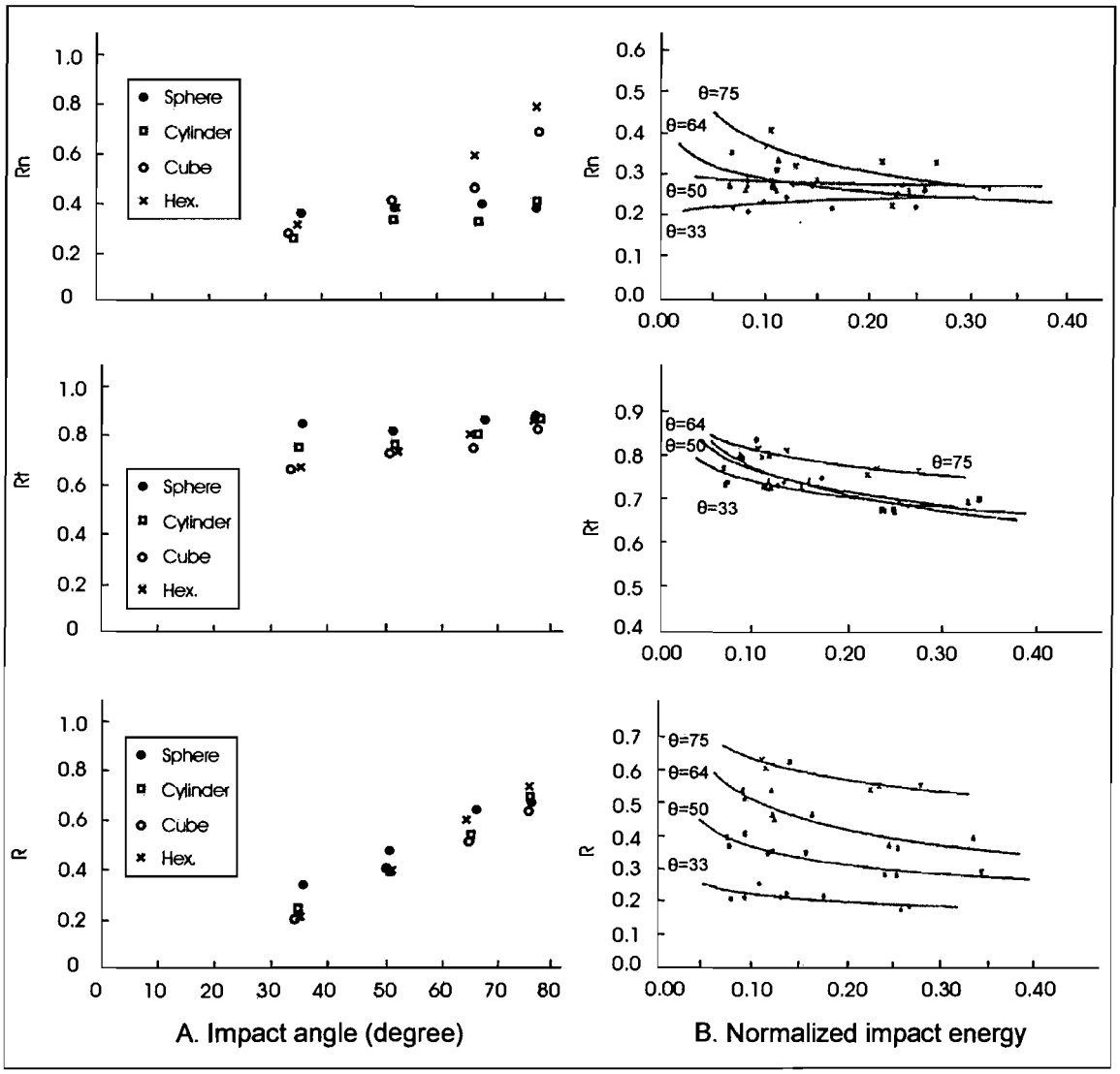

Figure 2-7: Plots showing the effects of boulder shape, impact angle and normalized impact energy on the coefficients of restitution (Chau *et al*, 1999)

Figure 2-7 shows the effects of boulder shape, impact angle θ (angle between the impact velocity and the normal to the slope) and the normalized impact energy (ratio of the impact energy to that required to fracture the same sample) on the coefficients of restitution. It is found from figure 2-7A that for $30^\circ < \theta < 50^\circ$ the normal coefficient of restitution is independent of boulder shape and θ, and for $60^\circ < \theta < 75^\circ$ the values of Rn are the largest for hexagonal boulders and smallest for cylindrical and spherical boulders. Values of Rn for spherical boulders are not sensitive to impact angle, while those for angular boulders increase with θ when $60^\circ < \theta < 75^\circ$. The tangential coefficient of restitution is not sensitive to both the boulder shape and the impact angle, while the energetic coefficient of restitution R (ratio of energies before and after impact) is not sensitive to shape effect but increases with impact angle. The normal coefficient of restitution (Rn) is not sensitive to the normalized energy when the impact angle is less than 50° but decreases slightly with the normalized energy when $\theta > 50^\circ$, while Rt and R decreases with the normalized energy for all the four impact angles as shown in figure 2-7B (Chau et al, 1999).

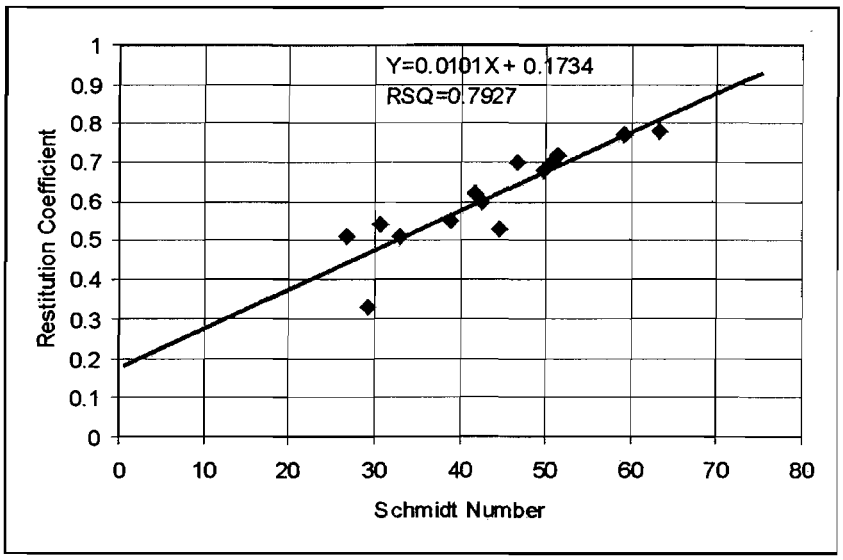

Figure 2-8: Plot showing the correlation between restitution coefficient and Schmidt number (Rayudu, 1997)

Rayudu(1997) tried to relate the coefficient of restitution to the Schmidt Hammer number of the rock forming the slope in order to find an easy means of determining the normal coefficient of restitution. In his test, a steel ball (diameter

4 cm) was dropped from 1m onto 14 different rock slabs, which were firmly clamped onto the concrete floor. A high-speed camera was used to record the dropping process and the coefficient of restitution was calculated from the dropping and rebound height. Rayudu found a linear relationship between the normal coefficient of restitution and the Schmidt rebound number (figure 2-8). Rayudu established a correlation between the coefficient of restitution and rock properties for the first time in rockfall research. The result shows that the coefficient of restitution can be determined directly from the Schmidt number of the materials forming the rock slope, instead of the expensive and risky field test. However, since the result was obtained from steel on rock impact, it cannot be used in rockfall simulation at this stage because of the difference of the elastic properties of rock and steel. Rayudu suggested that a good correlation between the coefficient of restitution and Schmidt number of rock–rock impact might also exist. Further laboratory tests are needed to examine the relationship between the coefficient of restitution and rock properties under more practical conditions before this approach can be practically used in rockfall simulation. These tests are described and discussed in the following chapters.

2.5 Syntheses

The coefficient of restitution was first defined in rigid-body dynamics, and then introduced to rockfall simulation. Three different definitions of the coefficient of restitution are used: the kinematic coefficient of restitution is defined as the normal velocity ratio before and after impact, the kinetic coefficient of restitution is defined as the ratio of normal impulse in the periods of restitution to that in the period of compression, and the energetic coefficient of restitution is defined as the ratio of work done by the normal impulse during the restitution period to that during the compression periods. Although the coefficient of restitution is defined in the normal direction in rigid-body dynamics, both normal and tangential coefficients of restitution are used to calculate the normal and tangential rebound velocities in rockfall analysis.

The values of the coefficient of restitution have usually been determined by field tests. Different authors have reported values of the restitution coefficient for

different conditions. Some laboratory tests have been carried out to investigate the relationship between the coefficient of restitution and rock properties. A significant study has been done by Rayudu (1997), who established a relationship between the coefficient of restitution and the Schmidt number of the slope. The result indicates that an easy method of determining the coefficient of restitution directly from the Schmidt number of rock slope materials is possible. Although the Schmidt number is only a rough measurement of rock strength, it is easy to carry out in the field and because it is based on impact it simulates the process of rockfall. Since the result was obtained from steel-rock impact, further tests are needed to verify this approach with more practical conditions. That is why this project has been proposed and laboratory and field tests have been carried out.

Chapter 3

Laboratory Tests to Determine the Coefficient of Restitution

3.1 Introduction

Rayudu (1997) suggested an easy method to determine the coefficient of restitution from the Schmidt number of rock slope materials. Since the Schmidt hammer rebound test is based on impact onto a surface which is similar to the process of rockfall, the Schmidt number can be used as an ideal parameter for rock property in rockfall analysis although it is only a rough measure of strength. The significance of the method is that the measurement of the Schmidt hammer number is easy to carry out in the field. But because his result is based on steel–rock impact, it can't be used to simulate rock–rock impact in computer simulation of rock falls.

The objectives of the laboratory tests are to obtain the coefficients of restitution of different rocks on different slopes, and to study the effects of rock properties (particularly the Schmidt number) and impact conditions (slope angle and impact velocity) on the coefficient of restitution, and try to establish a correlation between the coefficient of restitution and those factors. If successful, it will be possible to determine the restitution coefficient through those parameters.

Two phases of laboratory tests have been carried out, the first being the test with artificial rock spheres impacting polished rock slabs aimed at finding the relationship between the coefficient of restitution and the properties of rock slabs and rock spheres. The second test uses rough rock pieces and rock spheres impacting rough rock blocks, beds of debris and soil, aimed at finding the coefficient of restitution and verifying the relationship under more practical conditions.

3.2 Rock samples and their properties

3.2.1 Sample collection and preparation

Twenty-three different types of rock specimens were collected from different sources. Some of them were specimens collected from the field, and some from local stonemason companies. The large number of specimens is aimed at obtaining a large database for statistical analysis and all the specimens used for the tests are listed in table 3-1.

Rock slabs were made from all the above specimens (some of them are already slabs), and generally at least two slabs were prepared for one specimen in case of breaking in the bouncing test. The thickness of the rock slab was generally 2.5–5 cm. Slab surfaces were polished, and were generally smooth and flat (figure3-1).

Quasi-spherical rock balls were made from 18 of the above rock specimens by cutting and grinding, and at least two balls for each specimen were prepared for spare use. Diameters of rock spheres were generally 5.5–6 cm, which was of proximately the same mass as that of the steel ball used by Rayudu in his test so that the results could be compared directly (figure3-2).

A steel plate and 3 steel balls with diameter 3.5, 4.6, 5.0 cm were also prepared for the test to compare the difference between rock and steel, and to enable comparison with the study by Rayudu.

Table 3-1: Types of specimens used in the tests

Igneous	Metamorphic	Sedimentary
Basalt, Granite, Diorite, Rhyolite, Diorite-porphyry, Trachyte, Syenite, Gabbro, Granite- porphyry, Syenite-porphyry	Marble (4 types), Gneiss, Schist (2 types)	Limestone (3 types), Sandstone (3 types)

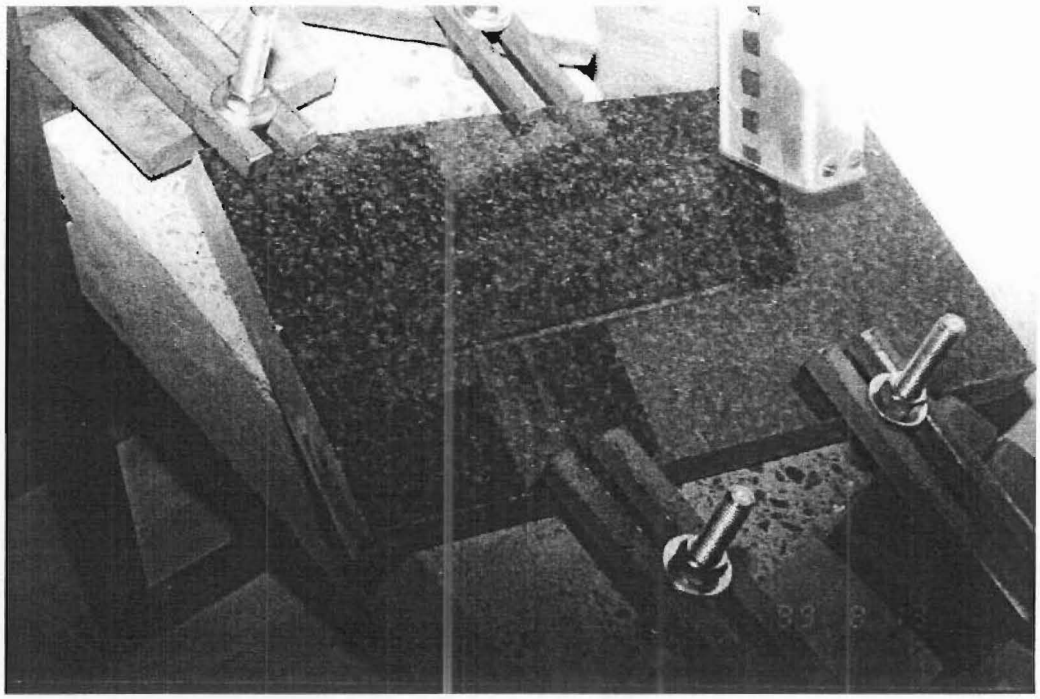

Figure 3-1: Rock slab clamped on concrete deck for rockfall laboratory test

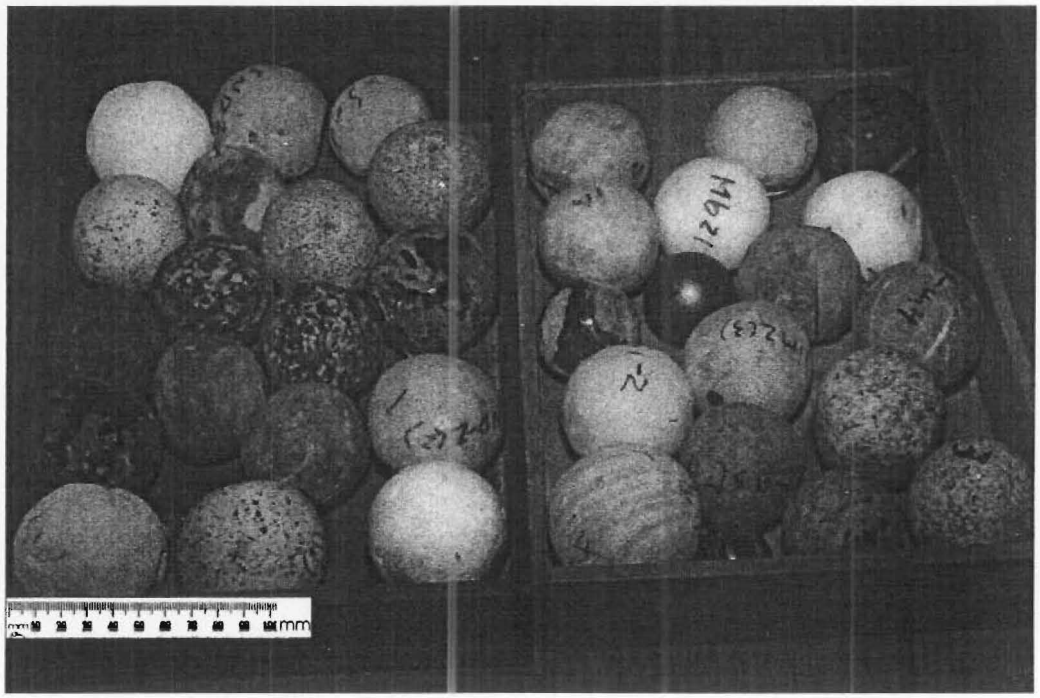

Figure 3-2: Rock and steel spheres for rockfall laboratory test

3.2.2 Measurement of Schmidt hammer numbers

The Schmidt hammer used in this test is of type L with impact energy 0.735 Nm. The Schmidt numbers for rock slabs and balls were measured using the ISRM suggested method (Brown, 1981). For rock slabs the Schmidt numbers were measured before the bouncing test with the slab firmly clamped on the concrete deck, and for rock balls this was done with a steel cradle which was clamped on the concrete deck together with the ball tested (figure3-3). At least 20 readings were taken for each specimen, the average of the upper 50% readings was calculated as the Schmidt number of the specimen as suggested by the ISRM.

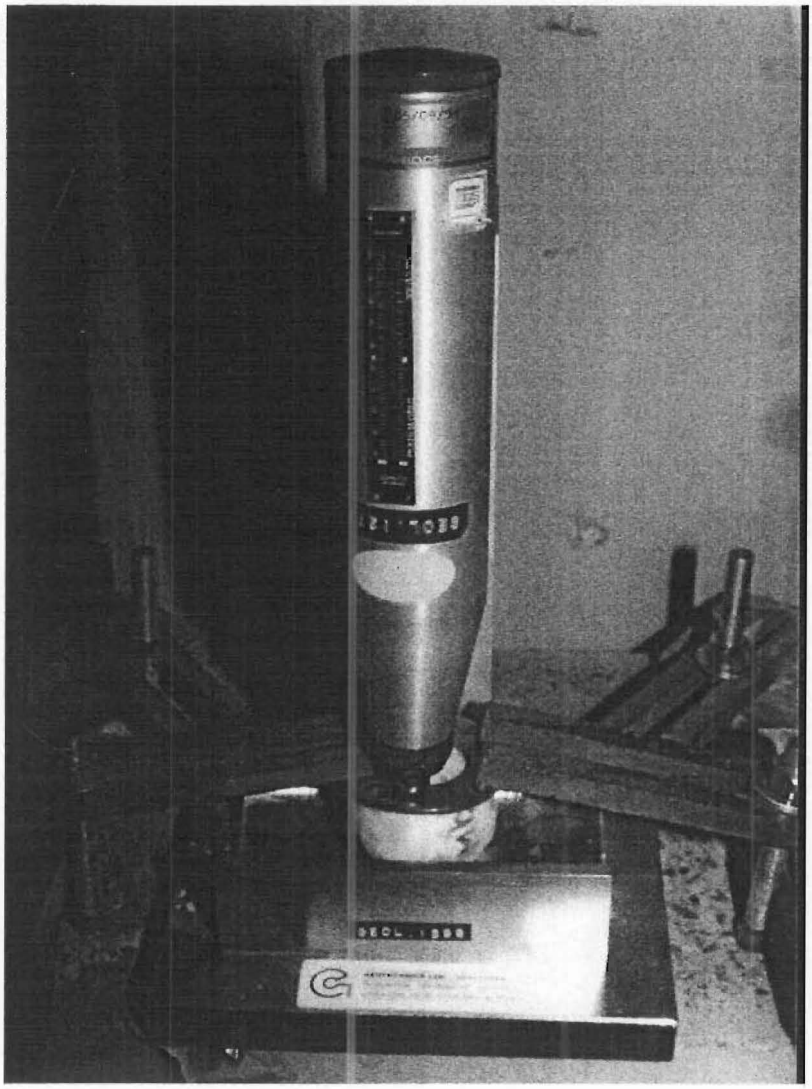

Figure 3-3: Set up for measuring the Schmidt number of rock spheres

Table 3-2: Mechanical properties of rock specimens

Slab Label	Rock type	Schmidt N1(mean)	Ball Label	Rock type	Schmidt N2(mean)	Sample	Density (Kg/m^3)	Edyn. (GPa)
bast1-1	Basalt	51.0	bast1-1	Basalt	41.0	Bast1	2890	81.29
dio1-1	Diorite	38.7	bast1-2	Basalt	46.7	Dio1	2890	27.80
Diop1	Diorite-porphyry	45.6	Bast1-3	Basalt	49.6	Gabbro	2900	48.26
Gabbro	Gabbro	49.4	dio1-1	Diorite	40.8	Gnss1	2780	49.91
gnss1-1	Gneiss	41.2	dio1-2	Diorite	41.8	Gnt1	2620	40.41
gnt1-1	Granite	39.9	diop1	diorite – porphyry	42.7	Lim1	1330	5.00
gnt1-2	Granite	52.2	Gnss1	Gneiss	33.4, 39.4(//)	Lim2	2690	38.47
gnt1-3	Granite	56.3	gnss2	Gneiss	32.3	Lim3	2630	56.91
lim2-1	Limestone	45.9	gnt1-1	Granite	50.3	Mb1	2660	27.85
lim3-1	Limestone	45.1	gnt1-2	Granite	44.9	Mb2	2700	49.82
mb1-2	Marble	25.8	Gnt1-3	granite	49.6	Mb3	2680	29.26
mb3-1	Marble	32.0	gnt2	Granite	58.2	Mb4	2510	43.78
mb4	Marble	41.8	Lime1-1	limestone	0	Rhy1	2340	31.09
rhy1-1	Rhyolite	48.1	lime2-1	Limestone	28.7	Scht1	2610	31.62
Scht1-1	Schist	49.7	lime2-2	Limestone	32.7	Scht2	2530	15.75
Scht1-2	Schist	45.7	lime2-3	Limestone	32.8	Snd1	2260	23.21
snd1-1	Sandstone	32.8	lime3-1	Limestone	34.9	Snd2	2440	27.47
snd1-2	Sandstone	37.1	Lime3-2	Limestone	32.9	Snd3-1	2040	15.77
Snd2-2	Sandstone	46.6	mb2-1	Marble	31.9	Snd3-2	2060	18.53
snd3	Sandstone	27.3	mb2-2	Marble	29.7	Sye1	2430	33.12
steel		43.9	mb3-1	Marble	26.6	Syep1	2600	34.49
Sye1-1	Syenite	44.0	mb3-2	Marble	30.2	Tra1	2510	22.38
Syep1	Syenite-porphyry	44.6	mb4	Marble	36.3			
tra1	Trachyte	47.9	rhyo1-1	Rhyolite	40.3			
			rhyo1-2	Rhyolite	42.0			
			scht1-1	Schist	33.4,40.5(//), 23.9(⊥)			
			scht1-2	Schist	32.0,37.5(//), 21.3(⊥)			
			snd1-1	sandstone	36.9			
			snd1-2	Sandstone	37.5			
			snd2-1	Sandstone	34.4			
			snd2-2	Sandstone	45.3			
			snd3-1	Sandstone	24.3			
			snd3-2	Sandstone	21.4			
			Snd3-3	Sandstone	24.6			
			Snd3-4	Sandstone	31.9			
			steel	d=4.6cm	44.4			
			Steel1	d=3.5cm	50.8			
			Steel2	d=5.0cm	49.6			
			sye1-1	Syenite	40.6			
			sye1-2	Syenite	36.9			
			tra1-2	Trachyte	48.0			

Notes: 1. The first number in the label refers to rock type, the second refers to number of sample, slab and ball.

2. //, ⊥: Measurements of Schmidt numbers parallel and perpendicular to foliation.

The mean Schmidt numbers of rock slabs and rock balls are shown in table 3-2. Measurement details are shown in Appendix A.

The values of the Schmidt number are affected by rock type, test direction, thickness and clamping conditions of rock slab. Rock slabs and balls made of the same rock specimen can have quite different values of Schmidt number. Generally igneous rocks have greater Schmidt numbers (with granite and basalt having the greatest value of N), while weak sedimentary rocks (such as sandstone and limestone) have smaller values of Schmidt number. For rocks with foliation (e.g. schist and gneiss), the values of Schmidt number are larger when the direction of the plunger is parallel to the foliation and smaller when the plunger is perpendicular to the foliation. Thicker slabs give a greater value of Schmidt number than thinner ones. When the contact between the slab and the concrete deck is not solid due to unsatisfactory clamping, the measured Schmidt number is smaller.

3.2.3 Other Properties

In order to study the relationship between the coefficient of restitution and other rock properties, cylindrical and cubic specimens were made from the remaining rock samples to measure the dynamic modulus of elasticity and density of rocks. Due to the limited samples, only 6 cylindrical specimens with the ISRM suggested dimensions (length 130 mm, diameter 50 mm) were made, and others are cubes with different size. Dynamic modulus of elasticity was obtained from the seismic transmission test. Samples for test are under natural moisture content, which is the condition of the rocks for laboratory impact tests. The travel times of compression and shear waves were measured using a seismic analyser, with which the velocities of both compression and shear waves were obtained, and then dynamic modulus of elasticity was calculated (Appendix A), which are tabulated in table 3-2. The value of the dynamic modulus of elasticity is the greatest for basalt (81.29 GPa) and smallest for the Oamaru limestone (5 GPa). However, the values of some limestone (56.91 for lim3-1) and marble (49.82 for mb2) are greater than that of granite (40.41). These unusual data are probably

caused by the limited samples, unsatisfactory sample dimensions and variations among rock materials.

3.3 Bouncing test for obtaining the coefficient of restitution

3.3.1 Test set-up

The bouncing test was carried out at Lincoln University with the prepared rock slabs and spheres. A concrete deck of dimension 460x260x100 mm was used to clamp the rock slabs, and a steel-supporting frame was used to set the slope angle of the deck (figure3-4). The spheres are released from a height of 1 m by a grabbing releaser (figure3-5), the bottom of which is controlled by springs and plug which minimize rotation of the falling rock at release. A high-speed camera (HSC250x2 of JCLab, able to take pictures of 200 frames / second) and a video recorder (Panasonic AG5700) were used to record the bouncing tests (figure3-5). Surveying rods were used as a reference system for measuring rebound height and distance.

3.3.2 Normal bounce

The bouncing tests were carried out with the slabs set to level. The test was done for a combination of a particular slab and a rock sphere. The sphere was bounced five times and the mean value of the restitution coefficient was calculated for each test. Generally a rock slab was tested once with a sphere from the same sample. For some rock slabs (e.g. gnt1-2, gnt1-3, syep1-1, schst1-1) that are not easy to damage, different rock spheres were used to bounce on the same slab to test the effect of the property of rock spheres on the coefficient of restitution.

In the previous chapter it was known that the coefficient of restitution is affected by the properties of both the rock slope and the falling rocks. From the bouncing tests using different spheres and slabs, it is possible to study the correlations between the coefficient of restitution and the properties of rock slabs, and between the coefficient of restitution and the properties of rock spheres. Although the slope and the falling rocks are often of the same rock type in the field, it is

necessary to consider the rock slab and rock sphere separately in the laboratory tests so that careful studies on the correlation for the coefficient of restitution can be carried out.

3.3.3 Inclined bounce

The angles of the concrete deck were set to 10°, 20°, 45° from the horizontal (actual angles for each slab may be slightly different as shown in table 3-3 due to the variation in thickness among a slab). For each angle, different combinations of slabs and spheres were tested. Generally one slab was tested once with one sphere from the same sample due to the limited number of specimens. Tests of different spheres on the same slab have then been carried out on the schist slab (scht1-1) that had not been not broken after the previous tests. No more such tests were done because of the limited samples and because a lot of tests with different spheres on the same slabs have been carried out in the normal bouncing tests. Figure 3-6 is a digitized picture from the video record showing the process of an inclined bounce.

The number of tests was limited due to the breakage of rock balls and slabs, but the overall test was rather successful with a large quantity of data (totally 138 sets) obtained. Breakage often occurred to rocks with low strength (e.g. marbles, sandstone and limestone) and thin slabs. The schist slab which was thicker (5 cm) than other slabs remained undamaged after all the bouncing tests. The tests would have been more successful if thicker slabs had been prepared. Another cause of slab breakage was unsatisfactory clamping, when the contact between the slab and the concrete deck was not totally solid at the impact point. Rock spheres of higher strength such as granite and basalt remained undamaged after all bouncing tests. When a slab or a sphere was broken, a spare one was used to complete the test, which might have caused some variations in the test result. When the spare slabs or spheres were also damaged, the test stopped. No more slabs and spheres have been made during the tests due to the limited samples, and the data obtained were considered enough to conduct necessary analysis.

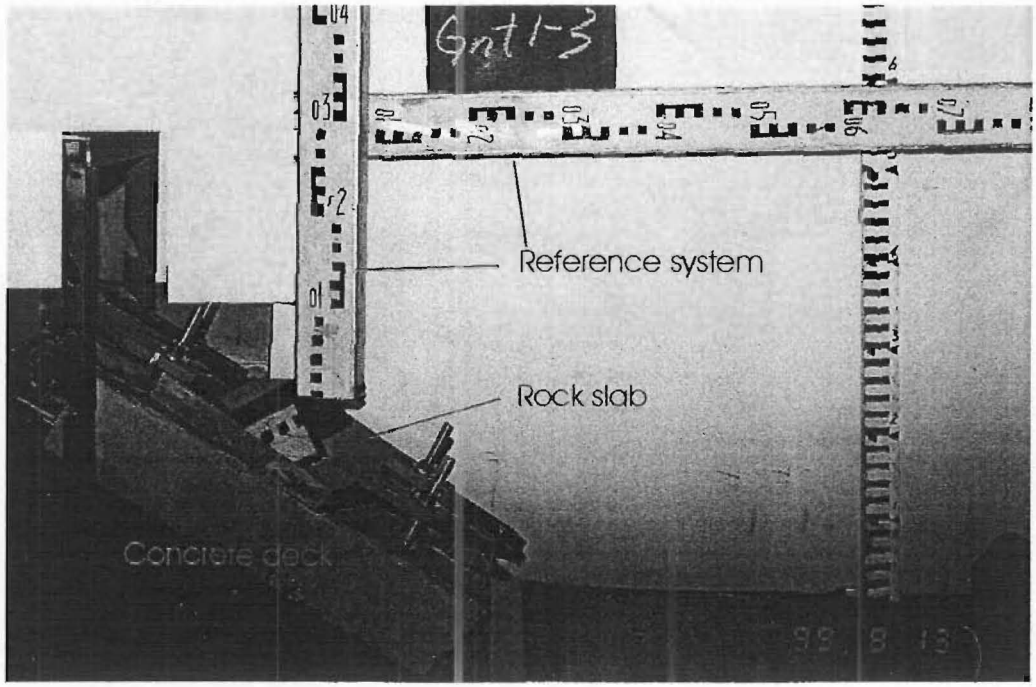

Figure 3-4: Rockfall laboratory test set up

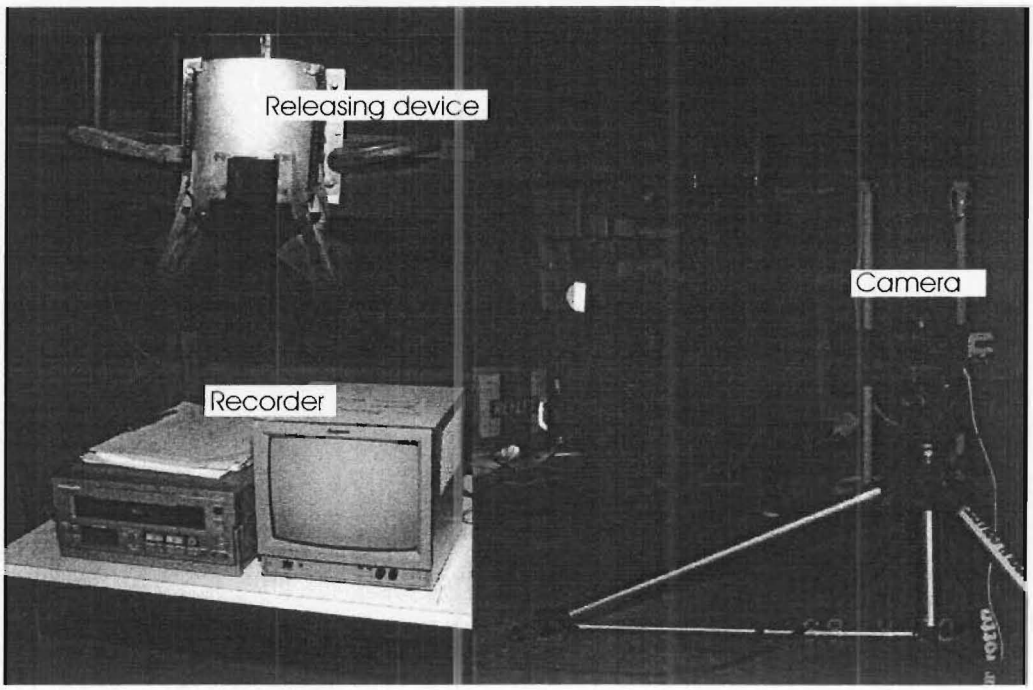

Figure 3-5: Rockfall laboratory test set up—camera, recorder and releasing device

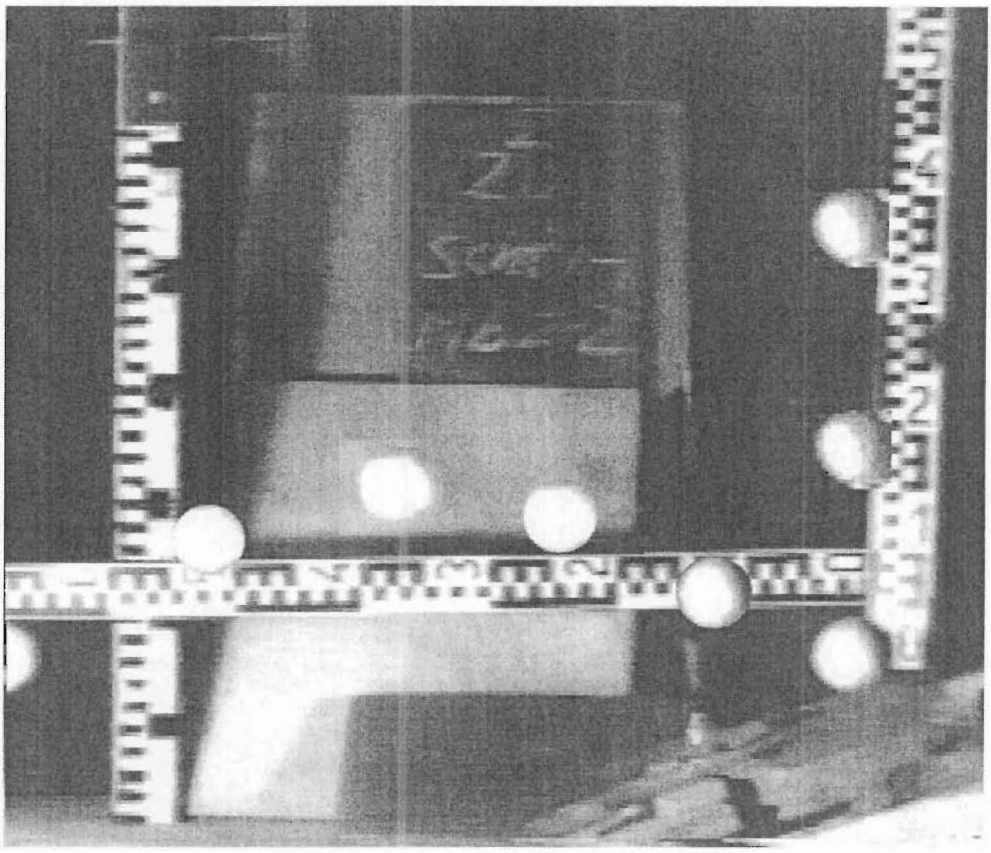

Figure 3-6: Digitised video picture showing the process of an inclined bounce in laboratory test with marble rock ball impacting on schist slab.

3.3.4 Image processing

The videotapes recording the bouncing test were processed with the high-speed recorder. For the normal bounce, rebound height (h) was measured from the video image and the reference rod used in the test (play the video frame by frame until the sphere reaches its apex, read the height from the reference rod). For the inclined bounce test, bouncing height, lateral distance and the time between bounces (or between point of impact and the apex of rebound trajectory) were measured (play the video tape frame by frame until the sphere reaches its apex or the floor for downward rebound, read the height and distance from the reference system, the number of frames gives the time) and recorded for later calculations. Figure 3-6 shows the trajectory of a sphere from the video tape and the parameter (bounce height and distance) relationship is shown in figure 3-7.

3.3.5 Calculation of restitution coefficient

For normal bounce, the coefficient of restitution was calculated through the dropping and rebound height according to:

$$R_n = \sqrt{\frac{h}{H}}$$

Where H – Height of drop (m)
h – height of rebound (m)

For inclined bouncing tests both normal and tangential coefficients of restitution were calculated from the measured parameters according to the following equations (the relationship of parameters is shown in figure 3-7):

$$Rn = \frac{Vrn}{Vin} \qquad Rt = \frac{Vrt}{Vit}$$

Where:

Vin = Vi cosA

Vit = Vi sinA

Vrn = Vrx sinA + Vry cosA (upward bounce),

or, Vrn = Vrx sinA – Vry cosA (downward bounce)

Vrt = Vrx cosA – Vry sinA (upward bounce),

or, Vrt = Vrx cosA + Vry sinA (downward bounce)

Vrx = S / t

Vry = $(h + 0.5g\ t^2)/t$ (upward bounce),

or, Vry = $(h - 0.5g\ t^2)/t$ (downward bounce)

Meanings of parameters:

Rn – Normal coefficient of restitution

Rt – Tangential coefficient of restitution

Vrn, Vrt – Normal and tangential components of rebound velocity

Vin, Vit – Normal and tangential components of impact velocity

Vix, Vrx – Horizontal components of impact and rebound velocity

Viy, Vry – Vertical components of impact and rebound velocity

S – Horizontal distance

t – Time interval(determined by counting frames between bounces)

A – Slab angle

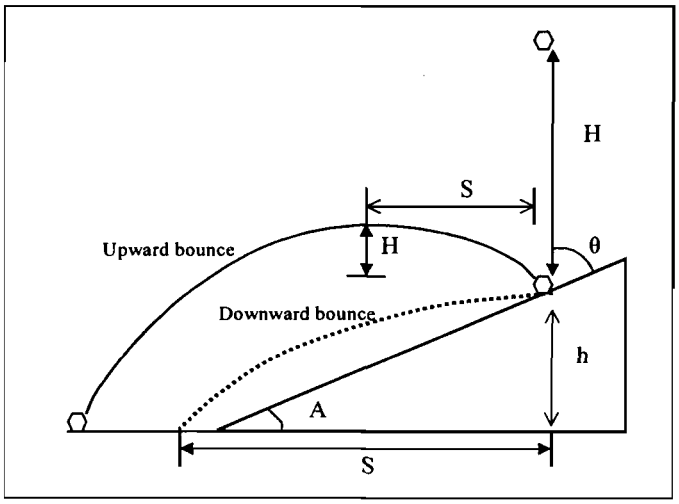

Figure 3-7: Inclined bouncing set-up and parameter relationship

The coefficient of restitution calculation details are presented in Appendix B. Table 3-3 shows the coefficients of restitution calculation results for impacts of each slabs with spheres from the same sample, data for slabs with different spheres are not presented here and are shown in Appendix B. The Schmidt numbers of slabs and spheres are also included in table 3 so that the relationship between the coefficient of restitution and the Schmidt number can be seen.

Table 3-3 shows that the normal coefficient of restitution (Rn) ranges from 0.18 (limestone) to 0.72 (granite), generally rocks with larger Schmidt numbers have higher values of Rn, indicating a possible correlation between Rn and the Schmidt number of rocks. However, some unusual data were found, for example, Rn for marble (mb3-1, Schmidt number N1 = 32,) is 0.66, which is greater than that of basalt (0.53) whose Schmidt number is much larger (N1 = 51). That is probably caused by variations of rock materials, shape effect and unsatisfactory clamping conditions.

Although the rock balls were made in quasi-spherical shapes, the shapes of different rock balls were different, some of them were close to a perfect sphere,

closer to a sphere bounced higher, resulting in larger values of Rn. The values of Rn obtained in this test are slightly smaller than that by Rayudu (1997, see chapter 2), possibly because of the clamping conditions (rock slabs were clamped on the concrete floor in Rayudu's test, which is more solid than the concrete deck). The values of Rn for steel on steel impact are smaller than those of some rocks (e.g. basalt and granite) whose Schmidt numbers are higher, indicating that the Schmidt number is a better parameter than compressive strength or the modulus of elasticity in the analysis of the coefficient of restitution.

The values of the tangential coefficient of restitution (Rt) range from 0.36 (mb3-1) to 0.88 (mb4), and are generally greater than 0.5. Rt seems to be independent of the Schmidt number, indicating that the Schmidt number is not a factor affecting the value of Rt. The Schmidt hammer test measures the impact property in the normal direction with the plunger normal to the surface, while the impact property in the tangential direction is affected mainly by friction. It was observed from the tests that the shape of rock sphere plays an important role in the rebound trajectory and thus the tangential coefficient of restitution. The trajectory of a perfect sphere will follow a theoretical parabola as assumed in the calculation of the coefficient of restitution. However when an irregular shape is involved, rotation of the rock sphere takes place and the resulting trajectory will be different from the theoretical parabola assumed in the calculation of the coefficient of restitution (figure 3-7), which will affect the values of the calculated coefficients of restitution (Rn and Rt) significantly.

3.4 Relationship between the coefficient of restitution and rock properties

In order to examine the effects of impact conditions on the coefficient of restitution, the relationships between the calculated coefficient of restitution and rock properties (Schmidt number, density, dynamic modulus of elasticity) and slope angle have been studied.

Table 3-3: Selected coefficient of restitution calculation results

Slab Label*	Slab Angle**	Ball Label	Slab N1	Ball N2	Rn	Rt
gnt1-1	0	gnt1-1	39.9	50.3	0.34	
bast1-1	0	bast1-1	51	41	0.49	
dio1-1	0	dio1-1	38.7	40.8	0.5	
scht1-1	0	scht1-1	49.7	40.5	0.58	
gnss1-1	0	gnss1-1	41.2	39.4	0.5	
mb1-2	0	mb2-1	25.8	31.9	0.24	
snd1-1	0	snd1-1	32.8	36.86	0.29	
mb4	0	mb4	41.8	36.25	0.42	
lim3-1	0	lim3-1	45.1	34.9	0.54	
snd2-2	0	snd2-2	46.6	45.3	0.49	
gnt1-2	0	gnt1-2	52.2	44.9	0.51	
schst1-1	0	schst1-2	49.7	37.5	0.57	
gnt1-3	0	gnt1-3	56.3	49.6	0.67	
mb1-2	0	mb2-1	25.8	31.9	0.24	
steel	0	steel	43.9	45	0.387	
lim3-2	10	lim3-2	45.1	32.9	0.18	0.44
mb4	10	mb4	41.8	36.3	0.35	0.54
scht1-1	10	scht1-2	49.7	37.5	0.56	0.61
snd3-1	10	snd3-3	27.3	24.6	0.5	0.58
bast1-1	12	bast1-1	51	41	0.48	0.76
dio1-1	12	dio1-1	38.7	40.8	0.25	0.67
gnt1-3	12	gnt1-3	56.3	49.6	0.67	0.71
mb1-2	12	mb2-2	25.8	29.7	0.29	0.46
mb3-1	12	mb3-2	32	30.2	0.39	0.49
snd1-2	12	snd1-2	37.1	37.5	0.42	0.42
lim1-1	20	lim1-1	0	0	0.25	0.6
scht1-1	20	scht1-2	49.7	37.5	0.6	0.75
gnt1-3	22	gnt1-3	56.3	49.6	0.72	0.6
mb1-2	22	mb2-2	25.8	29.7	0.32	0.67
snd1-2	22	snd1-2	37.1	37.5	0.43	0.66
bast1-1	23	bast1-1	51	41	0.45	0.58
dio1-01	23	dio1-1	38.7	40.8	0.27	0.49
mb3-1	23	mb3-2	32	30.2	0.39	0.36
mb4	23	mb4	41.8	36.3	0.3	0.48
snd3-1	23	snd3-4	27.3	31.9	0.37	0.67
bast1-1	46	bast1-3	51	41	0.53	0.61
dio1-1	46	dio1-1	38.7	40.8	0.37	0.67
gnt1-3	46	gnt1-3	56.3	49.6	0.68	0.69
lim1-1	46	lim1-1	0	0	0.4	0.53
mb1-2	46	mb2-2	25.8	29.7	0.53	0.69
mb4	46	mb4	41.8	36.3	0.38	0.88
snd1-2	46	snd1-2	37.1	37.5	0.58	0.59
mb3-1	48	mb3-2	32	30.2	0.66	0.69
snd3-1	48	snd3-3	27.3	24.6	0.46	0.53
steel	10	steel	43.9	44.4	0.42	0.64
steel	20	Steel	43.9	44.4	0.31	0.72
steel	46	steel	43.9	44.4	0.42	0.65

* Rock type for each label refer to table 3-2. ** Angle to horizontal.

3.4.1 Properties of rock slabs

3.4.1.1 Schmidt hammer number

The coefficient of restitution obtained from impact of the same ball on different slabs have been plotted against the Schmidt number of the slabs (N1) (figure 3-8), which shows that a linear correlation exists between the normal coefficient of restitution (Rn) and the Schmidt number of the slabs (N1) for most of the situations. Generally a good correlation (R^2 greater than 0.6) is found for rock balls with higher values of Schmidt number (such as granite, basalt and steel ball), while for rock balls with low value of Schmidt number (such as marble and limestone) the correlation is not as good as the former (R^2 generally less than 0.5). That is possibly because of the anisotropy of the sedimentary and metamorphic rocks, and because that other attribute factors such as shape effect become obvious when the Schmidt number is small. As the strength of rocks decreases, more destructive deformation occurs, which is affected by variations of rock materials such as grain bounding and defect, and thus the results of the coefficient of restitution are more varied. Irregular shape of rock balls causes the balls to bounce in directions other than the normal or theoretical direction (inclined slab) as achieved by a perfect sphere (such as a steel ball) due to the momentum generated at impact, as explained in the previous section.

For the tangential coefficient of restitution (Rt), a poor correlation with the Schmidt number (N1) was found, indicating that the Schmidt number of rocks is not a factor affecting the restitution behaviour of impact in the tangential direction and could not be used to determine the tangential coefficient of restitution of rocks. Theoretically the restitution behaviour in the normal direction is mainly affected by the mechanical properties of the material such as the Schmidt number, while that in the tangential direction is affected by friction on the contact surface (see chapter 2), which is confirmed by the above test results. The above analysis shows that the Schmidt number of rock slopes (N1) could only be used to determine the normal coefficient of restitution.

Figure 3-8 shows some of the plots of the coefficients of restitution (Rn and Rt) against the Schmidt number of rock slabs (N1) which were obtained with the same ball impacting on different slabs. Plots (a) to (d) are plots for normal bounces with granite (gnt1, gnt2), sandstone (snd1) and steel balls bouncing on different slabs, showing a fairly good correlation between Rn and N1 (R^2 from 0.62 to 0.81). Plot (e) shows a poor correlation between Rn and N1 for normal impact with a marble ball (mb2-1) bouncing on different slabs, with R^2 being 0.47. Plot (f) shows the relationship between the normal and tangential coefficients of restitution (Rn and Rt) and N1 for inclined bounces (slope angle 44°) with a granite ball (gnt1-3) bouncing on different slabs, where the correlation between Rn and N1 is good (R^2 0.95) while the correlation between Rt and N1 is poor (R^2 0.32)

3.4.1.2 Slope angle

The results of the restitution coefficients of different slope angles show that both the normal and tangential coefficient of restitution increases slightly with slope angle. Figure 3-9 is a plot of the average values of restitution coefficient for each slope angle (data sets for each angle are the same, so the average values are comparable between different angles) against slope angle, showing a good correlation (R^2 0.79 for Rn and 0.91 for Rt). That is similar to the result of Chau (1999) but different from the result of Wu (1985) where the mean normal coefficient of restitution decreases rapidly with impact angle θ (90° - A) while the tangential coefficient increases slightly with impact angle (see Chapter 2). Wu's result is doubted because Rn changes too sharply with the impact angle.

3.4.2 Properties of rock balls

In order to examine the effect of rock ball properties on the coefficient of restitution, bouncing tests of different rock balls impacting on the same rock slab have been carried out, and the results studied. In order to compare with Rayudu's (1997) test, the difference between rock and steel balls have been tested and studied.

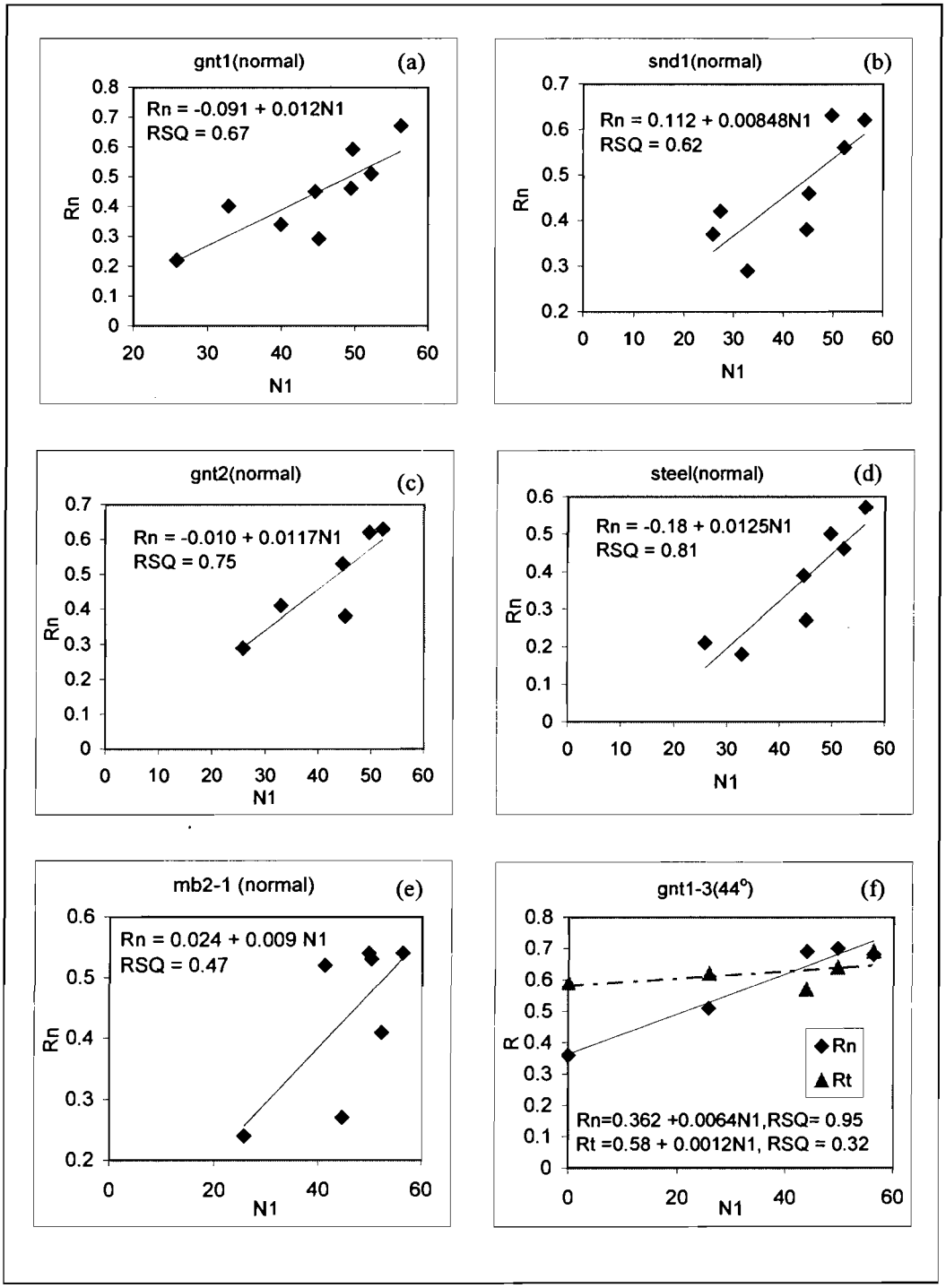

Figure 3-8: Plots of restitution coefficient(R) against the Schmidt number of slabs (N1), showing a good correlation for the normal coefficient (Rn) and a poor correlation for the tangential coefficient (Rt).

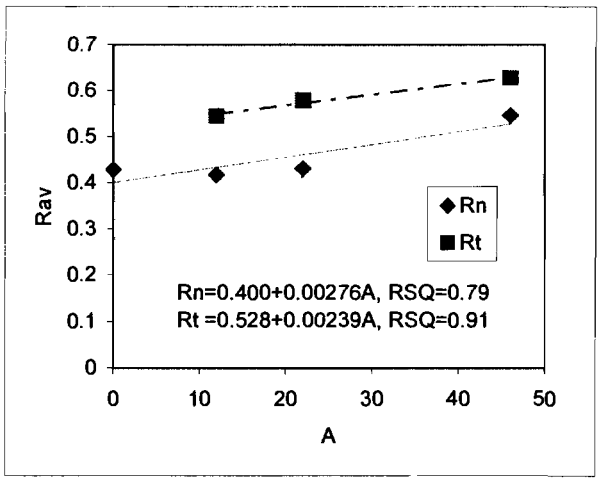

Figure 3-9: Plot showing the correlation between the average restitution coefficient (Rav) and slope angle (A).

3.4.2.1 Schmidt Hammer Number

The coefficients of restitution for impact of different balls impacting on the same slabs have been plotted against the Schmidt number of the rock balls (N2) (figure 3-10). The results show that a linear correlation exists between the normal coefficient of restitution (Rn) and the Schmidt number of rock balls (N2) for most of the situations (similar to the situation of rock slabs). For rock slabs with a higher value of Schmidt number (such as granite, syenite porphyry and steel), a better correlation is found with R^2 greater than 0.6, while for rock slabs with a low Schmidt number (such as marble and sandstone) correlation is not as good as the former (R^2 less than 0.5). That is probably because of the anisotropy of weak sedimentary and metamorphic rocks, and because that the effect of other factors such as shape on the coefficient of restitution become more significant when the Schmidt number is small, as discussed in the previous section. Density of rocks could affect the coefficient of restitution which will be discussed in 3.4.2.2. Unsatisfactory clamping conditions and variations during tests have also contributed to the scattering of data. The above results show that the Schmidt number of the falling rock (N2) is also a major factor affecting the normal coefficient of restitution (Rn) and could be used to determine the normal coefficient of restitution for rockfall analysis. The slopes of the Rn-N2 plots are generally flatter than those of the Rn-N1 plots as shown in figure 3-8 and figure 3-10, indicating that the effect of the properties of the falling rock is less significant than that of the slope properties.

For the tangential coefficient of restitution (Rt), such a correlation does not exist, indicating that the Schmidt number is not a major factor affecting the impact behaviour in the tangential direction as discussed in the previous section.

Figure 3-10 shows some of the plots of the coefficients of restitution (Rn, Rt) against the Schmidt numbers of rock balls (N2), including that for normal bounce on a granite slab (gnt1-3) (b), and those for normal and inclined bounces on schist slab (schst1-1) (a, c and d). The correlation coefficient (R^2) ranges from 0.749 to 0.858 for Rn (a, b and c), while that for Rt (d) is only 0.274. The value of the coefficient of restitution for a steel ball are plotted separately in the plots to show the difference between the steel and rock balls, which will be discussed in the following section.

3.4.2.2. Effect of density and the difference between rock and steel balls

Rayudu (1997) suggested that the restitution coefficient obtained from steel on rock impact should be greater that that from rock on rock impact, because steel is much more elastic than rocks. However, it is not the case in this test where the coefficients of restitution from steel on rock impacts are slightly lower than that of rock on rock impacts or have no apparent difference with the latter (figure3-10).

Figure 3-11 shows the results of bouncing tests on a steel plate. A linear correlation exists between the normal coefficient of restitution (Rn) and the Schmidt number of both rock balls and steel balls (N2). The normal restitution coefficients obtained by steel balls are lower than that by rock balls, especially in the case of normal impact, the differences are from 0.12 to 0.19.

An attempt to relate the differences between the coefficients of restitution obtained by steel and rock balls to the density of the dropping balls is quite successful, regression analysis of Rn with the Schmidt number (N2) and density (d) of the impacting balls gives a satisfactory correlation coefficient, for example, values of R^2 for the two situations shown in figure 3-11 (Rn with two parameters: N2 and d) are 0.92(normal bounce) and 0.85 (slope angle 10°) respectively, while

values of R^2 for Rn with N2 only are 0.29 and 0.44 (R^2 for rock balls only are 0.88 and 0.80 respectively). This result agrees with Thornton's (1997) conclusion that the coefficient of restitution decreases with the impact velocity and density. It is the density rather than mass that causes the difference in the restitution coefficient because density affects the contact area at impact, balls with greater density will have a smaller contact area at impact than those with the same mass but smaller density. The contact area at impact then affects the impacting stress. A greater stress causes a greater plastic deformation (indentation). Observations during testing have confirmed that conclusion.

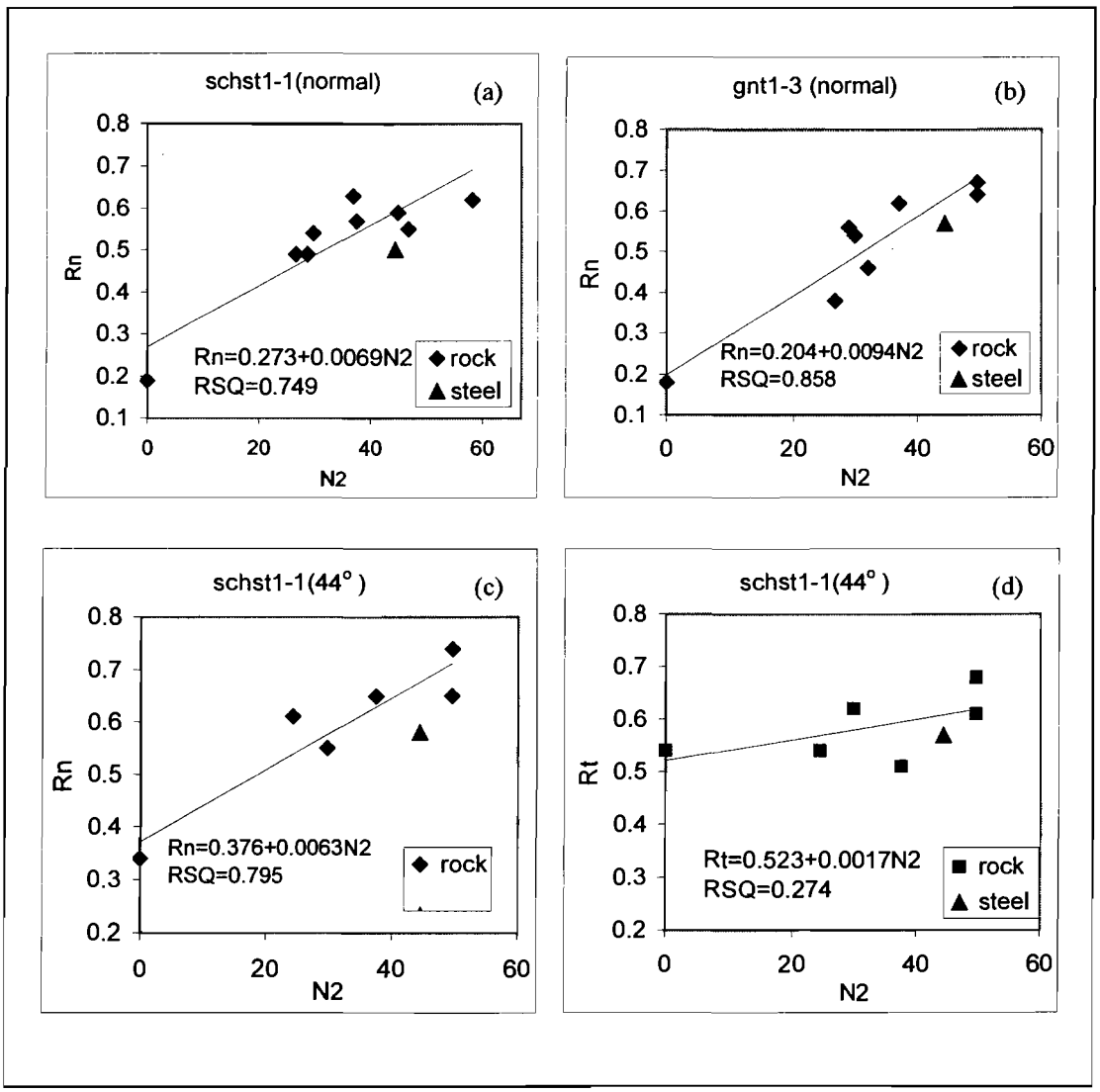

Figure 3-10: Plots showing the relationship between coefficient of restitution (Rn, Rt) and Schmidt number of dropping balls (N2), also showing the difference between rock and steel balls, normal and slope angle 44°.

The effects of density in the situations of impacts on rock slabs are not obvious. The difference in coefficient of restitution between impacts of steel on rock and rock on rock is not significant (as shown in figure 3-10). Marks of indentation on the steel plate were more clearly observed during tests than those on some hard rock slabs such as granite and basalt.

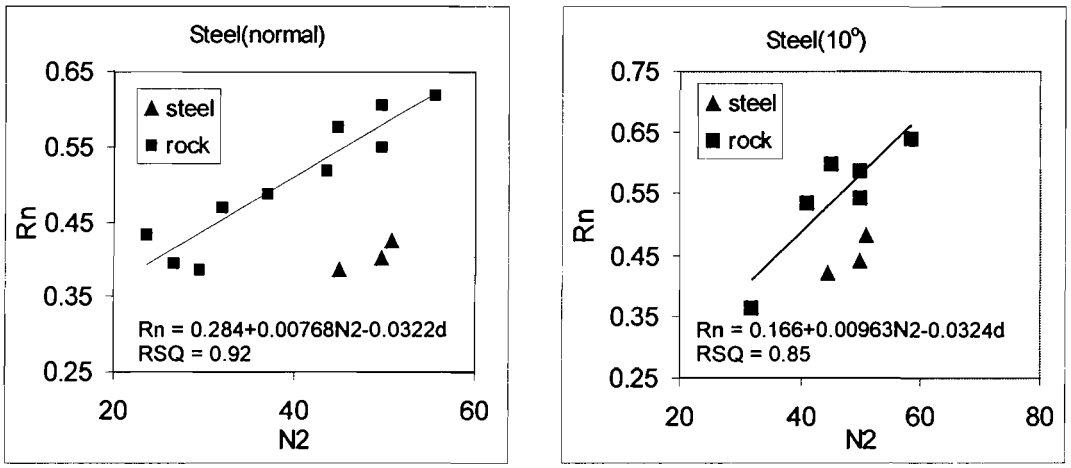

Figure 3-11: Plots of rock on steel and steel on steel bouncing tests, showing the difference between restitution coefficients of rock and steel balls and the effect of density (d) on Rn (trend lines are for rock balls only).

3.4.2.3. Dynamic modulus of elasticity

Theoretically, rocks that are more elastic should give a higher coefficient of restitution. An attempt has been made to relate the coefficient of restitution to the dynamic modulus of elasticity of the impacting balls, but the result is not good. For bounces with different balls impacting on the same slabs, correlation coefficients (R^2) between Rn and Edyn. are generally less than 0.2. Regression analysis for the normal coefficient of restitution (Rn) with the dynamic modulus of elasticity (Edyn.) in substitution of the Schmidt number of rock balls (N2) gives a poor correlation (R^2 0.38), while R^2 for Rn with the Schmidt numbers (N1, N2) for the same data set (90 data from normal bounce) is 0.66. That may indicate that the dynamic modulus of elasticity, which is calculated assuming a homogeneous and elastic medium, doesn't account for the variations among the rock materials,

and is not a proper parameter for the determination of the coefficient of restitution.

It should be noted that samples for the measurement of the elasticity modulus are not exactly the same as the rock balls (from different parts of the same rock specimen), and some samples are not of the standard dimension as suggested by ISRM due to the limited samples, therefore the reliability of the results is affected. That might have contributed to the poor correlation between the coefficient of restitution and the dynamic modulus of elasticity. Because of the variations of rock properties, different rock specimens are needed and different directions should be tested for the same rock to obtain a representative value of the dynamic modulus of elasticity, but such tests have not been done in this project because of the limited resource and because that the Schmidt hammer test is obviously a preferred method in the determination of the coefficient of restitution.

3.5 Empirical methods to determine coefficient of restitution

3.5.1 Empirical equation for normal coefficient

According to the above discussions, there is a linear correlation between the normal coefficient of restitution and the Schmidt numbers of rock slabs (N1) and rock balls (N2), and the slope angle (A). It is reasonable to try to establish a comprehensive empirical correlation between coefficient of restitution and the three attribute factors (N1, N2 and A). Regression analysis of the normal coefficient of restitution (Rn) with two factors (N1 and N2) for normal bounce, and three factors (N1, N2, and A) for inclined bounce, has been done. The initial correlation coefficients were not high (R^2 0.52-0.65), possibly because of some abnormal bounces caused by irregular shapes and/or unsatisfactory clamping conditions of rock slabs. Poor correlations also occur in cases of rock balls with low Schmidt number values such as the Oamaru limestone (lime1-1, N = 0). After studying all data and their test conditions, some abnormal data were removed and a better correlation was achieved. The regression analysis results are summarized in table 3-4.

Table 3-4: Regression analysis results

Data group	Equation	R^2
Normal bounce (65 data)	Rn = -0.138 + 0.00999N1 + 0.00368N2	0.76
Inclined bounce (29 data)	Rn = -0.158 + 0.00741N1 + 0.00314N2 + 0.00409A	0.84
Combined (90 data)	Rn = -0.110 + 0.00919N1 + 0.00392N2 + 0.00358A	0.82

Rn – normal coefficient of restitution, N1/N2 – Schmidt numbers of rock slab/rock ball, A – slope angle.

It can be seen from the equations that the Schmidt number of the slope materials (N1) is the primary factor affecting the coefficient of restitution (Rn), with its slope value more than twice as those of N2 and A, while the slope values of N2 and A are about the same. The result suggests that properties of slope materials is the most important factor in the determination of the coefficient of restitution, while the properties of the falling rock and impact angle are less important.

With the equations in table 3-4 it is possible to calculate the normal coefficient of restitution by measuring the Schmidt number of rocks and the slope angle. Since those factors are easy to measure in the field, this is a convenient approach to determine the coefficient of restitution. However, as the equations are established on laboratory tests under simplified conditions, it has to be verified for more practical conditions so that it can be applied in practical rockfall analysis.

3.5.2 Analysis of the tangential coefficient

Regression analysis on the tangential coefficient of restitution with the above three factors has also been done using the data from the inclined bouncing test, which shows that the tangential coefficient of restitution (Rt) does not have an apparent correlation with the above-mentioned three factors. The correlation coefficient (R^2) between Rt and the three factors (N1, N2 and A) for the data group of inclined bounce is only 0.17. This suggests that the tangential coefficient of restitution cannot be determined by the above approach as the normal coefficient of restitution.

In order to find an easy means to determine the tangential coefficient of restitution, the relationship between the tangential coefficient and normal

coefficient has been studied, the rolling friction coefficient for some rock samples has been measured, and its relationship with the tangential coefficient examined. Coefficient of restitution obtained with different rock spheres bouncing on different rock slabs from the laboratory tests have been used to study the relationship between Rn and Rt. The tangential coefficient Rt is plotted against the normal coefficient Rn (figure 3-12), but the plot shows that there is no correlation between the two coefficients (R^2 = 0.084). It was originally considered that the impact behaviour in the normal direction could affect that in the tangential direction, and the impact behaviour in the normal direction can be measured by the normal coefficient of restitution. In fact both elastic and plastic deformation contribute to the resistance to the movement in the tangential direction, while the normal coefficient of restitution is only a measure of the elastic deformation at impact. Furthermore, the friction between the impacting bodies is the predominant factor determining the tangential resistance. Therefore the normal coefficient of restitution cannot be used to determine the tangential coefficient of restitution.

The rolling friction coefficient is the tangent of the maximum inclination of a plane on which an initially stationary boulder just remains stationary (Lee & Elliot, 1998). The values of the rolling friction coefficient (Rf) of different spheres and slabs have been measured by the above approach (table 3-5), which have then been used to plot against the tangential coefficient of restitution Rt (figure 3-12). No correlation is found between Rt and Rf (R^2 = 0.02). The measured rolling friction angles (the maximum inclination of rock slabs on which an initially stationary rock ball just remains stationary) for the slabs are very low (1° - 5°), and are more controlled by the shapes of balls than by surface roughness, with the smallest value of Rf being that of the steel ball which is a perfect sphere as a result. This result indicates that the rolling friction coefficient, which is a measure of resistance to rotation under static conditions, does not represent the friction at the impact surface under dynamic condition. It is actually a resistance to sliding rather than to rolling at the impact surface, but the friction coefficient (sliding) is difficult to measure with a rock sphere.

Theoretically the impact behaviour in the tangential direction is controlled by the friction between the impacting bodies, which is determined by the friction coefficient and normal stress at the contact surface. Normal stress can be determined by the normal impact velocity that is the same for impacts with the same slope angle in this test as balls are dropped from the same height. The friction coefficient under dynamic conditions is difficult to obtain and is beyond the scope of this project. An easy and practical method for determining the tangential coefficient of restitution has not been found in this study and needs to be solved by further researches.

Table 3-5: Coefficient of restitution and rolling friction coefficient (Rf)

Slab* Label	Slab Angle (degree)	Ball* Label	Rn	Rt	Friction Angle (degree)	Rf
bast1-1	46	bast1-1	0.53	0.61	4	0.070
gnt1-3	12	gnt1-3	0.67	0.71	3	0.052
mb1-2	46	gnt1-3	0.54	0.59	4	0.070
mb1-2	12	mb2-2	0.29	0.46	4	0.070
mb1-2	46	mb2-2	0.53	0.69	4	0.070
scht1-1	44	bast1-3	0.74	0.61	3	0.052
scht1-1	44	gnt1-3	0.65	0.68	3	0.052
scht1-1	44	lim1-1	0.34	0.54	8	0.141
scht1-1	20	mb2-2	0.56	0.67	4	0.070
scht1-1	44	sand3-1	0.61	0.54	5	0.087
scht1-1	20	scht2-2	0.60	0.75	5	0.087
scht1-1	44	steel	0.58	0.57	1	0.017
steel	10	bast1-1	0.53	0.72	3	0.052
steel	10	bast1-3	0.54	0.74	4	0.070
steel	10	gnt1-2	0.60	0.62	3	0.052
steel	10	gnt1-3	0.59	0.68	3	0.052
steel	10	gnt2	0.64	0.60	3	0.052
steel	10	mb2-1	0.36	0.75	4	0.070
steel	46	snd1-2	0.62	0.51	4	0.070
steel	10	steel	0.42	0.64	2	0.035
steel	10	steel-1	0.48	0.62	1	0.017

* Meanings of labels refer to table 3-2.

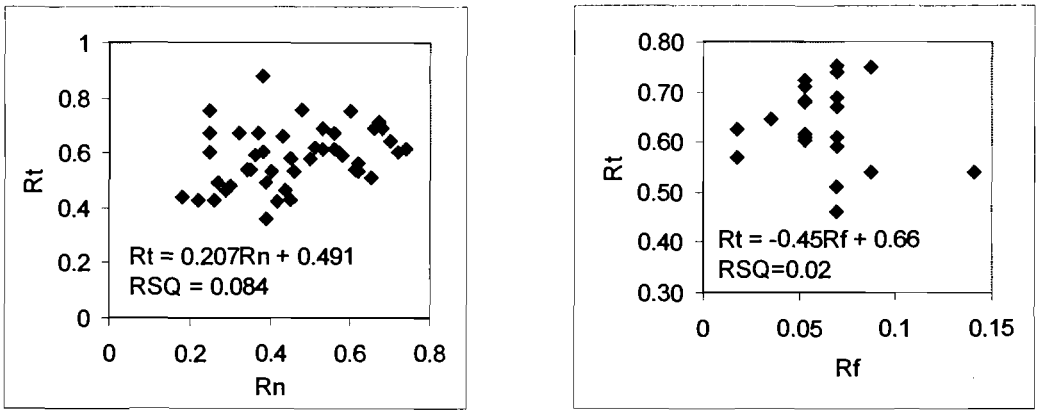

Figure 3-12: Plots of tangential coefficient of restitution (Rt) against normal coefficient of restitution (Rn) and rolling friction coefficient (Rf), both showing no correlation

3.6 Laboratory tests under practical conditions

As stated in the previous section, laboratory tests with fresh rock slabs and rock spheres to obtain the coefficient of restitution have shown a linear relationship between the coefficient of restitution and rock properties such as the Schmidt number of both rock slabs and dropping rocks, and the slope angle. It is now possible to determine the normal coefficient of restitution according to those rock parameters, but as this method is established under simplified conditions, calibration is needed for it to be applied in actual field conditions. Coefficients of restitution of rockfall on debris and soil slopes have to be determined for a complete rockfall analysis so that the coefficient of restitution for those slope materials can be determined according the test results in the following rockfall analysis. It was also planned to examine the effect of impact velocity on the value of the restitution coefficient, as the impact velocity is used as a scaling factor for the normal coefficient of restitution by some researchers (Pfeiffer and Bowen, 1989). For these purposes, laboratory tests with both rock spheres and rough rock pieces impacting on rough rock blocks (basalt, greywacke and limestone), beds of rock fragments, gravels, sands and loess soil have been carried out.

3.6.1 Test preparation

Three kinds of local rock samples have been collected for the tests: basalt from Banks Peninsula (figure 3-13), greywacke from Arthur's Pass and limestone from Porters Pass. These rocks are locally significant for rockfall hazards in the Canterbury region. Dimension of basalt block: 450x300x200mm, greywacke block: 400x200x150 mm, limestone block: 280x220x200 mm.

Two kinds of rock debris materials were prepared, one made mainly from limestone and basalts with diameter of 0.5 - 4 cm (angular), and the other of paving materials (angular limestone, diameter 0.5-2 cm); The gravels are from local sites with tabular shapes (dimension 1-6 x 1-6 x 0.3-1 cm), the sands are local coarse sands, and the soil in the test is loess from Port Hills. All the fragments, gravels, sands and soil were contained in a timber tray of dimension 300 x 600 x 100 mm, and the loess compacted with a timber rammer to make a compact bed.

To simulate the condition of a natural debris slope, fragments and paving materials were mixed (inter-layered) with soil and then compacted. Paving stones were inter-layered with soil and compacted in a galvanised iron box (50x50x20 cm) in a total of 5 layers laid and compacted with a timber rammer. Rock pieces used for dropping were basalt (tabular, cylindrical to cubic, 30-60x70-80x100-120 mm), greywacke (30-120 mm), and limestone (dimension 30-110mm); two rock balls (bast1-1, bast1-3) are also used in the tests to examine the shape effect.

Heights of dropping for rock blocks were: 0.6, 1.0, 1.5, 2.0, 2.5, 3.0 m, slope angle 0° and 40°, dropping height for beds of fragments, sands, gravels and soil was 1.5 m, slope angle 0° and 20°.

The Schmidt numbers of rocks have been measured before the bouncing tests which are listed in table 3-6, and measurement details are shown in Appendix B.

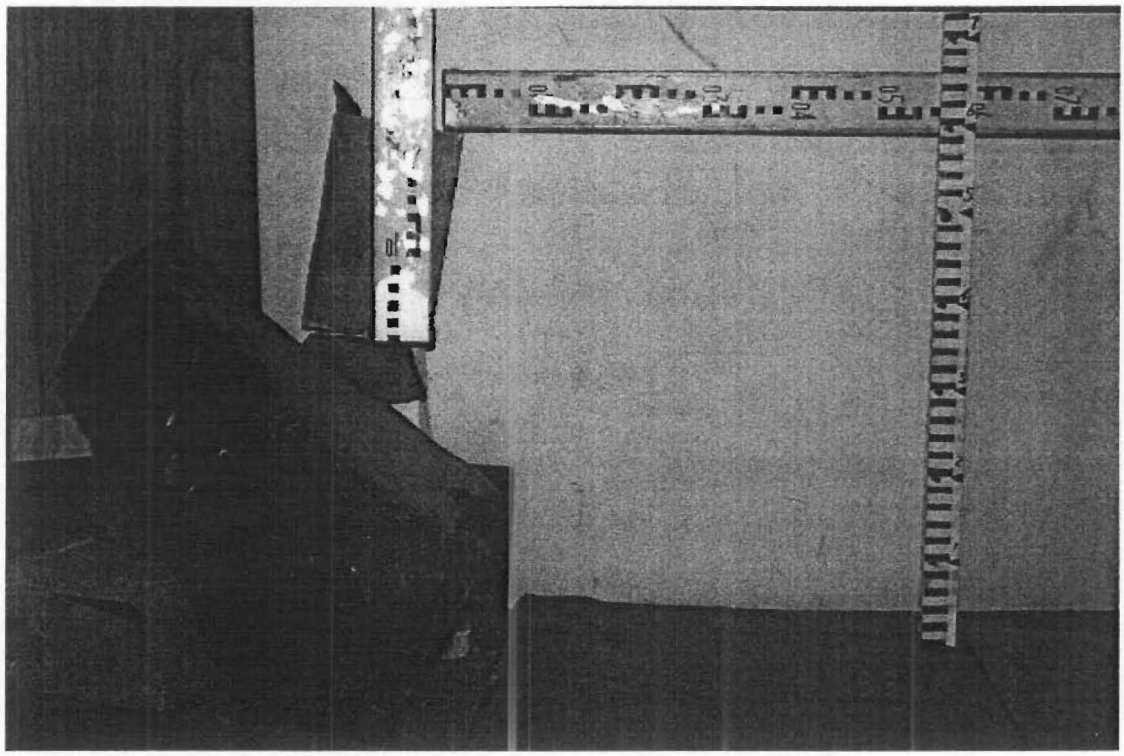

Figure 3-13: A basalt block (from Banks Peninsula) used in rockfall tests

3.6.2 Test results on rough rock blocks

3.6.2.1 Coefficient of restitution results and comparison with equation obtained values

The average values of the coefficient of restitution for different rocks bouncing on rock blocks are tabulated in table 3-6 (calculation details are shown in Appendix B). It is noted that the values of Rn of rock balls are much higher (about three times) than those of rough rock pieces. That is because of the shape effect of the falling rocks. A spherical rock bounces higher while an irregular shaped rock with sharp edges and corners will have crushing and rotation at impact and result in a lower bounce. The impact process of rough rock pieces is much more complicated than a rock sphere. Crushing of corners and edges, multipoint impacts, fast rotation and rotation direction change, sliding between contact surfaces before bouncing up were observed during the tests. All of these caused

energy dissipation and contributed to the smaller values of the restitution coefficient compared to those obtained by rock balls.

Table 3-6: Coefficient of restitution from test and equation

Slope		Falling rock		Slope angle	R test		R equation**
Label*	Mean N1	Label*	Mean N2	A (degree)	Rn	Rt	Req
limestone	42.2	bast1-1	41	0	0.484		0.43
basalt	53.9	bast1-3	49.6	0	0.818		0.58
basalt	53.9	bast1-3	49.6	40	0.83	0.538	0.72
grey	55.43	bast1-3	49.6	40	0.722	0.711	0.74
grey	55.43	bast1-3	49.6	0	0.735		0.60
basalt	53.9	bs	53.9	0	0.183		0.60
basalt	53.9	bs	53.9	40	0.29	0.731	0.74
grey	55.43	grey	55.43	40	0.255	0.824	0.76
grey	55.43	grey	55.43	0	0.184		0.62
limestone	42.2	lim	42.2	0	0.121		0.44
limestone	42.2	lim	42.2	40	0.21	0.621	0.59

*grey: greywacke, lim: limestone, bs: basalt, bast1-1, bast1-3: basalt rock balls.
**Req is calculated by the empirical equation shown in table 3-4 (Rn = -0.11 + 0.00919N1 +0.00392N2 + 0.00358A).

The values of the restitution coefficient were also calculated according to rock parameters by the empirical equations established in the previous section (table 3-4). The results are also tabulated in table 3-6 for comparison. Figure 3-14 is a plot of the coefficients of restitution from tests against those from calculation for both impacts with a basalt ball and with irregular rocks, showing a linear correlation between the test-obtained and calculated normal coefficients of restitution. The correlation for irregular rocks is better (R^2 0.88) than that for the basalt ball (R^2 0.56). The results suggest that the equation established on previous tests can be used to determine the coefficient of restitution for impact under more practical conditions with irregular-shaped rocks. That verified that the approach of determining the normal coefficient of restitution by the Schmidt number and slope angle is applicable for more practical conditions. However, the conditions for the above tests are still different from field conditions regarding the scale and slope properties, and further verification on the approach is needed before it is used for practical rockfall analysis.

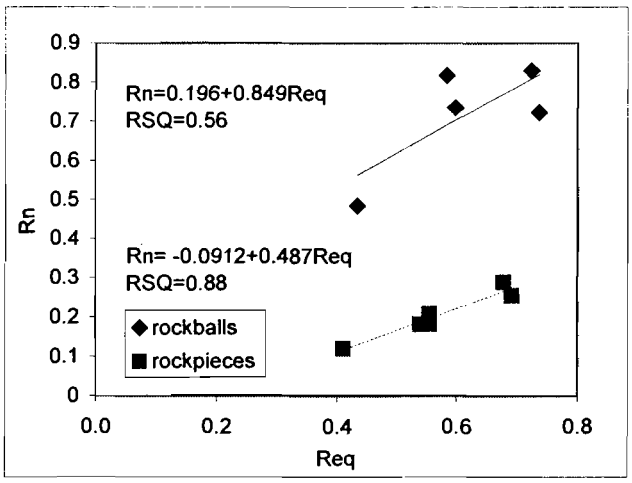

Figure 3-14: Plot of the coefficient of restitution from test against that from empirical equation (Req), showing a linear correlation for both rock balls and rock pieces.

3.6.2.2 Velocity dependence of the coefficient of restitution

The impact velocity affects the restitution coefficient by impact energy, with higher impact energy causing more plastic deformation and fracturing on the slopes and rock boulders and resulting in smaller coefficient of restitution. Pfeiffer and Bowen (1989) used a scaling factor to adjust the normal coefficient of restitution according to the impact velocity in their rockfall simulation program. Chau et al (1998) found that the coefficient of decreases slightly with the normalized impact energy (see Chapter 2).

To examine the effect of the impact velocity on the coefficient of restitution, different dropping heights (0.6, 1.0, 1.5, 2.0, 2.5, 3.0 m) have been used in the tests. The results of the restitution coefficients for different dropping heights are shown in table 3-7. Both normal and tangential coefficient of restitution is plotted against the impact velocity (Vi) in figure 3-15.

Figure 3-15 shows that the values of Rn are generally little changed or decrease slightly with Vi. The correlation between Rn and Vi is variable (R^2 from 0 to 0.82). For some rock pieces (basalt and limestone), Rn increases with Vi when Vi is less than 6.3 m/s (H = 2 m), and decreases when Vi exceeds that point (figure 3-15a). That is because that rock pieces do not bounce up completely at low dropping height, and the values of coefficient of restitution are too low. The tangential coefficient of restitution (Rt) increases with the impact velocity with a

Table 3-7: Coefficient of restitution for rough rocks

Slope Type*	Falling Rocks*	Slope angle	Drop height H (m)	Velocity Vi (m/s)	Rn	Rt
Basalt	bast1-3	0	0.6	3.43	0.82	
Basalt	bast1-3	0	1	4.43	0.82	
Basalt	bast1-3	0	1.5	5.43	0.80	
Basalt	bast1-3	0	2	6.26	0.82	
Basalt	bast1-3	0	2.5	7.00	0.82	
Basalt	BS	0	0.6	3.43	0.10	
Basalt	BS	0	1	4.43	0.15	
Basalt	BS	0	1.5	5.43	0.19	
Basalt	BS	0	2	6.26	0.25	
Basalt	BS	0	2.5	7.00	0.21	
Basalt	BS	0	3	7.67	0.20	
Lime	bast1-1	0	0.65	3.57	0.53	
Lime	bast1-1	0	1.03	4.50	0.54	
Lime	bast1-1	0	1.5	5.43	0.41	
Lime	bast1-1	0	2	6.26	0.46	
Lime	lim	0	0.6	3.43	0.06	
Lime	lim	0	1	4.43	0.11	
Lime	lim	0	1.5	5.43	0.11	
Lime	lim	0	2	6.26	0.18	
Lime	lim	0	2.5	7.00	0.16	
Lime	lim	0	3	7.67	0.11	
grey	bast1-3	0	0.65	3.57	0.72	
grey	bast1-3	0	1	4.43	0.74	
grey	bast1-3	0	1.5	5.43	0.74	
grey	bast1-3	0	2	6.26	0.73	
grey	bast1-3	0	2.5	7.00	0.74	
grey	grey	0	0.65	3.57	0.18	
grey	grey	0	1	4.43	0.16	
grey	grey	0	1.5	5.43	0.18	
grey	grey	0	2	6.26	0.17	
grey	grey	0	2.5	7.00	0.20	
grey	grey	0	3	7.67	0.21	
Basalt	bast1-3	40	0.6	3.43	0.88	0.50
basalt	bast1-3	40	1	4.43	0.84	0.45
basalt	bast1-3	40	1.5	5.43	0.80	0.59
basalt	bast1-3	40	2	6.26	0.81	0.56
basalt	bast1-3	40	2.5	7.00	0.80	0.60
basalt	Bs	40	0.6	3.43	0.26	0.64
basalt	Bs	40	1	4.43	0.31	0.66
basalt	Bs	40	1.5	5.43	0.28	0.76
basalt	Bs	40	2	6.26	0.34	0.77
basalt	Bs	40	2.5	7.00	0.28	0.76
basalt	Bs	40	3	7.67	0.26	0.80

Table 3-7 continued

Slope type	Falling rocks	Slope angle	Drop height H (m)	Velocity Vi (m/s)	Rn	Rt
Lime	Lim	40	1	4.43	0.19	0.49
Lime	Lim	40	1.5	5.43	0.20	0.66
Lime	Lim	40	2	6.26	0.22	0.59
Lime	Lim	40	2.5	7.00	0.25	0.63
Lime	Lim	40	3	7.67	0.20	0.74
grey	bast1-3	40	0.6	3.43	0.84	0.59
grey	bast1-3	40	1	4.43	0.70	0.73
grey	bast1-3	40	1.5	5.43	0.79	0.67
grey	bast1-3	40	2	6.26	0.63	0.84
grey	bast1-3	40	2.5	7.00	0.65	0.74
grey	Grey	40	0.6	3.43	0.28	0.77
grey	Grey	40	1	4.43	0.29	0.82
grey	Grey	40	1.5	5.43	0.33	0.84
grey	Grey	40	2	6.26	0.29	0.84
grey	Grey	40	2.5	7.00	0.15	0.85
grey	Grey	40	3	7.67	0.20	0.83

*grey: greywacke, lim: limestone, bs: basalt, bast1-1, bast1-3: basalt rock balls.

fairly good correlation (R^2 from 0.53 to 0.89). This result does not seem to agree with the impact theory for the tangential coefficient of restitution, because both the normal and tangential coefficients of restitution are assumed to decrease with the impact velocity as more deformation and fracturing occurs. The reasons for that are probably variations caused by test set up and the limited falling height. When the falling height and the impact velocity is small, there is no significant deformation at impact, and the effect of impact velocity is less significant compared with other factors affecting the tangential coefficient of restitution such as shape of boulders. Further tests with greater drop height are needed to examine the relationship between the tangential coefficient of restitution and the impact velocity.

3.6.3 Tests on beds of debris and soil materials

A basalt ball (bast1-3) and basalt rock pieces (basalt is a common rock in Banks Peninsula, a rockfall field trial will be carried out in Lyttelton Quarry where the slope is formed by basalt) were used to drop onto all the different beds. Results for the coefficient of restitution are shown in table 3-8, and compacted materials

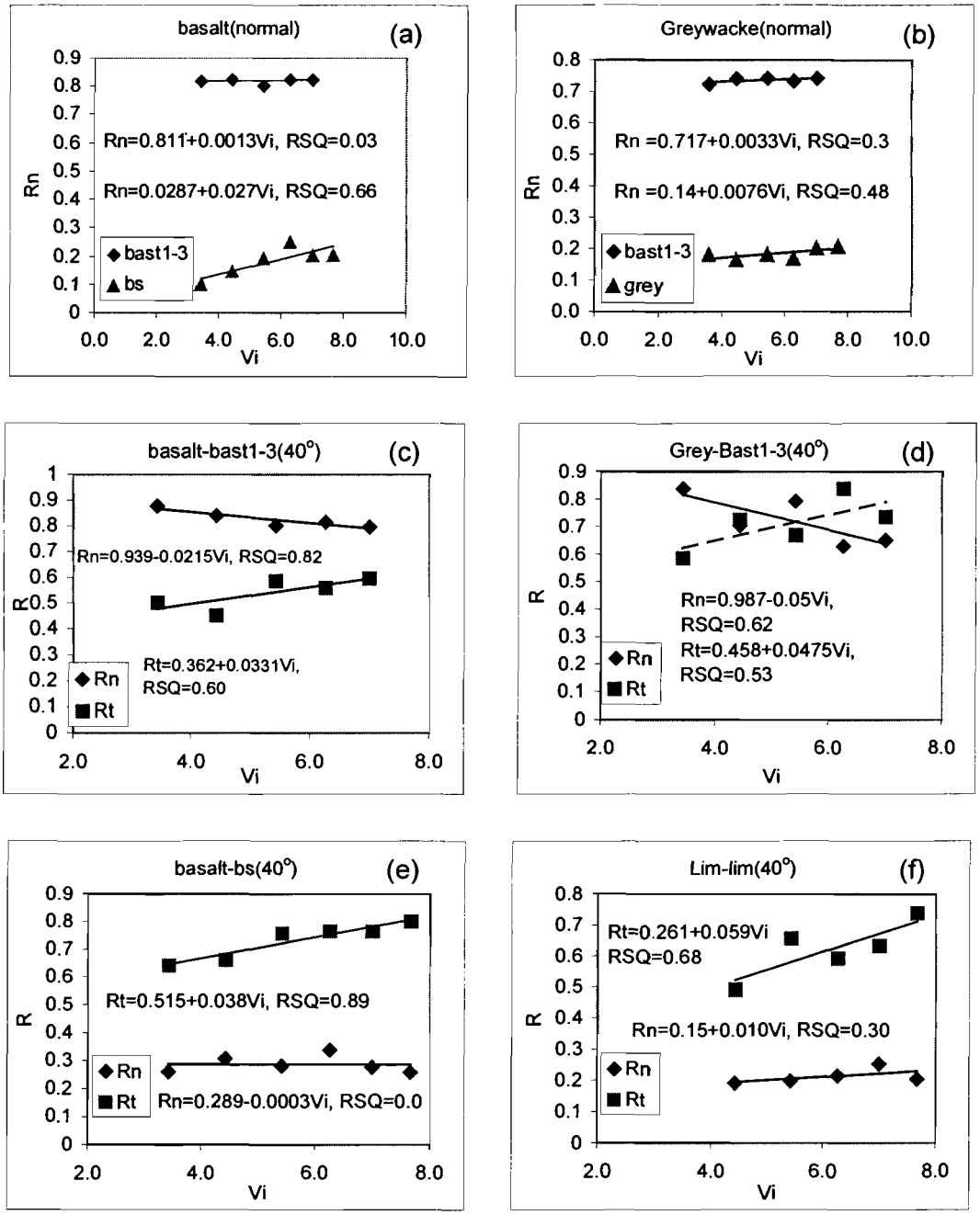

Figure 3-15: Plots of coefficient of restitution (Rn, Rt) against impact velocity (Vi) for rock balls and rough rock boulders impacting on different rough rock surfaces. (a). normal bounce of basalt ball and basalt boulders on basalt block, (b). normal bounce of basalt ball and greywacke boulders on greywacke block, (c). inclined bounce of basalt ball on basalt block, (d). inclined bounce of basalt ball on greywacke block, (e). inclined bounce of basalt boulders on basalt block, and (f). inclined bounce of limestone boulders on limestone block.

Table 3-8: Coefficient of restitution for beds of debris and soil materials

Beds*	A (degree)	Falling Rocks*	H (m)	Rn	Rt
sand	0	bast1-3	1.5	0.00	
gravel	0	bast1-3	1.5	0.06	
frag#	0	bast1-3	1.5	0.07	
paving#	0	bs	1.5	0.08	
frag	0	bast1-3	1.5	0.09	
paving#	0	bast1-3	1.5	0.09	
loess#	0	bast1-3	1.5	0.10	
frag#	0	bs	1.5	0.10	
loess#	0	bs	1.5	0.12	
sand	20	bast1-3	1.5	0.19	-0.01
gravel	20	bast1-3	1.5	0.14	0.31
frag	20	bast1-3	1.5	0.17	0.33
loess#	20	bast1-3	1.5	0.17	0.35
frag	40	bast1-3	1.5	0.22	0.39
paving#	20	bs	1.5	0.15	0.57
paving#	20	bast1-3	1.5	0.15	0.58
loess#	20	bs	1.5	0.23	0.61
frag#	20	bast1-3	1.5	0.16	0.61
frag#	20	bs	1.5	0.17	0.67

-- Compacted beds. frag – fragment, paving – paving stones, bs – basalt, bast1-3 – basalt ball.

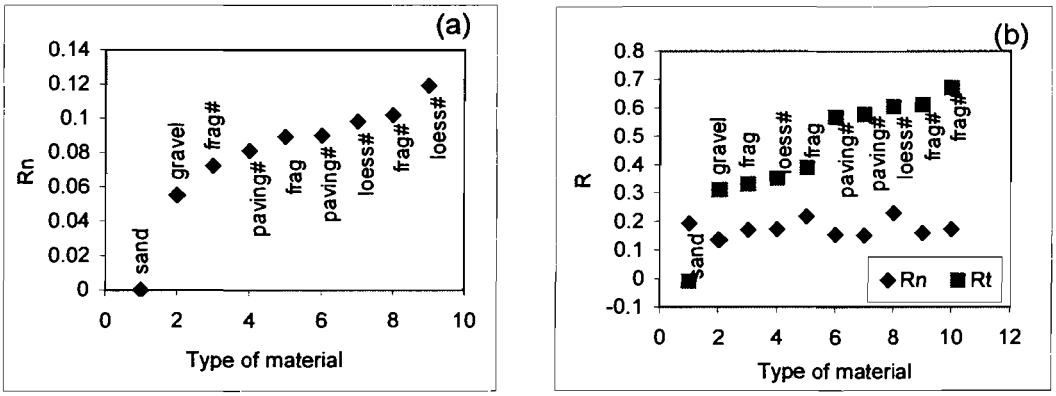

Figure 3-16: Plots of coefficients of restitution for bounces of basalt ball and basalt boulders on beds of different materials, showing the effect of the degree of compaction on the coefficient of restitution (compacted beds are marked by #). (a). Normal bounce, (b). Inclined bounce.

are marked by a "#" in the table, gravels, fragments and paving stones were mixed with loess and then compacted as explained previously. The results show that loose sand has the least restitution coefficient (Rn 0-0.19), while compact loess and fragments have a higher coefficient of restitution than the loose materials. Generally Rn is less than 0.2 for all the materials and Rt is in the range of 0.31–0.39 for loose materials and 0.57–0.67 for compact materials. Figure 3-16 shows the effect of the degree of compaction on the coefficients of restitution. The effect of compaction on the tangential coefficient is more significant, with Rt for compact materials being about twice of that of loose materials. It should be noted that loose sand has a negative tangential coefficient of restitution, that is because that dropping rocks often sink into the sands at impact, resulting in a large tangential resistance, indicating that sand is a good material for ditch bed in rockfall protection. The result in table 3-8 also shows the shape effect of the dropping rocks. Rough rocks generally have a higher coefficient of restitution, because those rock pieces have a larger size and thus a larger contact surface at impact than rock balls. Generally no obvious difference is found between the different bed materials except for sands, indicating that the property of the bed material is not an important factor in the determination of the coefficients of restitution of such materials while the degree of compaction is the principal factor. The result suggests that the coefficients of restitution for debris slope could be determined by the degree of compaction.

3.7 Conclusions and discussions

1) A comprehensive laboratory test to examine the effects of rock properties and impact set up on the coefficient of restitution has achieved good results. The test shows that a linear relationship exists between the normal restitution coefficient and the Schmidt numbers of the rock slabs, the falling rock balls, and the slope angle. For the tangential coefficient of restitution, a poor correlation with the Schmidt numbers has been found.

2) Comprehensive equation to calculate the normal restitution coefficient (Rn) with the Schmidt numbers of rock slabs and rock balls (N1, N2), and slope

angle (A) with good correlation coefficient has been established through regression analysis:

$$Rn = -0.11 + 0.00919N1 + 0.00392N2 + 0.00358A \quad (R^2 = 0.82) \qquad (1)$$

This method is confirmed by later tests with angular rock pieces impacting rough rock surfaces. The normal coefficient of restitution from tests with rough rocks has a linear correlation with that calculated by equation (1) (Req):

$$Rn = -0.0912 + 0.487Req \quad (R^2 = 0.88) \qquad (2)$$

The two equations can be used to calculate the normal coefficient of restitution for rockfall simulations but further verification with field conditions is needed.

3) Laboratory tests with rock balls and rough rock pieces impacting on rough rock blocks, beds of rock fragments, gravels, sands and soil provided valuable data of the coefficient of restitution for those materials, which can be used to determine the coefficient of restitution of similar materials in rockfall simulation.

4) The values of the normal coefficient of restitution of rock balls bouncing on rock blocks are much higher (about three times) than those of rock pieces, showing that boulder shape is an important factor affecting the coefficient of restitution. The coefficients of restitution of debris and soil beds increase with the degree of compaction (Rt of compacted materials is about twice of that of loose materials), indicating a possible method of determining the coefficient of restitution of soil and debris slopes by measuring the degree of compaction.

5) Analysis to find a simple means to determine the tangential coefficient of restitution shows a poor correlation between the tangential coefficient and normal coefficient, and between the tangential coefficient of restitution and the rolling friction coefficient. This indicates that the two parameters cannot represent the surface friction at impact under dynamic conditions. An easy

and practical method of determining the tangential coefficient of restitution has not been found in this test.

6) An attempt to relate the coefficient of restitution to the dynamic modulus of elasticity of falling balls was not successful, possibly because of the sample quality and limited number of tests. This might also indicate that the dynamic modulus of elasticity is not a good parameter for the determination of the coefficient of restitution, as a large number of samples are needed to obtain a representative result of the dynamic modulus of elasticity.

7) Analysis to examine the velocity dependence of the coefficient of restitution shows that the values of the normal coefficients of restitution are little changed or decrease slightly with the impact velocity, with variable correlations (R^2 from 0 to 0.82), while the tangential coefficient of restitution increases slightly with the impact velocity (R^2 0.53-0.68).

8) The Schmidt hammer test is widely used as a practical, non-destructive method for evaluation of rock strength. Although it is only a rough a measure of rock compressive strength, but because its principle is based on impact, simulating the process of rockfall, the Schmidt number has a better correlation with the normal coefficient of restitution than other rock properties such as dynamic modulus of elasticity; and because it is easy to carry out in the field, it is a preferable method for the determination of the coefficient of restitution.

Chapter 4

Rockfall Field Trial and Simulation Study

4.1 Introduction

Rockfall analysis is often carried out by either field test or computer simulation. Early researchers like Ritchie (1960) conducted in situ field tests to understand rockfall behaviour for the design of protective measures. Such field tests have also been reported by Mak and Blomfield (1986), Chan and Au (1986), Azzoni and de Freitas (1995), and others. Observing actual rockfall processes in the field will provide the most accurate information for rockfall analysis. However, it is expensive and impractical to carry out such tests in most situations where space is limited or public safety is a concern. The significance of the field trial data is also limited by the number of rocks rolled. Computer simulation has become a cheap and efficient means of rockfall analysis and mitigation design in recent years. Large number of both random and repeatable rockfall simulations can be carried out by computers. Since computer programs use simplified models to simulate field condition and rockfall behaviour, calibration is often needed; the input of parameters are critical to the results of computer simulation.

This chapter compares a rockfall field trial and the relevant computer simulation results. For this purpose, a rockfall field trial was carried out in a local hard rock quarry. In situ tests for the coefficients of restitution were conducted with free falling of rock boulders. Forty rocks were dropped down a particular slope, and three cameras were used to record the process. Computer simulations of rockfalls on the same slope were carried by two recently revised programs (CRSP and RocFall), the results of which have been used to compare with the field trial data.

4.2 Rockfall field trial

4.2.1 Site description

The site for the field trial is at Lyttelton Quarry, where several benches (10-15 m high) provide steep rock slopes (figure 4-1 and figure 4-2). Basalt boulders from quarrying are available on the bench floors for use. The bench slopes are generally steep (about 80^0), but locally rock slopes of 45°–60 ° are present. Scree slopes (with or without vegetation) are available near the bottom of the slopes. Large basalt blocks (diameter 2-4m) are also available on the bench floors, which can be used as rock base for parameter (coefficients of restitution) testing.

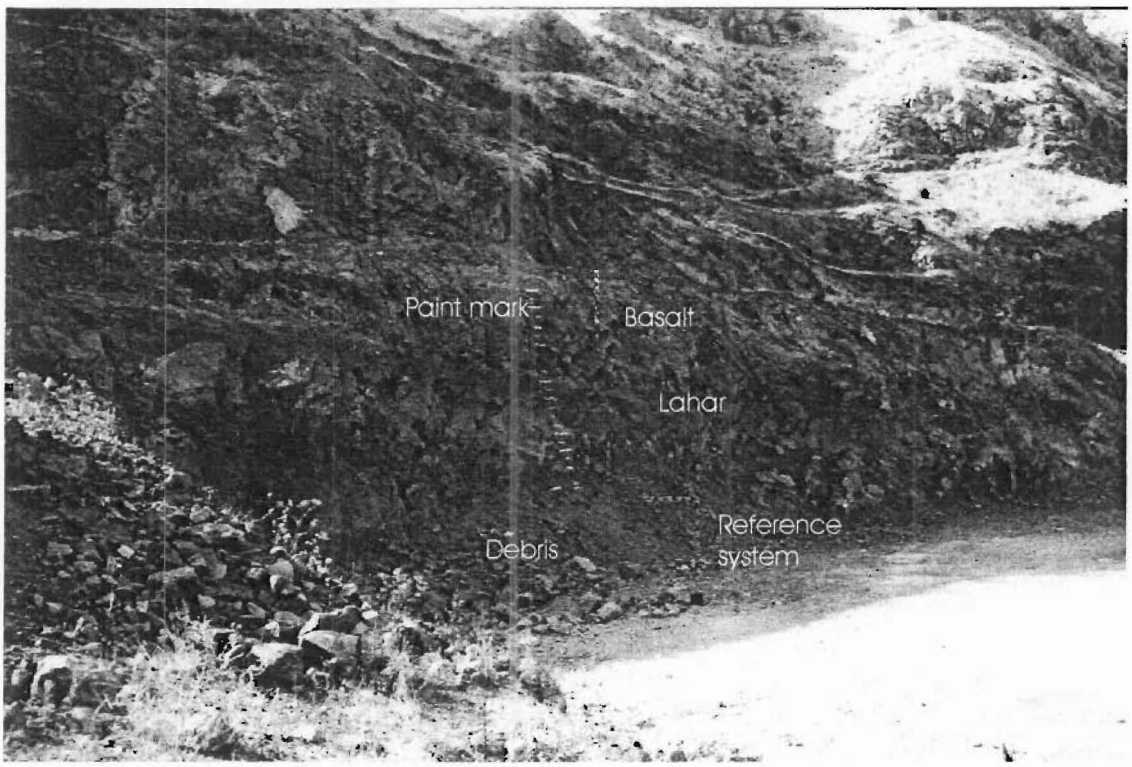

Figure 4-1: Site for rockfall field trial, Lyttelton Quarry

Rocks forming the slope are mainly basalts, with two kinds of basalts present in the quarry: massive lava and rubbly lava. Massive lava is slightly to moderately weathered, grey to black, hard (Schmidt number ranges from 50.5 to 61, average 53.1), with generally smooth surface. Rubbly lava is slightly to moderately weathered, pinkish, brown to grey, hard (weaker than massive lava, with Schmidt number ranges from 31 to 43, average 35.6), the exterior surface is generally

rough. Mixed type is found between the two kinds of basalts. Layers of lahar deposits (1-2 m thick) are found between the two basalt flows, and are moderately weathered, red to brown, weak (Schmidt number ranges from 18.5 to 22.5, average 20.3), with grey gravels (size 0.5-2 cm) scattered among a brown ash base. Scree at the bottom of the slope are comprised of basalt fragments (5-10 cm, maximum 40 cm) and debris, which is loose to moderately compact. The slope profile for the field trial from EDM surveys is shown in Figure 4-2.

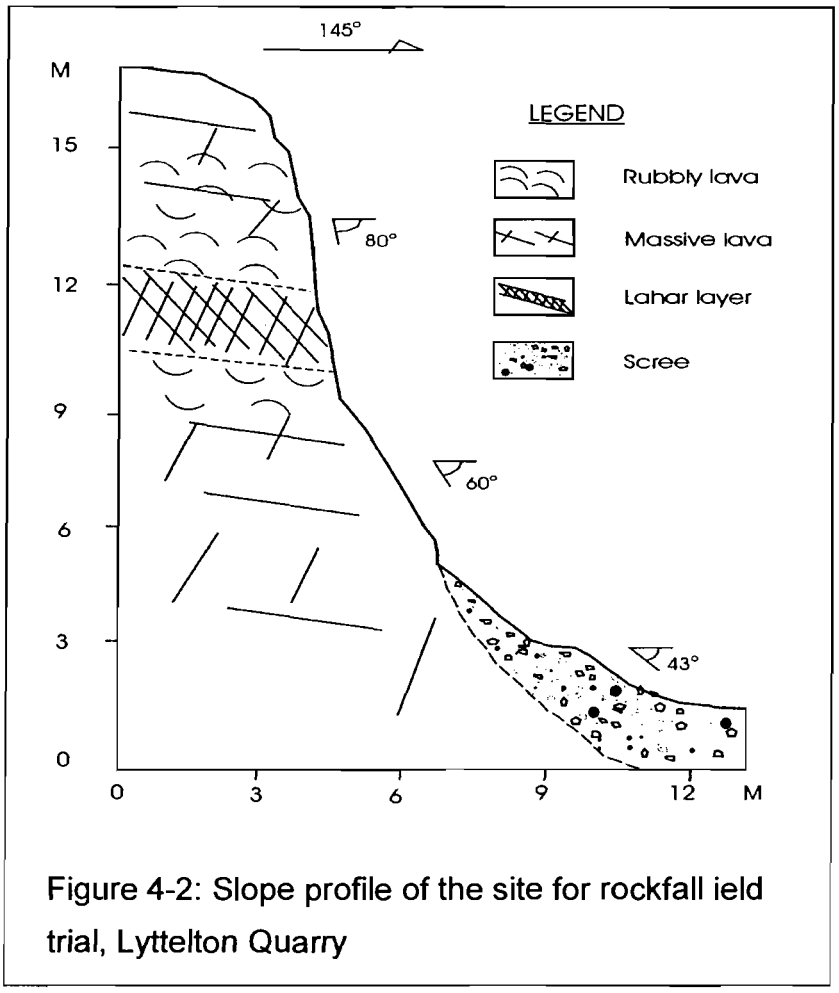

Figure 4-2: Slope profile of the site for rockfall ield trial, Lyttelton Quarry

4.2.2 Site investigation

Site investigation inside the quarry area has been carried out to select a preferable slope profile for the field trial and to determine parameters for rockfall simulation. The profile chosen for the field trial is a steep to moderately steep rock slope (60°-80°) at the upper part and a scree slope at the lower part (figure 4-1 and figure 4-2), wide area is available on the bottom bench to prevent rocks

from rolling out. Detailed Schmidt hammer measurements have been done on different rocks on the slope face (Appendix C). Detailed face logging has also been done on the slope face.

Table 4-1: Surface Roughness of Slope

Cell No	Slope properties			Remarks
	Mean angle (degree)	Stdev.	S value	
1	59.0	8.0	0.03	From survey
2	50.0	8.0	0.03	From survey
3	74.0	8.0	0.03	From survey
4	52.0	8.0	0.03	From survey
5	81.5	12.0	0.04	From survey
6	59.0	8.0	0.03	From survey
7	87.2	12.4	0.04	From survey
8	65.0	9.5	0.03	From survey
9	82.0	9.5	0.03	From survey
10	51.5	3.5	0.01	From survey
11	53.2	8.7	0.03	Compass measured
12	45.8	5.2	0.02	Compass measured
13	64.2	8.7	0.03	Compass measured
14	37.7	9.9	0.04	Compass measured
15	18.7	5.8	0.02	Compass measured
16	34.4	8.9	0.03	Compass measured
17	30.5	11.2	0.03	Compass measured
18	20.3	10.4	0.04	Compass measured
19	4.3	2.6	0.01	Compass measured
20	13.8	6.3	0.02	Compass measured
21	-0.6	5.2	0.02	Compass measured

Note: S value is the surface roughness defined by the CRSP program as the perpendicular variation within a slope distance equal to the radius of the boulder.

Detailed profile survey has been carried out on the selected slope profile with an EDM surveying device; the survey interval is 0.5 m. Survey data for the slope profile is shown in Appendix C.

The measurement for surface roughness has been carried out on the lower part of the slope (including the scree slope and the lower part of rock slope) with a geological compass fixed on a straight edge 30 cm long. The length of the edge is determined according to the size of rocks to be dropped on the slope. For the upper part of the slope, it is too difficult to conduct the surface roughness measurement with the compass, and the slope roughness of this part has been determined from survey data (measurement details are shown in appendix C). Because the slope is very steep at this part ($80^{o}\pm$), there will not be much impact

on this area during rockfall, so the accuracy of surface roughness by survey data is enough. Surface roughness in terms of the standard deviation of slope angle (Stdev.) and in terms of the perpendicular variation within a slope distance equal to the radius of the boulder (S value) for each cell of the slope is shown in table 4-1.

4.2.3 Field trial preparation

Before the rockfall field trial, paint marks at intervals of 0.5 m were made on the rock slope for reference. A timber reference system was also established on the lower part of the slope. A poly-nylon belt was hung on a steel rod from the top bench for reference on the upper part of the slope (figure 4-1 and figure 4-3).

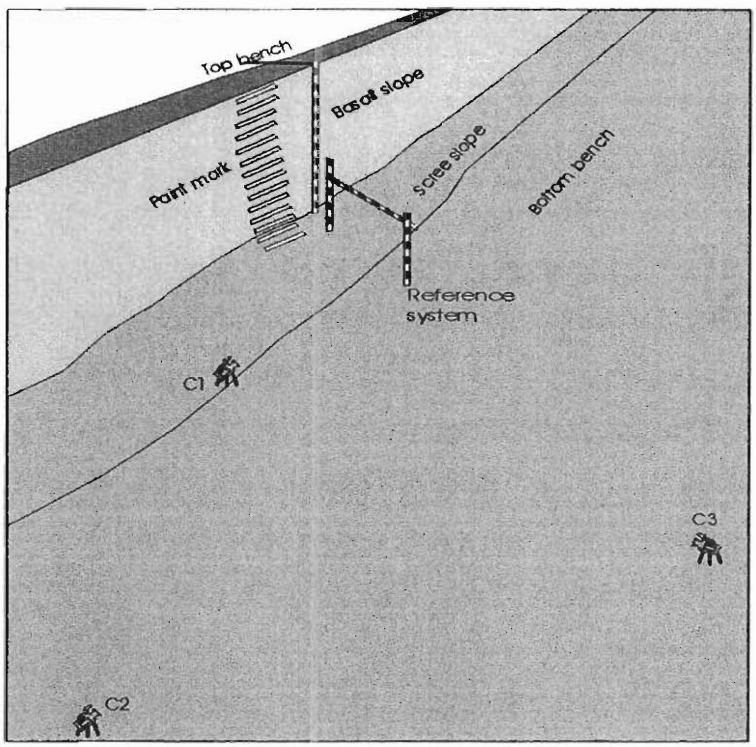

Figure 4-3: Rockfall field trial site set-up.

Three cameras were employed for photography of the field trial. A high-speed camera (C1) was used to take photograph of the lower part of the slope, a

conventional movie camera (C2) was used to take picture of the whole slope from the west side, and another conventional camera (C3) was used to take pictures from the front of the slope (figure4-3).

In total 40 basalt boulders were collected for the field trial, which were near-spherical to tabular shaped, with average size: 33.03 (25-48) x 26.4 (20-35) x 20.95 (17-30) cm. The size of all the boulders is shown in appendix C.

For the computer simulation of rockfall on the slope, a parameter test was prepared to obtain the coefficients of restitution. An excavator was employed to release rock boulders onto basalt rock surfaces and the scree slope. Because there is no bare rock outcrop on the bench floors, two big rock blocks were used for this purpose. One was massive basalt, with down-slope angle 10°-14° and size 2.2x2.5x1.5m; the other was rubbly basalt, with down-slope angle 28°-30°, and size 2.5x2.8x1.2m. Both of them rested on the ground firmly.

4.2.4 Parameter test

The purpose of the test was to obtain the coefficients of restitution under field conditions, to provide parameters for computer simulations, and to compare with those obtained from laboratory tests. Basalt boulders of a sirnilar size to those for the field trial were dropped by an excavator from about 4 m onto different surfaces (figure 4-4): a scree surface at the toe of the slope (slope angle 10°-20°), massive and rubbly basalt blocks (slope angle 12° and 28°). About 15 drops were done for each type of surface. Timber reference systems were established and a high-speed camera was used to record the process.

Coefficients of restitution were calculated from video image processing by the same method as in the laboratory tests. The coefficients of restitution for the three materials are shown in table 4-2 (calculation details are shown in appendix B). The results of the coefficients of restitution from previous laboratory tests on basalt block and beds of compacted fragments and paving stones are also listed in table 4-2 for comparison, which are similar to those from the field test.

Table 4-2: Coefficients of restitution from tests and equations

Slope type	Property			Rn from calculation		R from field test		R from lab test*	
	Angle	N_{field}	N_{lab}	With N_{field}	With N_{lab}	Rn	Rt	Rn	Rt
Massive basalt	12°	53.1	53.7	0.22	0.22	0.25	0.77	0.18 - 0.29	0.6 - 0.74
Rubbly Basalt	28°	35.6	47.9	0.17	0.22	0.23	0.66		
Scree/beds of debris	10°- 20°					0.17	0.68	0.15- 0.17	0.57- 0.67

* Results from lab tests on basalt block and beds of compacted fragments and paving stones.

Figure 4-4: Digitised picture showing the process of a boulder bouncing on a basalt block. An excavator (left) is used to release boulders.

The normal coefficients of restitution for the two kinds of basalts (massive and rubbly basalt) were calculated using the equations suggested in chapter 3, which are shown in table 4-2 for comparison. Two groups of data for the Schmidt number were used in the calculation, one is from field measurement (N_{field}), the other was measured in laboratory (N_{lab}) on fresh smooth surfaces of samples

taken from the field. It can be seen that for the rubbly basalt the calculated Rn using field measured Schmidt numbers (N_{field}) are smaller than those from field test, while those calculated using laboratory measured Schmidt numbers (N_{lab}) are similar to filed results. There is no significant difference for the massive basalt. This is because that the Schmidt number measured in the field is smaller than that measured in laboratory due to the effect of weathering, roughness and the variations of average rubbly material along the surface of the rubbly basalt.

These effects are not so obvious for a rockfall impact with a larger energy and contact area at impact than the plunger of the Schmidt hammer. With a large contact area, the effect of the small undulations on the surface can be minimized, while with large impact energy, the effect of the thin weathered layer on the surface can be reduced. This suggests that the determination of the coefficient of restitution should not only rely on the Schmidt number and equations, field conditions influencing the Schmidt hammer measurement should also be taken into account. The rubbly basalt has a rough surface and thus a smaller Schmidt number, but the small scale undulation on the surface does not have much effect on the restitution of a falling rock with an impact area much larger than that with the plunger of the Schmidt hammer. Therefore, when determining the coefficient of restitution, the Schmidt hammer measurement should be examined carefully from field investigation and adjusted before being used for calculation, or an adjusting factor should be used for the calculated coefficient of restitution.
A proper way for that is to make a fresh and smooth surface on the rock and carry out the Schmidt hammer tests on it. This could be done in the field as well as in the laboratory by taking samples back.

4.2.5 Rockfall field trial

All 40 basalt boulders were released by hand from the top of the slope. Rocks bounced down the slope onto the bottom bench, changed to rolling and sliding, and finally stopped (figure 4-5 and figure 4-7). The paths of rocks are largely along the profile line (the line of analysis), with larger variation at the lower part. The final positions of rocks are shown in figure4-6.

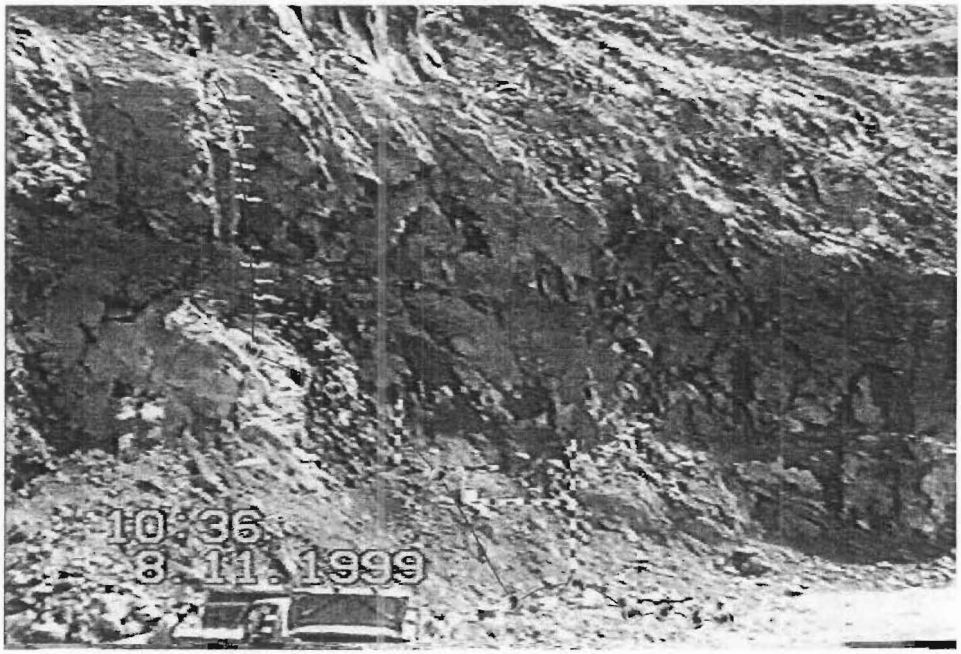

Figure 4-5: Digitised picture showing the trajectory of a falling rock in the field trial

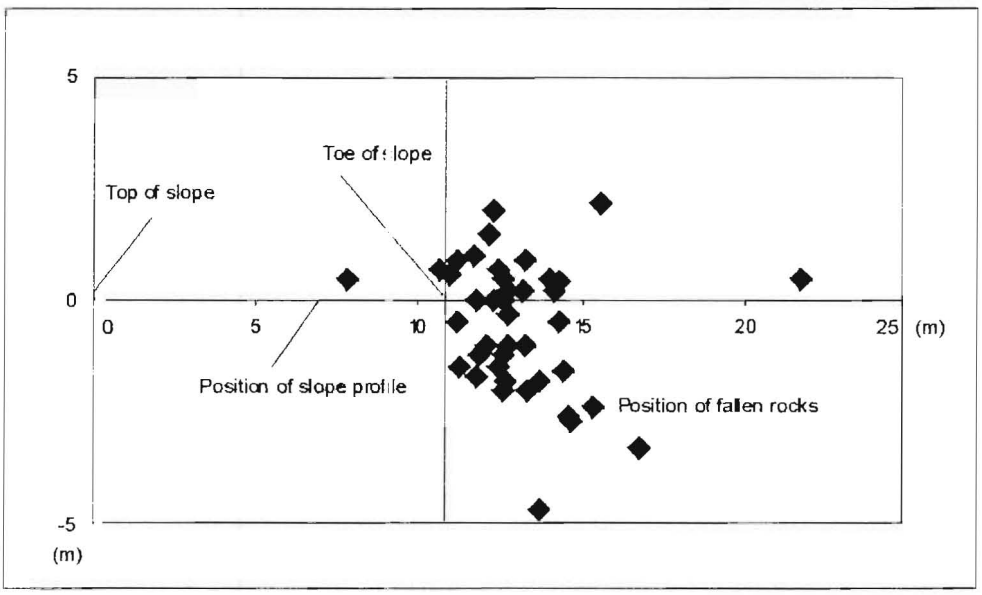

Figure 4-6: A plan view of the rest positions of fallen rocks from rockfall field trial

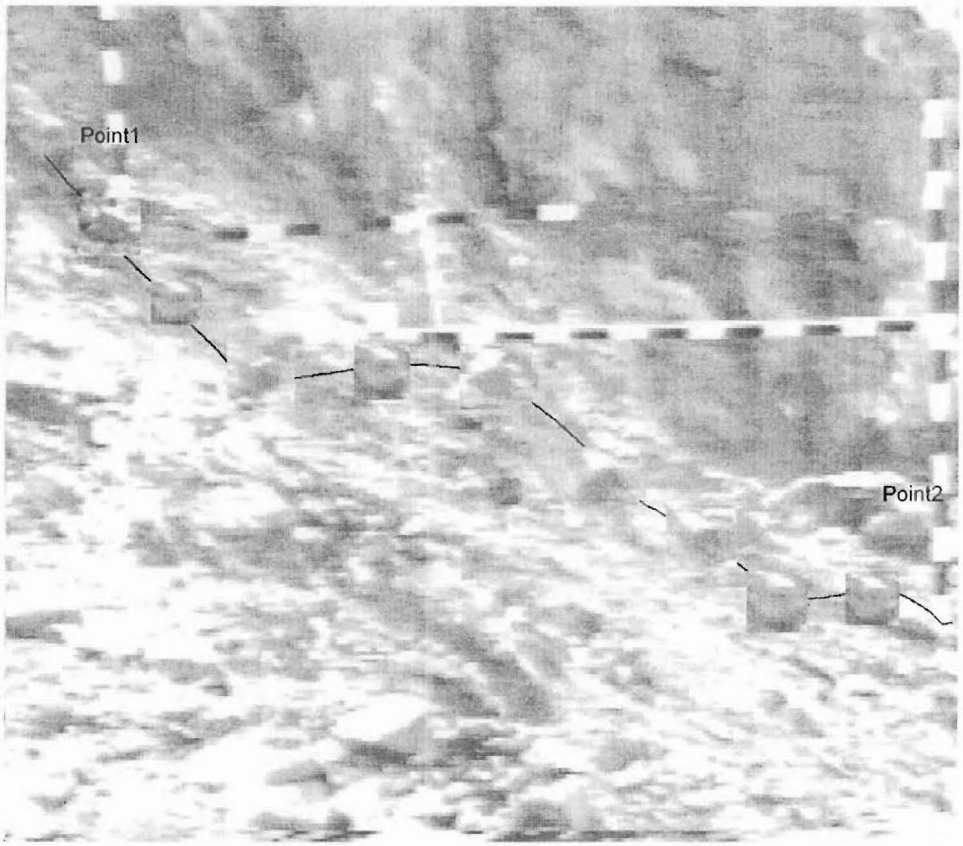

Figure 4-7: Picture taken by the high-speed camera, showing rockfall trajectory at the lower part of the slope and the analysis points.

The rockfall process was recorded by the three cameras at three different positions, which were then processed for rockfall trajectory analysis. Three analysis points were determined: the base of the rock slope (point 1), the toe of the slope (point 2) and the first survey point on the bottom bench (point 3) (6.8 m from the toe of slope). Bounce height and velocity of each rock passing the three positions were measured and calculated from the video record (appendix C), which are shown in table4-3. The percentages of rocks passing point1, point2 and point 3 are 100%, 95.2% and 2.5% respectively.

Table 4-3: Rockfall Field Trial Results

Index	Point 1		Point 2		Point 3	
	Height(m)	Velocity(m/s)	Height(m)	Velocity(m/s)	Height(m)	Velocity(m/s)
Mean	1.26	12.12	0.29	9.76	0	0
Max.	3.20	16.67	1.51	16.67	0	0
Min.	0.10	8.33	0.00	5.00	0	0
Stdev.	0.91	2.00	0.30	3.09	0	0

4.3 Rockfall simulation programs

4.3.1 Introduction

The first computer simulation program for rockfall analysis was developed by Piteau and Clayton (1977). After that, several programs were developed by various authors, including Azimi et al. (1982), Shie Shin Wu (1986), Hoek (1987), Hungr and Evans (1988), Spang and Rautenstrauch (1988), Pfeiffer and Bowen (1989), Elliot (1992), Azzoni *et al.* (1995) and Stevens (1998). Some of the recently revised programs are as follows:

- CADMA: a commercial program developed by Azzoni (1995) of ISMES SpA and ENEL CRIS of Italy;
- CRSP: first developed in 1989 by Pfeiffer and Bowen at the Colorado Department of Transportation, revised (version4.0) in 1997 by Jones, Higgins and Andrew, a program in public domain;
- RocFall: developed by Stevens of the University of Toronto (1998), based on the model developed by Hoek (1987);
- Rockfal3: developed from rockfal2 (Elliot 1992) by Golder Associates in 1997, first developed to improve upon CRSP.

The main features of the programs are shown in table 4-4 (modified from Lee and Elliot 1998).

Table 4-4: Main features of rockfall simulation programs

Features	CRSP	CADMA	RocFall	Rockfal 3
Boulder type	Sphere, cylinder, disc	Ellipsoid (most general)	Particle	Sphere, cube
Boulder source	All boulders in a simulation have identical size & shape Originated within a zone with coordinates of both ends specified Probably using uniform distribution	Variable boulder size & shape Variable starting velocity Originated within a zone as CRSP Probably using uniform distribution	Variable boulder mass Originated within a line or a point Probably using uniform distribution	Identical boulder size & shape Originated from a point with the same starting velocity
Slope	Slope roughness as perpendicular variation	Slope roughness as fraction of slope angle of cell	Slope roughness as standard deviation of slope angle Random distribution of slope vertices	Slope roughness as standard deviation of slope angle
Restitution coefficients	Separate coefficients of normal and tangential directions Applied to velocity loss	Single coefficient applied to energy loss	Separate coefficients of normal and tangential directions Applied to velocity loss	Separate coefficients of normal and tangential directions Applied to velocity loss
Rolling Mode	Modelled as a series of short bounces. Tangential restitution (braking) applied at each bounce and not continuously. Normal restitution (cushioning) erroneously applied at each step	Uses equation of motion Applies true rolling friction coefficient	Normal & tangential coefficients applied in projectile mode Friction angle applied in sliding mode	Uses equation of energy conservation Assumes rolling friction coefficient as a function of the tangential restitution coefficient
Output	Shows boulder trajectory, bounce height, velocity and energy distribution, and statistics at analysis points Windows 95, 98 or Windows NT 4.0	Windows 95 Prints directly to printers	Shows boulder trajectory, bounce height, velocity and energy distribution, and statistics at analysis points Windows 95, 98 or Windows NT 4.0	Shows boulder trajectory, bounce height, velocity and energy distribution, and statistics at analysis points DOS, use screen capture for printing

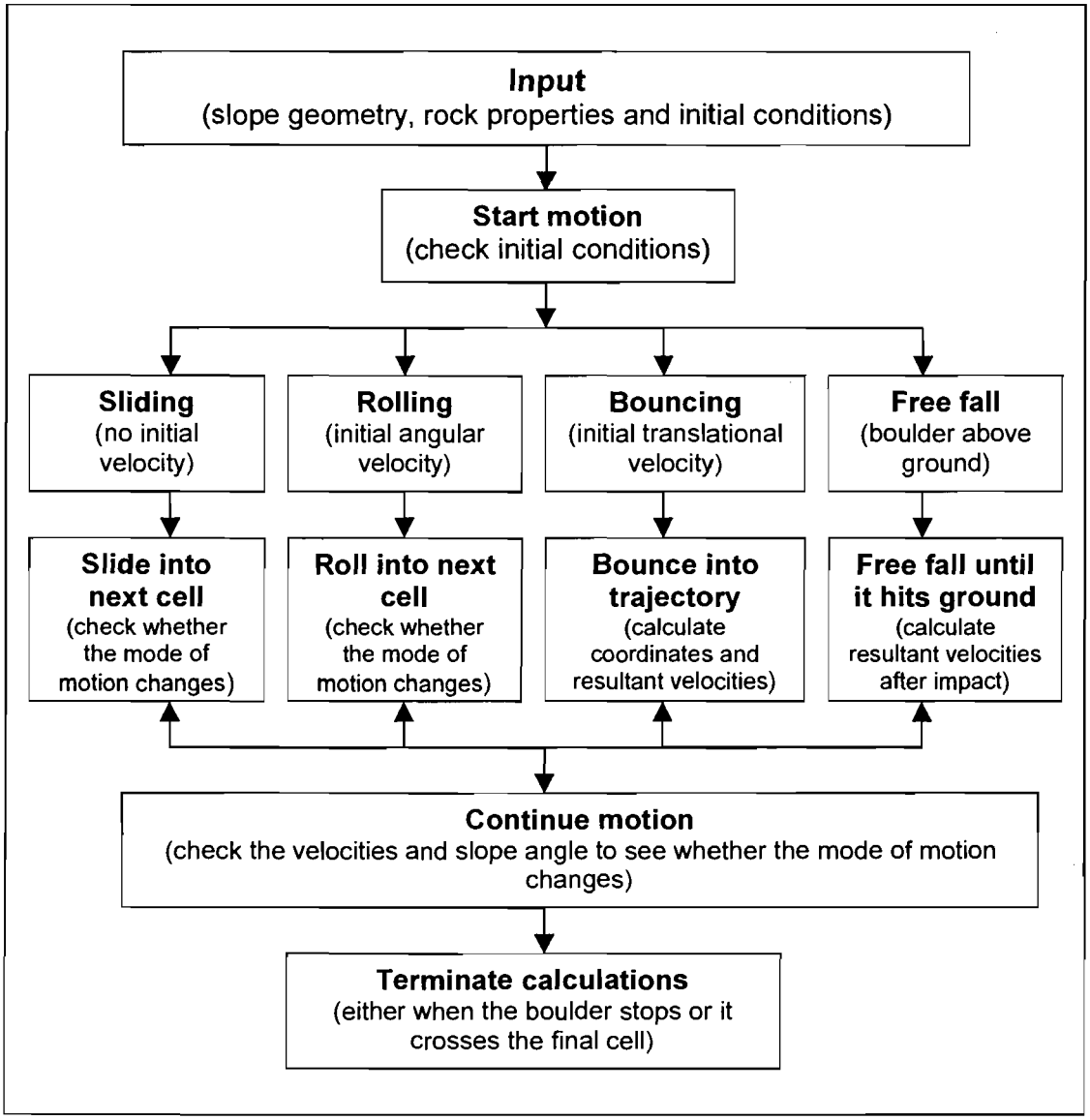

Figure 4-8: General algorithm for rockfall computer simulation (from Rayudu, 1997)

All the simulation programs use the equation of rigid body motion and properties of the slope and rocks to calculate velocity and bounce characteristics of the rock as it travels down the slope. In order to reduce the number of parameters in rockfall simulation, the following general assumptions are made for all computer programs discussed in this chapter (specific assumptions are used for individual programs):

- The effect of air friction on the movement of rock is negligible;

- Rockfall motion is considered in a plane perpendicular to the slope, and lateral variation of slope is not considered in the program;
- There is no break-up of rocks during the process of rockfall.

Although the simulation algorithms of different programs differ from each other, the general algorithm is the same; it involves determining the mode of the boulder (bounce, slide or roll), calculating the velocity at the end of each impact, and detecting whether the boulder has stoped or moved beyond the area of interest. The basic algorithm of rockfall simulation is shown in figure 4-8.

4.3.2 Parameter input

Behaviour of rockfall is influenced by slope properties, slope geometry, boulder properties and initial conditions of rockfall. Parameters that should be specified for rockfall simulation are shown in table 4-5.

4.3.2.1 Slope properties

Slope parameters in rockfall simulation include slope geometry, surface roughness and the restitution coefficients of slope materials. Slope geometry is the primary factor in defining impact position and zones of acceleration and deceleration. Surface roughness accounts for the variation of slope angle at impact from the overall slope segment, as well as the transverse undulation of slope. The coefficients of restitution are important in calculating velocities of the rock after impact.

Slope geometry is defined by dividing the slope profile into a suitable number of cells, and entering the coordinates of both ends of each cell. Slope roughness and coefficients of restitution are then entered for each cell. The number of cells is usually unlimited for most programs. Variation of coordinates in slope geometry is considered in the RocFall program, assigning a random distribution of slope vertex. This is useful to simulate the effect of lateral variation of the slope profile, to analyse the sensitivity of the current profile to changes in the location of vertices, and to determine where remedial measures would be of most use.

Table 4-5: Parameters in rockfall simulation

Factor	Parameter
Slope properties	Slope geometry (coordinates of cells) Surface roughness Coefficients of restitution Friction angle
Boulder properties	Rock size (mass) Rock shape
Initial conditions	Starting zone Initial velocity

Slope roughness is usually defined as the angle of variation from the slope cell angle, while in the program CRSP it is defined as the maximum perpendicular variation within a slope distance equal to the radius of the boulder. Impact angles are randomly created by the mean angle of the cell and surface roughness. The value of surface roughness is influenced by the boulder size, and larger boulders will experience smaller variation in slope angle. Surface roughness can be determined by measuring the slope angle in the field with a straight edge or from detailed profile surveys. The standard variation of the measured angles is the value of surface roughness. The length of the straight edge is determined by the boulder size.

Normal and tangential coefficients of restitution are entered for each cell of the slope, while for the program CADMA a single coefficient of restitution is used. A normal scaling factor is used by CRSP and RocFall to adjust the normal coefficient of restitution (Rn) according to the impact velocity. The friction angle is used by RocFall to reduce velocity in the sliding mode. Almost all parameters in RocFall can be defined by either a constant or a random variable which specify the mean value and standard deviation of parameters, while in CRSP they are defined as constant.

4.3.2.2 Boulder properties

Boulder properties include boulder shape, size, mass and density (table 4-4). Spherical, discoidal and cylindric shapes are specified for CRSP, with size specified by the diameter and thickness. In RocFall, the boulder is modelled as a particle with specified mass. The mass of the boulder can be randomly variable.

The program CADMA uses a three dimensional boulder (specified by axial ratio and volume) to perform the simulation.

4.3.2.3 Initial conditions

Initial conditions of the boulder include the initial horizontal and vertical velocities, and the starting position of the boulder. Before a simulation can begin, the initial location and velocity of rocks must be defined. The starting location for CRSP is a vertical zone above the top slope defined by the Y-coordinates of the top and the base. In RocFall, both line and point seeders can be defined. In line seeding, the initial location of each rock is determined randomly along the length of a source line, which can be defined in any length and direction above the slope.

4.3.3 Simulation algorithms

The process of rockfall in most simulation programs includes impact and bouncing, rolling and sliding, and stopping. The initial movement of the boulder depends upon the initial condition specified. The boulder starts movement by free falling if the initial position is above the ground. It then enters impact and bouncing motion after the first impact. If the initial position is on the slope, the initial movement of the boulder may be rolling and sliding, or bouncing if it is given an initial velocity. A boulder can change from rolling into bouncing when there is a sudden increase in slope angle. The movement of the boulder transforms from bouncing into rolling and sliding when the velocity becomes less than a minimum velocity (in Rockfal3 this is defined as the velocity that could lift the boulder to a height of one twentieth of the boulder radius). The boulder stops when its velocity becomes zero or a specified small value (0.1 m/s in Rockfal3). Impact and bouncing is the most important stage in rockfall simulation.

The trajectory of a bouncing rock is assumed to be parabolic, which is determined by the initial velocity and the force of gravity. The boulder will strike the slope when the parabola intersects the slope surface. The essence of the bouncing algorithm is to find the location of intersection between the boulder path and the slope line. Once the impact point is found, the reflected velocity is calculated according to the coefficient of restitution. The resultant velocity is

checked to determine the mode of movement, if the velocity is still in the category of bouncing, the process will repeat again.

The equations for calculating the coordinates of impact are as follows:
The parametric equation for slope line is given by:

$$Y = aX + b \quad (1)$$

where a, b are constants defined by coordinates of the end points of the cell.

The parametric equation for the parabolic boulder trajectory:

$$Y = Y_0 + \frac{Vy_0}{Vx_0}(X - X_0) + \frac{g}{2Vx_0^2}(X - X_0)^2 \quad (2)$$

where: X_0 ,Y_0 , Vx_0, Vy_0 are the initial coordinates and velocities.

The position of the boulder is checked with cell coordinates and the coordinates of impact can be solved from equations (1) and (2).

Resultant velocities after impact are calculated using the coefficients of restitution. Different programs use different calculation methods. The algorithms used by CRSP and RocFall are outlined below:

CRSP (Pfeiffer and Bowen)

The velocity of the boulder is resolved into normal and tangential components to calculate the reflected velocities using the normal and tangential coefficients of restitution. The new normal velocity is obtained by the normal coefficient of restitution and a velocity dependent scaling factor:

$$V_{rn} = B\, R_n\, V_{in} \quad (3)$$

where V_{rn} ,V_{in} are the incoming and reflected normal velocities.

$B = \frac{1}{1+(V_{in}/30)^2}$ is the scaling factor.

The new tangential velocity is calculated using the conservation of energy:

$$(\tfrac{1}{2} I\, \omega_i^2 + \tfrac{1}{2} mV_{it}^2)\, f(F)\, SF = \tfrac{1}{2} I\, \omega_r^2 + \tfrac{1}{2} mV_{rt}^2 \quad (4)$$

where :

m = rock mass

I = rock moment of inertia

ω_i, ω_r= initial and final rotational velocity

V_{it}, V_{rt} = initial and final tangential velocity

$f(F) = R_t + \dfrac{1 - R_t}{1.5 + \left(\dfrac{V_{it} - \omega_i r}{10}\right)^2}$ is the friction function

$SF = \dfrac{R_t}{1 + \left(\dfrac{V_{in}}{50}\right)^2}$ is the scaling factor

r = radius of the boulder

Because it is assumed that there is no sliding between the boulder and the slope at impact, the relationship between the translational and rotational velocity is as follows:

$$V_{rt} = \omega_r r \tag{5}$$

The new tangential velocity can be solved from equation (4) and (5):

$$V_{rt} = \sqrt{\frac{r^2(I\omega_i^2 + mV_{it}^2) f(F) SF}{I + mr^2}} \tag{6}$$

RocFall (Stevens)

The new normal and tangential velocities are calculated directly from the normal and tangential coefficients of restitution:

$V_{rn} = R_n V_{in}$

$V_{rt} = R_t V_{it}$

where V_{in} / V_{it}, V_{rn} / V_{rt} are the incoming and reflected normal and tangential components of velocity.

The post-impact velocities are transformed into horizontal and vertical components according to:

$V_{rx} = (V_{rn}) \sin\theta + (V_{rt}) \cos\theta$

$V_{ry} = (V_{rt}) \sin\theta + (V_{rn}) \cos\theta$

where V_{rx} / V_{ry} are the reflected horizontal and vertical components of velocity.

θ is the slope angle.

The program CADMA uses the principle of conservation of angular momentum to simulate impact conditions; a single energy coefficient of restitution is used to calculate the final velocity. Other programs use either the principle of energy conservation or the simple method used by RocFall.

The boulder starts rolling when the velocity is not high enough to put the boulder into a bouncing trajectory. A minimum velocity is usually used to define the transition point from bounce to rolling mode by most of the simulation programs. For CRSP, the boulder is considered to be rolling if the travel distance between bounces is less than its radius. The rolling mode is modelled as a series of short bounces. In RocFall, rolling and sliding is simulated using basic physical laws of motion based on the friction angle specified. CADMA uses the dynamic equilibrium equations of a rigid body to calculate the velocity of the boulder during rolling or sliding motion.

4.3.4 Simulation output

Both CRSP and RocFall use the Windows system. Data output includes graphs of rock trajectory, graphic and statistical data for particular analysis points. Bounce height, velocity and kinetic energy are the three parameters provided by the simulation output.

An overall graph of boulder trajectory and graphs of the distribution of bounce height and maximum velocity along the slope are provided by CRSP (figure 4-9). Up to three analysis points can be selected on the slope, graphic and statistic data for each point are provided by the program, including the distribution of bounce height, velocity and kinetic energy (figure 4-10). Rockfall characteristics at particular sites are helpful for determination of the location of remedial works.

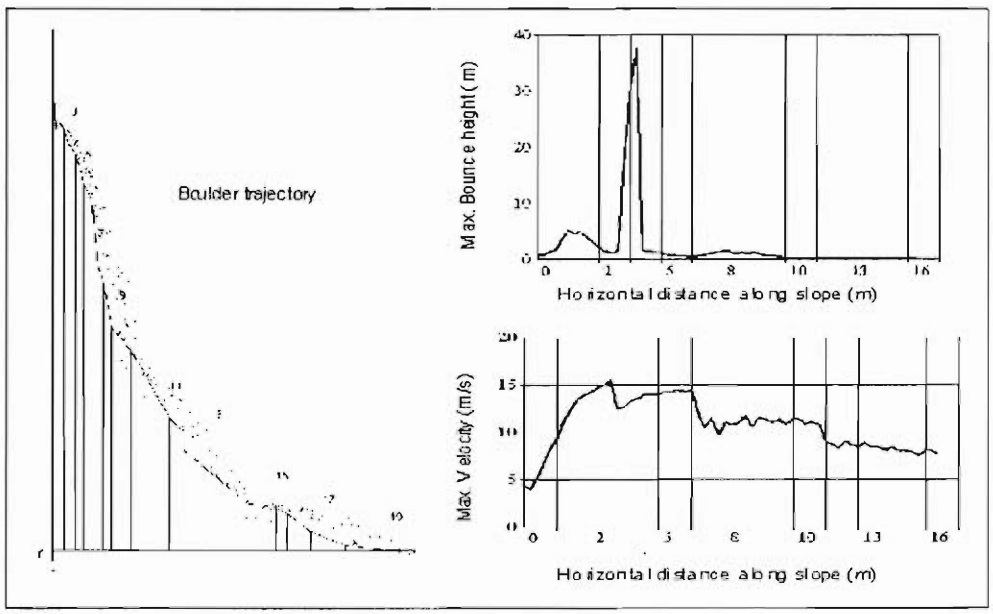

Figure 4-9: CRSP simulation output - Graphs

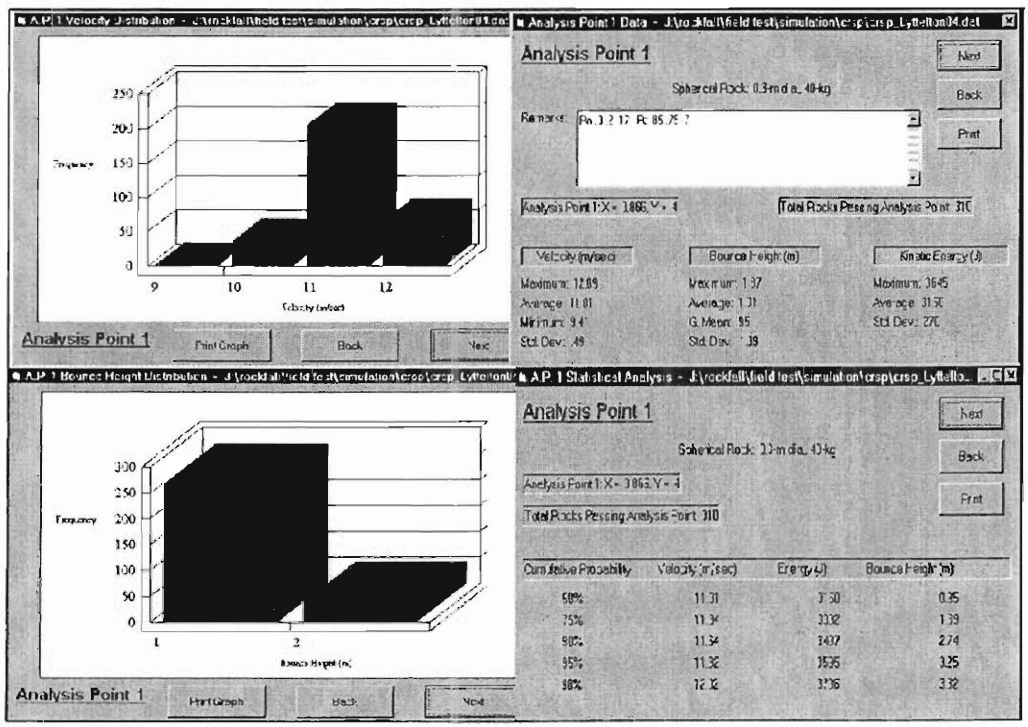

Figure 4-10: CRSP simulation output – Statistics.

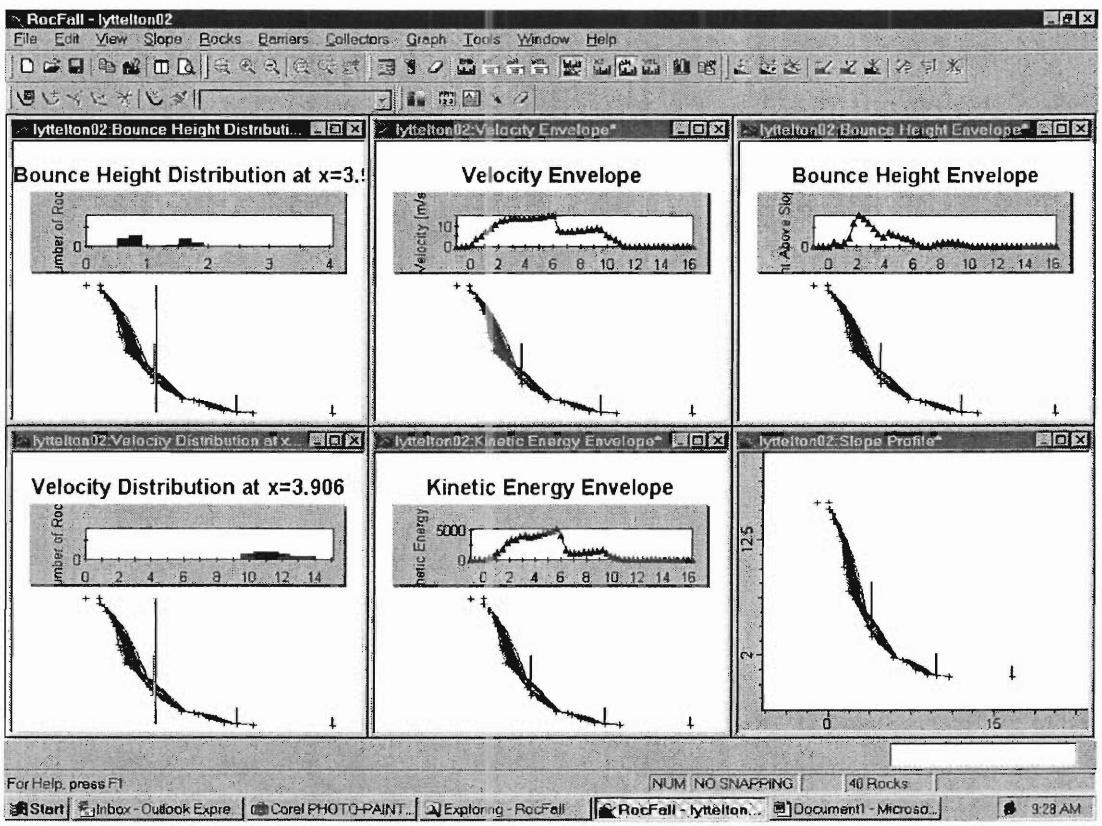

Figure 4-11: RocFall simulation output – Graphs

The program RocFall produces boulder trajectory as well as envelopes of maximum bounce height, velocity and kinetic energy along the slope. Bounce height and velocity distributions at any location can be displayed above the profile by moving the slider (a vertical line across the profile) with a mouse (figure 4-11).

In order to assist with the design of remedial measures, RocFall provides data collectors to gather statistical information of rocks passing particular locations along the slope. A data collector is a single line segment that can be placed anywhere along the slope. After the simulation has been performed, a data collector can present statistics on bounce height, velocity and kinetic energy of rocks passing that point. Data collectors are useful when designing barriers, designing parameters can be obtained by placing a data collector at the position of interest, and running the simulation again.

A special feature of RocFall output is the barrier. Barriers are modelled in the program like a slope segment, with the same set of material properties (coefficients of restitution and friction angle). A barrier is a line segment (with one end on the slope) that can be placed anywhere along the slope surface. Impact capacity is required when defining a barrier to test its ability to resist rockfall impact. The simulation of barriers is useful because it allows the test of remedial measures with more simulations. For example, a sensitivity analysis can be performed with a barrier in the simulation. This study would reveal the conditions for the design to fail. The probability of the conditions could be evaluated and the adequacy of the design decided.

4.4 Computer simulation and comparison with field trial results

4.4.1 Determination of parameters

The slope is separated into 21 cells for simulation based on differences in slope angle and material types. Coordinates and surface roughness of each cell are determined in the slope survey and from site investigation. For CRSP surface roughness is determined as the perpendicular distance (S value) within a slope distance equal to the boulder radius (0.15m), while for RocFall it is determined as the standard deviation of slope angle (Stdev.) (table 4-1).

As discussed in Section 4.2.4, the normal coefficients of restitution calculated using field measured Schmidt number are smaller than those from the field test and need to be adjusted according to field conditions. The normal coefficients of restitution for massive and rubbly basalts from field test are 0.246 and 0.226. Note that the slope angle for the field tests is from 12° to 28°, while the slope angle for the field trial is 60°-80°, so the coefficient of restitution for this slope should be larger than the values from field tests as the normal coefficient of restitution increases with slope angle. Applying the equations in Chapter 3 using the Schmidt number measured on fresh surface (N_{lab}), Rn is calculated as 0.303 and 0.301 for massive and rubbly basalts respectively. Therefore the value of Rn is assumed to be 0.3 for both types of basalts. Coefficients of restitution for the lahar are determined according to its Schmidt number compared with basalt. The

coefficients of restitution for scree slope are from field tests result. The coefficients of restitution in simulation are shown in table 4-6.

Three analysis points (data collectors) are used in the simulation to get statistics at specific positions and compare with the field trial. The three points are the same as those used in field trial observation.

Table 4-6: Coefficients of restitution in simulation

Material	Rn	Rt
Basalt	0.3	0.85
Lahar	0.2	0.75
Scree	0.17	0.7

Table 4-7: Statistics of bounce height from CRSP simulation and field trial

	No	40 – run simulation				400 – run simulation				1000 – run simulation			
		%Pass	Max.	Mean	Stdev.	%Pass	Max.	Mean	Stdev.	%Pass	Max.	Mean	Stdev.
Point 1	1	77.5	1.8	1	1.45	77.5	1.87	1.02	1.41	77.4	1.88	1.02	1.41
	2	77.5	1.82	1.04	1.41	77.5	1.86	1.01	1.42	77.4	1.88	1.02	1.42
	3	77.5	1.83	0.96	1.4	77.5	1.87	1.03	1.43	77.4	1.87	1	1.42
	4	77.5	1.84	0.96	1.49	77.5	1.88	1.02	1.4	77.4	1.88	1.02	1.41
	5	77.5	1.76	0.95	1.4	77.5	1.87	1.02	1.41	77.4	1.86	1.02	1.43
	6	77.5	1.87	1.08	1.43	77.5	1.87	1.01	1.39	77.4	1.88	1.03	1.41
	Field	**100**	**3.2**	**1.26**	**0.91**	**100**	**3.2**	**1.26**	**0.91**	**100**	**3.2**	**1.26**	**0.91**
Point 2	1	77.5	0.84	0.31	10.53	77.5	0.87	0.36	8.2	77.4	0.89	0.36	7.83
	2	77.5	0.85	0.36	15.36	77.5	0.87	0.36	8.4	77.4	0.87	0.36	8.83
	3	77.5	0.81	0.41	8.03	77.5	0.88	0.35	9.38	77.4	0.91	0.36	8.78
	4	77.5	0.71	0.36	6.03	77.5	0.85	0.35	9.02	77.4	0.88	0.35	8.27
	5	77.5	0.73	0.34	8.09	77.5	0.88	0.35	7.16	77.4	0.87	0.35	8.38
	6	77.5	0.77	0.26	14.22	77.5	0.87	0.37	9.49	77.4	0.87	0.35	7.79
	Field	**95.2**	**1.51**	**0.29**	**0.3**	**95.2**	**1.51**	**0.29**	**0.3**	**95.2**	**1.51**	**0.29**	**0.3**
Point 3	1	75	0.05	-0.01	3.39	75.25	0.06	0	4.09	76	0.05	0	4
	2	70	0.06	0	4.31	76.5	0.06	0	4.05	75.8	0.06	0	4.12
	3	77.5	0.05	0	4.76	76.5	0.06	0	9.98	75.2	0.06	0	4.16
	4	77.5	0.05	-0.01	4.02	76.5	0.06	0	3.91	74.9	0.06	0	4.37
	5	75	0.05	0	4.33	75	0.07	0	4.27	73.9	0.07	0	4.15
	6	77.5	0.06	0	3.94	76.75	0.06	-0.01	4.13	75	0.07	0	4.11
	Field	**2.5**	**0**	**0**	**0**	**2.5**	**0**	**0**	**0**	**2.5**	**0.06**	**0**	**0**

Note: pass% - percentage of boulders passed, stdev.- standard deviation.

4.4.2 CRSP simulation

Three series of simulations have been performed. The first series consists of six 40 run simulations, corresponding to the boulders rolled in the field trial. 400 and 1000 run simulations have also been conducted to decide the suitable number of runs. The statistics of bounce height and velocity from the simulations are summarised in table 4-7 and table 4-8. The corresponding results from the field trial are also presented in the tables for comparison purpose. The following features can be concluded from the simulation results:

(1) The distributions from the six 400 run simulations in table 4-7 are essentially identical, suggesting that 400 runs are probably sufficient for the simulation.

(2) The percentages of rocks passing point 1 and point 2 are slightly lower than those (77% to more than 95%) from the field trial, while that passing point 3 is much higher (75% to 2.5 %). This is probably due to the spherical shape used in the simulation, which rolled further on the ground, while the shapes of boulders in the field trial are rather irregular, and boulders are often blocked by boulders previously rolled down the slope.

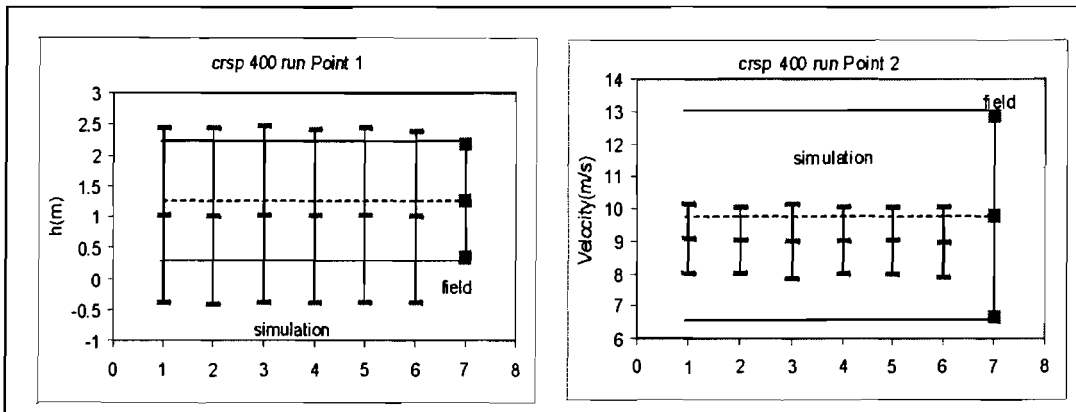

Figure 4-12: Plots showing the comparison between CRSP simulation and field trial results – mean and range of bounce height and velocity.

(3) The mean value of bounce height from simulation is slightly lower than that from field trial at point 1, but slightly higher at point 2. They are identical at point 3. The maximum bounce heights from the simulation are lower than those from field trial at point 1 and point 2. This is probably due to the lateral variation of the slope. The scree slope is higher to the east than the surveyed profile, which may have caused the higher bounce height. The overall agreement is fairly good. Figure 4-12 shows the comparison of the ranges (mean plus or minus standard deviation) and means (dotted line) between simulations and field trial. The agreement in bounce height is rather close at point 1. The standard deviations of bounce height at point 2 and point 3 are unreasonably large (larger than the maximum bounce height). It can be seen from the boulder trajectory simulation that boulders go below the slope surface at the lower part of the slope, which implies that negative values of bounce height occurred during the simulation. That revealed a problem in the CRSP program. This problem is said to have been solved in the latest version of the program.

(4) The velocities from simulation are slightly lower than those from field trial at point 1 and point 2, with rather close agreement in mean velocity (figure 4-12). However, they are quite different at point 3. That is due to the effect of boulder shape as explained in (1).

Table 4-8: Statistics of velocity from CRSP simulation (400 run) and field trial

No	Point1				Point2				Point3			
	%Pass	Max.	Mean	Stdev.	%Pass	Max.	Mean	Stdev.	%Pass	Max.	Mean	Stdev.
1	77.5	12	10.96	0.54	77.5	10.76	9.06	1.05	75.25	7.69	5.63	1.21
2	77.5	12.19	10.98	0.53	77.5	10.58	9.02	1.01	76.75	7.82	5.53	1.25
3	77.5	12.03	10.98	0.51	77.5	10.93	8.98	1.15	75	7.9	5.57	1.22
4	77.5	12.1	10.97	0.52	77.5	11.23	9.01	1.04	76.5	7.71	5.47	1.24
5	77.5	12.08	10.95	0.52	77.5	11.09	9.02	1.03	76.5	7.62	5.46	1.24
6	77.5	12.02	10.93	0.53	77.5	10.7	8.96	1.07	76.5	7.62	5.46	1.21
Field	**100**	**16.67**	**12.12**	**2**	**95.24**	**16.67**	**9.76**	**3.09**	**2.5**	**0**	**0**	**0**

Note: pass% - percentage of boulders passed, stdev.- standard deviation.

4.4.3 RocFall simulation

40, 400 and 1000 run simulations have been conducted as was done in the CRSP simulation. Statistics of bounce height and velocity at the three analysis points are tabulated in table 4-9 and table 4-10, and corresponding data from field trial are also presented in the tables.

Table 4-9: Statistics of bounce height from RocFall simulation and field trial

	No	40 – run simulation				400 – run simulation				1000 – run simulation			
		%Pass	Max.	Mean	Stdev.	%Pass	Max.	Mean	Stdev.	%Pass	Max.	Mean	Stdev.
Point 1	1	100	1.66	0.91	0.42	100	1.86	0.96	0.44	99.9	1.86	0.98	0.44
	2	100	1.68	1.02	0.43	100	1.86	1.01	0.45	100	1.98	1.00	0.45
	3	100	1.82	1.05	0.45	100	1.81	1.00	0.44	100	1.82	0.98	0.44
	4	100	1.66	0.93	0.43	100	1.83	0.99	0.44	99.9	1.89	1.00	0.44
	5	100	1.78	0.87	0.42	100	1.85	0.99	0.45	100	1.95	1.00	0.44
	6	100	1.82	1.03	0.47	100	1.76	1.03	0.45	100	1.92	0.99	0.44
	Field	**100**	**3.2**	**1.26**	**0.91**	**100**	**3.2**	**1.26**	**0.91**	**100**	**3.2**	**1.26**	**0.91**
Point 2	1	32.5	0.32	0.068	0.114	26.25	0.553	0.058	0.11	27.4	0.671	0.064	0.112
	2	38.3	0.38	0.11	0.154	26.5	0.492	0.077	0.114	28.2	0.549	0.059	0.103
	3	37.5	0.53	0.10	0.146	25.25	0.386	0.055	0.092	27.2	0.648	0.057	0.109
	4	17.5	0.13	0.042	0.063	25.75	0.456	0.057	0.11	27.1	0.606	0.066	0.11
	5	25	0.47	0.059	0.106	30.5	0.473	0.059	0.106	28.7	0.455	0.057	0.095
	6	40	0.22	0.087	0.08	23.5	0.609	0.087	0.14	26.6	0.572	0.057	0.11
	Field	**95.2**	**1.51**	**0.29**	**0.3**	**95.2**	**1.51**	**0.29**	**0.3**	**95.2**	**1.51**	**0.29**	**0.3**
Point 3	1	0	0	0	0	0	0	0	0	0	0	0	0
	2	0	0	0	0	0	0	0	0	0	0	0	0
	3	0	0	0	0	0	0	0	0	0	0	0	0
	Field	**2.5**	**0**	**0**	**0**	**2.5**	**0**	**0**	**0**	**2.5**	**0.06**	**0**	**0**

Note: pass% - percentage of boulders passed, stdev.- standard deviation.

Table 4-10: Statistics of velocity from RocFall simulation (400 run) and field trial

No	Point1				Point2				Point3			
	%Pass	Max.	Mean	Stdev.	%Pass	Max.	Mean	Stdev.	%Pass	Max.	Mean	Stdev.
1	100	14.17	11.12	1.22	30.5	10.27	5.49	2.9	0	0	0	0
2	100	14.31	11.09	1.27	23.5	10.39	5.74	3	0	0	0	0
3	100	14.15	11.16	1.25	29.5	10.7	5.73	2.8	0	0	0	0
4	100	14.33	11.02	1.19	24	10.03	5.07	2.87	0	0	0	0
5	100	14.11	11.13	1.18	26.25	10.59	5.27	2.91	0	0	0	0
6	100	14.17	10.95	1.27	26.5	10.05	5.91	2.75	0	0	0	0
Field	**100**	**16.67**	**12.12**	**2**	**95.24**	**16.67**	**9.76**	**3.09**	**2.5**	**0**	**0**	**0**

Note: pass% - percentage of boulders passed, stdev.- standard deviation.

It is found that the simulation results of both bounce height and velocity at point1 and point 2 are smaller than the field trial results, with the difference at point1 smaller than point2. No rock reaches point3, which is much like the situation in the field (only one boulder passes that point).

Figure 4-13 shows the mean values and ranges of bounce height from the simulation and the field trial, the difference at point2 is significant (difference in average bounce height 77%). The reason for such big differences is possibly the input coefficients of restitution and the relatively small and overall steep characteristics of this slope (the next chapter will show that bounce heights from RocFall are smaller than those from CRSP for steep slopes but larger for flat slope sections).

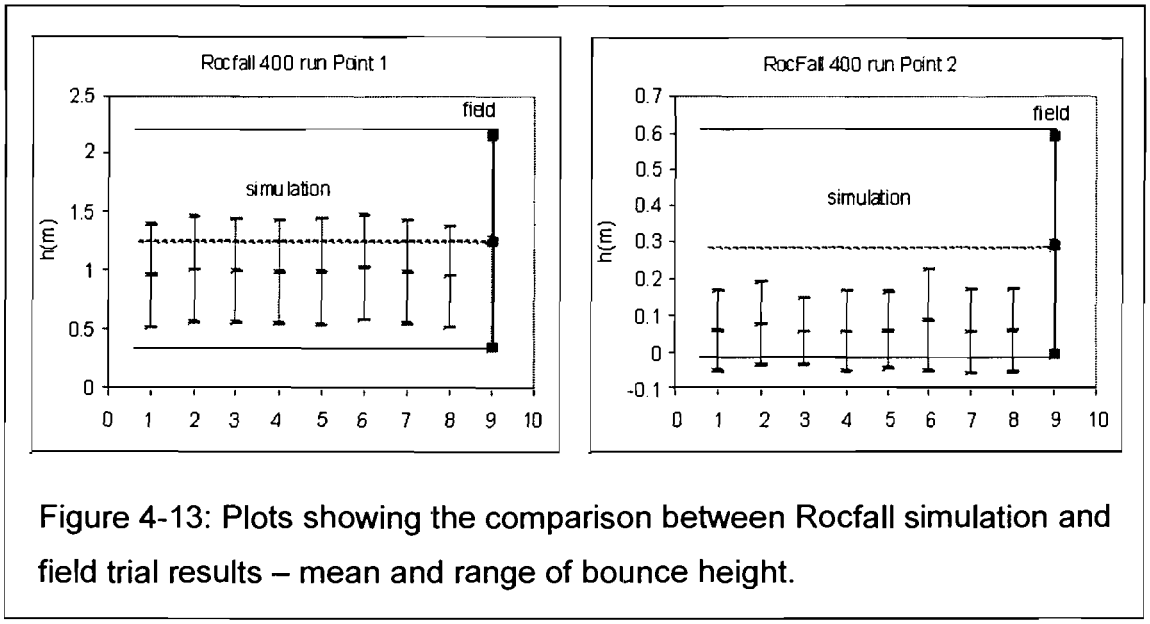

Figure 4-13: Plots showing the comparison between Rocfall simulation and field trial results – mean and range of bounce height.

Table 4-11 shows the coefficients of restitution suggested by both CRSP and RocFall, and those used for this simulation. The restitution coefficients suggested by RocFall for both bedrock and talus are much higher than those used for the simulation of Lyttelton Quarry, while the coefficients suggested by CRSP are less different. The difference in the coefficients of restitution might have caused the difference in the simulation results. Note that the coefficients of restitution obtained from this research (both from laboratory and field tests) are smaller than

those of similar slope materials reported by some earlier researchers (refer to table 2-1 in Chapter 2).

Table 4-11: Parameters suggested by simulation programs

Materials	Bed rock		Talus		Soil	
	Rn	Rt	Rn	Rt	Rn	Rt
CRSP	0.37-0.42	0.87-0.92	0.3-0.33	0.8-0.87	0.28-0.32	0.8-0.83
RocFall	0.53	0.99	0.32	0.82	0.3	0.8
Lyttelton	0.3	0.85	0.17	0.7		

A back analysis has been conducted with different combinations of parameters for basalt, lahar and scree, to compare with the field trial results. The results are presented in table 4-12. It is found that parameter combination with Rn=0.55, Rt=0.85 for basalt, Rn=0.35, Rt=0.75 for lahar, and Rn=0.35, Rt=0.7 for scree (Group1) has the closest simulation result to the field trial. This group of parameters is similar to those suggested by the program RocFall, but quite different from field data.

The above rockfall simulation study shows that there is a fairly good agreement between the CRSP simulation results and field trial results, while the simulation results by RocFall are different from the field trial. This suggests that CRSP is more suitable than RocFall for the situation in Lyttelton Quarry. Parameter input, especially the coefficients of restitution, is very important to rockfall simulation results

Table 4-12: RocFall simulation results with varied parameters

Group	Parameters*						Point1				Point2			
	RnB	RtB	RnL	RtL	RnS	RtS	%Pass	Max.	Mean	Stdev.	%Pass	Max.	Mean	Stdev.
1	0.55	0.85	0.35	0.75	0.35	0.7	100	3.53	1.18	0.62	88.75	1.04	0.33	0.24
2	0.55	0.85	0.35	0.8	0.35	0.8	100	3.85	1.21	0.66	98.5	1.02	0.37	0.27
3	0.55	0.85	0.35	0.8	0.3	0.75	100	3.50	1.24	0.65	90.75	0.88	0.18	0.22
4	0.5	0.85	0.35	0.8	0.3	0.75	100	3.17	1.12	0.56	94.25	0.99	0.21	0.24
5	0.5	0.85	0.35	0.8	0.35	0.8	100	3.79	1.14	0.6	99.5	0.98	0.37	0.26
6	0.55	0.85	0.4	0.8	0.4	0.8	100	3.42	1.21	0.63	99.75	1.21	0.45	0.31
Field							**100**	**3.2**	**1.26**	**0.91**	**95.24**	**1.51**	**0.29**	**0.3**

*RnB, RtB, RnL, RtL, RnS, RtS represent the restitution coefficients of basalt, lahar and scree.

4.5 Conclusions and discussion

(1) Rockfall field tests carried out on basalt blocks and scree slope materials show that the coefficients of restitution from field tests are similar to the results from the previous laboratory tests. Comparison between the normal coefficients of restitution from field test and those calculated using the equations suggested in Chapter 3 shows that the calculated coefficient of restitution using field measured Schmidt numbers is smaller than that from the field test, especially for the rubbly basalt which has a smaller Schmidt number. This is because the Schmidt number measured in the field is smaller than that measured on smooth surface in the laboratory due to the effect of weathering, defects and roughness of the surface. These effects are not so obvious for a rockfall impact with a larger energy and contact area than the Schmidt hammer. This suggests that the determination of the coefficient of restitution should not only rely on the equations, because field conditions influence the Schmidt measurement and restitution coefficient and should also be taken into account. The Schmidt number should be examined carefully with field investigations and adjusted before being used for the calculation of the coefficient of restitution. A proper way for that is to measure the Schmidt number on fresh and smooth surface.

(2) Comparison between the results from the rockfall field trial carried out on the bench slope and those from simulations by the CRSP shows a fairly good agreement (difference in average bounce height less than 20%). The rest positions of boulders from simulation are further away from the slope than the field trial, due to the spherical shape of boulders used in the simulation. The overall result suggests that CRSP provides a reasonable result and is suitable for the slope conditions at Lyttelton Quarry.

(3) The simulation results by RocFall are different from the field trial, especially at the toe (difference in average bounce height 77%). This is possibly because of the coefficient of restitution and the slope geometry characteristics at this site. The coefficients of restitution used in the simulation (determined by field tests) are smaller than those

recommended in the program, which might have resulted in the small bounce heights and velocities in the simulations. The relatively small scale of the slope in Lyttelton Quarry might have also contributed to the variations because boulders only experience a few impacts before stop. The effect of slope geometry characteristics on the simulation results will be discussed in the next chapter. The simulation results suggest that RocFall is not suitable for the situations in Lyttelton Quarry.

Chapter 5

Rockfall Analysis at Marine Apartments, Sumner

5.1 Introduction

Chapter 3 and chapter 4 presented the results of laboratory and field tests to obtain the coefficient of restitution. An approach of determining the coefficient of restitution by rock slope properties has been developed and tested under field conditions. It is now possible to apply this approach to practical rockfall analysis.

The site for this analysis was the Marine Apartments, Sumner, where the existing Marine Tavern building is bounded on the southern side by a steep cliff face of 35–45 m. Between the cliff face and the building is a car park. A tower block of some 32 m high was proposed at this site (figure 5-1), but was rejected on planning ground. Rockfalls from the cliff face pose a hazard to the car park and the proposed tower block. Face inspection has been carried out by Bell *et al* (Bell, 1996). Topographic surveys carried out by Eliot Sinclair and Partners Ltd. provided a series of profiles using stereoscopic ground photographic pairs and appropriate computer software.

This chapter presents the results of rockfall analysis at the Marine apartments, using the simulation programs CRSP and RocFall. Although rockfall hazards assessments have been carried out by Bell (1996) and Richards (1996) on the proposed tower block and the proposed buildings was rejected on planning grounds, rockfall hazards at this site has been further assessed in this study as an application of rockfall analysis. Additional site investigations have been carried out to assist in determining parameters. Rockfall hazard to the car park has been evaluated using the Rockfall Hazard Rating System (RHRS). A semi-quantitative risk analysis has carried out for the site to calculate the probability of accidents and assess the level of risk at the car park.

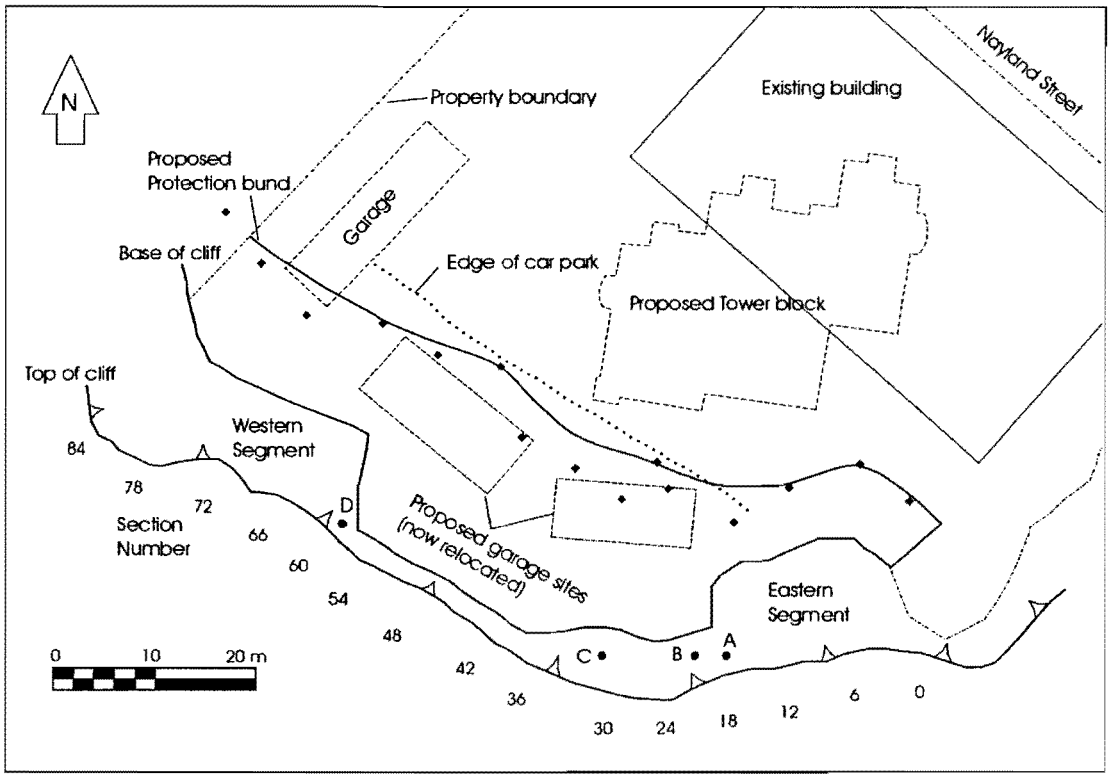

Figure 5-1: Site sketch plan of Marine apartments, Sumner (modified from Bell 1996)

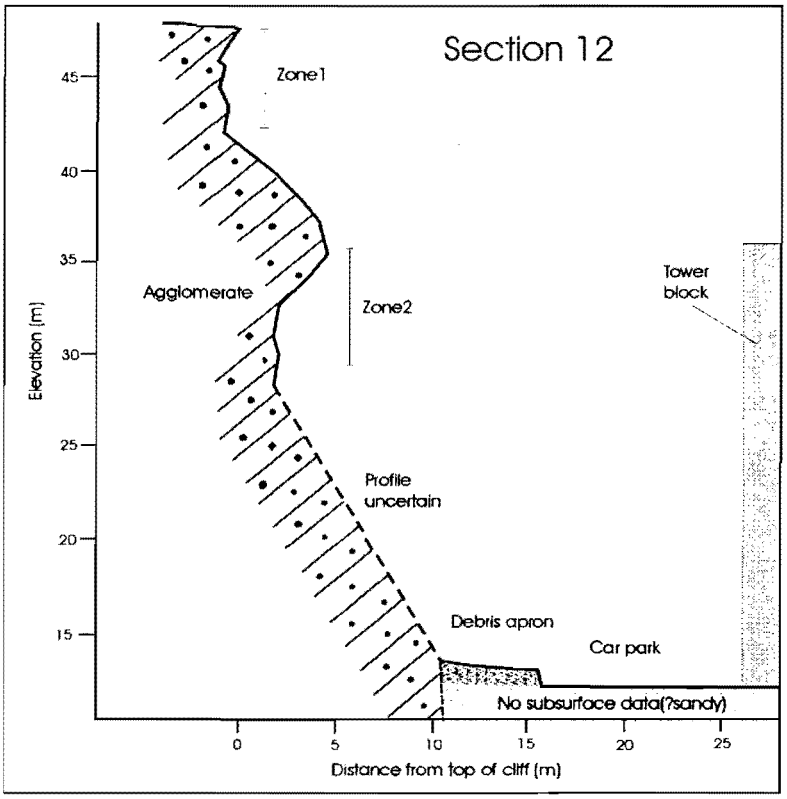

Figure 5-2: A typical profile of the cliff face showing source zones in rockfall simulation, section position refer to figure 5-1.

5.2 Site description

5.2.1 Geology

The cliff face on the southern side of the site consists of a basalt lava flow 6–8 m thick overlying volcanic agglomerate. The agglomerate forms the major part of the face, and is at least 30 m thick, with blocks of strong andesitic lava in a matrix of weak to moderately weak ash material. Block size is generally 10–30 cm in diameter, with a maximum 2 m. The Schmidt number of the blocks ranges from 20–49, with an average 38. This unit is the result of a localised explosive eruption of volcanic debris during the formation of the sequence (Bell, 1996). Between the basaltic lava and the agglomerate is a weak to very weak red ash horizon at least 1 m thick (figure 5-3). A sub-vertical basaltic dyke some 2–3 m wide forms the prominent ridge at the extreme eastern end of the site, and local caves have formed by weathering and erosion to a horizon depth of about 3 m into the base of the cliff. A debris (or talus) apron is present at the base of the cliff, which varies from less than 3 m to a maximum of about 9 m in thickness, and extends from about 12 m to more than 20 m in plan width out from the base of the cliff. The apron is composed predominantly of loess and fine debris with minor agglomerate and basaltic blocks of 10–30 cm in diameter, with a maximum block size 1.2 m. The geological features of the site are shown in figure 5-3.

The cliff itself formed initially by wave action when sea level reached its present elevation some 6,500 years ago, and the debris apron at its base has accumulated both during this erosive event and subsequently by weathering processes. The local moderately to highly weathered nature of the agglomerate is attributed primarily to hydrothermal alteration and secondarily to weathering processes operating since the cliffing event in Postglacial times. There is no information on the nature or depth underlying the debris apron, and it is assumed that beach sands are present as is the case elsewhere in the Sumner-Redcliffs area (Bell, 1996).

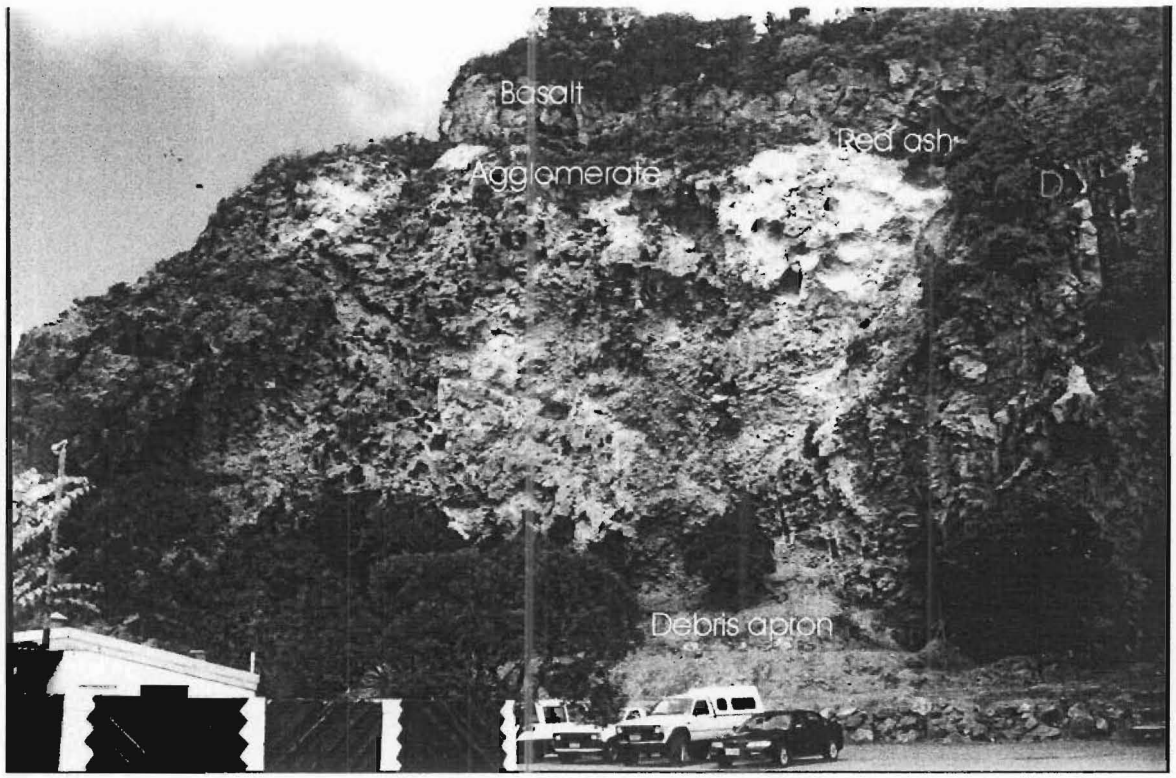

Figure 5-3: Picture of the cliff face showing geological features and source areas (A, B, C and D)

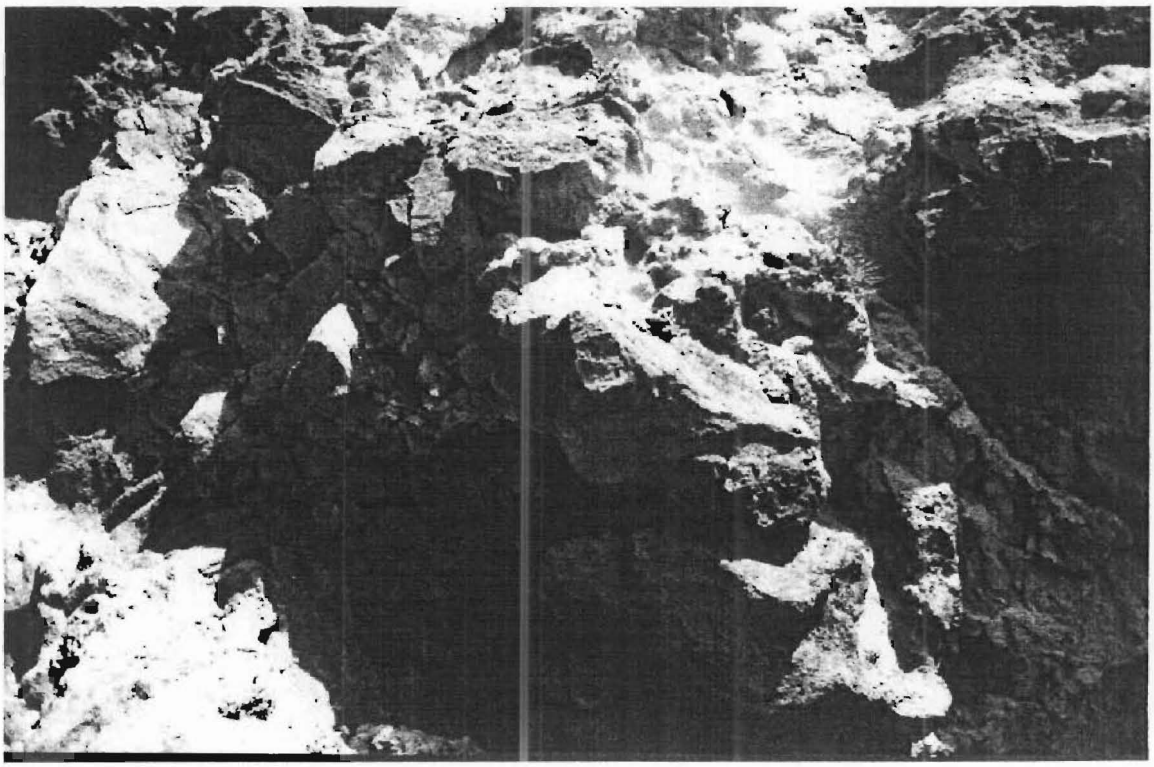

Figure 5-4: Picture showing extensively fractured agglomerate in area A

5.2.2 Source of rockfalls

Inspection of the cliff face and debris apron has shown evidence for continuing release of rockfall materials, with dimensions of individual blocks varying from about 150 mm to more than 1.2 m. Four problem areas have been identified on the face (figure 5-1 and figure 5-3) by Bell (1996) as follows:

1) Area A: located near the south-eastern ridge line, it involves a face area of approximately 5m by 5m in which the rock mass is extensively fractured with joints open up to about 100 mm (figure 5-4), and further significant rockfalls are anticipated with some blocks up to about 1 t in mass.
2) Area B: located below and to the west of Area A, and again it involves an area of about 5m by 5m in which penetrative joints open to about 150 mm dip steeply into the face, and provide a toppling release mode for blocks up to about 1 t in mass.
3) Area C: located in the approximate centre of the face, although there is no immediate concern regarding rockfall generation, it involves a significant overhang in the relatively weak bonded agglomerate from which blocks up to 0.5 t could be released.
4) Area D: is located to the west of the face, where a cavern approximately 2 m deep and 2-3 m wide and high has developed in the red ash horizon immediately beneath the overhanging grey basaltic lava flow. Further cavern enlargement could result in a significant rockfall by undermining the basalt flow in the longer term (100+ years).

Areas A, B and C are located within the weak and fractured agglomerate and are of immediate concern to the car park and proposed buildings. In addition, localised small failures must also been anticipated elsewhere in the agglomerate on the face, especially the eastern part of the cliff.

5.2.3 Triggering mechanisms

A variety of natural triggering mechanisms have been identified for rockfall generation in the volcanic rocks of Banks Peninsula (Bell, 1996). These include: dynamic loading during a large earthquake, high pore (or cleft) water pressure

due to prolonged rainfall, differential weathering and erosion (e.g. of red ash horizons) and slope unloading and progressive opening of joints promoting wedge failures. The following mechanisms have been identified for the Marine site (Bell, 1996):

1) Rainfall: Presently only one minor area of ground water seepage was identified in the central western part, and large pore pressure–generated failures are considered most unlikely because of the presence of the red ash horizon in the upper part of the profile which will limit vertical infiltration of water. In the eastern part of the cliff face where the ash horizon is not preserved, a localised association of rockfalls with prolonged wet periods may still occur because of the ready entry of infiltrating water along open fractures in the agglomerate.
2) Differential weathering: differential weathering of the red ash horizon beneath the upper grey basaltic lava has been identified as a matter of long-term concern in Area D, as this failure mechanism has been considered responsible for the June 1992 rockfall of c. 50 m^3 in Raekura Place, Red cliffs (Bell, 1996), and is a relatively common form of long-term (100+ years) cliff retreat due to the weak and slaking nature of the ash materials. General face deterioration over time in the two areas of open fracturing (A & B) will result in continuing block failures.
3) Earthquake: large earthquakes can be considered to have affected the cliff face with a frequency of some 250–500 years since its formation some 6,500 years ago and therefore to have contributed to episodic debris release.

5.2.4 Rockfall history

There is no documented records of rockfall-associated injuries and damage so far at this site. Anecdotal information suggests that only minor episodic debris release from the cliff face has occurred during the last 100 years. Bell (1996) estimated the rate of debris accumulation assuming that the apron has been accumulated uniformly in the past 6,500 years:

Segment	Debris Accumulation per 100 years	
	Volume (m^3)	Mass (t)
Western	5	12
Eastern	30	65
Total	35	77

Although the simplified assumptions that were made may be incorrect, the above figures are nevertheless considered realistic in their order of magnitude. They also provided quantitative confirmation that the western part of the cliff has been much more stable over time than the eastern segment. The historical data indicates that annually 0.35 m^3 of material is to be expected on average, with the great majority from the eastern part of the face. It is also probable that the rate of accumulation has declined over time following the retreat of the sea from the base of the cliff, so this estimate may well be high (Bell, 1996).

5.3 Rockfall trajectory prediction at Marine Tavern site

In this section, rockfall trajectories from the cliff face are predicted by computer simulation of rockfalls on 15 profiles along the cliff face using the CRSP and RocFall programs. Profile surveying data from Eliot Sinclair and Partners Ltd. has been used for the simulations. Source areas are assumed to be along near-vertical or overhung slope segments where rockfalls are more likely to occur. Parameters were determined from field investigation and the results from previous tests. Rockfall characteristics at four different positions has been analyzed. To effectively retain rockfalls from the cliff, a ditch and bund protection system has been designed by Bell (1996), the position of which has been further assessed by the simulations.

5.3.1 Parameter input

Sections: Survey data of the profiles for simulation are provided by Eliot Sinclair and Partners Ltd, which are derived from stereoscopic ground photographic pairs. Slope information for the lower parts of the agglomerate slopes are uncertain due to blockage from building and trees, which will affect the simulation results. In total 15 sections spaced at 6 m interval have been used in the simulation. The

locations of the sections are shown in figure 5-1, while survey data for those sections are shown in Appendix C.

Source areas: As described above, the most likely source areas of rockfalls are from the agglomerate cliff face, and two source areas of fractured rock (areas A & B) have been identified on the eastern part of the cliff, while two other areas (areas C & D) of potential long-term concern have also been identified. For computer simulation, source areas are assumed to be along near-vertical or overhung segments and above flatter parts of the slope which would give a ski-jump effect to falling rocks, and this would provide a conservative result. Generally two source zones are used for each section (figure 5-2): **zone1** on the upper part and **zone2** on the lower part of the slope. Zone2 is among agglomerate cliff face and is the major source of rockfalls, while zone1 is in agglomerate or basalt face and is considered a minor source.

Boulder size: Investigations on the cliff face and the debris apron showed that blocks are generally 0.1–0.3 m in diameter, with maximum block size 1.2 m. The diameter of 0.3 m is thus used for the simulations. To examine the effect of boulder size on the simulation results, simulations with diameter 0.8 m (used by the previous study) have also been done on certain sections. It is considered that smaller rocks will travel further down the slope.

Coefficient of restitution and surface roughness: Field measurement showed that the average Schmidt number of the agglomerate is 38, according to the equations in chapter 3, the normal coefficient of restitution is calculated as 0.21 (±0.04). As discussed in chapter 4, the calculated value needs to be adjusted because the surface of the agglomerate is often rough and coated with ash materials. Because the surface conditions of the agglomerate are similar to those of the rubbly basalt in Lyttelton, which has an average Schmidt number of 35.6 in the field (similar to that of agglomerate) and 48 on fresh surface, the coefficients of restitution of the rubbly basalt in Lyttelton were adopted for the agglomerate in this analysis. As the agglomerate is composed of hard blocks as well as weak ash matrix, the actual coefficient of restitution should be smaller than that of the rubbly basalt.

The coefficients of debris materials were also determined according to field tests in Lyttelton. The coefficients of restitution for the car park (asphalt surface) were determined according to its relative hardness to rock and debris (weaker than rock so that its value of Rn is determined smaller than that of rock slope but larger than debris).

Slope roughness has been measured at the lower part of the agglomerate slope and the debris slope using a compass and a straight edge of 0.3 m long (Appendix C). The slope angle of the upper part of the slope has not been measured due to difficulty of access, and the surface roughness the lower part is adopted. Coefficients of restitution (Rn, Rt) and surface roughness (Rf) for different slope materials in the simulation are shown in table 5-1:

Table 5-1: Parameters for rockfall simulations

Slope	Rn	Rt	Rf
Rock slope	0.3	0.85	15°
Debris slope	0.17	0.70	10°
Car park (asphalt)	0.25	0.80	0°

Analysis points: To collect data about rockfall characteristics at particular positions concerned, four analysis points have been selected -- Point1: edge of the car park, Point2: 1m from the edge of the car park, Point3: original site of the proposed garage, Point4: site of the proposed tower block. Although the plan for the tower block was rejected and the garages were relocated as a result of previous rockfall assessment by Bell (1996), rockfall trajectory analysis have been planed for these sites in this study as an application of rockfall trajectory analysis.

Ditch and bund: A protection ditch was designed by bell (1996) to protect the proposed tower block from rockfall impact but not built as the proposal was rejected, which includes a catch ditch, a 2 m high engineered rock bund and a 1.8 m high wire mesh fence placed on top. The position of the inner side of the bund has been further assessed by simulations in this study.

Table 5-2: Computer simulation results (bounce height) of Marine Apartment

Section No	Source Zone	Type	Bounce height (m)												Bund Position (m)
			Point1			Point2			Point3			Point4			
			max	mean	N%	max	mean	N%	max	mean	N%	max	mean	N%	
0	Zone1	crsp	1.81	0.12	99.5	0.22	0.04	98.9							15
		roc	0	0	32	0	0	2							10
6	zone1	crsp	1.84	0.59	78	0.49	0.1	77.8							20.1
		roc	3.08	0.4	100	1.65	0.22	100							19
6	zone2	crsp	1.44	0.16	85	0.35	0.06	85							
		roc	0.86	0.11	98.8	0.26	0.08	81.8							
12	zone1	crsp	0.99	0.01	62.2	0.28	0.05	49.6				0	0	0	17.5
		roc	1.13	0.34	67.8	0.66	0.15	28.5				0	0	0	17.5
12	zone2	crsp	0.24	0.03	99.8	0.19	0.03	99.8				0	0	0	
		roc	0.01	0	3.75	0	0	0				0	0	0	
18	Zone1	crsp	0.54	0.05	99.8	0.13	0.01	99.8	0.25	0.05	99.8	0	0	0	15.6
		roc	0	0	3.75	0	0	0	0.39	0.11	20.3	0	0	0	15.6
24	zone1	crsp	0.69	0.09	87.1	0.05	0	86.5	13.8	3.91	99.6	0	0	0	21.2
		roc	1.54	0.54	66	1.08	0.27	53.3	11.1	2.47	100	0.16	0.08	25.5	21.5
24	zone2	crsp	0.62	0.06	39.9	0.06	0	39.2	0.16	0.01	56.7	0	0	0	
		roc	0	0	0.5	0	0	0	0.89	0.14	22.3	0	0	0	
30	zone1	crsp	0.08	0.01	97.1	0.08	0	93.6	7.74	0.77	99.8	0	0	0	18.5
		roc	0.01	0	3.75	0	0	2	1.26	0.42	97	0	0	0	19
30	zone2	crsp	0.14	0.01	73.2	0.14	0.01	68.4	0.2	0.01	83	0	0	0	
		roc	0	0	0	0	0	0	2.98	0.16	49.8	0	0	0	
36	zone1	crsp	0.17	0.03	97.8	0.04	0	97.2	20.1	18.3	99.5	0	0	4.25	24
		roc	1.09	0.14	52.5	0.55	0.11	20.8	19.7	17	100	0.16	0.11	16.8	24
36	zone2	crsp	0.1	0.01	21.7	0.01	0	20.5	0.06	0	23.8	0	0	0	
		roc	0	0	0.25	0	0	0	4.22	0.68	75.3	0	0	0	
42	zone1	crsp	0.17	0.02	91.7	0.02	0	90.3	11	1.3	91.8	0	0	0	18.5
		roc	0	0	1.75	0	0	0	6.48	0.76	100	0	0	0	18.5
42	zone2	crsp	0.08	0.01	26.1	0	0	20.7	0.13	0.02	27.2	0	0	0	
		roc	0	0	0	0	0	0	5.74	1.03	77.8	0	0	0	
48		crsp	1.21	1.01	99.8	1.06	0.62	99.7							17.5
		roc	1.71	0.87	26.3	1.51	0.42	16.3							23.5
54	zone1	crsp	2.16	0.54	74	1.21	0.15	73	15.7	11.2	97.2				24
		roc	9.18	1.49	74.3	7.95	1.12	71.3	16.9	12.5	89.8				30
60	zone1	crsp	1.45	0.43	51.8	0.83	0.04	51.7	14	5.95	79.7				20
		roc	2.38	1.04	25.3	2.18	0.6	25	12.1	2.99	60.5				24
60	zone2	crsp	0.91	0.28	16.5	0.07	0.01	16.4	9.26	5.5	22.8				
		roc	1.14	0.19	4.25	0.49	0.2	1.25	6.01	1.45	90.3				
66	zone1	crsp	0.8	0.5	15	0.51	0.08	11.8							20.1
		roc	0	0	0	0	0	0							20
66	zone2	crsp	1.16	0.74	81.7	1.05	0.4	87.4							
72		crsp	0.11	0.02	99.8	0.14	0.04	99.8							15.2
		roc	0	0	0	0	0	0							16
78		crsp	0.1	0.03	91.3	0	0	77.5							22.2
		roc	0	0	0	0	0	0							20
84		crsp	0.2	0.02	99	0.17	0	79.8							23.2
		roc	0	0	0	0	0	0							21

5.3.2 Simulation results

CRSP and RocFall simulations for the 15 sections have been performed. Bounce height, velocity and percentage of rocks passed (N%) at the four analysis points and the bund position (distance from top of the cliff to the inner side of the bund) are shown in table 5-2 and table 5-4. The bund positions were determined by simulations of rockfalls from zone1, with slope geometry changed on the lower part of the slope (with a ditch and bund replacing the debris apron). An analysis point is set at the inner side of the bund, and the bund position was determined by moving from near the cliff base outward until no rocks reached the analysis point (as shown in figure 5-7). Simulation results with boulder diameter 0.8 m are shown in table 5-3. The following conclusions can be drawn from the results:

1) A majority of the rocks from the cliff face reach the edge of the car park (point1), with maximum bounce height more than 2 m, indicating that vehicles in the row close to the edge are prone to rockfall hazards without protection measures. The site of the proposed tower block (point4) is generally not affected by rockfalls, only a few rocks from sections 24 & 36 reach this position, with very small bounce height (0-0.6 m). This result is similar to that from previous study (Bell, 1996).
2) Rocks from zone1 bounce higher and travel further down the slope. In fact the bounce heights of rocks from zone2 at point1 & 2 for most sections are very small. Considering the small probability of rockfalls from near the top of the slope where basalt and agglomerate rocks are less fractured, the probability of rocks reaching the car park would be small. That explains why there is no reported car damages from the car park so far. Figure 5-5 shows the difference of trajectories of rockfalls from zone1 and zone2.
3) Bounce heights of rocks with diameter 0.8 m are smaller than those of rocks with diameter 0.3 m (table 5-3), indicating that analysis results with diameter 0.3 m are on the safe side in terms of rockfall hazards because a worse condition is considered.

Table 5-3: Simulated bounce heights of boulders with different diameters (CRSP simulation, source zone1)

Section No	Diameter (m)	Bounce height (m)												Bund* Position (m)
		Point1			Point2			Point3			Point4			
		max	mean	N%	max	mean	N%	max	mean	N%	max	mean	N%	
24	0.3	0.69	0.09	87.1	0.05	0	86.5	13.8	3.91	99.6	0	0	0	21.2
	0.8	0	0	0	0	0	0	12.4	6.26	63	0	0	0	21.2
36	0.3	0.17	0.03	97.8	0.04	0	97.2	20.1	18.3	99.5	0	0	4.25	24
	0.8	0.03	0	2.5	0.02	0	2.5	19.2	18	99.5	0	0	0	22
54	0.3	2.16	0.54	74	1.21	0.15	73	15.7	11.2	97.2				24
	0.8	1.04	0.4	95.3	0.69	0.18	95.3	14.6	13.5	99.8				24
66	0.3	0.8	0.5	15	0.51	11.8	3.75							20.1
	0.8	0	0	0	0	0	0							18

* Bund position is from top of cliff, N% is percentage of rocks passed.

Table 5-4: CRSP simulation results (velocity)

Section No	Source Zone	Velocity (m/s)								Bund Position (m)*	
		Point1		Point2		Point3		Point4			
		max	mean	max	mean	max	mean	max	mean	Ritchie	crsp
0		18.9	9.25	10.3	7.23						15
6	zone1	19.6	12	15.2	8.5					21.1	20.1
	zone2	14.4	8.12	13.9	6.87						
12	zone1	23.8	5.84	23.8	4.68					18.9	17.5
	zone2	9.36	5.35	9.67	5.61						
18		11.9	7.8	9.6	6.98	10.8	7.33			20	15.6
24	zone1	8.57	6.47	6.51	4.89	25	14.4			14	21.2
	zone2	10.6	6.13	10.4	4.87	10.4	5.23				
30	zone1	5.95	4.56	5.8	4.24	26.2	10.5			14.1	18.5
	zone2	8.39	4.95	8.09	4.75	9.77	6.18				
36	zone1	8.93	6.62	7.67	5.77	15.6	11.9	5.3	3.88	16.2	24
	zone2	7.23	5.7	6.14	5.06	6.06	4.94				
42	zone1	7.93	6.05	7.25	5.55	26.3	12			11.1	18.5
	zone2	6.23	5.02	5.91	4.7	7.05	5.87				
48	zone1	7.94	7.11	8.44	7.1					12.8	17.5
	zone2	8.9	7.19	9.25	7.66						
54	zone1	22.3	7.74	22.6	6.87	20.1	13.5			14	24
	zone2	0	0	0	0	0	0				
60	zone1	9.04	6.97	9.66	5.14	26.1	18.1			15.7	20
	zone2	7.86	6.72	7.96	4.51	19.9	13.2				
66	zone1	9.25	5.47	9.52	4.14					20.3	20.1
	zone2	9.45	6.97	9.93	7.1						
72		10.3	6.26	9.77	5.85	11.3	7.78			21.4	15.2
78		9.75	6.28	9.42	6.37					22.4	22.2
84		9.79	6.02	9.85	6.07					24.5	23.2

* Bund position is from top of cliff.

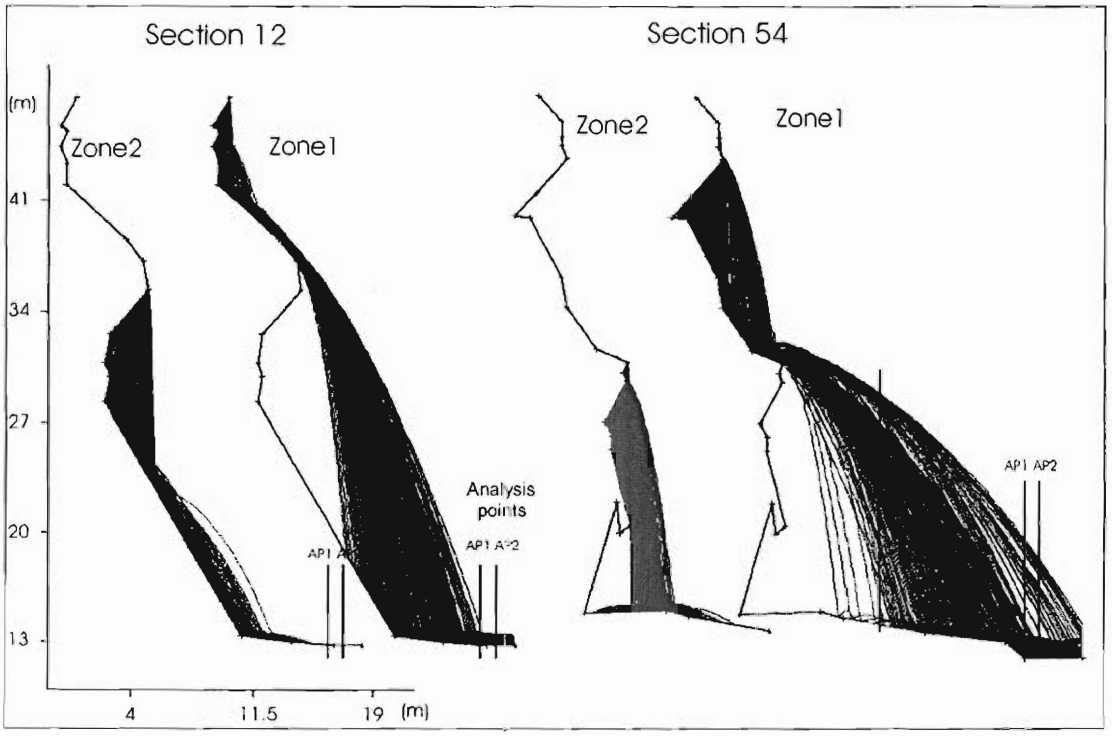

Figure 5-5: Picture showing the trajectory difference of rocks from source zone1 and zone2 (RocFall simulation)

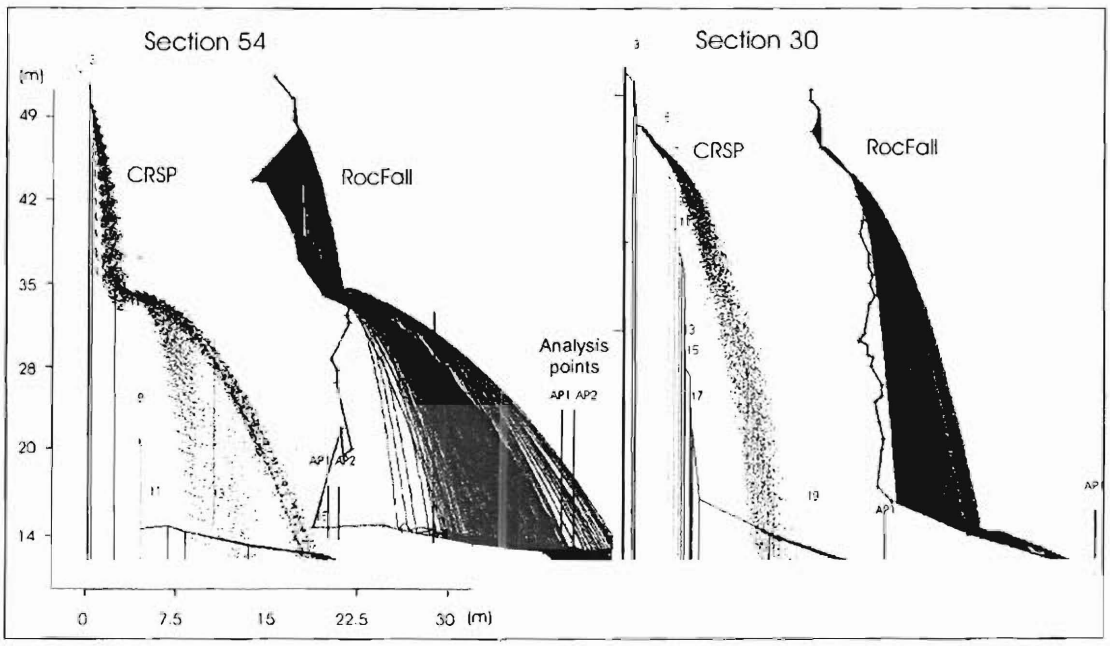

Figure 5-6: Picture showing the ski jump effects of CRSP and RocFall simulations.

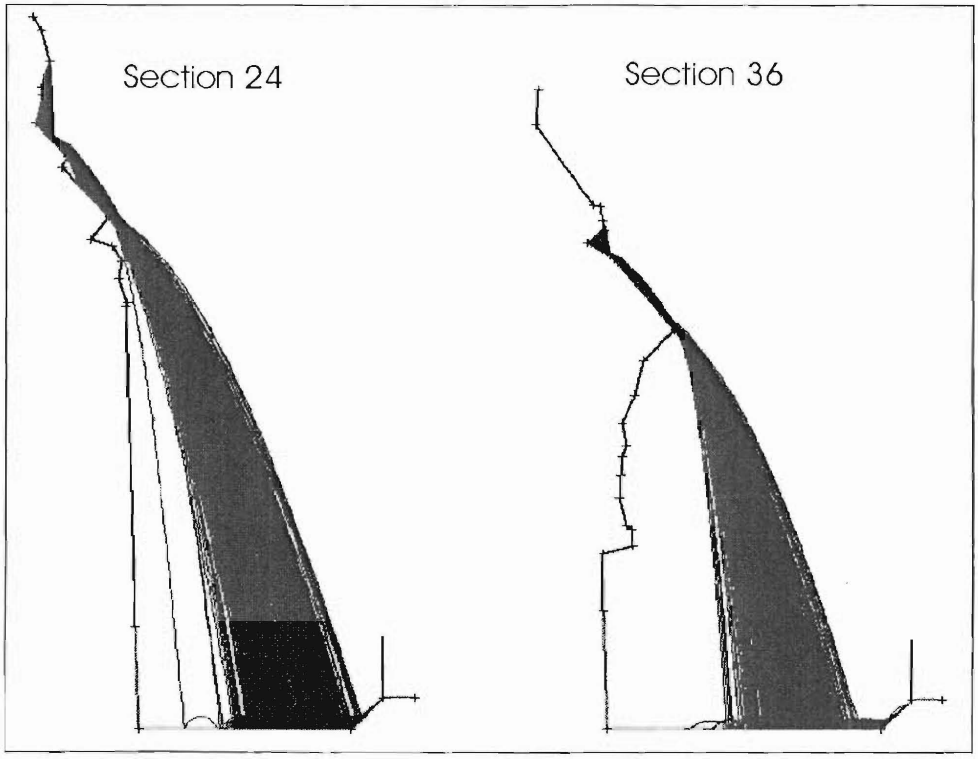

Figure 5-7: RocFall simulation to determine bund position

4) Bounce heights from RocFall simulation are generally smaller than those from CRSP simulation; however, they are higher at sections 12, 24, 36, 54 and 66 where significant flat slope segments exist below zone1 (figure 5-6). This indicates that the ski-jump effect is more obvious in the RocFall simulation.
5) The results for bund positions from simulation are compared with those determined from Ritchie's criteria (table 5-4). The results show that the distances between the bund and the cliff from simulations are close to those from Ritchie's method at the steep sections, while for sections with a significant flat slope segment below zone1 (such as sections 12, 24, 36, 54) the simulated distance is larger due to the ski jump effect. Ritchie's method is based on uniformly shaped excavated slopes and does not take irregular slope geometry into account. Although the overall slopes of those sections are steep, there is a flat segment between two very steep slope segments which causes rocks from above (zone1) to bounce further away from the cliff face as shown in figure 5-5 and figure 5-7, while this effect is not accounted for in Ritchie's method which uses an average slope angle. However, because the bund positions are determined in the simulations by

rockfalls from zone1 which is only a minor source of rockfalls, the above ski jump effect might have been over estimated.

5.4 Rockfall hazard rating

5.4.1 Rockfall Hazard Rating System (RHRS)

The RHRS is a system of determining the priority of rock slopes in highway rockfall management, developed by the United States Department of Transportation. The severity that a rock slope is subject to rockfall hazards is assessed in this system by several factors. It allows highway agencies to better allocate their mitigation funds when dealing with large number of rock slopes. The process involves the following steps:

1) Slope inventory: Creating the database of rockfall locations.
2) Preliminary rating: Grouping rockfall sites into three broad, manageable sized categories and deciding the priority of slopes for detailed rating.
3) Detailed rating: Prioritising the identified rockfall sites for rockfall management.
4) Preliminary design and cost estimate: Adding remediation information to the rockfall database.
5) Project identification and development: Advancing rockfall correction projects toward construction.
6) Annual review and update: Maintaining the rockfall database.

The detailed rating considers 12 factors which contributes to the overall rockfall hazard (table 5-5). The four benchmark criteria to the right of the table correspond to logical breaks in the increasing (in logarithmic scale) risk associated with each category. The scores for each category are then totalled and the slopes with higher scores present greater risk. The scoring system is explained in detail in the RHRS Participant's Manual (1993).

5.4.2 Detailed rating for Marine Tavern site

The RHRS system has been developed for highway rockfall management. It deals with rockfall hazards to vehicles on highways, but can be adopted to evaluate rockfall hazards to vehicles in the car park at Marine apartments.

Table 5-5: Rockfall Hazard Rating System

Category			Rating criteria and score			
			Point 3	Point 9	Point 27	Point 81
Slope height			25 ft	50 ft	75 ft	100 ft
Ditch effectiveness			Good catchment	Moderate catchment	Limited catchment	No catchment
Average vehicle risk			25% of the time	50% of the time	75% of the time	100% of the time
Percent of decision sight distance			Adequate sight distance, 100% of low design value	Moderate sight distance, 80% of low design value	Limited sight distance, 60% of low design value	Very limited sight distance, 40% of low design value
Roadway width including paved shoulders			44 ft	36 ft	28 ft	20 ft
Geology character	Case 1	Structural condition	Discontinuous joints, favourable orientation	Discontinuous joints, random orientation	Discontinuous joints, adverse orientation	Continuous joints, adverse orientation
		Rock friction	Rough, irregular	Undulating	Planar	Clay infilling or slickensided
	Case 2	Structural condition	Few differential erosion features	Occasional erosion features	Many erosion features	Major erosion features
		Difference in erosion rates	Small difference	Moderate difference	Large difference	Extreme difference
Block size Quantity of Rockfall/event			1 ft 3 cubic yards	2 ft 6 cubic yards	3 ft 9 cubic yards	4 ft 12 cubic yards
Climate and presence of water on slope			Low to moderate precipitation, no freezing periods, no water on slope	Moderate precipitation, or short freezing periods, or intermittent water on slope	High precipitation, or long freezing periods, or continual water on slope	High precipitation, and long freezing periods, or continual water on slope and long freezing periods
Rockfall history			Few falls	Occasional falls	Many falls	Constant falls

Because there is only one slope of 88 m long in this analysis, hazard rating is actually unnecessary in terms of RHRS. However, considering the difference between the eastern and western segments, and in order to see the hazard score of the slope, it was decided to perform a detailed rating on the eastern and western segments of the slope. Preliminary rating is not considered.

Table 5-6 shows the rating results for the eastern and western segments of the slope at Marine Tavern site. 11 categories have been scored according to the guidelines of the RHRS Participant's Manual. The category "Roadway width

including paved shoulders" is not applicable in this case because it is a car park rather than a roadway that is subject to rockfall. Scores of the two segments are different in the "ditch effectiveness", "geology structure", "climate and presence of water" and "rockfall history" categories.

Table 5-6: Rockfall hazard rating for Marine apartment site

Category	Eastern segment		Western segment	
	Value	Score	Value	Score
Slope height	124	100	123	100
Ditch effectiveness		27		18
Average vehicle risk		81		81
Percent of decision sight distance	100	3	100	3
Roadway width including paved shoulders				
Geology structure		50		27
Block size		3		3
Climate and presence of water on slope		18		6
Rockfall history		18		6
Total		300		244

- **Ditch effectiveness**: the debris apron between the base of the cliff and the car park can be treated as a ditch (as suggested in the RHRS Participant's Manual), the sketch plan of the site (figure 5-1) shows that the catchment zone in the western segment is wider than that in the eastern segment, but both provide limited catchments to rockfalls from the cliff face according to rockfall simulations.
- **Geology structure**: the agglomerates which form the majority of the cliff face are supported by weak ash matrix, with obvious differential erosion features. The agglomerates in the eastern segment are intensively fractured. Therefore, the eastern segment gets a score of 50 while the western segment receives a score of 27 according to the RHRS manual.
- **Climate and presence of water on slope**: due to the fracturing and lack of basalt cape in the eastern segment, the cliff face has a moderate to high precipitation and scored 18 in this category. The western segment is better protected by the basalt on top and less fractured and therefore gets a lower score.

- **Rockfall history**: rockfalls of this site are occasional but according to the volume of debris in the two segments, the eastern segment gets a higher score.

The rating result shows that the eastern segment has a higher total score and therefore priority should be given to the eastern segment for rockfall protection.

5.5 Risk assessment of rockfalls at Marine Tavern site

5.5.1 Introduction

Varnes (1984) defined risk as a measure of the probability of an event and the resulting death, injuries or damage. Risk is expressed in several forms depending on the entity at risk. For natural hazards, the two most commonly used risk parameters are the probability of an individual death, PDI (Morgan 1991 and 1992, Ale 1991) and the probability of death to the exposed population for specified time period, P(D) (Whitman 1984, Salmon 1994, Ale 1991). Bunce (1994) presented a methodology of risk analysis for rockfalls on highways. The annual probability of an accident and the annual probability of an individual's vehicle being in an accident were used in his rockfall risk calculation. By calculating these parameters, it is possible to compare rockfall risks to other published risk levels for natural hazards, engineering projects and specific activities and occupations.

The Canadian Standards Association (CAN/CSA 1991) presented several forms of risk analysis. "Methods of Analysis of Engineering Systems" was chosen by Bunce (1994) for the quantification of risk posed by rockfalls on highways. Six stages are considered in risk analysis, including scope definition, hazard identification, risk estimation, documentation, verification and analysis update.

Risk analysis methods proposed by Bunce (1994) include frequency and consequence analysis, selection of either qualitative or quantitative analysis methods, fault tree and event tree analysis, and calculation of risk parameters. The event tree analysis and risk calculation provide a quantitative expression of

risk and will be applied to the risk analysis of this site, the calculated risk will then be compared to other published level of risks to see whether it is acceptable.

5.5.2 Event tree analysis

The event tree analysis considers a range of possible events that lead to specific outcomes. In this case the outcome is a fatality by rockfalls, the initial event is rainfall. The probability of occurrence for each event in a sequence is determined based on analysis of site conditions, from which the probability of rockfall fatality is derived. Figure 5-8 shows an event tree analysis of roclfalls at the car park of Marine apartments.

The probability of each event has been determined based on the following assumptions:

1) The probability of occurrence of rain heavy enough to initiate rockfall event is estimated as 15 days per annum or 4%.
2) The probability of a rockfall being triggered by heavy rain, based on the debris accumulation rate and rockfall history of the site, has been estimated as 5%.
3) The probability of a falling rock reaching the car park is estimated as 15% of rockfalls from the cliff face according to rockfall trajectory analysis (average percentages of falling rocks reaching car park are 82.9% for zone1 and 29.6% for zone2, the area percentages of zone1 and zone2 are 10% and 20% of the cliff face respectively).
4) The probability of a vehicle parking in the row close to the cliff being impacted by a rockfall is estimated as 3.4% given that a fockfall event occurs, assuming that an average of 4 vehicles are present in the row during daytime (12 hours), the average width (direction of vehicle perpendicular to cliff face) of vehicles be 1.5 m. The probability is: 1.5*2/88 = 3.4%.
5) Rocks with bounce height over 1 m are considered to be able to cause fatalities (hit people in a vehicle). According to trajectory analysis, the percentage of rocks with bounce height over 1 m is 5% of rocks reaching the car park. Assuming that the average parking time for each vehicle is 1

hour and the time that people are inside the vehicle is 2 minutes, the probability of people being hit in a rockfall accident (given the vehicle is impacted) is 5%*2/60 = 0.17%

6) As the Marine apartment is now the place of a bar, the number of occupants impacted has been estimated between 1 and 2 for the most cases.

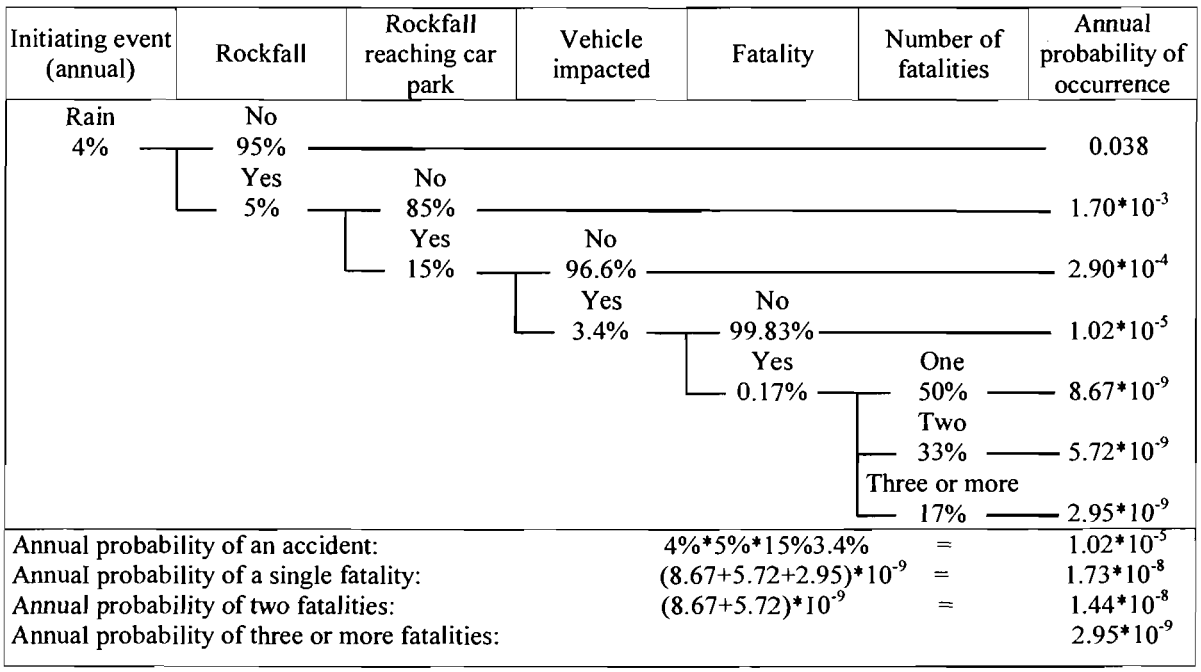

Figure 5-8: Event tree analysis of Marine site

The above-calculated probabilities of accident and fatalities are very low, for example, the probability of accident is $1.02*10^{-5}$ which is equivalent to one event in 98,000 years. The annual probability of rainfall (4%) is actually a daily probability because there will always be heavy rain during the period of a year (15 days). This may have explained the very low probabilities obtained. It is decided to use such a percentage value in order to be consistent with other authors (Bunce 1994, Rayudu 1997, Hoek 1998). The calculated risk in figure 5-8 is to be compared with the level of risks from other engineering projects and guidelines in section 5.5.4.

5.5.3 Risk calculation

Bunce (1994) used two parameters to calculate probability in his rockfall risk calculation:

$$P = P(S:H)*P(T:S)$$

where P(S:H) is the probability of a spatial impact, i.e. that a vehicle is affected by a rockfall given that a rockfall occurs. P(T:S) is the probability of a temporal impact, i.e. that the vehicle occupies the location of the rockfall impact given that it occurs. The probability of at least one accident (P(A)) and the probability of an individual being in the accident (PAV) are calculated as quantitative expression of risk from rockfalls on highways.

Three different rockfall hazards have been identified by Bunce (1994): a falling rock hitting a moving vehicle, a falling rock hitting a stationary vehicle, and a moving vehicle hitting a fallen rock. Bunce (1994) provided different methods of risk calculation for each of the cases. The method for a falling rock hitting a stationary vehicle has been adopted to the calculation of rockfall risk to vehicles in the car park at the Marine site. The following assumptions have been made in the calculation:

- The temporal distribution of vehicles during daytime (12 hours) is uniform. The average number of vehicles in the row close to the cliff of the car park is 4 during 12 hours (equivalent to 2 throughout 24-hour period).
- The spatial distribution of vehicles is uniform in the row at risk.
- The spatial distribution of rockfalls within the cliff area is uniform.
- The timing of each rockfall is independent and therefore the temporal distribution of rockfalls is uniform.
- The vehicle location and the rockfall location are independent.

Risk of rockfalls at the Marine site is calculated using Bunce's method as follows:

1) The probability of accident (a vehicle being impactd by a rock):

The probability of a spatial impact given that a rockfall occurs, P(S:H) equals the fraction of the car park occupied by vehicles times the probability of a rockfall reaching the car park(Pr):

$P(S:H) = Pr*Fv = Pr*Nv*Lv*/Lc = 0.15*2*1.5/88 = 5.11*10^{-3}$

where Nv is the average number of vehicles at risk and is estimated as 4 at daytime or 2 for a day.
Lv is the average width of vehicles, Lc is the length of the car park under rockfall hazards.
Pr is the probability that a falling rock reaching the car park and is estimated as 15% by trajectory analysis in the previous section.

The probability that one or more vehicles are impacted by a rockfall is calculated using the following equation:

$P(S) = 1- \{(1- P(S:H)\}^{Nr}$

$= 1 – (1-5.11*10^{-3})^1 = 5.11*10^{-3}$

where Nr is the number of rockfalls per year and is estimated as 1 according to debris accumulation rate and historical record.

Since the car park is assumed to be occupied by an average of 2 vehicles throughout 24 hours, the temporal probability P(T:S) is unity. Therefore the probability of at least one accident:

$P(A) = P(S) *P(T:S) = 5.11*10^{-3}*1 = 5.11*10^{-3}$

As stated in the previous section, the probability of people being hit by a rockfall is 0.17% given that a vehicle is impacted. Therefore the probability of fatality:

$P(F) = 5.11*10^{-3}*0.17\% = 8.69*10^{-6}$

2) The probability of an individual vehicle being in an accident

$P(S:H) = Pr*Fv = Pr*Lv/Lc = 0.15*1.5/88 = 2.55*10^{-3}$

$P(S) = 1- \{(1- P(S:H)\}^{Nr}$

$= 1 – (1-2.55*10^{-3})^1 = 2.55*10^{-3}$

The probability of a temporal impact given that a rockfall occurs equals the proportion of a year the vehicle occupies the section of the car park:

P(T:S) = t / 8760

Assuming the time a vehicle parking in the car park is 1 hour and for a single trip per year:

$P(T:S) = 1/8760 = 1.14*10^{-4}$

The probability of an individual vehicle being in an accident:

$PAV = P(S)*P(T:S) = 2.55*10^{-3} * 1.14*10^{-4} = 2.91*10^{-7}$

The results show that the risk of an accident (a vehicle being impacted by a rockfall from the cliff face) is moderate ($5.11*10^{-3}$, equivalent to one in 195 years), which is reasonable as there have been no reported accidents and injuries at this site in more than 100 years. The risk of fatality (people being hit by a rockfall) ($8.69*10^{-6}$) and the risk for a particular vehicle for one trip per year ($2.91*10^{-7}$) are very low. The calculated risk will be compared with the acceptable risks in other engineering projects in the following section.

The above probabilities are calculated based on the assumption that 1 rockfall event occurs in a year. That is estimated according to debris accumulation rate (0.35 m^3 per year, equivalent to 3 rocks of 0.3 m in diameter), considering that the accumulation rate has declined over time since the retreat of the sea from the base of the cliff (Bell, 1996) and that not all the debris apron has been formed by individual rockfalls.

5.5.4 Comparison of risk level

Figure 5-9 is a summary of published and proposed guidelines for tolerable risk of fatalities for "Major Civil Engineering Projects" (Nielsen 1994). The hazard posed by rockfalls can be compared with the hazard posed by major civil engineering projects because both of these come under "occasional major risks" and the risks to the public must be reduced to acceptable levels. The so-called "acceptable levels" may vary from different counties and different times.

The calculated probabilities of fatalities of this site from event tree analysis and from risk calculation have been plotted against the risk criteria in figure 5-9. The

results show that both the estimated risks from event tree analysis and the calculated probability of fatality are under all the proposed risk acceptable guidelines. This indicates that the level of risk of fatalities from rockfalls at the Marine Tavern site is low and acceptable according to the risk guidelines.

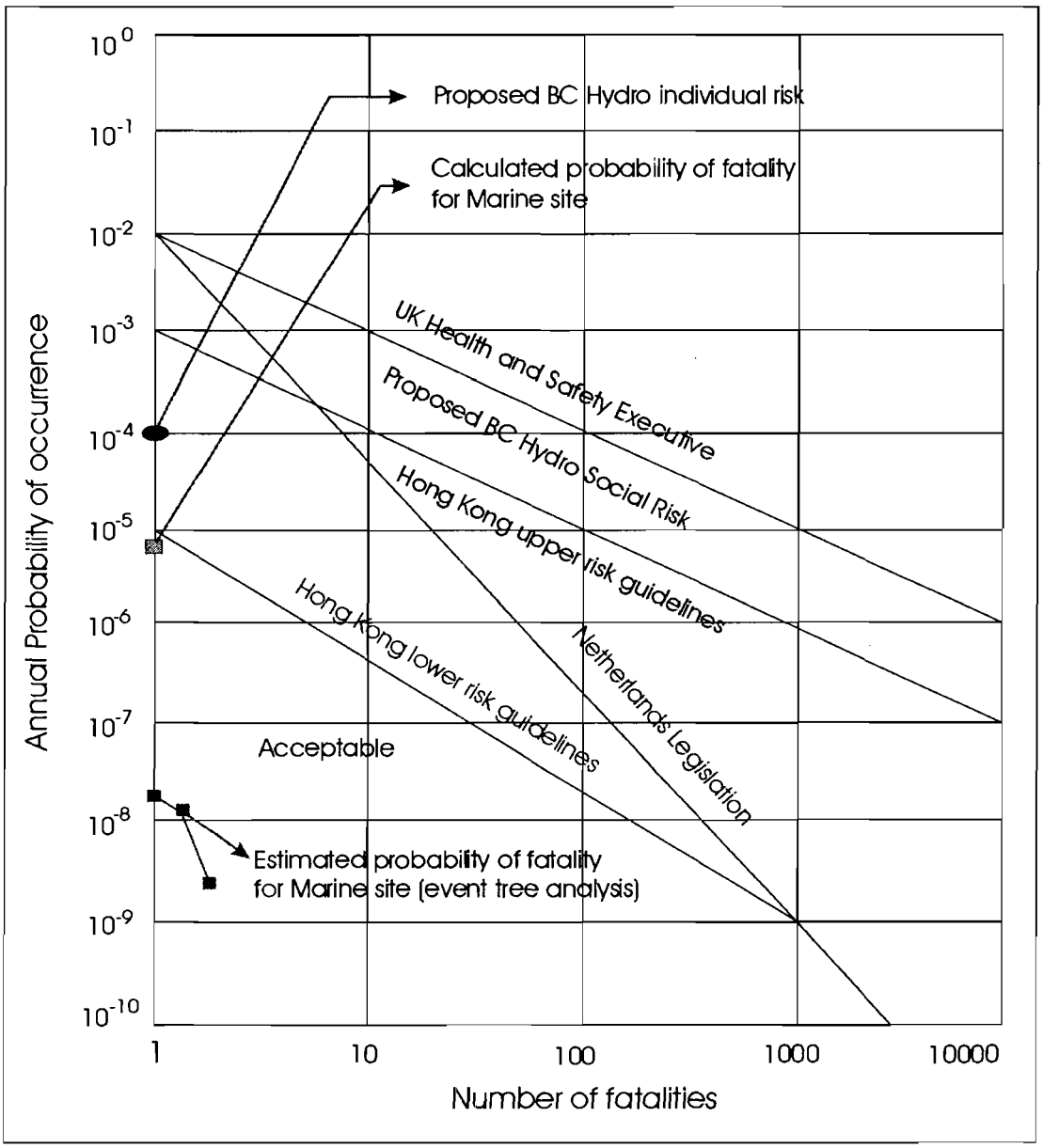

Figure 5-9: Comparison between calculated risk of fatality and published and proposed acceptable risk criteria.

5.6 Conclusions and discussion

Site investigation, rockfall trajectory analysis and risk evaluation at the Marine Tavern site have led to the following conclusions:

1). The cliff face consists mainly of agglomerate poses a rockfall hazard to the car park and the proposed buildings below. The blocks among the agglomerate are supported by weak ash matrix and the agglomerate is intensively fractured in certain areas. Overhung slopes are common in the cliff face. Two source areas of intensively fractured rock each about 5x5 m have been identified on the eastern part of the cliff, and two other areas of potential long-term concern have also been identified in the western segment. Historic data suggest that only minor episodic debris release from the cliff face has occurred during the last 100 years. Analysis of data from debris accumulations forming the talus apron at the base of the cliff suggests an average rockfall volume of 0.35 m^3 per year since the initial cliff formation by sea erosion some 6,500 years ago, with a majority in the eastern segment.

2). Computer simulations of rockfalls from the cliff face by two programs show that a majority of rocks from the upper part of the cliff (zone1) reaches the edge of the car park, which suggests that rockfall hazards to the car park need to be assessed.

3). Risk analysis of rockfalls from the cliff face suggests that the annual probability of at least one vehicle being impacted by a rockfall is moderate ($5.11*10^{-3}$ or one in 195 years), the probability of fatality (people being hit by a falling rock) ($8.69*10^{-6}$) is low and acceptable according to the proposed risk criteria for "Major Civil Engineering Projects".

4). The simulated bounce heights from the program RocFall are generally smaller than those from CRSP, the reason for that are thought to be the value of the recommended coefficient of restitution in chapter 4. However, RocFall gives a larger bounce height for slopes with significant flat slope segment at the upper part. Considering the experience of simulations in chapter 4, it is concluded that CRSP provides a more reasonable result for such conditions as at Lyttelton Quarry and the Marine Tavern site.

5). As the calculated risk of accident (one in 195 years) in the car park is significant rockfall prevention measures are needed for vehicles in the car park. The proposed ditch and bund protection system is a long-term solution. Before this system could be constructed, simple measures such as a fence at the edge of the car park should be considered. Warning sign should be erected at entrance of the car park.

Chapter 6

Conclusions

6.1 Investigation programme

This project has been focused on the coefficient of restitution – a key parameter in computer rockfall simulations which is difficult to determine. All the works have been planned and carried out to achieve the three main objectives: to find an easy method of determining the coefficient of restitution through laboratory tests, to verify the method under field conditions and to conduct rockfall trajectory analysis and risk evaluation at a particular site. The process and overall achievements of the programme are summarised as follows (results from each stages of the research will be presented in the following sections):

6.1.1 The first objective has been achieved through two stages of laboratory tests. The process and results are described in Chapter 3. The first stage of laboratory tests is a series of impact tests with simplified conditions sirnilar to those assumed in the algorithms of computer simulation programs. Quasi-spherical rock balls and rock slabs made from 23 different rock specimens were used in these tests. After obtaining the coefficients of restitution of different combinations of rock ball, rock slab and slope angle, the relationship between the coefficient of restitution and the Schmidt number of rocks and the slope angle has been studied through regression analysis. The relationships between the coefficient of restitution and other rock properties such as the dynamic modulus of elasticity and the rolling friction coefficient have also been studied to find possible ways of determining the coefficient of restitution. Finally an empirical equation to calculate the coefficient of restitution from the Schmidt number of rocks and slope angle has been established. This provides an easy and practical means of determining the coefficient of restitution. The second stage of the laboratory tests tried to verify the results of the first stage with more practical conditions. Three different

rocks of local significance have been used in this test. Angular rock boulders were dropped on to large rock blocks which were set to different angles. The result confirmed the correlation concluded in the first stage, indicating that the method established by the first stage could be used for more practical conditions. The effect of the impacting velocity on the coefficient of restitution have been studied by releasing boulders from different heights (0.6, 1.0, 1.5, 2.0, 2.5, 3.0 m) in the laboratory, and tests have also been carried out on beds of soil, gravel, sand and fragment to find the coefficients of restitution of these materials. Summarised results from field tests will be presented in section 6.2.

6.1.2 For the second objective, field parameter tests and a rockfall field trial have been carried out at Lyttelton Quarry. Large basalt boulders were dropped on to rock and debris slopes with an excavator to obtain the coefficient of restitution. Forty rock boulders were rolled down a bench slope of 16 m to test for rockfall behaviours. The results were then compared with rockfall simulations on the same slope by two programs. Results from field tests will be summarised in section 6.3.

6.1.3 The third objective is an application of rockfall analysis, which has been presented out in Chapter 5. Site investigations have been carried out to identify rockfall hazards; computer simulations of rockfalls were carried out at the Marine Tavern site. Rockfall hazards have been assessed using the RHRS rating system, risk from rockfall hazards have been calculated and evaluated at this site. Summarised results for this analysis will be presented in section 6.4.

As there has not been a simple method to determine the coefficient of restitution so far, the works of this research are undoubtedly significant in this area although the proposed approach is limited to the normal coefficient of restitution and needs to be tested with more practical situations. The Schmidt hammer test is a simple, non-destructive method for evaluation of rock strength. It is easy to carry out in the field. To determine the coefficient of restitution by Schmidt hammer test is therefore preferable for practical use. The rockfall analysis carried out at the Marine Tavern site is helpful for the property owner and local authorities to make decisions to mitigate rockfall hazards at this and other similar sites.

6.2 Conclusions from Laboratory tests

6.2.1 Laboratory tests with rock balls impacting rock slabs shows that there is a linear relationship between the normal coefficient of restitution and the Schmidt numbers of both the rock slabs and the falling rock balls. The correlation is better (R^2 >0.6) for rocks with higher value of Schmidt number (such as granite and basalt). However, such a correlation does not exist for the tangential coefficient of restitution.

6.2.2 A comprehensive equation to calculate the normal coefficient of restitution through the Schmidt numbers and slope angle are established through regression analysis of the data from the tests:

$$Rn = -0.110 + 0.00919N1 + 0.00392N2 + 0.00358A \quad (R^2 = 0.82) \qquad (1)$$

where N1, N2 are the Schmidt numbers of the rock slope and the falling rock, A is the slope angle (degree).

6.2.3 The coefficients of restitution (especially the normal coefficient) obtained from laboratory tests with angular rough rocks are much smaller than those with simplified conditions (rock balls and polished slabs). The value of Rn for basalt ball on basalt block is 0.82 while that for angular basalt boulders on basalt block is 0.3. This indicates that shape effect is a major concern in determining the coefficient of restitution. The normal coefficient of restitution obtained from tests correlates linearly with those calculated from rock properties using equation(1):

$$Rn = -0.0912 + 0.487Req \quad (R^2 = 0.88) \qquad (2)$$

where Req is the calculated normal coefficient of restitution.
Equations (1) and (2) can be used to determine the normal coefficient of restitution for rockfall analysis but the Schmidt number measured in the field should be examined.

6.2.4 Coefficients of restitution for debris, soil, sand and fragment materials obtained from laboratory tests show that the coefficients (especially the tangential coefficients) of those materials increase with the degree of compaction of the beds impacted. This suggests a possible way of determining the coefficient of restitution for debris and soil slope.

6.2.5 Analysis on the tangential coefficient of restitution has not achieved the expected result. Attempts to correlate the tangential coefficient of restitution with the Schmidt numbers and slope angle, the normal coefficient, and the rolling friction coefficient have all led to poor correlation results. This indicates that the tangential coefficient of restitution is not determined by the above parameters, and the factors affecting the tangential dynamic behaviour of impact are complicated (involving friction under dynamic conditions) and difficult to measure in as simple a way as that for the normal coefficient of restitution.

6.2.6 The density of falling balls affects the coefficient of restitution as it determines the impacting stress on the slabs. There is a difference between the coefficient of restitution obtained by steel balls and rock balls due to the different densities. Normal coefficient of restitution of a steel ball is smaller than that of a rock ball with the same Schmidt number value, because the steel ball with a larger density makes a larger indentation on the slab impacted.

6.2.7 The correlation between the coefficient of restitution and the dynamic modulus of elasticity is not obvious (with R^2 less than 0.2) according to analysis on the test data, possibly because of the reliability of test results due to the limited samples, and because the destructive effect of impact is not represented by the dynamic modulus of elasticity.

6.2.8 Impact tests carried out with rocks dropping from different heights onto rock slopes show that the normal coefficients of restitution are little changed or decrease slightly with the impact velocity with variable correlation coefficients (R^2 from 0 to 0.82), while the tangential coefficients increase linearly with the impact velocity (R^2 from 0.53 to 0.89). It is considered that the coefficient of restitution should decrease with the impact velocity because high impact energy will cause more deformation and fracturing on the rock slope and thus less restitution. A scaling factor is used to adjust the normal coefficient of restitution according to the impact velocity in some rockfall simulation programs. However, the result from this test are not consistent with that, possibly because of the scattering caused by shape effect and other impact conditions.

6.3 Conclusions from field tests

6.3.1 Coefficients of restitution for basalt and debris slope have been obtained from field tests in Lyttleton Quarry (Rn/Rt for massive basalt, rubbly basalt and debris slope are 0.25/0.77,0.23/0.66 and 0.17/0.68 respectively), which are similar to those from laboratory tests with angular rocks, indicating that the scale of test does not have much effect on the coefficient of restitution. However, the normal coefficient of restitution calculated by the empirical equations from laboratory tests is smaller than that from field test. This is because that the Schmidt number measured in the field is smaller than that measured in the laboratory due to weathering, defect and roughness of the surface. These effects are not so obvious for a rockfall impact with a larger energy and a larger contact area than the Schmidt hammer. Schmidt number measured in the field should be examined with field conditions when using the empirical equations to calculate the coefficient of restitution, and a proper way is to carry out the Schmidt measurement on fresh smooth rock surface.

6.3.2 The comparison between the field trial on a bench slope in Lyttelton Quarry and the computer simulation results on the same slope shows that there is a fairly good agreement between field trial and the results of CRSP simulation, while simulation results from RocFall are different from the field trial. This is possibly because that the recommended coefficient of restitution in RocFalll is higher than that of this site for the same slope material, and that the slope is rather small and steep. Computer simulations carried out for the Marine Tavern site suggest that bounce heights from RocFall simulation for slopes with a flat segment in the upper part are higher than those from CRSP, and reverse for steep slopes. The experience of this research suggests that CRSP provides a more reasonable result for the situations of Lyttelton Quarry and the Marine Tavern site.

6.4 Rockfall analysis at Marine Tavern site

6.4.1 Site investigations on the cliff face at the Marine apartments shows that the agglomerate cliff poses a rockfall hazard to the car park and the proposed

buildings at the base. Two source areas of intensively fractured rock have been identified on the eastern part of the cliff, and two other areas of potential long-term concern have also been identified on the western part. Debris accumulation rate has been estimated as 0.35 m^3 per year according to historic data.

6.4.2 Computer simulations of rockfalls from the cliff face by two programs (CRSP and RocFall) show that a majority of rocks from the upper part of the cliff (zone1) reaches the edge of the car park. The result suggests that rockfall hazards to the car park need to be assessed. Mitigation measures are needed to protect vehicles in the car park from rockfall hazards.

6.4.3 Rockfall hazards rating have been carried out on the eastern and western segments of the cliff using the RHRS system. The results show that the eastern segment is of higher priority with a score of 300 while the western segment is scored 244. Although the RHRS system is developed for highway slopes and for the management of large number of slopes, this analysis is still helpful by determining the scores and quantifying the difference of rockfall hazards between the eastern and western segments.

6.4.4 Risks of rockfalls to vehicles in the car park have been assessed through event tree analysis and a calculation method developed by Bunce (1994). The annual probability of an accident and a single fatality from event tree analysis is 1.02 $*10^{-5}$ and $1.73*10^{-8}$ respectively, while those from risk calculation are $5.11*10^{-3}$ and $8.69*10^{-6}$ respectively. Comparison between the calculated risks and proposed risk criteria for "Major Civil Engineering Projects" shows that the level of risk of fatality from rockfalls at the site is low and acceptable to the proposed criteria. The calculated probability of accident is significant (one in 195 years), suggesting that certain mitigation measures are needed at the car park although the expected loss from damages for a vehicle being impacted by a falling rock may not be high.

6.5 Discussions and future work

The method of determining the coefficient of restitution from the Schmidt hammer test is quite helpful for rockfall analysis. However, the measured Schmidt

numbers can vary dramatically for the same rock in the field, due to rock defect and surface properties. The determination of the coefficient of restitution should not only rely on the Schmidt hammer test and the equations, field conditions influencing the Schmidt measurement and restitution coefficient should also been taken into account. The Schmidt number should be examined carefully with field investigations and adjusted before being used for calculation.

Attempts at finding a method to determine the tangential coefficient of restitution has not been successful in this research. Shape effect and friction are main factors affecting the rebound behaviours in the tangential direction according to observations during the tests. Further work on the tangential coefficient of restitution could consider these factors.

The approach of determining the coefficient of restitution by Schmidt hammer test developed in this research is only applicable for clean rock slopes. Methods of determining the coefficients of restitution of soil and debris slopes have not been developed. Laboratory tests in this research show that the degree of compaction is an important factor, with compacted materials having higher coefficients of restitution. As quantitative measurement on the degree of compaction has not been made and bounce tests on materials with different degree of compaction has not been carried out in this study, it is not possible to analyse the relationship between the coefficients of restitution and the degree of compaction at this stage. Further work in this area could consider the possibility of determining the coefficient of restitution of debris and soil materials by the degree of compaction through a type of penetration test.

References

Aggistalis G., Alivizatos A., Stamoulis D. and stournaras G. (1996). Correlating uniaxial compressive strength with Schmidt hardness, point load index, Young's modulus, and mineralogy of gabbros and basalts (North Greece). Bull. International association of Engineering Geology, 54, pp.3-11.

Ale B.J.M. (1991). Risk analysis and risk policy in the Netherlands and the EEC. Journal of Loss Prevention in the Process Industry. Vol. 4.

Auberger M. and Rinehart J.S. (1960). Energy loss associated with impact of steel spheres on rocks. Journal of Geophysical Research. Vol.65, No.12, pp.4157-4164.

Azimi C., Desvarreux P. and Giraud A. (1982). Method of calculating the dynamics of rockfalls. Application to the study of a mountainside at La Pale (Vercors). Bull. Liasion Lab Ponts Chaussees, N122, Nov-Dec, pp.93-102.

Azzoni A. and de Freitas M.H. (1995). Experimental gained parameters, decisive for rockfall analysis. Rock Mech. And Rock Enging. 28(2), 111-124.

Azzoni A. Barbera G. LA. And Zaninetti A. (1995). Analysis and prediction of rockfalls using a mathematical model. International Journal of Rock Mechanics, Vol.32, No.7, pp709-724, 1995.

Azzoni A., Drigo E., Giani G.P., Rossi P.P., and Zaninetti A. (1992). In situ observation of rockfall analysis. Proceedings of the 6th International Symposium on Landslides, Christchurch, pp.307-314.

Azzoni A., Rossi P.P., Drigo E., Giani G.P. and Zaninetti A. (1991). In situ observation of rockfall analysis parameters. Proceedings of the 6th International Symposium on Landslides, Christchurch, pp.307-314.

Battle J.A. (1993). On Newton's and Poison's rules of percussive dynamics. American Society for Mechanical Engineers (ASME) Journal of Applied Mechanics, vol.60, pp.376-381.

Bell, D.H. (1996). Building on marginal land. Proceedings Tech Group IPENZ v.22, Issue 1(G), 87-100.

Bell. D.H. (1996). Rockfall Hazards Evaluation and Mitigation, Marine Apartments, Nayland Street, Sumnar. Report submitted to Marine Properties Ltd.

Bieniawski Z.T. (1976). Rock mass classification in rock engineering. Proceedings of the Symposium on Exploration for Rock Engineering. Balkema, Rotterdam, Vol.1, pp.97-106.

Bowman R. (1995). Coefficient of restitution as an indication of impact resistance. Standards Association of Australia, 1995.

Brach R.M. (1984). Friction, restitution, and energy loss in planner collisions. American Society for Mechanical Engineers (ASME) Journal of Applied Mechanics, vol.51, pp.164-170.

Brach R.M. (1988). An impact model with applications to erosion and wear. International Journal of Impact Engineering, Vol.7, No.1.

Brach R.M. (1989). Rigid body collision. American Society for Mechanical Engineers (ASME) Journal of Applied Mechanics, vol.56, pp.133-138.

Brach R.M. (1991). Mechanical impact dynamics. John Wiley and Sons, New York.

Brach R.M. (1997). Impact coefficients and tangential coefficients. American Society for Mechanical Engineers (ASME) Journal of Applied Mechanics, vol.64, pp.1014-1016.

Broili L. (1976). Relations between scree slope morphometry and dynamics of accumulation processes. Meeting on rockfall dynamics and protective works effectiveness, Bergamo, 20-21, 1976.

Brown E.T. (1981). Rock Characterisation testing and Monitoring-ISRM Suggested Methods. Published for the Commission of Testing Methods, International Society for Rock Mechanics (ISRM).

Budetta P. and Santo A. (1994). Morphostructural evolution and related kinematics of rockfalls in Campania (Southern Italy): A case study. Engineering Geology, 36, pp.197-210.

Bunce C.M. (1994). Risk analysis for rockfalls on highways. M.Sc. thesis, Dept. of Civil Engineering, University of Alberta.

Bunce C.M., Cruden D.M. and Morgeensten N.R. (1997). Assessment of the hazard from rockfall on a highway. Canadian Geotechnical Journal, vol. 34, 1997.

CAN/CSA (1991). Risk analysis requirement and guidelines, Quality management. A national standard of Canada. Q634 – M91. Canadian Standards Association, Rexdale, Canada.

Chan Y. C., Chan C. F. and Au W. C. (1986). Design of a boulder fence in Hong Kong. Conference on Rock Engineering and Excavation in an Urban Environment. Institute of Mining and Metallurgy, Hong Kong. 24-27, pp.87-96.

Chau K. T. and Lee C. F. (1998). Experimental studies on rockfall and debris flow. Planning, Design and Implementation of Debris Flow and Rockfall Hazards Mitigation Measures, Hong Kong, 1998.

Chau K.T., Liu J., Chan T.C.P., Yu T.X. and Chen X.W. (1999). Dynamic impacts on finite solid circular cylinders. Proceedings of the 6th Pan American congress of Applied Mechanics, PACAM VI, Rio Brazil, Applied Mechanics in Americas, 7, pp. 967-970.

Chau K.T., Wong R.H.C. and Lee C.F. (1998). Rockfall problems in Hong Kong and some new experimental results for coefficient of restitution. International Journal if rock Mechanics and Mining Science, 35(4-5), pp.662-663.

Chau K.T., Wong R.H.C., Liu J. and Wu J.J. (1999). Shape effect on the coefficient of restitution during rockfall impacts. 9th International Congress on Rock Mechanics, 1999.

Chen H., Chen R. and Huang T. (1994). An Application of An Analytical Model to A Slope Subject To Rockfalls. Bulletin of the Association of Engineering Geologists, vol. XXXI, No.4, 1994, pp. 447-458.

Componuovo G. F. (1976). ISMES' experience on the model of S Martino. Meeting on rockfall dynamics and protective works effectiveness, Bergamo, 20-21, 1976.

Cundall P.A. (1971). Acomputer model for simulating progressive, large scale movements in blocky rock system. International Society for Rock Mechanics Symposium on Rock Fracture, Nancy, Paper II-8.

Descoeutere F. and Zimmermann T. (1987). Three-dimensional dynamic calculation of rockfalls. Proceedings of the 6th Int. Conf. on Rock Mechanics, Montreal, pp337-342.

Elliott G.M. (1992). Rockfall simulation using Rockfal2. Unpublished notes.

Elliott G.M. and Rippere K.H. (1990). Performance analysis in rockfall simulation. 41st Highway Geology Symposium, New Mexico, 1990.

Evans S. G. and Hungr O. (1993). The assessment of rockfall hazard at a base of talus slopes. Canadian Geotechnical Journal, 30, pp.620-636.

Falcone G. and Piperno F. (1998). The restitution coefficient: A new interpretation. American Journal of Physics, Vol.65, pp.332-334.

Fookes P.G. and Weltman A. J. (1989). Rock Slope: Stabilization and Remedial Measures against Degradation in Weathered and Fresh Rock. Proc. Instn Civ. Engs, Part 1, 1989, 86, Apr. 359-380.

Fornaro M., Peila D. and Nebbia M. (1990). Block falls on rock slope – Application of a numerical program to some real cases. Proc. 6th Int. Congress IAEG. Amsterdam, Balkema, Rotterdam, pp.2173-2180.

Fumagalli E. (1976). Introduction au probleme du Mont St. Martino. Meeting on rockfall dynamics and protective works effectiveness. Bergamo, 20-21, 1976.

GEOBRUGG. (1993). Rockfall data collecting and analysis procedure. FATZER AG Romanshom Switzerland, 1993.

Goldsmith W. (1952). The coefficient of restitution. Bull. Mech. Div., Am. Soc. Eng. Ed., 2, pp.10-3-13.

Hoek E. (1987). Rockfall – A Program in Basic for the Analysis of Rockfalls from Slopes. Department of Civil engineering, University of Toronto, Canada.

Hoek E. (1998). Practical Rock Engineering. Rocscience website: http://www.rocscience.com/Hoekcorner.htm

Hungr O. and Evens S.G. (1988). Engineering evaluation of fragmental rockfall hazards. Proceedings of the 5th International Symposium on Landslides, Lausanne, pp.685-690.

Hunt R.E. (1992). Slope failure risk mapping for highways: methodology and case history. Rockfall prediction and control and landslide histories, Transportation Research Record, National research Council, Washington, No. 1343, pp.42-51.

Keller J.B. (1986). Impact with friction. American Society for Mechanical Engineers (ASME) Journal of Applied Mechanics, vol.53, pp.1-4.

Kolaiti E. and Papadopoulos Z. (1993). Evaluation of Schmidt rebound hammer testing: A critical approach. Bull. International association of Engineering Geology, 48, pp.69-76.

Lee K. and Elliott G. (1998). Rockfall: Application of Computer Simulation to Design of Preventive Measures. Planning, Design and Implementation of Debris Flow and Rockfall Hazards Mitigation Measures, Hong Kong, 1998.

Lied K. (1977). Rockfall Problems in Norway. ISEMS, 90 51-53, Bergamo.

Lundy P.A. (1995). Engineering Geological Evaluation of Rockfall Hazards on Banks Peninsula, Canterbury. A thesis submitted in partial fulfillment of the requirements for the degree of Master of Science in Engineering Geology, University of Canterbury.

Mak N. and Blomfield D. (1986). Rock trap design for presplit rock slopes. Conference on Rock Engineering and Excavation in an Urban Environment. Institute of Mining and Metallurgy, Hong Kong. 24-27, pp.263-270.

Marghitu D.B. and Humuzlu Y. (1995). Three-Dimensional rigid-Body Collisions with Multiple contact Points. American Society for Mechanical Engineers (ASME) Journal of Applied Mechanics, vol.62, pp.725-732.

Martin D.C. (1988). Rockfall control: an update (technical note). Bull. Assoc. Eng'g. Geol., Vol.13, No.14, pp.329-335.

Morgan G.C. (1991) Qualification of Risks from Slope Hazards. *In* Landslides Hazards in the Canadian Cordillera, Geological Association of Canada, Special Publication.

Morgan G.C., Rawlings G.E. and Sobkowicz J.C. (1992). Evaluating total risk to the communities from large debris flows. Geological and Natural Hazards, Vancouver Geotechnical Society and Canadian Geotechnical Society, Vancouver, British Columbia, May 1992, pp.225-236.

Morin A. (1855). Notions fondamentales de mecanique. Hachette, Paris.

Newton I. (1686). Philosophiae naturalis principia mathematica. Reg. Soc. Praeses, London.

Nielsen H. (1994). A geological hazard assessment for the lower Fox Valley, Arino 1994. Department of Conservation, Conservation advisory science notes: 121.

Norrish N.I. and Wyllie D.C. (1996). Rock slope stability analysis. In Landslides: Investigation and Mitigation, Transportation research board, National research council, Special report 247, pp.391-418.

Pfeiffer T.J. and Bowen T.D. (1989). Computer simulation of rockfalls. Bull. Ass. Engng. Geol. XXVI, 135-146.

Pierson L.A., Davis S.A. and Van Vickle R. (1991). Rockfall Hazard Rating System Implementation Manual. Federal Highway Administration Report. FHWA-OR-EG-90-01. FHWA, U.S. Department of Transportation.

Piteau D.R. (1977). Computer rockfall model. Proc. Meet. Rockfall Dynamics Protective Works Effectiveness. 90, 123-125.

Piteau D.R. and Clayton R. (1977). Discussion of paper "Computerized design of rock slopes using interactive graphics for the input and output of geometrical data" by P.A. Cundall, M.D. Voegele and C. Fairhurst. Proceedings 16th Symposium on Rock Mechanics, pp.62-63.

Piteau D.R. and Peckover F.L. (1978). Rock Slope Engineering. In Schuster R.L. and Krizek R.J. (Editors) "Landslides: analysis and control". Transportation Research Board Special Report 176, National Academy of Sciences, Washington DC, pp.489.

Poisson S.D. (1817). Mechanics. Longmans, London.

Richards L.R. (1988). Rockfall protection: a review of current analytical and design methods. *Secondo Ciclo Conferenze di Mechanica e Ingrenaria delle Rocce, MIR, Politecnico di Torino,* pp. 11.1-11.13.

Richards L.R. (1996). Rockfall Protection Measures, Marine Apartment, Nayland Street, Sumner. Unpublished report.

Ritchie A.M. (1963). Evaluation of rockfalls and its control. Highways Research Record. 17, 14-28.

Robotham M.E., Wang H. and Walton G. (1995). Assessment of risk from rockfall from active and abandoned quarry slopes. Transections of the Institute of Mining and Metallurgy A, 1995, 104(1-4), A25-33.

Romana M. (1988). Practice of SMR classification for slope appraisal. Proceedings of the 5th International Symposium on landslides, Lausanne. Vol.2, pp.1227-1229.

Romana M. (1991). SMR classification. Proceedings of the 7th International Congress on Rock Mechanics (ISRM), Aachen, Germeny. Vol.2, pp.955-960.

Routh E.J. (1860). Dynamics of a system of rigid bodies. Macmillan and Co., London.

Sachpazis C.I. (1990). Correlating Schmidt hardness with compressive strength and Young's modulus of carbonate rocks. Bull. International association of Engineering Geology, 42, pp.75-83.

Smith C.E. (1991). Predicting rebounds using rigid body dynamics. American Society for Mechanical Engineers (ASME) Journal of Applied Mechanics, vol.58, pp.754-758.

Smith C.E. (1991). Predicting rebounds using rigid-body dynamics. American Society for Mechanical Engineers (ASME) Journal of Applied Mechanics, vol.58, pp.754-758.

Smith C.E. and Liu P.P. (1992). Coefficient of restitution. American Society for Mechanical Engineers (ASME) Journal of Applied Mechanics, vol.59, pp.963-969.

Smotzyk U. (1983). Deep compaction. General report, Speciality session 3. Proc. VIII. ECSMFE, 3, pp.1105-1116, Helsinki.

Spang R. M (1998). Rockfall Barriers: Design and Practice in Europe. Planning, Design and Implementation of Debris Flow and Rockfall Hazards Mitigation Measures, Hong Kong, 1998.

Spang R. M and Sonser TH. (1995). Optimized rockfall protection by "ROCKFALL". Proceedings 8th International Congress on Rock Mechanics, Tokyo, 1995.

Spang R.M. and Rautenstrauch R.W. (1988). Empirical and mathematical approaches top rockfall protection and their practical application. Proceedings of the 5th International Symposium on Landslides, Lausanne, pp.1237-1243.

Stevens W. D. (1998). RocFall: A Tool for Probabilistic Analysis, Design of Remedial Measures and Prediction of Rockfalls. A thesis submitted in conformity with the requirements for the degree of Master of Applied Science, University of Toronto, 1998.

Stronge W.J. (1990). Rigid body collision with friction. Proceedings of Royal Society, London, Vol.A431, pp.169-181.

Stronge W.J. (1991). Unravelling paradoxical theories for rigid body collisions. American Society for Mechanical Engineers (ASME) Journal of Applied Mechanics, vol.58, pp.1049-1055.

Thornton C. (1997). Coefficient of restitution for collinear collisions of elastic-perfectly plastic spheres. American Society for Mechanical Engineers (ASME) Journal of Applied Mechanics, vol.64, pp.383-386.

U.S. Department of Transportation (1993). Rockfall Hazard Rating System, Participant's Manual. FHWA – SA – 93 –057.

Varnes D.J. (1978). Slope movement types and processes. Schuster, R.L. and Krizek, R.J. Landslides – Analysis and Control, Transportation Research Board Special Report 176, National Academy of Sciences, Washington D.C., pp. 11-33.

Varnes D.J. (1984). Landslide Hazard Zonation: a review of principals and practice. Natural Hazards 3. UNESCO, Paris, 63pp.

Wang Y. and Mason M.T. (1992). Two-dimensional rigid-body collisions with friction. American Society for Mechanical Engineers (ASME) Journal of Applied Mechanics, vol.59, pp.635-642.

Whiteside P.G.D. (1986). Discussion on rockfall protection measures. Conference on Rock Engineering and Excavation in an Urban Environment. Institute of Mining and Metallurgy, Hong Kong. 24-27, pp.490-492.

Whitman R.V. (1984). Evaluating Calculated Risk in Geotechnical Engineering. Journal of Geotechnical Engineering Division, ASCE, Vol.37, pp.83-143.

Whittaker E.T. (1904). A treatise on the analytical dynamics of particles and rigid bodies. Cambridge University Press, U.K.

Wu S.S (1985). Rockfall evaluation by computer simulation. Transportation Research Record, No.1031, pp. 1-5.

Wyllie D.C. and Norrish N.I. (1996). Stabilisation of Rock Slopes. In Landslides: Investigation and Mitigation, Transportation research board, National research council, Specisl report 247, pp.474-500.

Appendix A

Rock Property Measurements

A1. Mechanical Properties of Rocks

In order to study the relationship between the coefficient of restitution and properties of rocks, density and dynamic modulus of elasticity (Edyn.) of rocks used in the laboratory tests have been measured using cubic and cylindrical specimens. The results are listed in table A-1.

Table A-1: Measurement of mechanical properties of rock samples

Sample	Length (mm)	Volume (cm^3)	Weight (g)	Density (g/cm^3)	tp delay (ms)	tp (ms)	Vp (m/s)	ts delay (ms)	ts (s)	Vs (m/s)	Edyn. (Gpa)
Bast1-1	133.65	261.07	754.20	2.89	10.70	30.90	6616	8.00	49.30	3236	81.3
Dio1-1	136.21	266.03	767.60	2.89	10.70	54.10	3138	8.00	73.10	2092	27.8
Gabbro	59.63	95.40	276.90	2.90	10.70	19.60	6700	8.00	32.70	2414	48.3
Gneiss1-1	78.99	165.52	460.40	2.78	10.70	28.30	4488	8.00	37.00	2724	49.9
Gnt1-1	137.10	268.88	705.80	2.62	10.70	43.30	4205	8.00	62.70	2506	40.4
Lim1-1	132.62	252.99	336.00	1.33	10.70	72.30	2153	8.00	116.70	1220	5.0
Lim2-1	72.26	144.71	389.70	2.69	10.70	29.60	3823	8.00	36.40	2544	38.5
Lim3-1	60.64	92.86	244.40	2.63	10.70	20.80	6004	8.00	29.50	2820	56.9
Mb1-2	88.64	190.64	507.20	2.66	10.70	26.00	5793	8.00	54.50	1906	27.9
Mb2	133.42	260.84	704.60	2.70	10.70	38.70	4765	8.00	57.40	2701	49.8
Mb3-1	79.51	159.08	427.10	2.68	10.70	26.30	5097	8.00	48.50	1963	29.3
Mb4	59.06	83.29	208.80	2.51	10.70	18.50	7572	8.00	32.00	2461	43.8
Rhy1-1	61.15	186.46	436.20	2.34	10.70	24.40	4464	8.00	35.40	2232	31.1
Scht1	61.65	154.22	402.30	2.61	10.70	23.00	5012	8.00	37.60	2083	31.6
Scht2	64.27	173.68	439.60	2.53	10.70	23.00	5225	8.00	52.00	1461	15.8
Snd1-1	138.45	266.35	602.10	2.26	10.70	50.70	3461	8.00	75.90	2039	23.2
Snd2	60.22	147.05	359.20	2.44	10.70	27.10	3672	8.00	36.40	2120	27.5
Snd3-1	59.75	124.52	254.60	2.04	10.70	29.80	3128	8.00	42.40	1737	15.8
Snd3-2	50.60	91.63	188.60	2.06	10.70	25.60	3396	8.00	35.00	1874	18.5
Sye1-1	34.52	108.66	264.40	2.43	10.70	18.50	4426	8.00	21.60	2538	39.3
Sye1-1	62.57	108.66	264.40	2.43	10.70	24.70	4469	8.00	39.20	2005	26.9
Syep1-1	92.73	169.76	441.50	2.60	10.70	34.30	3929	8.00	48.00	2318	34.5
tra	57.08	142.27	356.90	2.51	10.70	21.00	5542	8.00	40.50	1756	22.4

Note: tp, Vp: P-wave travel time and velocity; ts, Vs: S-wave travel time and velocity.

A2. Schmidt Hammer measurements

Schmidt hammer measurement results (upper 50% of all measurements) for rock slabs, rock balls and rough rocks are shown in table A2-1 to A2-3.

Table A2-1: Schmidt number test results (slabs)

Slab Label	Schmidt number (N1)											
	1	2	3	4	5	6	7	8	9	10	Mean	Stdev.
bast1-1	56.8	53.8	55.8	40.2	48.3	47.0	48.5	50.6	55.5	53.5	51.0	5.1
dio1-1	36.4	34.2	41.0	39.5	42.5	39.5	37.5	39.5	39.0	37.5	38.7	2.4
diop1-1	47.8	45.8	47.5	41.0	46.1	42.5	47.5	46.2	48.5	43.5	45.6	2.5
gabbro	51.0	50.2	52.0	48.2	45.5	48.8	49.5	51.8	46.8	50.5	49.4	2.1
gneiss1-1	40.5	39.5	36.2	46.2	43.5	37.2	42.5	45.0	39.2	42.2	41.2	3.3
gnt1--1	43.8	37.9	38.4	41.0	38.2	38.2	37.6	41.2	39.8	42.5	39.9	2.2
gnt1-2	53.0	52.0	50.2	51.8	54.2	52.5	49.8	53.8	54.0	50.5	52.2	1.6
gnt1-3	60.0	55.5	54.5	54.3	57.0	55.8	58.2	54.5	55.0	58.5	56.3	2.0
lim2-1	46.2	45.5	45.0	47.2	45.5	44.8	47.2	46.0	45.8	46.2	45.9	0.8
lim3-1	49.5	48.5	48.3	29.5	49.5	42.8	46.5	48.5	43.8	44.0	45.1	6.0
mb1-2	29.2	26.1	24.5	25.2	23.8	24.0	26.0	26.2	24.8	28.5	25.8	1.8
mb3-1	33.5	34.2	32.2	30.0	30.2	29.8	33.8	32.5	33.0	30.8	32.0	1.7
mb4	44.8	42.5	39.0	43.0	39.5	40.6	42.5	42.0	43.8	40.2	41.8	1.9
rhy1-1	46.2	50.2	48.2	47.5	48.5	47.0	45.5	47.5	51.5	48.5	48.1	1.8
scht1-2	46.5	41.0	47.5	45.5	48.0	42.8	46.2	45.8	47.5	46.0	45.7	2.2
scht1-1	49.2	49.0	49.5	51.2	49.5	51.0	49.0	48.2	50.5	49.5	49.7	1.0
snd1-1	39.2	33.5	33.8	27.5	30.0	27.5	32.8	36.6	36.2	31.0	32.8	3.9
snd1-2	38.5	39.5	38.2	34.0	34.0	35.5	36.8	38.8	37.0	38.5	37.1	2.0
snd2-2	47.5	47.0	42.5	48.2	47.6	42.8	47.5	46.8	48.0	48.5	46.6	2.2
snd3	25.5	26.0	27.2	32.0	25.6	26.0	31.8	26.8	27.5	25.0	27.3	2.5
sye1-1	45.0	44.5	45.5	41.0	44.0	42.2	46.5	43.5	41.6	45.8	44.0	1.9
syep	47.5	45.2	39.8	43.5	47.2	42.2	43.8	44.5	45.5	46.5	44.6	2.4
tra1	50.5	49.2	42.5	47.2	50.2	45.8	50.2	49.5	45.0	48.5	47.9	2.7

Table A2-3: Schmidt number test results (rough rocks)

Rocks	Schmidt numbers											
	1	2	3	4	5	6	7	8	9	10	Mean	Stdev.
Basalt	56	50.5	50	54.5	55.5	55.5	55	54	54.2	54	53.9	2.1
Limestone	40.5	46	38.5	45.5	38.5	40.2	43	39	44.5	46	42.2	3.2
Greywacke	56.6	54.5	55	52.8	52.5	54.4	57.5	57.5	56.5	57	55.4	1.9

Table A2-2: Schmidt number test results (balls)

Ball Label	Schmidt Number (N2)											
	1	2	3	4	5	6	7	8	9	10	Mean	Stdev.
basalt1-1	41.8	37.5	43.5	40.2	42.2	42	41.5	40	39.6	42	41	1.7
basalt1-2	43.5	51.2	45.9	47	46	48	43.8	44.5	49	47.8	46.7	2.4
basat1-3	52.5	48.6	47	49.4	52	50.6	48.5	47.5	49	51	49.6	1.9
dio1-1	44.2	43.8	45.5	42.5	43.6	38.5	36	37.2	37	39.8	40.8	3.5
dio1-2	42.5	45.8	38.5	46	46	40.8	38.2	39.5	39.2	41.2	41.8	3.1
diop1	47	40.5	47.5	45.5	41.8	46.5	40.2	39.5	38	40	42.7	3.6
gneiss1	24.5	25.5	30.5	28.2	28.8	40.5	36.8	38.8	41.5	39.2	33.4	6.6
gneiss1(//)						40.5	36.8	38.8	41.5	39.2	39.4	1.8
gneiss2	30.2	31.2	29.5	31.9	27.1	33.2	34.8	34.8	36.2	33.8	32.3	2.8
gnt1-1	48	53.8	50.5	49	50	48.8	52	47.5	51.2	52.5	50.3	2.1
gnt1-2	45	45.5	45.8	48.3	45.2	42	41.8	43.5	44.5	47.5	44.9	2.1
gnt1-3	48.2	49.5	50	49.2	49.5	49.5	49.8	49.8	50	50	49.6	0.5
gnt2	59.2	55.6	56	60.3	60.1	57.8	58.5	60.2	56.5	57.5	58.2	1.8
lime1-1	0	0	0	0	0	0	0	0	0	0	0	0.0
lime2-1	26	22.2	23.2	29	27	34.5	32.8	33.2	28.5	30.5	28.7	4.2
lime2-2	36	32	29.6	39	30.3	32	34	31.5	30.5	32	32.7	2.9
lime2-3	29.9	27	32.1	33.6	34.5	35.5	29.8	36	33.8	35.8	32.8	3.0
lime3-1	35.2	30.1	33.9	37	37.5	35.5	33.5	35	35.8	35	34.9	2.1
lime3-2	29.8	35.2	33.8	36	33.5	30.4	29.5	32.5	34.8	33	32.9	2.3
mb2-1	31	28	34.1	33.2	33.5	29	30.8	32.8	33.5	33	31.9	2.1
mb2-2	28.5	27.2	31.8	32.1	33.8	28.2	29.5	28.5	27	30.5	29.7	2.3
mb3-1	31.2	23	28.5	22	26.5	28.1	25.5	27	28.5	26	26.6	2.7
mb3-2	28.9	29.9	28.1	31.9	32.1	32	28.2	32	28.5	30	30.2	1.7
mb4	30.5	37.8	36.5	33	35.9	39.2	35.5	38.5	38	37.8	36.3	2.7
rhyo1-1	39.9	40	41.8	37.8	42.2	40.5	39.4	38.5	40.5	42.8	40.3	1.6
rhyo1-2	42.5	48.1	43.5	44	45	39.2	40.2	38.5	39	40.2	42	3.1
scht1-1	42.5	38.5	39.5	41.8	41	25	24.2	26	26.5	28.5	33.4	7.9
scht1-1(//)						42.5	38.5	39.5	41	40.8	40.5	1.5
scht1-1(⊥)	25	24.2	22	25.2	23.2						23.9	1.3
scht1-2	36	35.5	39.6	37.5	36.5	30.5	25.6	25.2	26	28	32	5.6
scht1-2(//)	38	36.8	39.5	34.8	36	39.5	38	37.5	37.8	37	37.5	1.4
scht1-2(⊥)	22.5	18.5	25.2	19.5	21						21.3	2.6
snd1-1	35.5	38.1	35.2	38.2	32.2	34.5	39.8	37.2	39.5	38.5	36.9	2.4
snd1-2	38.5	35.2	34.2	36.1	39.5	36.5	37.9	39	38.8	39.5	37.5	1.9
snd2-1	31.5	32.5	36	31.5	30.8	35.8	36.5	36	36.2	37.5	34.4	2.5
snd2-2	47.5	43.8	45.8	48.9	48.9	42.8	43	44	43.5	45.2	45.3	2.4
snd3-1	24.6	24.8	29.2	24.3	20	23	22.5	23.8	25	25.5	24.3	2.4
snd3-2	20.5	22	19.8	22	25.5	19	21.2	19	21.8	23.5	21.4	2.0
snd3-3	27.5	28.5	27	23.5	22.8	21	22.5	23	24.5	25.6	24.6	2.5
snd3-4	32	31.8	31.5	33.5	29.5	32.6	31.8	32.8	32	31.5	31.9	1.1
steel	45	43.5	45.5	46	42.5	43.6	42.8	45.6	45	44.5	44.4	1.2
steel1	51.2	51.5	48.5	49	50.5	52.4	48.8	52	52.5	51.8	50.8	1.5

Table 2-2 continued

Ball Label	Schmidt Number (N2)											
	1	2	3	4	5	6	7	8	9	10	Mean	Stdev.
steel2	50	51.2	49.5	48	47.6	50	50.5	50.5	48	51	49.6	1.3
sye1-1	42.6	44	42.2	43.5	39	40.2	38.6	38.5	39	38.2	40.6	2.3
sye1-2	33	32	34.1	40.1	34.1	42.5	36	39.5	38	39.5	36.9	3.5
tra1-2	41.9	50	44.2	50	50.5	49.8	50	47.2	47	49	48	2.9

Appendix B

Coefficient of Restitution Calculation

Various tests have been carried out to obtain the coefficient of restitution both in laboratory and in the field. These include: laboratory tests with rock and steel balls impacting on rock slabs and steel plate; laboratory tests with rock balls and angular rock boulders impacting on rough rock blocks and beds of gravels, sands and fragments; field tests with rock boulders impacting on rock and scree base. The calculation details are listed below.

B.1 Laboratory test with rock slabs and steel plate

The calculations of restitution coefficient of normal bounce on rock and steel slabs are shown in table B1-1. Equations for calculation are shown in chapter 3.

Meaning of symbols:

R: coefficient of restitution, H: height of drop,

h: height of rebound, frames: frames from point of impact to the highest point of bounce.

Table B1-1: Coefficient of restitution calculation (normal bounce on rock and steel slabs)

Slab Label	Slab Angle	Ball Label	No. Drop	Drop H(m)	Bounce h(m)	Frames (1/200s)	Horiz. Dist.(m)	R	Notes
Gnt1-1	0	Gnt1-1	1	1	0.15	36			
			2		0.13	28			
			3		0.09	20			
			4		0.13	30			
			5		0.09	24			
			Av		0.12			0.344	Average
Bast1-1	0	Bast1-1	1	1	0.15	34			
			2		0.30	40			
			3		0.18	33			
			4		0.27	48			
			5		0.29	49			
			Av	1	0.24			0.488	
Dio1-1	0	Dio1-1	1	1	0.14	30			
			2		0.25	48			
			3		0.41	55			
			4		0.22	40			
			5		0.25	45			
			Av	1	0.25			0.504	

Table B1-1 continued

Slab Label	Slab Angle	Ball Label	No. Drop	Drop H(m)	Bounce h(m)	Frames (1/200s)	Horiz. Dist.(m)	R	Notes
Diop1-1	0	Diop1-1	1	1.01	0.07	15			
			2		0.14				
			3		0.21				
			4						
			5						
			Av	1.01	0.18			0.416	
Rhy1-1	0	Rhy1-1	1	1	0.18				
			2		0.27				
			3		0.24				
			4		0.26				
			5		0.25				
			Av	1	0.24			0.490	
Scht1-1	0	Scht1-1	1	0.97	0.33				
			2		0.18				
			3		0.37				
			4		0.34				
			5		0.39				
			Av	0.97	0.32			0.576	
Gnss1-1	0	Gnss1-1	1	1	0.21				
			2		0.30				
			3						
			4						
			5						
			Av	1	0.26			0.505	
		Mb2-2	1		0.31				
			2		0.25				
			3		0.27				
			4		0.24				
			Av	1	0.27			0.517	
Mb1-2	0	Mb2-1	1	1.01	0.06				
			2		0.07				
			3		0.05				
			4		0.05				
			5		0.06				
			Av	1.01	0.06			0.240	
		Mb3-1	1		0.12				
			2		0.06				
			3		0.04				
			4		0.05				
			5		0.05				
			Av	1.01	0.06			0.252	
		Gnt1-1	1		0.04				
			2		0.03				
			3		0.10				
			4		0.03				
			5		0.05				
			Av	1.01	0.05			0.222	
		gnt2	1		0.08				
			2		0.07				

Table B1-1 continued

Slab Label	Slab Angle	Ball Label	No. Drop	Drop H(m)	Bounce h(m)	Frames (1/200s)	Horiz. Dist.(m)	R	Notes
			3		0.08				
			4		0.11				
			Av	1.01	0.09			0.290	
		Steel	1		0.03				
			2		0.05				
			3		0.06				
			4						
			Av	1.01	0.05			0.215	
		Bast1-1	1		0.02				
			2		0.02				
			3		0.10				
			4		0.14				
			AV	1.01	0.07			0.263	
		Snd1-1	1		0.15				
			2		0.12				
			3		0.11				
			4		0.18				
			Av	1.01	0.14			0.372	
		snd3-1	1		0.10				
			2		0.11				
			3		0.08				
			4		0.08				
			Av	1.01	0.09			0.303	
		Lim1-1	1		0.02				
			2		0.02				
			3		0.02				
			4						
			Av	1.01	0.02			0.135	
		Snd2-1	1		0.10				
			2		0.10				
			3		0.08				
			4						
			Av	1.01	0.09			0.304	
Syep1-1	0	Syep1-1	1	0.985	0.16				
			2		0.24				
			3		0.17				
			4		0.19				
			5						
			Av	0.985	0.19			0.438	
		Gnt1-1	1		0.19				
			2		0.18				
			3		0.28				
			4		0.15				
			Av	0.985	0.20			0.449	
		Gnt2	1		0.23				
			2		0.28				
			3		0.28				
			4		0.31				
			Av	0.985	0.27			0.526	

Table B1-1 continued

Slab Label	Slab Angle	Ball Label	No. Drop	Drop H(m)	Bounce h(m)	Frames (1/200s)	Horiz. Dist.(m)	R	Notes
		Steel	1		0.16				
			2		0.16				
			3		0.13				
			4		0.14				
			Av	0.985	0.15			0.385	
		Bast1-1	1		0.13				
			2		0.04				
			3		0.04				
			4						
			Av	0.985	0.07			0.263	
		Snd1-1	1		0.12				
			2		0.12				
			3		0.12				
			4		0.22				
			Av	0.985	0.15			0.384	
		Snd3-1	1		0.12				
			2		0.19				
			3		0.09				
			4		0.13				
			Av	0.985	0.13			0.365	
		Mb2-1	1		0.03				
			2		0.09				
			3		0.06				
			4		0.12				
			AV	0.985	0.07			0.274	
		Dio1-1	1		0.06				
			2		0.06				
			3		0.08				
			4		0.14				
			AV	0.985	0.08			0.292	
		Mb3-1	1		0.04				
			2		0.07				
			3		0.07				
			4		0.07				
			Av	0.985	0.06			0.252	
Snd1-1	0	Snd1-1	1	1	0.09				
			2		0.10				
			3		0.09				
			4		0.06				
			5						
			Av	1	0.08			0.289	
		Gnt1-2	1		0.33				
			2		0.08				
			3		0.08				
			4						
			Av	1	0.16			0.404	
		Gnt2	1		0.16				
			2		0.24				
			3		0.17				

Table B1-1 continued

Slab Label	Slab Angle	Ball Label	No. Drop	Drop H(m)	Bounce h(m)	Frames (1/200s)	Horiz. Dist.(m)	R	Notes
			4		0.11				
			Av	1	0.17			0.412	
		steel	1		0.02				slab break
			2		0.07				here
			3		0.03				reclamped
			4		0.02				
			Av	1	0.03			0.180	
		Bast1-1	1		0.11				
			2		0.15				
			3		0.30				
			4						
			Av	1	0.19			0.432	
		Snd3-1	1		0.32				slab N
			2		0.28				abnomal
			3		0.26				here
			4						46-50
			Av	1	0.29			0.535	
		Mb2-1	1		0.26				
			2		0.42				
			3		0.16				
			Av	1	0.28			0.529	
Sye1-1	0	Sye1-1	1	1	0.14				
			2		0.07				
			3		0.08				
			4		0.12				
			5		0.09				
			Av	1	0.10			0.315	
Gabr		Gnt1-2	1	1.02	0.19				
			2		0.16				
			3		0.29				
			4		0.23				
			Av	1.02	0.22			0.462	
Mb4		Mb4	1	1.01	0.20				
			2		0.18				
			3		0.21				
			4		0.19				
			5		0.13				
			Av	1.01	0.18			0.424	
Scht1-2	0	Scht1-2	1	1	0.24				
			2		0.15				
			3		0.24				
			4		0.19				
			5		0.20				
			Av	1	0.20			0.448	
Mb3-1	0	Mb3-1	1	1.01	0.04				
			2		0.05				
			3		0.06				
			4		0.07				

Table B1-1 continued

Slab Label	Slab Angle	Ball Label	No. Drop	Drop H(m)	Bounce h(m)	Frames (1/200s)	Horiz. Dist.(m)	R	Notes
			5		0.06				
			Av	1.01	0.06			0.233	
		Gnt1-2	1		0.11				
			2		0.08				
			3		0.06				
			4						
			Av	1.01	0.08			0.287	
		Steel	1		0.07				
			2		0.08				
			3		0.08				
			4		0.07				
			Av	1.01	0.08			0.273	
		Bast1-1	1		0.04				
			2		0.05				
			3		0.06				
			4		0.05				
			Av	1.01	0.05			0.222	
		Snd1-1	1		0.26				
			2		0.20				
			3		0.21				
			4		0.17				
			Av	1.01	0.21			0.456	
		Gnt2	1		0.12				
			2		0.08				
			3		0.17				
			4		0.20				
			Av	1.01	0.14			0.376	
		Snd3-2	1		0.10				
			2		0.09				
			3		0.09				
			4						
			Av	1.01	0.09			0.304	
Lim2-1	0	Lim2-1	1	1.01	0.12				
			2		0.09				
			3		0.13				
			4		0.08				
			5		0.09				
			Av	1.01	0.10			0.318	
Lim3-1	0	Lim3-1	1	1	0.02				
			2		0.37				
			3		0.40				
			4		0.37				
			5		0.30				
			Av	1	0.29			0.538	
Snd2-2	0	Snd2-2	1	1	0.26				
			2		0.23				
			3		0.24				

Table B1-1 continued

Slab Label	Slab Angle	Ball Label	No. Drop	Drop H(m)	Bounce h(m)	Frames (1/200s)	Horiz. Dist.(m)	R	Notes
			4		0.25				
			5		0.22				
			Av	1	0.24			0.489	
snd3	0	Mb3-2	1	0.99	0.12				
			2		0.22				
			3		0.19				
			4		0.22				
			Av	0.99	0.19			0.435	
snd3	0	lim1-1	1	0.99	0.04				
			2		0.03				
			3		0.06				
			Av	0.99	0.04			0.205	
snd3	0	snd1-1	1		0.27				
			2		0.15				
			3		0.13				
			4		0.14				
			Av	0.99	0.17			0.417	
tra1	0	tra1-2	1		0.36				
			2		0.31				
			3		0.23				
			4		0.40				
			Av	1.01	0.33			0.567	
gnt1-2	0	gnt1-2	1		0.28				
			2		0.17				
			3		0.32				
			4		0.22				
			5		0.30				
			Av	1.01	0.26			0.505	
gnt1-2	0	bast1-1	1		0.28				
			2		0.27				
			3		0.24				
			4		0.29				
			Av	1.01	0.27			0.517	
gnt1-2	0	gnt2	1		0.36				
			2		0.42				
			3		0.40				
			4		0.43				
			5		0.36				
			6		0.42				
			7		0.43				
			Av	1.01	0.40			0.632	

Table B1-1 continued

Slab Label	Slab Angle	Ball Label	No. Drop	Drop H(m)	Bounce h(m)	Frames (1/200s)	Horiz. Dist.(m)	R	Notes
gnt1-2	0	steel	1		0.16				
			2		0.24				
			3		0.24				
			4		0.21				
			Av	1.01	0.21			0.459	
gnt1-2	0	snd1-2	1		0.33				
			2		0.34				
			3		0.36				
			4		0.21				
			5		0.32				
			Av	1.01	0.31			0.556	
gnt1-2	0	mb2-1	1		0.20				
			2		0.10				
			3		0.22				
			Av	1.01	0.17			0.414	
gnt1-2	0	mb3-1	1		0.21				
			2		0.16				
			3		0.17				
			4		0.21				
			Av	1.01	0.19			0.431	
		lim1-1	1		0.02				
			2		0.04				
			3		0.02				
			Av	1.01	0.03			0.157	
		lim2-1	1		0.26				
			2		0.24				
			3		0.24				
			4		0.22				
			Av	1.01	0.24			0.486	
schst1-1	0	schst1-2	1		0.31				
			2		0.34				
			3		0.34				
			4		0.27				
			Av	0.98	0.32			0.567	
		gnt1-2	1		0.27				
			2		0.37				
			3		0.38				
			4		0.33				
			Av	0.98	0.34			0.587	
		bast1-1	1		0.25				
			2		0.33				

Table B1-1 continued

Slab Label	Slab Angle	Ball Label	No. Drop	Drop H(m)	Bounce h(m)	Frames (1/200s)	Horiz. Dist.(m)	R	Notes
			3		0.34				
			4		0.25				
			Av	0.98	0.29			0.546	
		snd1-1	1		0.40				
			2		0.36				
			3		0.39				
			4		0.40				
			Av	0.98	0.39			0.629	
		gnt2	1		0.40				
			2		0.44				
			3		0.33				
			4		0.32				
			Av	0.98	0.37			0.617	
		mb2-2	1		0.29				
			2		0.29				
			3		0.30				
			4		0.29				
			Av	0.98	0.29			0.544	
schst1-1	0	mb3-1	1		0.22				
			2		0.27				
			3		0.21				
			4		0.23				
			Av	0.98	0.23			0.486	
		lim2-1	1		0.20				
			2		0.14				
			3		0.33				
			4		0.29				
			Av	0.98	0.24			0.494	
		steel	1		0.12				
			2		0.32				
			3		0.24				
			4		0.31				
			Av	0.98	0.25			0.503	
		lim1-1	1		0.04				
			2		0.03				
			Av	0.98	0.04			0.189	
gnt1-3	0	gnt1-3	1		0.53				
			2		0.49				
			3		0.46				
			4		0.36				
			5		0.43				

Table B1-1 continued

Slab Label	Slab Angle	Ball Label	No. Drop	Drop H(m)	Bounce h(m)	Frames (1/200s)	Horiz. Dist.(m)	R	Notes
			Av	1	0.45			0.674	
		bast1-3	1		0.26				
			2		0.36				
			3		0.48				
			4		0.52				
			Av	1	0.41			0.636	
		snd1-1	1		0.41				
			2		0.32				
			3		0.43				
			4		0.37				
			Av	1	0.38			0.618	
		snd3-4	1		0.26				
			2		0.24				
			3		0.19				
			4		0.14				
			Av	1	0.21			0.456	
gnt1-3	0	mb2-2	1		0.31				
			2		0.31				
			3		0.27				
			4		0.27				
			Av	1	0.29			0.539	
gnt1-3		mb3-1	1		0.17				
			2		0.07				
			3		0.19				
			Av	1	0.14			0.379	
gnt1-3		lim2-1	1	1	0.31			0.557	
gnt1-3		lim1-1	1	1	0.04				
			2		0.03				
			Av	1	0.03			0.180	
gnt1-3		steel	1		0.42				
			2		0.13				
			3		0.44				
			Av	1	0.33			0.574	
Steel	0	steel	1	1.005	0.11			0.331	
			2	1.005	0.1			0.315	
			3	1.005	0.17			0.411	
			4	0.8	0.13			0.403	
			5	0.8	0.16			0.447	
			6	0.8	0.135			0.411	
			7	1	0.12			0.346	

Table B1-1 continued

Slab Label	Slab Angle	Ball Label	No. Drop	Drop H(m)	Bounce h(m)	Frames (1/200s)	Horiz. Dist.(m)	R	Notes
			8	1	0.17			0.412	
			9	1	0.12			0.346	
			10	1	0.165			0.406	
			11	1	0.185			0.430	
Steel	0	steel	Av					0.387	
Steel	0	steel1	1	1	0.17			0.412	
			2	1	0.19			0.436	
			3	1	0.21			0.458	
			4	1	0.17			0.412	
			5	1	0.16			0.400	
Steel	0	steel1	Av					0.424	
Steel	0	steel2	1	1	0.2			0.447	
			2	1	0.12			0.346	
			3	1	0.11			0.332	
			4	1	0.25			0.500	
			5	1	0.15			0.387	
Steel	0	steel2	Av					0.403	
Steel	0	gnt1-3	1	1.005	0.42			0.646	
			2	1.005	0.34			0.582	
			3	1.005	0.36			0.599	
			4	1	0.365			0.604	
			5	1	0.37			0.608	
			6	1	0.34			0.583	
			7	1	0.37			0.608	
Steel	0	gnt1-3	AV					0.604	
Steel	0	gnt1-2	1	1.005	0.34			0.582	
			2	1.005	0.24			0.489	
			3	1.005	0.36			0.599	
			4	1.005	0.3			0.546	
			5	1	0.4			0.632	
			6	1	0.3			0.548	
			7	1	0.35			0.592	
			8	1	0.38			0.616	
Steel	0	gnt1-2	Av					0.575	
Steel	0	bast1-1	1	1.005	0.36			0.599	
			2	1.005	0.31			0.555	
			3	1.005	0.23			0.478	
			4	1	0.31			0.557	
			5	1	0.3			0.548	
			6	1	0.18			0.424	
			7	1	0.21			0.458	
Steel	0	bast1-1	Av					0.517	
Steel	0	bast1-3	1	1	0.28			0.529	

Table B1-1 continued

Slab Label	Slab Angle	Ball Label	No. Drop	Drop H(m)	Bounce h(m)	Frames (1/200s)	Horiz. Dist.(m)	R	Notes
			2	1	0.25			0.500	
			3	1	0.37			0.608	
			4	1	0.31			0.557	
Steel	0	bast1-3	Av					0.549	
Steel	0	snd1-1	1	1	0.25			0.500	
			2	1	0.22			0.469	
			3	1	0.23			0.480	
			4	1	0.25			0.500	
Steel	0	snd1-1	Av					0.487	
Steel	0	gnt2	1	1.005	0.44			0.662	
			2	1	0.37			0.608	
			3	1	0.37			0.608	
			4	1	0.375			0.612	
			5	1	0.41			0.640	
			6	1	0.34			0.583	
Steel	0	gnt2	Av					0.619	
Steel	0	mb2-2	1	1.005	0.23			0.478	
Steel	0	mb2-1	1	1	0.26			0.510	
			2	1	0.17			0.412	
			3	1	0.215			0.464	
			4	1	0.23			0.480	
Steel	0	mb2-1	Av					0.469	
Steel	0	mb3-2	1	1	0.13			0.361	
			2	1	0.16			0.400	
			3	1	0.16			0.400	
			4	1	0.15			0.387	
Steel	0	mb3-2	Av					0.387	
Steel	0	snd3-1	1	1	0.24			0.490	
			2	1	0.17			0.412	
			3	1	0.16			0.400	
Steel	0	snd3-1	AV	1				0.434	
Steel	0	snd3-3	1	1	0.18			0.424	
			2	1	0.17			0.412	
			3	1	0.12			0.346	
Steel	0	snd3-3	Av					0.394	

The coefficients of restitution calculation of inclined bounce on rock and steel slabs are shown in table B1-2. Calculation equations and parameter relationship are shown in Chapter 3. Notations of symbols:

H', h', S': initial recorded drop height, bounce height and horizontal distance;

H, h, S: corrected (with reference system) drop height, bounce height and horizontal distance;

S1, S2: correction factors for distance and height (difference between the point of impact and the origin of the reference system);

Vi, Vrx, Vry: velocity of impact and rebound velocities in X and Y direction;

Vin, Vit, Vrn, Vrt: impact and rebound velocities in normal and tangential direction;

Rn, Rt: normal and tangential coefficients of restitution

Table B1-2: Coefficient of restitution calculation (bounce on inclined rock and steel slabs)

Slab label	Slab Angle	Ball Label	No. Drop	Drop H'(m)	Drop H(m)	Bounce h'(m)	Bounce h(m)	Frames (1/200 s)	Horiz. Distance S'(m)	Horiz. Distance S(m)	S1 (m)	S2 (m)	Vi (m/s)	Vrx (m/s)	Vry (m/s)	Vin (m/s)	Vit (m/s)	Vrn (m/s)	Vrt (m/s)	Rn	Rt
mb4	10	mb4	1	1	1.01	0.135	0.145	33	0.14	0.11	0.03	0.01	4.45	0.67	1.69	4.38	0.77	1.78	0.36	0.41	0.47
	10		2	1	1.01	0.1	0.11	32	0.16	0.13	0.03	0.01	4.45	0.81	1.47	4.38	0.77	1.59	0.54	0.36	0.70
	10		3	1	1.01	0.085	0.095	30	0.12	0.09	0.03	0.01	4.45	0.60	1.37	4.38	0.77	1.45	0.35	0.33	0.46
	10		4	1	1.01	0.06	0.07	22	0.1	0.07	0.03	0.01	4.45	0.64	1.18	4.38	0.77	1.27	0.42	0.29	0.55
			Av	1	1															0.35	0.54
mb4	23	mb4	1	0.99	1	0.01	0.02	19	0.14	0.13	0.01	0.01	4.43	1.37	0.68	4.08	1.73	1.16	1.00	0.28	0.58
	23		2	0.99	1.01	-0.005	0.015	7	0.06	0.05	0.01	0.02	4.45	1.43	0.60	4.10	1.74	1.11	1.08	0.27	0.62
	23		3	0.99	1.01	0.06	0.08	30	0.19	0.18	0.01	0.02	4.45	1.20	1.27	4.10	1.74	1.64	0.61	0.40	0.35
	23		4	0.99	1.01	0.03	0.05	18	0.13	0.12	0.01	0.02	4.45	1.33	1.00	4.10	1.74	1.44	0.84	0.35	0.48
	23		5	0.99	0.98	0.015	0.005	12	0.05	0.07	-0.02	-0.01	4.38	1.17	0.38	4.04	1.71	0.80	0.93	0.20	0.54
	23		6	0.99	1.01	0.03	0.05	19	0.11	0.1	0.01	0.02	4.45	1.05	0.99	4.10	1.74	1.32	0.58	0.32	0.33
			Av	0.99	0.99															0.30	0.48
mb4	46	mb4	1	0.9	0.91	-0.2	-0.19	23	0.25	0.26	-0.01	0.01	4.23	2.26	1.09	2.94	3.04	0.87	2.35	0.30	0.77
	46		2	0.9	0.94	-0.2	-0.16	19	0.27	0.27	0	0.04	4.29	2.84	1.22	2.98	3.09	1.20	2.85	0.40	0.92
	46		3	0.9	0.97	-0.2	-0.13	18	0.27	0.23	0.04	0.07	4.36	2.56	1.00	3.03	3.14	1.14	2.50	0.38	0.80
	46		4	0.9	0.94	-0.11	-0.07	9	0.12	0.12	0	0.04	4.29	2.67	1.33	2.98	3.09	0.99	2.81	0.33	0.91
	46		5	0.9	0.93	-0.2	-0.17	20	0.32	0.32	0	0.03	4.27	3.20	1.21	2.97	3.07	1.46	3.09	0.49	1.01
			Av	0.9	0.9															0.38	0.88
gnt1-3	12	gnt1-3	1	1.02	1.03	0.31	0.32	50	0.34	0.3	0.04	0.01	4.50	1.20	2.51	4.40	0.93	2.70	0.65	0.61	0.70
	12		2	1.02	1.03	0.43	0.44	62	0.16	0.13	0.03	0.01	4.50	0.42	2.94	4.40	0.93	2.96	-0.20	0.67	
	12		3	1.02	1.03	0.31	0.32	49	0.33	0.3	0.03	0.01	4.50	1.22	2.51	4.40	0.93	2.71	0.68	0.62	0.72
	12		4	1.02	1.03	0.45	0.46	59	0.42	0.39	0.03	0.01	4.50	1.32	3.01	4.40	0.93	3.22	0.67	0.73	0.71
	12		5	1.02	1.03	0.47	0.48	60	0.23	0.2	0.03	0.01	4.50	0.67	3.07	4.40	0.93	3.14	0.01	0.71	0.01
			Av																	0.67	0.71
gnt1-3	22	gnt1-3	1	0.97	0.99	0.31	0.33	50	0.46	0.46	0	0.02	4.41	1.84	2.55	4.09	1.65	3.05	0.75	0.75	0.46

Table B1-2 continued

Slab label	Slab Angle	Ball Label	No. Drop	Drop H'(m)	Drop H(m)	Bounce h'(m)	Bounce h(m)	Frames (1/200 s)	Horiz. Distance S'(m)	Horiz. Distance S(m)	S1 (m)	S2 (m)	Vi (m/s)	Vrx (m/s)	Vry (m/s)	Vin (m/s)	Vit (m/s)	Vrn (m/s)	Vrt (m/s)	Rn	Rt
	22		2	0.97	1	0.24	0.27	42	0.49	0.46	0.03	0.03	4.43	2.19	2.32	4.11	1.66	2.97	1.16	0.72	0.70
	22		3	0.97	1	0.11	0.14	35	0.45	0.42	0.03	0.03	4.43	2.40	1.66	4.11	1.66	2.44	1.60	0.59	0.97
	22		4	0.97	0.99	0.4	0.42	57	0.49	0.47	0.02	0.02	4.41	1.65	2.87	4.09	1.65	3.28	0.45	0.80	0.27
			Av																	0.72	0.60
gnt1-3	46	gnt1-3	1	0.96	1.01	-0.16	-0.11	35	0.6	0.58	0.02	0.05	4.45	3.31	-0.23	3.09	3.20	2.54	2.14	0.82	0.67
	46		2	0.96	0.94	-0.16	-0.18	43	0.62	0.65	-0.03	-0.02	4.29	3.02	-0.22	2.98	3.09	2.33	1.94	0.78	0.63
	46		3	0.96	1.02	-0.16	-0.1	30	0.46	0.43	0.03	0.06	4.47	2.87	-0.07	3.11	3.22	2.11	1.94	0.68	0.60
	46		4	0.96	0.99	-0.16	-0.13	30	0.46	0.45	0.01	0.03	4.41	3.00	0.13	3.06	3.17	2.07	2.18	0.68	0.69
			Av	0.96	0.96															0.68	0.69
bast1-1	12	bast1-3	1	1.04	1.04	0.22	0.22	45	0.33	0.35	-0.02	0	4.52	1.56	2.08	4.42	0.94	2.36	1.09	0.53	1.16
	12		2	1.04	1.05	0.14	0.15	34	0.07	0.07	0	0.01	4.54	0.41	1.72	4.44	0.94	1.76	0.05	0.40	0.05
	12		3	1.04	1.06	0.25	0.27	45	0.29	0.26	0.03	0.02	4.56	1.16	2.30	4.46	0.95	2.49	0.65	0.56	0.69
	12		4	1.04	1.06	0.34	0.36	50	0.13	0.11	0.02	0.02	4.56	0.44	2.67	4.46	0.95	2.70	-0.12	0.61	
	12		5	1.04	1.06	0.12	0.14	33	0.26	0.24	0.02	0.02	4.56	1.45	1.66	4.46	0.95	1.92	1.08	0.43	1.14
	12		Av	1.04	1.04															0.48	0.76
bast1-1	23	bast1-3	1	1	1.04	0.12	0.16	40	0.37	0.34	0.03	0.04	4.52	1.70	1.78	4.16	1.76	2.30	0.87	0.55	0.49
	23		2	1	1.04	-0.01	0.03	19	0.12	0.09	0.03	0.04	4.52	0.95	0.78	4.16	1.76	1.09	0.57	0.26	0.32
	23		3	1	1.01	0.07	0.08	30	0.27	0.27	0	0.01	4.45	1.80	1.27	4.10	1.74	1.87	1.16	0.46	0.67
	23		4	1	1.01	0.1	0.11	34	0.4	0.38	0.02	0.01	4.45	2.24	1.48	4.10	1.74	2.24	1.48	0.55	0.85
	23		Av	1	1															0.45	0.58
bast1-1	46	bast1-1	1	0.96	0.98	-0.06	-0.04	9	0.115	0.115	0	0.02	4.38	2.56	0.67	3.05	3.15	1.37	2.26	0.45	0.72
	46		2	0.96	0.99	-0.14	-0.11	22	0.29	0.26	0.03	0.03	4.41	2.36	0.46	3.06	3.17	1.38	1.97	0.45	0.62
	46		3	0.96	0.99	-0.15	-0.12	29	0.35	0.32	0.03	0.03	4.41	2.21	0.12	3.06	3.17	1.51	1.62	0.49	0.51
	46		4	0.96	0.97	-0.15	-0.14	32	0.44	0.43	0.01	0.01	4.36	2.69	0.09	3.03	3.14	1.87	1.93	0.62	0.62
	46		5	0.96	0.95	-0.15	-0.16	39	0.56	0.56	0	-0.01	4.32	2.87	-0.14	3.00	3.11	2.16	1.90	0.72	0.61

Table B1-2 continued

Slab label	Slab Angle	Ball Label	No. Drop	Drop H'(m)	Drop H(m)	Bounce h'(m)	Bounce h(m)	Frames (1/200 s)	Horiz. Distance S'(m)	Horiz. Distance S(m)	S1 (m)	S2 (m)	Vi (m/s)	Vrx (m/s)	Vry (m/s)	Vin (m/s)	Vit (m/s)	Vrn (m/s)	Vrt (m/s)	Rn	Rt
	46		6	0.96	1	-0.15	-0.11	30	0.45	0.42	0.03	0.04	4.43	2.80	0.00	3.08	3.19	2.02	1.94	0.66	0.61
	46		Av	0.96	0.96															0.53	0.61
dio1-1	12	dio1-1	1	1.04	1.04	0.05	0.055	21	0.05	0.06	-0.01	0.005	4.52	0.57	1.04	4.42	0.94	1.13	0.34	0.26	0.37
	12		2	1.04	1.05	0.07	0.08	29	0.15	0.12	0.03	0.01	4.53	0.83	1.26	4.43	0.94	1.41	0.55	0.32	0.58
	12		3	1.04	1.04	0.05	0.05	25	0.08	0.09	-0.01	0	4.51	0.72	1.01	4.41	0.94	1.14	0.49	0.26	0.53
	12		4	1.04	1.04	0.01	0.015	13	0.08	0.08	0	0.005	4.52	1.23	0.55	4.42	0.94	0.79	1.09	0.18	1.16
	12		5	1.04	1.05	0.03	0.04	21	0.1	0.09	0.01	0.01	4.53	0.86	0.90	4.43	0.94	1.05	0.65	0.24	0.69
	12		Av	1.04	1.04															0.25	0.67
dio1-1	23	dio1-1	1	1.01	1.02	0.01	0.02	16	0.09	0.11	-0.02	0.01	4.47	1.38	0.64	4.12	1.75	1.13	1.01	0.27	0.58
	23		2	1.01	1.03	0.01	0.03	15	0.09	0.08	0.01	0.02	4.50	1.07	0.77	4.14	1.76	1.12	0.68	0.27	0.39
	23		3	1.01	1.02	0.01	0.02	15	0.08	0.1	-0.02	0.01	4.47	1.33	0.63	4.12	1.75	1.11	0.98	0.27	0.56
	23		4	1.01	1.03	0.01	0.03	19	0.13	0.12	0.01	0.02	4.50	1.26	0.78	4.14	1.76	1.21	0.86	0.29	0.49
	23		5	1.01	1.02	0.005	0.01	17	0.07	0.09	-0.02	0.005	4.46	1.06	0.53	4.11	1.74	0.91	0.77	0.22	0.44
	23		Av	1.01	1.01															0.27	0.49
dio1-1	46	dio1-1	1	0.94	0.98	-0.19	-0.15	25	0.27	0.27	0	0.04	4.38	2.16	0.59	3.05	3.15	1.15	1.92	0.38	0.61
	46		2	0.94	0.98	-0.19	-0.15	32	0.37	0.37	0	0.04	4.38	2.31	0.15	3.05	3.15	1.56	1.72	0.51	0.54
	46		3	0.94	0.98	-0.19	-0.15	25	0.28	0.28	0	0.04	4.38	2.24	0.59	3.05	3.15	1.20	1.98	0.40	0.63
	46		4	0.94	0.95	-0.11	-0.1	11	0.11	0.13	-0.02	0.01	4.32	2.36	1.55	3.00	3.11	0.62	2.76	0.21	0.89
	46		Av	0.94	0.94															0.37	0.67
mb3-1	12	mb3-2	1	1.04	1.05	0.1	0.11	33	0.14	0.12	0.02	0.01	4.54	0.73	1.48	4.44	0.94	1.59	0.40	0.36	0.43
	12		2	1.04	1.05	0.1	0.11	30	0.11	0.09	0.02	0.01	4.54	0.60	1.47	4.44	0.94	1.56	0.28	0.35	0.30
	12		3	1.04	1.05	0.22	0.23	49	0.31	0.28	0.03	0.01	4.54	1.14	2.14	4.44	0.94	2.33	0.67	0.53	0.71
	12		4	1.04	1.05	0.05	0.06	25	0.15	0.13	0.02	0.01	4.54	1.04	1.09	4.44	0.94	1.29	0.79	0.29	0.84
	12		5	1.04	1.05	0.17	0.18	40	0.13	0.11	0.02	0.01	4.54	0.55	1.88	4.44	0.94	1.95	0.15	0.44	0.16
	12		Av	1.04	1.04															0.39	0.49

Table B1-2 continued

Slab label	Slab Angle	Ball Label	No. Drop	Drop H'(m)	Drop H(m)	Bounce h'(m)	Bounce h(m)	Frames (1/200 s)	Horiz. Distance S'(m)	Horiz. Distance S(m)	S1 (m)	S2 (m)	Vi (m/s)	Vrx (m/s)	Vry (m/s)	Vin (m/s)	Vit (m/s)	Vrn (m/s)	Vrt (m/s)	Rn	Rt
mb3-1	23	mb3-2	1	1.01	1.04	0.08	0.11	29	0.25	0.22	0.03	0.03	4.52	1.52	1.47	4.16	1.76	1.95	0.82	0.47	0.47
	23		2	1.01	1.03	0.05	0.07	29	0.15	0.14	0.01	0.02	4.50	0.97	1.19	4.14	1.76	1.48	0.42	0.36	0.24
	23		3	1.01	1.06	-0.03	0.02	12	0.1	0.02	0.08	0.05	4.56	0.33	0.63	4.20	1.78	0.71	0.06	0.17	0.03
	23		4	1.01	1.02	0.05	0.06	26	0.17	0.18	-0.01	0.01	4.47	1.38	1.10	4.12	1.75	1.55	0.85	0.38	0.48
	23		5	1.01	1.03	0.14	0.16	35	0.34	0.33	0.01	0.02	4.50	1.89	1.77	4.14	1.76	2.37	1.04	0.57	0.59
	23		Av	1.01	1.01															0.39	0.36
mb3-1	48	mb3-2	1	0.93	0.96	-0.19	-0.16	30	0.47	0.43	0.04	0.03	4.34	2.87	0.33	2.90	3.23	1.91	2.16	0.66	0.67
	48		2	0.93	0.96	-0.19	-0.16	25	0.41	0.38	0.03	0.03	4.34	3.04	0.67	2.90	3.23	1.81	2.53	0.62	0.78
	48		3	0.93	0.97	-0.19	-0.15	26	0.42	0.37	0.05	0.04	4.36	2.85	0.52	2.92	3.24	1.77	2.29	0.61	0.71
	48		4	0.93	0.96	-0.19	-0.16	31	0.5	0.46	0.04	0.03	4.34	2.97	0.27	2.90	3.23	2.02	2.19	0.70	0.68
	48		5	0.93	0.96	-0.19	-0.16	34	0.54	0.5	0.04	0.03	4.34	2.94	0.11	2.90	3.23	2.11	2.05	0.73	0.63
	48		Av	0.93	0.93	-0.19	-0.19													0.66	0.69
snd1-2	12	snd1-2	1	1.02	1.02	0.11	0.11	33	0.17	0.17	0	0	4.47	1.03	1.48	4.38	0.93	1.66	0.70	0.38	0.75
	12		2	1.02	1.03	0.19	0.2	40	0.11	0.1	0.01	0.01	4.50	0.50	1.98	4.40	0.93	2.04	0.08	0.46	0.08
	12		Av	1.02	1.02															0.42	0.42
snd1-2	12	bast1-3	1	1.02	1.02	0.08	0.08	30	0.06	0.07	-0.01	0	4.47	0.47	1.27	4.38	0.93	1.34	0.19	0.31	0.21
	12		2	1.02	1.02	0.05	0.05	26	0.12	0.13	-0.01	0	4.47	1.00	1.02	4.38	0.93	1.21	0.77	0.28	0.82
	12		3	1.02	1.02	0.02	0.02	20	0.03	0.03	0	0	4.47	0.30	0.69	4.38	0.93	0.74	0.15	0.17	0.16
	12		4	1.02	1.03	0.05	0.06	25	0.11	0.09	0.02	0.01	4.50	0.72	1.09	4.40	0.93	1.22	0.48	0.28	0.51
	12		Av	1.02	1.02															0.26	0.43
snd1-2	22	snd1-2	1	0.99	1	0.06	0.07	25	0.25	0.22	0.03	0.01	4.43	1.76	1.17	4.11	1.66	1.75	1.19	0.43	0.72
	22		2	0.99	1	0.06	0.07	25	0.22	0.19	0.03	0.01	4.43	1.52	1.17	4.11	1.66	1.66	0.97	0.40	0.58
	22		3	0.99	0.99	0.09	0.09	27	0.19	0.18	0.01	0	4.41	1.33	1.33	4.09	1.65	1.73	0.74	0.42	0.45
	22		4	0.99	0.99	0.07	0.07	21	0.23	0.22	0.01	0	4.41	2.10	1.18	4.09	1.65	1.88	1.50	0.46	0.91

Table B1-2 continued

Slab label	Slab Angle	Ball Label	No. Drop	Drop H'(m)	Drop H(m)	Bounce h'(m)	Bounce h(m)	Frames (1/200 s)	Horiz. Distance S'(m)	Horiz. Distance S(m)	S1 (m)	S2 (m)	Vi (m/s)	Vrx (m/s)	Vry (m/s)	Vin (m/s)	Vit (m/s)	Vrn (m/s)	Vrt (m/s)	Rn	Rt
	22		Av	0.99	0.99															0.43	0.66
snd1-2	22	bast1-3	1	0.99	1	0.03	0.04	20	0.21	0.18	0.03	0.01	4.43	1.80	0.89	4.11	1.66	1.50	1.34	0.37	0.80
	22		2	0.99	1	0.05	0.06	20	0.17	0.14	0.03	0.01	4.43	1.40	1.09	4.11	1.66	1.54	0.89	0.37	0.54
	22		3	0.99	0.99	0.06	0.06	23	0.16	0.15	0.01	0	4.41	1.30	1.09	4.09	1.65	1.50	0.80	0.37	0.49
	22		4	0.99	0.99	0.09	0.09	27	0.27	0.26	0.01	0	4.41	1.93	1.33	4.09	1.65	1.95	1.29	0.48	0.78
	22		5	0.99	0.99	0.04	0.04	20	0.12	0.11	0.01	0	4.41	1.10	0.89	4.09	1.65	1.24	0.69	0.30	0.42
	22		Av	0.99	0.99															0.38	0.60
snd1-2	46	snd1-2	1	0.93	0.93	-0.15															
	46		2	0.93	0.95	-0.15	-0.13	33	0.47	0.44	0.03	0.02	4.32	2.67	-0.02	3.00	3.11	1.93	1.84	0.64	0.59
	46		3	0.93	0.91	-0.15	-0.17	33	0.36	0.37	-0.01	-0.02	4.23	2.24	0.22	2.94	3.04	1.46	1.72	0.50	0.56
	46		4	0.93	0.95	-0.15	-0.13	30	0.39	0.36	0.03	0.02	4.32	2.40	0.13	3.00	3.11	1.64	1.76	0.55	0.57
	46		Av	0.93	0.95	-0.15	-0.13	30	0.44	0.41	0.03	0.02	4.32	2.73	0.13	3.00	3.11	1.88	1.99	0.63	0.64
																				0.58	0.59
snd1-2	46	bast1-3	1	0.93	0.95	-0.15	-0.13	31	0.38	0.35	0.03	0.02	4.32	2.26	0.08	3.00	3.11	1.57	1.63	0.52	0.52
	46		2	0.93	0.96	0.15	0.18	32	0.35	0.32	0.03	0.03	4.34	2.00	1.91	3.01	3.12	2.77	0.02	0.92	0.00
	46		3	0.93	0.96	-0.15	-0.12	29	0.39	0.36	0.03	0.03	4.34	2.48	0.12	3.01	3.12	1.71	1.81	0.57	0.58
	46		4	0.93	0.95	-0.15	-0.13	32	0.4	0.37	0.03	0.02	4.32	2.31	0.03	3.00	3.11	1.64	1.63	0.55	0.52
	46		5	0.93	0.95	-0.15	-0.13	29	0.39	0.36	0.03	0.02	4.32	2.48	0.19	3.00	3.11	1.66	1.86	0.55	0.60
	46		Av	0.93	0.93						0.03									0.62	0.56
snd3-1	10	snd3-3	1	1.02	1.03	0.15	0.16	38	0.2	0.17	0.03	0.01	4.48	0.89	1.77	4.42	0.78	1.90	0.57	0.43	0.74
	10		2	1.02	1.03	0.28	0.29	48	0.14	0.1	0.04	0.01	4.48	0.42	2.39	4.42	0.78	2.42	0.00	0.55	
	10		3	1.02	1.03	0.18	0.19	37	0.25	0.22	0.03	0.01	4.48	1.19	1.93	4.42	0.78	2.11	0.84	0.48	1.07
	10		4	1.02	1.03	0.28	0.295	50	0.22	0.17	0.05	0.015	4.50	0.68	2.41	4.43	0.78	2.49	0.25	0.56	0.32
	10		5	1.02	1.03	0.2	0.21	46	0.18	0.15	0.03	0.01	4.48	0.65	2.04	4.42	0.78	2.12	0.29	0.48	0.37
	10		6	1.02	1.03	0.23	0.24	42	0.18	0.15	0.03	0.01	4.48	0.71	2.17	4.42	0.78	2.26	0.33	0.51	0.42
	10		Av	1.02	1.02															0.50	0.58

Table B1-2 continued

Slab label	Slab Angle	Ball Label	No. Drop	Drop H'(m)	Drop H(m)	Bounce h'(m)	Bounce h(m)	Frames (1/200 s)	Horiz. Distance S'(m)	Horiz. Distance S(m)	S1 (m)	S2 (m)	Vi (m/s)	Vrx (m/s)	Vry (m/s)	Vin (m/s)	Vit (m/s)	Vrn (m/s)	Vrt (m/s)	Rn	Rt
snd3-1	20	snd3-3	1	0.98	0.98	0.07	0.07	28	0.19	0.18	0.01	0	4.38	1.29	1.19	4.12	1.50	1.55	0.80	0.38	0.53
	20		2	0.98	0.98	0.12	0.12	34	0.18	0.17	0.01	0	4.38	1.00	1.54	4.12	1.50	1.79	0.41	0.43	0.28
	20		3	0.98	0.99	0.13	0.14	34	0.27	0.26	0.01	0.01	4.41	1.53	1.66	4.14	1.51	2.08	0.87	0.50	0.58
	20		Av	0.98	0.98						0.01									0.44	0.46
snd3-1	23	snd3-4	1	0.99	1.01	0.015	0.035	15	0.17	0.13	0.04	0.02	4.45	1.73	0.83	4.10	1.74	1.45	1.27	0.35	0.73
	23		2	0.99	1.01	0.03	0.05	21	0.18	0.15	0.03	0.02	4.45	1.43	0.99	4.10	1.74	1.47	0.93	0.36	0.53
	23		3	0.99	1.01	0.03	0.05	23	0.24	0.21	0.03	0.02	4.45	1.83	1.00	4.10	1.74	1.63	1.29	0.40	0.74
	23		Av	0.99	1.01							0.02	4.45							0.37	0.67
snd3-1	48	snd3-3	1	0.93	0.96	-0.19	-0.16	26	0.35	0.33	0.02	0.03	4.34	2.54	0.59	2.90	3.23	1.49	2.14	0.51	0.66
	48		2	0.93	0.96	-0.19	-0.16	30	0.35	0.33	0.02	0.03	4.34	2.20	0.33	2.90	3.23	1.41	1.72	0.49	0.53
	48		3	0.93	0.96	-0.19	-0.16	29	0.4	0.39	0.01	0.03	4.34	2.69	0.39	2.90	3.23	1.74	2.09	0.60	0.65
	48		4	0.93	0.94	-0.19	-0.18	42	0.53	0.53	0	0.01	4.29	2.52	-0.17	2.87	3.19	1.99	1.56	0.69	0.49
	48		5	0.93	0.96	-0.19	-0.16	32	0.38	0.18	0.2	0.03	4.34	1.13	0.22	2.90	3.23	0.69	0.91	0.24	0.28
	48		Av	0.93	0.93															0.46	0.53
lim3-2	10	lim3-2	1	1.04	1.04	0.14	0.14	34	0	0	0	0	4.51	0.00	1.66	4.44	0.78	1.63	-0.29	0.37	
	10		2	1.04	1.04	0.04	0.04	26	0.09	0.09	0	0	4.51	0.69	0.95	4.44	0.78	1.05	0.52	0.24	0.66
	10		3	1.04	1.04	0.01	0.01	15	0.02	0.02	0	0	4.51	0.27	0.50	4.44	0.78	0.54	0.18	0.12	0.22
	10		Av	1.04	1.04															0.18	0.44
lim1-1	12	lim1-1	1	1.02	1.04	0.02	0.04	25	0.11	0.1	0.01	0.02	4.52	0.80	0.93	4.42	0.94	1.08	0.59	0.24	0.63
	12		2	1.02	1.04	0.035	0.055	23	0.04	0.01	0.03	0.02	4.52	0.09	1.04	4.42	0.94	1.04	-0.13	0.23	
	12		4	1.02	1.04	0.01	0.03	20	0.07	0.04	0.03	0.02	4.52	0.40	0.79	4.42	0.94	0.86	0.23	0.19	0.24
	12		Av	1.02	1.02															0.22	0.43
lim1-1	20	lim1-1	1	0.99	1.02	-0.12	-0.09	40	0.26	0.24	0.02	0.03	4.47	1.20	-0.53	4.20	1.53	0.91	0.95	0.22	0.62

Table B1-2 continued

Slab label	Slab Angle	Ball Label	No. Drop	Drop H'(m)	Drop H(m)	Bounce h'(m)	Bounce h(m)	Frames (1/200 s)	Horiz. Distance S'(m)	Horiz. Distance S(m)	S1 (m)	S2 (m)	Vi (m/s)	Vrx (m/s)	Vry (m/s)	Vin (m/s)	Vit (m/s)	Vrn (m/s)	Vrt (m/s)	Rn	Rt
	20		2	0.99	1.03	-0.12	-0.08	38	0.33	0.28	0.05	0.04	4.50	1.47	-0.51	4.22	1.54	0.98	1.21	0.23	0.79
	20		3	0.99	1.01	-0.12	-0.1	56	0.38	0.38	0	0.02	4.45	1.36	-1.02	4.18	1.52	1.42	0.93	0.34	0.61
	20		4	0.99	1.01	0.005	0.025	20	0.06	0.06	0	0.02	4.45	0.60	0.74	4.18	1.52	0.90	0.31	0.22	0.20
	20		5	0.99	0.99	-0.12	-0.12	44	0.3	0.32	-0.02	0	4.41	1.45	-0.53	4.14	1.51	1.00	1.18	0.24	0.79
	20		Av	0.99	0.99															0.25	0.60
lim1-1	46	lim1-1																			
	46		1	0.93	1.02	-0.18	-0.09	23	0.27	0.25	0.02	0.09	4.47	2.17	0.22	3.11	3.22	1.41	1.67	0.45	0.52
	46		2	0.93	0.97	-0.18	-0.14	26	0.23	0.26	-0.03	0.04	4.36	2.00	0.44	3.03	3.14	1.13	1.71	0.37	0.54
	46		3	0.93	0.97	-0.18	-0.14	28	0.27	0.29	-0.02	0.04	4.36	2.07	0.31	3.03	3.14	1.27	1.66	0.42	0.53
	46		4	0.93	0.97	-0.18	-0.14	26	0.22	0.25	-0.03	0.04	4.36	1.92	0.44	3.03	3.14	1.08	1.65	0.36	0.53
			Av																	0.40	0.53
lim1-1	46	gnt1-3	1	0.93	1	-0.18	-0.11	21	0.24	0.22	0.02	0.07	4.43	2.10	0.53	3.08	3.19	1.14	1.84	0.37	0.58
	46		2	0.93	0.95	-0.18	-0.16	27	0.27	0.28	-0.01	0.02	4.32	2.07	0.52	3.00	3.11	1.13	1.82	0.38	0.59
	46		3	0.93	0.97	-0.2	-0.16	25	0.24	0.25	-0.01	0.04	4.36	2.00	0.67	3.03	3.14	0.98	1.87	0.32	0.60
	46		Av	0.93	0.93															0.36	0.59
lim1-1	20	gnt1-3	1	0.99	1.02	-0.14	-0.11	43	0.31	0.3	0.01	0.03	4.47	1.40	-0.54	4.20	1.53	0.99	1.13	0.23	0.74
	20		2	0.99	1.01	-0.14	-0.12	48	0.38	0.37	0.01	0.02	4.45	1.54	-0.68	4.18	1.52	1.16	1.22	0.28	0.80
	20		3	0.99	1	-0.14	-0.13	44	0.28	0.28	0	0.01	4.43	1.27	-0.49	4.16	1.51	0.89	1.03	0.21	0.68
	20		4	0.99	1.03	-0.14	-0.1	45	0.38	0.34	0.04	0.04	4.50	1.51	-0.66	4.22	1.54	1.14	1.19	0.27	0.78
	20		Av	0.99	0.99	-0.14	-0.14													0.25	0.75
mb1-2	12	mb2-2	1	1.05	1.06	0.01	0.02	20	0.08	0.08	0	0.01	4.55	0.80	0.69	4.45	0.95	0.84	0.64	0.19	0.68
	12		2	1.05	1.07	0.035	0.055	23	0.12	0.1	0.02	0.02	4.57	0.87	1.04	4.47	0.95	1.20	0.63	0.27	0.67
	12		3	1.05	1.06	0.04	0.05	31	0.22	0.21	0.01	0.01	4.55	1.35	1.08	4.45	0.95	1.34	1.10	0.30	1.16
	12		4	1.05	1.05	0.05	0.05	27	0.04	0.06	-0.02	0	4.53	0.44	1.03	4.43	0.94	1.10	0.22	0.25	0.23
	12		5	1.05	1.05	0.18	0.18	42	0.12	0.14	-0.02	0	4.53	0.67	1.89	4.43	0.94	1.98	0.26	0.45	0.28
	12		Av	1.05	1.05															0.29	0.46

Table B1-2 continued

Slab label	Slab Angle	Ball Label	No. Drop	Drop H'(m)	Drop H(m)	Bounce h'(m)	Bounce h(m)	Frames (1/200 s)	Horiz. Distance S'(m)	Horiz. Distance S(m)	S1 (m)	S2 (m)	Vi (m/s)	Vrx (m/s)	Vry (m/s)	Vin (m/s)	Vit (m/s)	Vrn (m/s)	Vrt (m/s)	Rn	Rt
mb1-2	22	mb2-2	1	1.01	1.04	-0.12	-0.09	46	0.36	0.35	0.01	0.03	4.52	1.52	-0.74	4.19	1.69	1.25	1.13	0.30	0.67
	22		2	1.01	1.03	-0.12	-0.1	46	0.45	0.44	0.01	0.02	4.50	1.91	-0.69	4.17	1.68	1.36	1.51	0.33	0.90
	22		3	1.01	1.04	0.02	0.05	25	0.16	0.15	0.01	0.03	4.52	1.20	1.01	4.19	1.69	1.39	0.73	0.33	0.43
	22		4	1.01	1.02	0.01	0.02	18	0.12	0.14	-0.02	0.01	4.47	1.56	0.66	4.15	1.68	1.20	1.19	0.29	0.71
	22		5	1.01	1.02	-0.12	-0.11	53	0.38	0.4	-0.02	0.01	4.47	1.51	-0.88	4.15	1.68	1.39	1.07	0.33	0.64
	22		Av	1.01	1.01															0.32	0.67
mb1-2	22	gnt1-3	1	1.01	1.02	0.01	0.02	36	0.07	0.07	0	0.01	4.47	0.39	0.99	4.15	1.68	1.07	-0.01	0.26	
	22		2	1.01	1.03	0.09	0.11	29	0.18	0.19	-0.01	0.02	4.50	1.31	1.47	4.17	1.68	1.85	0.66	0.44	0.39
	22		3	1.01	1.01	0.11	0.11	31	0.19	0.22	-0.03	0	4.45	1.42	1.47	4.13	1.67	1.89	0.77	0.46	0.46
	22		Av	1.01	1.01															0.45	0.43
mb1-2	46	gnt1-3	1	0.94	1	-0.18	-0.12	25	0.34	0.32	0.02	0.06	4.43	2.56	0.35	3.08	3.19	1.60	2.03	0.52	0.64
	46		2	0.94	1	-0.18	-0.12	20	0.24	0.22	0.02	0.06	4.43	2.20	0.71	3.08	3.19	1.09	2.04	0.35	0.64
	46		3	0.94	1	-0.18	-0.12	26	0.34	0.32	0.02	0.06	4.43	2.46	0.29	3.08	3.19	1.57	1.92	0.51	0.60
	46		4	0.94	0.99	-0.18	-0.13	32	0.46	0.44	0.02	0.05	4.41	2.75	0.03	3.06	3.17	1.96	1.93	0.64	0.61
	46		Av	0.94	0.94	-0.18	-0.18				0.02									0.51	0.62
mb1-2	46	mb2-2	1	0.94	1	-0.18	-0.12	22	0.31	0.3	0.01	0.06	4.43	2.73	0.55	3.08	3.19	1.58	2.29	0.51	0.72
	46		2	0.94	0.99	-0.18	-0.13	22	0.32	0.31	0.01	0.05	4.41	2.82	0.64	3.06	3.17	1.58	2.42	0.52	0.76
	46		3	0.94	0.97	-0.18	-0.15	30	0.38	0.38	0	0.03	4.36	2.53	0.26	3.03	3.14	1.64	1.95	0.54	0.62
	46		4	0.94	0.96	-0.18	-0.16	30	0.39	0.4	-0.01	0.02	4.34	2.67	0.33	3.01	3.12	1.69	2.09	0.56	0.67
	46		Av	0.94	0.94	-0.18	-0.18													0.53	0.69
scht1-1	10	scht1-2	1	1	1.01	0.27	0.28	50	0.28	0.28	0	0.01	4.45	1.12	2.35	4.38	0.77	2.51	0.70	0.57	0.90
	10		2	1	1.01	0.22	0.23	40	0.17	0.18	-0.01	0.01	4.45	0.90	2.13	4.38	0.77	2.25	0.52	0.51	0.67
	10		3	1	1.01	0.33	0.34	50	0.22	0.21	0.01	0.01	4.45	0.84	2.59	4.38	0.77	2.69	0.38	0.61	0.49
	10		4	1	1.01	0.28	0.29	48	0.16	0.17	-0.01	0.01	4.45	0.71	2.39	4.38	0.77	2.47	0.28	0.56	0.37

Table B1-2 continued

Slab label	Slab Angle	Ball Label	No. Drop	Drop H'(m)	Drop H(m)	Bounce h'(m)	Bounce h(m)	Frames (1/200 s)	Horiz. Distance S'(m)	Horiz. Distance S(m)	S1 (m)	S2 (m)	Vi (m/s)	Vrx (m/s)	Vry (m/s)	Vin (m/s)	Vit (m/s)	Vrn (m/s)	Vrt (m/s)	Rn	Rt
	10		5	1	1.01	0.21	0.22	43	0.36	0.36	0	0.01	4.45	1.67	2.08	4.38	0.77	2.34	1.29	0.53	1.67
	10		Av	1	1.01							0.01	4.45							0.56	0.61
													0.00								
scht1-1	20	scht1-2	1	0.93	0.95	0.21	0.23	39	0.34	0.32	0.02	0.02	4.32	1.64	2.14	4.06	1.48	2.57	0.81	0.63	0.55
	20		2	0.93	0.94	0.19	0.2	40	0.39	0.39	0	0.01	4.29	1.95	1.98	4.04	1.47	2.53	1.15	0.63	0.79
	20		3	0.93	0.95	0.23	0.25	48	0.41	0.38	0.03	0.02	4.32	1.58	2.22	4.06	1.48	2.63	0.73	0.65	0.49
	20		4	0.93	0.93	0.1	0.1	32	0.28	0.3	-0.02	0	4.27	1.88	1.41	4.01	1.46	1.97	1.28	0.49	0.88
	20		5	0.93	0.95	0.14	0.16	38	0.44	0.44	0	0.02	4.32	2.32	1.77	4.06	1.48	2.46	1.57	0.61	1.06
	20		Av	0.93	0.93															0.60	0.75
scht1-1	20	mb2-2	1	0.93	0.93	0.1	0.1	32	0.28	0.29	-0.01	0	4.27	1.81	1.41	4.01	1.46	1.94	1.22	0.48	0.84
	20		2	0.93	0.94	0.12	0.13	30	0.34	0.33	0.01	0.01	4.29	2.20	1.60	4.04	1.47	2.26	1.52	0.56	1.03
	20		3	0.93	0.94	0.26	0.27	50	0.33	0.31	0.02	0.01	4.29	1.24	2.31	4.04	1.47	2.59	0.38	0.64	0.26
	20		4	0.93	0.94	0.13	0.14	33	0.34	0.34	0	0.01	4.29	2.06	1.66	4.04	1.47	2.26	1.37	0.56	0.93
	20		Av	0.93	0.93															0.56	0.67
scht1-1	44	mb2-2	1	0.92	0.95	-0.2	-0.17	41	0.51	0.51	0	0.03	4.32	2.49	-0.18	3.11	3.00	1.85	1.67	0.60	0.56
	44		2	0.92	0.95	-0.2	-0.17	40	0.5	0.5	0	0.03	4.32	2.50	-0.13	3.11	3.00	1.83	1.71	0.59	0.57
	44		3	0.92	0.96	-0.2	-0.16	40	0.5	0.47	0.03	0.04	4.34	2.35	-0.18	3.12	3.01	1.76	1.56	0.56	0.52
	44		4	0.92	0.95	-0.2	-0.17	30	0.43	0.41	0.02	0.03	4.32	2.73	0.40	3.11	3.00	1.61	2.24	0.52	0.75
	44		Av	0.92	0.92	-0.2	-0.2													0.57	0.60
scht1-1	44	scht1-2	1	0.92	0.94	-0.2	-0.18	44	0.54	0.53	0.01	0.02	4.29	2.41	-0.26	3.09	2.98	1.86	1.55	0.60	0.52
	44		2	0.92	0.94	0.02	0.04	18	0.25	0.23	0.02	0.02	4.29	2.56	0.89	3.09	2.98	2.41	1.22	0.78	0.41
	44		3	0.92	0.94	-0.2	-0.18	42	0.57	0.56	0.01	0.02	4.29	2.67	-0.17	3.09	2.98	1.98	1.80	0.64	0.60
	44		4	0.92	0.93	-0.2	-0.19	43	0.5	0.5	0	0.01	4.27	2.33	-0.17	3.07	2.97	1.74	1.55	0.57	0.52
	44		Av	0.92	0.92															0.65	0.51
scht1-1	44	gnt1-3	1	0.92	0.95	-0.2	-0.17	37	0.57	0.56	0.01	0.03	4.32	3.03	0.01	3.11	3.00	2.09	2.19	0.67	0.73

Table B1-2 continued

Slab label	Slab Angle	Ball Label	No. Drop	Drop H'(m)	Drop H(m)	Bounce h'(m)	Bounce h(m)	Frames (1/200 s)	Horiz. Distance S'(m)	Horiz. Distance S(m)	S1 (m)	S2 (m)	Vi (m/s)	Vrx (m/s)	Vry (m/s)	Vin (m/s)	Vit (m/s)	Vrn (m/s)	Vrt (m/s)	Rn	Rt
	44		2	0.92	0.95	-0.2	-0.17	45	0.65	0.65	0	0.03	4.32	2.89	-0.35	3.11	3.00	2.26	1.84	0.73	0.61
	44		3	0.92	0.95	-0.2	-0.17	41	0.56	0.56	0	0.03	4.32	2.73	-0.18	3.11	3.00	2.02	1.84	0.65	0.61
	44		4	0.92	0.99	-0.2	-0.13	42	0.64	0.61	0.03	0.07	4.41	2.90	-0.41	3.17	3.06	2.31	1.80	0.73	0.59
	44		Av	0.92	0.92	-0.2	-0.2													0.70	0.64
scht1-1	44	steel	1	0.92	0.94	-0.2	-0.18	42	0.46	0.49	-0.03	0.02	4.29	2.33	-0.17	3.09	2.98	1.75	1.56	0.56	0.52
	44		2	0.92	0.93	-0.2	-0.19	44	0.54	0.56	-0.02	0.01	4.27	2.55	-0.22	3.07	2.97	1.92	1.68	0.63	0.57
	44		3	0.92	0.93	-0.2	-0.19	46	0.55	0.57	-0.02	0.01	4.27	2.48	-0.30	3.07	2.97	1.94	1.57	0.63	0.53
	44		4	0.92	0.93	-0.2	-0.19	45	0.53	0.55	-0.02	0.01	4.27	2.44	-0.26	3.07	2.97	1.88	1.58	0.61	0.53
	44		Av	0.92	0.92	-0.2	-0.2													0.61	0.54
scht1-1	44	snd3-1	1	0.92	0.96	-0.2	-0.16	40	0.52	0.52	0	0.04	4.34	2.60	-0.18	3.12	3.01	1.94	1.74	0.62	0.58
	44		2	0.92	1	-0.2	-0.12	35	0.43	0.39	0.04	0.08	4.43	2.23	-0.17	3.19	3.08	1.67	1.48	0.52	0.48
	44		3	0.92	0.95	-0.2	-0.17	47	0.61	0.62	-0.01	0.03	4.32	2.64	-0.43	3.11	3.00	2.14	1.60	0.69	0.53
	44		4	0.92	0.95	-0.2	-0.17	44	0.57	0.56	0.01	0.03	4.32	2.55	-0.31	3.11	3.00	1.99	1.62	0.64	0.54
	44		Av	0.92	0.92	-0.2	-0.2													0.62	0.53
scht1-1	44	lim1-1	1	0.92	0.95	-0.2	-0.17	24	0.24	0.23	0.01	0.03	4.32	1.92	0.83	3.11	3.00	0.74	1.95	0.24	0.65
	44		2	0.92	0.98	-0.2	-0.14	31	0.31	0.28	0.03	0.06	4.38	1.81	0.14	3.15	3.05	1.15	1.40	0.37	0.46
	44		3	0.92	0.97	-0.2	-0.15	29	0.3	0.28	0.02	0.05	4.36	1.93	0.32	3.14	3.03	1.11	1.61	0.35	0.53
	44		4	0.92	0.95	-0.2	-0.17	34	0.34	0.34	0	0.03	4.32	2.00	0.17	3.11	3.00	1.27	1.55	0.41	0.52
	44		Av	0.92	0.92	-0.2	-0.2													0.34	0.54
scht1-1	44	bast1-3	1	0.92	0.94	-0.19	-0.17	49	0.67	0.67	0	0.02	4.29	2.73	-0.51	3.09	2.98	2.26	1.61	0.73	0.54
	44		2	0.92	0.97	-0.19	-0.14	45	0.7	0.66	0.04	0.05	4.36	2.93	-0.48	3.14	3.03	2.38	1.78	0.76	0.59
	44		3	0.92	0.95	-0.19	-0.16	42	0.65	0.64	0.01	0.03	4.32	3.05	-0.27	3.11	3.00	2.31	2.01	0.74	0.67
	44		4	0.92	0.95	-0.19	-0.16	42	0.63	0.62	0.01	0.03	4.32	2.95	-0.27	3.11	3.00	2.24	1.94	0.72	0.65
	44		Av	0.92	0.92	-0.19	-0.19													0.75	0.60

Table B1-2 continued

Slab label	Slab Angle	Ball Label	No. Drop	Drop H'(m)	Drop H(m)	Bounce h'(m)	Bounce h(m)	Frames (1/200 s)	Horiz. Distance S'(m)	Horiz. Distance S(m)	S1 (m)	S2 (m)	Vi (m/s)	Vrx (m/s)	Vry (m/s)	Vin (m/s)	Vit (m/s)	Vrn (m/s)	Vrt (m/s)	Rn	Rt
steel	10	steel	1	1.01	1.02	0.035	0.045	13	0.02	0.02	0	0.01	4.474	0.308	1.011	4.406	0.777	1.049	0.127	0.2382	0.164
	10		2	1.01	1.02	0.02	0.03	13	0.02	0.01	0.01	0.01	4.474	0.154	0.78	4.406	0.777	0.795	0.016	0.1805	0.021
	10		3	1.01	1.03	0.14	0.16	37	0.18	0.16	0.02	0.02	4.495	0.865	1.772	4.427	0.781	1.896	0.544	0.4282	0.697
	10		4	1.01	1.02	0.125	0.135	37	0.16	0.15	0.01	0.01	4.474	0.811	1.637	4.406	0.777	1.753	0.514	0.3979	0.662
	10		5	1.01	1.03	0.15	0.17	36	0.16	0.14	0.02	0.02	4.495	0.778	1.827	4.427	0.781	1.935	0.449	0.437	0.575
	10		Av																	0.421	0.645
	10																				
	10	steel-1	1	1.01	1.02	0.27	0.28	42	0.21	0.2	0.01	0.01	4.474	0.952	2.363	4.406	0.777	2.493	0.528	0.5658	0.679
	10		2	1.01	1.03	0.17	0.19	40	0.2	0.17	0.03	0.02	4.495	0.85	1.931	4.427	0.781	2.049	0.502	0.4629	0.643
	10		3	1.01	1.03	0.15	0.17	38	0.165	0.145	0.02	0.02	4.495	0.763	1.827	4.427	0.781	1.931	0.434	0.4363	0.556
	10		4	1.01	1.02	0.18	0.19	41	0.18	0.17	0.01	0.01	4.474	0.829	1.932	4.406	0.777	2.047	0.481	0.4646	0.619
	10		Av	1.01	1.01		0													0.4824	0.624
	10				0		0														
	10	steel-2	1	1.01	1.02	0.14	0.15	32	0.15	0.15	0	0.01	4.474	0.938	1.722	4.406	0.777	1.859	0.624	0.422	0.804
	10		2	1.01	1.02	0.14	0.15	33	0.14	0.14	0	0.01	4.474	0.848	1.718	4.406	0.777	1.84	0.537	0.4176	0.692
	10		3	1.01	1.02	0.175	0.185	35	0.15	0.14	0.01	0.01	4.474	0.8	1.916	4.406	0.777	2.025	0.455	0.4597	0.586
	10		4	1.01	1.02	0.18	0.19	38	0.18	0.17	0.01	0.01	4.474	0.895	1.932	4.406	0.777	2.058	0.546	0.4671	0.702
	10		Av	1.01	1.01		0			0										0.4416	0.696
	10				0		0			0											
	10	gnt1-3	1	1.01	1.02	0.33	0.34	55	0.2	0.2	0	0.01	4.474	0.727	2.585	4.406	0.777	2.672	0.267	0.6066	0.344
	10		2	1.01	1.02	0.33	0.34	51	0.13	0.13	0	0.01	4.474	0.51	2.584	4.406	0.777	2.633	0.053	0.5977	0.069
	10		3	1.01	1.02	0.27	0.28	51	0.3	0.29	0.01	0.01	4.474	1.137	2.349	4.406	0.777	2.511	0.712	0.5699	0.917
	10		4	1.01	1.02	0.28	0.29	48	0.26	0.25	0.01	0.01	4.474	1.042	2.386	4.406	0.777	2.53	0.612	0.5743	0.787
	10		Av	1.01	1.01		0			0										0.5871	0.683
	10				0		0			0											
	10	gnt1-2	1	1.01	1.02	0.285	0.29	52	0.2	0.21	-0.01	0.005	4.463	0.808	2.391	4.395	0.775	2.495	0.38	0.5676	0.491
	10		2	1.01	1.02	0.38	0.39	59	0.23	0.23	0	0.01	4.474	0.78	2.769	4.406	0.777	2.862	0.287	0.6497	0.369
	10		3	1.01	1.02	0.28	0.29	48	0.38	0.38	0	0.01	4.474	1.583	2.386	4.406	0.777	2.624	1.145	0.5957	1.474
	10		4	1.01	1.02	0.31	0.315	48	0.12	0.13	-0.01	0.005	4.463	0.542	2.49	4.395	0.775	2.546	0.101	0.5793	0.13

Table B1-2 continued

Slab label	Slab Angle	Ball Label	No. Drop	Drop H'(m)	Drop H(m)	Bounce h'(m)	Bounce h(m)	Frames (1/200 s)	Horiz. Distance S'(m)	Horiz. Distance S(m)	S1 (m)	S2 (m)	Vi (m/s)	Vrx (m/s)	Vry (m/s)	Vin (m/s)	Vit (m/s)	Vrn (m/s)	Vrt (m/s)	Rn	Rt
	10		Av	1.01	1.01		0			0										0.5981	0.616
	10				0		0			0											
	10	bast1-3	1	1.01	1.02	0.26	0.265	42	0.25	0.25	0	0.005	4.463	1.19	2.292	4.395	0.775	2.464	0.774	0.5606	0.999
	10		2	1.01	1.01	0.23	0.23	41	0	0.02	-0.02	0	4.452	0.098	2.127	4.384	0.773	2.112	-0.27	0.4818	-0.35
	10		3	1.01	1.02	0.29	0.3	46	0.31	0.31	0	0.01	4.474	1.348	2.432	4.406	0.777	2.63	0.905	0.5969	1.165
	10		4	1.01	1.02	0.23	0.235	42	0.25	0.27	-0.02	0.005	4.463	1.286	2.149	4.395	0.775	2.34	0.893	0.5324	1.152
	10		Av	1.01	1.01		0			0										0.5429	0.741
	10				0		0			0											
	10	bast1-1	1	1.01	1.02	0.26	0.27	45	0.28	0.29	-0.01	0.01	4.474	1.289	2.304	4.406	0.777	2.492	0.869	0.5657	1.119
	10		2	1.01	1.02	0.13	0.14	35	0.29	0.29	0	0.01	4.474	1.657	1.658	4.406	0.777	1.921	1.344	0.436	1.73
	10		3	1.01	1.02	0.27	0.28	40	0.15	0.15	0	0.01	4.474	0.75	2.381	4.406	0.777	2.475	0.325	0.5618	0.419
	10		4	1.01	1.02	0.2	0.21	40	0.14	0.15	-0.01	0.01	4.474	0.75	2.031	4.406	0.777	2.13	0.386	0.4836	0.497
	10		5	1.01	1.02	0.36	0.37	50	0.08	0.09	-0.01	0.01	4.474	0.36	2.706	4.406	0.777	2.728	-0.12	0.6191	-0.15
	10		Av	1.01	1.01		0			0										0.5333	0.723
	10				0		0			0											
	10	gnt2	1	1.01	1.02	0.4	0.41	52	0.18	0.18	0	0.01	4.474	0.692	2.852	4.406	0.777	2.929	0.187	0.6649	0.24
	10		2	1.01	1.02	0.36	0.37	52	0.29	0.29	0	0.01	4.474	1.115	2.698	4.406	0.777	2.851	0.63	0.6472	0.811
	10		3	1.01	1.02	0.32	0.33	50	0.21	0.2	0.01	0.01	4.474	0.8	2.546	4.406	0.777	2.646	0.346	0.6007	0.445
	10		4	1.01	1.02	0.39	0.395	51	0.04	0.06	-0.02	0.005	4.463	0.235	2.8	4.395	0.775	2.798	-0.25	0.6367	-0.33
	10		5	1.01	1.03	0.36	0.375	50	0.24	0.23	0.01	0.015	4.484	0.92	2.726	4.416	0.779	2.845	0.433	0.6441	0.556
	10		Av	1.01	1.01		0			0										0.6387	0.604
	10				0		0			0											
steel	10	mb3-2	1	1.01	1.02	0.05	0.06	26	0.16	0.16	0	0.01	4.474	1.231	1.099	4.406	0.777	1.296	1.021	0.2942	1.315
	10	mb2-1	2	1.01	1.02	0.12	0.13	35	0.12	0.13	-0.01	0.01	4.474	0.743	1.601	4.406	0.777	1.706	0.454	0.3872	0.584
	10		3	1.01	1.02	0.11	0.12	30	0.08	0.08	0	0.01	4.474	0.533	1.536	4.406	0.777	1.605	0.259	0.3643	0.333
	10		4	1.01	1.03	0.18	0.2	40	0.22	0.21	0.01	0.02	4.495	1.05	1.981	4.427	0.781	2.133	0.69	0.4819	0.884
	10		5	1.01	1.03	0.05	0.07	25	0.1	0.09	0.01	0.02	4.495	0.72	1.173	4.427	0.781	1.28	0.505	0.2892	0.647
	10		Av	1.01	1.01		0			0										0.3634	0.753
	10				0		0			0											

Table B1-2 continued

Slab label	Slab Angle	Ball Label	No. Drop	Drop H'(m)	Drop H(m)	Bounce h'(m)	Bounce h(m)	Frames (1/200 s)	Horiz. Distance S'(m)	Horiz. Distance S(m)	S1 (m)	S2 (m)	Vi (m/s)	Vrx (m/s)	Vry (m/s)	Vin (m/s)	Vit (m/s)	Vrn (m/s)	Vrt (m/s)	Rn	Rt
steel	20	steel	1	0.96	0.97	0.03	0.04	19	0.14	0.14	0	0.01	4.362	1.474	0.887	4.099	1.492	1.338	1.081	0.3263	0.725
	20		2	0.96	0.97	0.03	0.04	18	0.12	0.13	-0.01	0.01	4.362	1.444	0.886	4.099	1.492	1.326	1.054	0.3236	0.707
	20		3	0.96	0.97	0.025	0.035	18	0.11	0.13	-0.02	0.01	4.362	1.444	0.83	4.099	1.492	1.274	1.073	0.3108	0.719
	20		4	0.96	0.97	0.02	0.03	18	0.11	0.13	-0.02	0.01	4.362	1.444	0.775	4.099	1.492	1.222	1.092	0.2981	0.732
	20		Av	0.96	0.96		0			0										0.3147	0.721
	20				0		0			0											
	20	steel-1	1	0.96	0.97	0.075	0.085	25	0.2	0.21	-0.01	0.01	4.362	1.68	1.293	4.099	1.492	1.79	1.136	0.4366	0.762
	20		2	0.96	0.98	0.08	0.1	24	0.2	0.19	0.01	0.02	4.385	1.583	1.422	4.12	1.5	1.878	1.002	0.4557	0.668
	20		3	0.96	0.96	0.07	0.07	28	0.2	0.23	-0.03	0	4.34	1.643	1.187	4.078	1.484	1.677	1.138	0.4112	0.767
	20		4	0.96	0.97	0.07	0.08	22	0.18	0.2	-0.02	0.01	4.362	1.818	1.267	4.099	1.492	1.812	1.275	0.4421	0.855
	20		Av	0.96	0.96		0			0										0.4364	0.763
	20				0		0			0											
	20	steel-2	1	0.97	0.98	0.04	0.05	20	0.13	0.15	-0.02	0.01	4.385	1.5	0.991	4.12	1.5	1.444	1.071	0.3504	0.714
	20		2	0.97	0.98	0.045	0.055	20	0.14	0.16	-0.02	0.01	4.385	1.6	1.041	4.12	1.5	1.525	1.148	0.3701	0.765
	20		3	0.97	0.98	0.04	0.05	20	0.15	0.17	-0.02	0.01	4.385	1.7	0.991	4.12	1.5	1.512	1.259	0.367	0.839
	20		4	0.97	0.98	0.05	0.06	22	0.16	0.18	-0.02	0.01	4.385	1.636	1.085	4.12	1.5	1.579	1.167	0.3833	0.778
	20		Av	0.97	0.97		0			0										0.3677	0.774
	20				0		0			0											
	20	gnt2	1	0.97	0.98	0.12	0.13	31	0.32	0.35	-0.03	0.01	4.385	2.258	1.599	4.12	1.5	2.275	1.575	0.5521	1.05
	20		2	0.97	0.99	0.2	0.22	40	0.36	0.37	-0.01	0.02	4.407	1.85	2.081	4.141	1.507	2.588	1.027	0.625	0.681
	20		3	0.97	0.98	0.19	0.2	38	0.35	0.39	-0.04	0.01	4.385	2.053	1.985	4.12	1.5	2.567	1.25	0.623	0.834
	20		4	0.97	0.98	0.19	0.2	36	0.33	0.37	-0.04	0.01	4.385	2.056	1.994	4.12	1.5	2.577	1.25	0.6254	0.833
	20		5	0.97	0.98	0.2	0.21	38	0.34	0.36	-0.02	0.01	4.385	1.895	2.037	4.12	1.5	2.562	1.084	0.6219	0.723
	20		Av	0.97	0.97		0			0										0.6094	0.824
	20				0		0			0											
	20	bast1-3	1	0.97	0.97	0.02	0.02	20	0.04	0.1	-0.06	0	4.362	1	0.691	4.099	1.492	0.991	0.704	0.2417	0.472
	20		2	0.97	0.99	0.16	0.18	36	0.34	0.35	-0.01	0.02	4.407	1.944	1.883	4.141	1.507	2.434	1.183	0.5878	0.785
	20		3	0.97	0.98	0.22	0.23	40	0.3	0.32	-0.02	0.01	4.385	1.6	2.131	4.12	1.5	2.55	0.775	0.6188	0.517
	20		4	0.97	0.98	0.1	0.11	29	0.28	0.33	-0.05	0.01	4.385	2.276	1.47	4.12	1.5	2.16	1.636	0.5241	1.091

Table B1-2 continued

Slab label	Slab Angle	Ball Label	No. Drop	Drop H'(m)	Drop H(m)	Bounce h'(m)	Bounce h(m)	Frames (1/200 s)	Horiz. Distance S'(m)	Horiz. Distance S(m)	S1 (m)	S2 (m)	Vi (m/s)	Vrx (m/s)	Vry (m/s)	Vin (m/s)	Vit (m/s)	Vrn (m/s)	Vrt (m/s)	Rn	Rt
	20		5	0.97	0.98	0.12	0.13	32	0.29	0.31	-0.02	0.01	4.385	1.938	1.597	4.12	1.5	2.164	1.274	0.5251	0.85
	20		Av	0.97	0.97		0			0										0.564	0.743
	20				0		0			0											
	20	gnt1-3	1	0.97	0.98	0.26	0.27	40	0.35	0.37	-0.02	0.01	4.385	1.85	2.331	4.12	1.5	2.823	0.941	0.6852	0.628
	20		2	0.97	0.97	0.17	0.17	40	0.25	0.32	-0.07	0	4.362	1.6	1.831	4.099	1.492	2.268	0.877	0.5532	0.588
	20		3	0.97	0.98	0.15	0.16	34	0.29	0.34	-0.05	0.01	4.385	2	1.775	4.12	1.5	2.352	1.272	0.5708	0.848
	20		4	0.97	0.99	0.16	0.18	36	0.3	0.32	-0.02	0.02	4.407	1.778	1.883	4.141	1.507	2.377	1.027	0.574	0.681
	20		Av	0.97	0.97		0			0										0.5958	0.686
					0		0			0											
steel	46	steel	1	0.9	0.94	-0.22	-0.18	30	0.32	0.34	-0.02	0.04	4.295	2.267	0.464	2.983	3.089	1.308	1.909	0.4385	0.618
	46		2	0.92	0.95	-0.22	-0.19	30	0.33	0.36	-0.03	0.03	4.306	2.4	0.531	2.991	3.097	1.358	2.049	0.4539	0.662
	46		3	0.92	0.93	-0.22	-0.21	31	0.29	0.35	-0.06	0.01	4.26	2.258	0.595	2.959	3.064	1.211	1.996	0.4093	0.651
	46		4	0.92	0.93	-0.22	-0.21	30	0.3	0.34	-0.04	0.01	4.26	2.267	0.664	2.959	3.064	1.169	2.052	0.3951	0.67
	46		Av	0.92	0.92		0			0										0.4242	0.65
	46				0		0			0											
steel	46	steel-1	1	0.92	0.96	-0.22	-0.18	26	0.31	0.31	0	0.04	4.329	2.385	0.747	3.007	3.114	1.196	2.194	0.3979	0.705
	46		2	0.92	0.96	-0.22	-0.18	26	0.33	0.34	-0.01	0.04	4.329	2.615	0.747	3.007	3.114	1.362	2.354	0.4531	0.756
	46		3	0.92	0.95	-0.22	-0.19	27	0.35	0.37	-0.02	0.03	4.306	2.741	0.745	2.991	3.097	1.454	2.44	0.4861	0.788
	46		4	0.92	0.94	-0.22	-0.2	28	0.38	0.42	-0.04	0.02	4.283	3	0.742	2.975	3.081	1.643	2.618	0.5521	0.85
	46		Av	0.92	0.92		0			0										0.4723	0.774
	46				0		0			0											
steel	46	steel-2	1	0.92	0.96	-0.22	-0.18	26	0.32	0.36	-0.04	0.04	4.329	2.769	0.747	3.007	3.114	1.473	2.461	0.4899	0.79
	46		2	0.92	0.96	-0.22	-0.18	22	0.26	0.3	-0.04	0.04	4.329	2.727	1.097	3.007	3.114	1.2	2.684	0.3991	0.862
	46		3	0.92	0.96	-0.22	-0.18	23	0.26	0.29	-0.03	0.04	4.329	2.522	1.001	3.007	3.114	1.119	2.472	0.372	0.794
	46		4	0.92	0.96	-0.22	-0.18	22	0.26	0.29	-0.03	0.04	4.329	2.636	1.097	3.007	3.114	1.135	2.62	0.3773	0.842
	46		Av	0.92	0.92		0			0										0.4096	0.822
	46				0		0			0											
steel	46	gnt-2	1	0.92	0.92	-0.22	0.02	36	0.43	0.49	-0.06	0	4.249	2.722	0.645	2.951	3.056	2.406	1.427	0.8154	0.467
	46		2	0.92	0.97	-0.22	0	34	0.43	0.44	-0.01	0.05	4.362	2.588	0	3.03	3.138	1.862	1.798	0.6144	0.573

Table B1-2 continued

Slab label	Slab Angle	Ball Label	No. Drop	Drop H'(m)	Drop H(m)	Bounce h'(m)	Bounce h(m)	Frames (1/200 s)	Horiz. Distance S'(m)	Horiz. Distance S(m)	S1 (m)	S2 (m)	Vi (m/s)	Vrx (m/s)	Vry (m/s)	Vin (m/s)	Vit (m/s)	Vrn (m/s)	Vrt (m/s)	Rn	Rt
	46		3	0.92	0.95	-0.22	0	35	0.45	0.48	-0.03	0.03	4.317	2.743	0	2.999	3.106	1.973	1.905	0.6579	0.614
	46		4	0.92	0.95	-0.22	0.02	40	0.5	0.53	-0.03	0.03	4.317	2.65	0.645	2.999	3.106	2.354	1.377	0.7851	0.443
	46		Av	0.92	0.92		0			0										0.7182	0.524
	46				0		0			0											
	46	gnt1-3	1	0.92	0.95	-0.22	0	45	0.57	0.6	-0.03	0.03	4.317	2.667	0	2.999	3.106	1.918	1.852	0.6396	0.596
	46		2	0.92	0.95	-0.22	0.02	42	0.54	0.58	-0.04	0.03	4.317	2.762	0.65	2.999	3.106	2.438	1.451	0.813	0.467
	46		3	0.92	0.95	-0.22	0	40	0.5	0.54	-0.04	0.03	4.317	2.7	0	2.999	3.106	1.942	1.876	0.6476	0.604
	46		4	0.92	0.94	-0.22	0	42	0.53	0.56	-0.03	0.02	4.295	2.667	0	2.983	3.089	1.918	1.852	0.643	0.6
	46		Av	0.92	0.92		0			0										0.6858	0.567
	46				0		0			0											
steel	46	bast1-3	1	0.92	0.95	-0.22	-0.19	32	0.37	0.4	-0.03	0.03	4.317	2.5	0.403	2.999	3.106	1.519	2.026	0.5064	0.652
	46		2	0.92	0.95	-0.22	-0.19	42	0.48	0.52	-0.04	0.03	4.317	2.476	-0.13	2.999	3.106	1.868	1.63	0.623	0.525
	46		3	0.92	0.94	-0.22	-0.2	36	0.46	0.49	-0.03	0.02	4.295	2.722	0.228	2.983	3.089	1.8	2.055	0.6033	0.665
	46		4	0.92	0.94	-0.22	-0.2	32	0.38	0.41	-0.03	0.02	4.295	2.563	0.465	2.983	3.089	1.52	2.115	0.5096	0.685
	46		Av	0.92	0.92		0			0										0.5605	0.632
	46				0		0			0											
	46	mb2-1	1	0.92	0.97	-0.22	-0.17	25	0.24	0.25	-0.01	0.05	4.362	2	0.747	3.03	3.138	0.92	1.927	0.3035	0.614
	46		2	0.92	0.95	-0.22	-0.19	32	0.29	0.33	-0.04	0.03	4.317	2.063	0.403	2.999	3.106	1.204	1.722	0.4014	0.555
	46		3	0.92	0.96	-0.22	-0.18	22	0.21	0.24	-0.03	0.04	4.34	2.182	1.097	3.015	3.122	0.808	2.305	0.2679	0.738
	46		Av	0.92	0.92		0			0										0.3243	0.636
	46				0		0			0											
steel	46	snd1-2	1	0.92	0.94	-0.22	-0.2	39	0.47	0.52	-0.05	0.02	4.295	2.667	0.069	2.983	3.089	1.87	1.902	0.6269	0.616
	46		2	0.92	0.96	-0.21	-0.17	45	0.5	0.53	-0.03	0.04	4.34	2.356	-0.35	3.015	3.122	1.936	1.386	0.6422	0.444
	46		3	0.92	0.97	-0.22	-0.17	40	0.44	0.46	-0.02	0.05	4.362	2.3	-0.13	3.03	3.138	1.745	1.503	0.576	0.479
	46		Av	0.92	0.92		0			0										0.615	0.513

B.2 Laboratory tests with rough rocks

Coefficient of restitution calculation on rough rocks and beds of debris and soil materials are calculated using equations as the previous section. Normal coefficient of restitution calculation results are shown in table B 2-1. Notation of symbols:

Bast1-3: basalt ball Bs: basalt boulder;
lim: limestone; Grey: greywacke;
frag: rock fragment; Paving: paving stone;
represents compacted materials (inter-layered with soil).

Table B 2-1: Coefficient of restitution calculation (Normal bounce on rough rocks and beds of debris and soil materials)

Slope	Rock	No. drop	Drop H (m)	Bounce h (m)	Frames (1/200 s)	R
Basalt	bast1-3	1	0.6	0.32		0.730
Basalt	bast1-3	2	0.6	0.42		0.837
Basalt	bast1-3	3	0.6	0.42		0.837
Basalt	bast1-3	4	0.6	0.45	52	0.866
Basalt	bast1-3	av	0.6			0.817
Basalt	bast1-3	1	1	0.68	77	0.825
Basalt	bast1-3	2	1	0.65	77	0.806
Basalt	bast1-3	3	1	0.68		0.825
Basalt	bast1-3	4	1	0.72		0.849
Basalt	bast1-3	5	1	0.7		0.837
Basalt	bast1-3	6	1	0.65	73	0.806
Basalt	bast1-3	av	1			0.824
Basalt	bast1-3					
Basalt	bast1-3	1	1.5	0.7		0.683
Basalt	bast1-3	2	1.5	0.99		0.812
Basalt	bast1-3	3	1.5	1.07		0.845
Basalt	bast1-3	4	1.5	1.09		0.852
Basalt	bast1-3	5	1.5	0.98		0.808
Basalt	bast1-3	av	1.5			0.800
Basalt	bast1-3					
Basalt	bast1-3	1	2	1.23		0.784
Basalt	bast1-3	2	2	1.28		0.800
Basalt	bast1-3	3	2	1.43		0.846
Basalt	bast1-3	4	2	1.5		0.866
Basalt	bast1-3	av	2			0.824
Basalt	bast1-3					
Basalt	bast1-3	1	2.5	1.74		0.834
Basalt	bast1-3	2	2.5	1.85		0.860

Table B 2-1 continued

Slope	Rock	No. drop	Drop H (m)	Bounce h (m)	Frames (1/200 s)	R
Basalt	bast1-3	3	2.5	1.68		0.820
Basalt	bast1-3	4	2.5	1.42		0.754
Basalt	bast1-3	5	2.5	1.82		0.853
Basalt	bast1-3	av	2.5			0.824
Basalt	BS	1	0.6	0.01		0.129
Basalt	BS	2	0.6	0		0.000
Basalt	BS	3	0.6	0.02		0.183
Basalt	BS	4	0.6	0		0.000
Basalt	BS	5	0.6	0		0.000
Basalt	BS	6	0.6	0.09		0.387
Basalt	BS	7	0.6	0.02		0.183
Basalt	BS	8	0.6	0		0.000
Basalt	BS	9	0.6	0		0.000
Basalt	BS	av	0.6			0.098
Basalt	BS	1	1	0.03		0.173
Basalt	BS	2	1	0.02		0.141
Basalt	BS	3	1	0		0.000
Basalt	BS	4	1	0.05		0.224
Basalt	BS	5	1	0.05		0.224
Basalt	BS	6	1	0.01		0.100
Basalt	BS	7	1	0.03		0.173
Basalt	BS	av	1			0.148
Basalt	BS	1	1.5	0.21		0.374
Basalt	BS	2	1.5	0		0.000
Basalt	BS	3	1.5	0.02		0.115
Basalt	BS	4	1.5	0.02		0.115
Basalt	BS	5	1.5	0.01		0.082
Basalt	BS	6	1.5	0.1		0.258
Basalt	BS	7	1.5	0.1		0.258
Basalt	BS	8	1.5	0.09		0.245
Basalt	BS	9	1.5	0.1		0.258
Basalt	BS	av	1.5			0.190
Basalt	BS	1	2	0.3		0.387
Basalt	BS	2	2	0.32		0.400
Basalt	BS	3	2	0.19		0.308
Basalt	BS	4	2	0.27		0.367
Basalt	BS	5	2	0		0.000
Basalt	BS	6	2	0.21		0.324
Basalt	BS	7	2	0.03		0.122
Basalt	BS	8	2	0.2		0.316
Basalt	BS	9	2	0.01		0.071
Basalt	BS	10	2	0.1		0.224
Basalt	BS	Av	2			0.252

Table B 2-1 continued

Slope	Rock	No. drop	Drop H (m)	Bounce h (m)	Frames (1/200 s)	R
Basalt	BS	1	2.5	0.15		0.245
Basalt	BS	2	2.5	0.06		0.155
Basalt	BS	3	2.5	0.4		0.400
Basalt	BS	4	2.5	0.03		0.110
Basalt	BS	5	2.5	0.03		0.110
Basalt	BS	6	2.5	0.2		0.283
Basalt	BS	7	2.5	0.15		0.245
Basalt	BS	8	2.5	0		0.000
Basalt	BS	9	2.5	0.15		0.245
Basalt	BS	10	2.5	0.17		0.261
Basalt	BS	Av	2.5			0.205
Basalt	BS	1	3	0.15		0.224
Basalt	BS	2	3	0.02		0.082
Basalt	BS	3	3	0.11		0.191
Basalt	BS	4	3	0.08		0.163
Basalt	BS	5	3	0.17		0.238
Basalt	BS	6	3	0.21		0.265
Basalt	BS	7	3	0.28		0.306
Basalt	BS	8	3	0.08		0.163
Basalt	BS	av	3			0.204
Lime	bast1-3	1	0.65	0.22		0.582
Lime	bast1-3	2	0.65	0.14		0.464
Lime	bast1-3	3	0.65	0.13		0.447
Lime	bast1-3	4	0.65	0.27		0.645
Lime	bast1-3	av	0.65			0.534
Lime	bast1-3	1	1.03	0.27		0.512
Lime	bast1-3	2	1.03	0.26		0.502
Lime	bast1-3	3	1.03	0.47		0.676
Lime	bast1-3	4	1.03	0.25		0.493
Lime	bast1-3	5	1.03	0.33		0.566
Lime	bast1-3	6	1.03	0.23		0.473
Lime	bast1-3	7	1.03	0.23		0.473
Lime	bast1-3	8	1.03	0.35		0.583
Lime	bast1-3	av	1.03			0.535
Lime	bast1-3	1	1.5	0.23		0.392
Lime	bast1-3	2	1.5	0.55		0.606
Lime	bast1-3	3	1.5	0.2		0.365
Lime	bast1-3	4	1.5	0.1		0.258
Lime	bast1-3	5	1.5	0.25		0.408
Lime	bast1-3	6	1.5	0.27		0.424
Lime	bast1-3	av	1.5			0.409
Lime	bast1-3	1	2	0.45		0.474
Lime	bast1-3	2	2	0.42		0.458
Lime	bast1-3	3	2	0.25		0.354

Table B 2-1 continued

Slope	Rock	No. drop	Drop H (m)	Bounce h (m)	Frames (1/200 s)	R
Lime	bast1-3	4	2	0.32		0.400
Lime	bast1-3	5	2	0.28		0.374
Lime	bast1-3	6	2	0.62		0.557
Lime	bast1-3	7	2	0.58		0.539
Lime	bast1-3	8	2	0.48		0.490
Lime	bast1-3	av	2			0.456
Lime	lim	1	0.6	0		0.000
Lime	lim	2	0.6	0.02		0.183
Lime	lim	3	0.6	0.02		0.183
Lime	lim	4	0.6	0		0.000
Lime	lim	5	0.6	0.02		0.183
Lime	lim	6	0.6	0		0.000
Lime	lim	7	0.6	0		0.000
Lime	lim	8	0.6	0		0.000
Lime	lim	9	0.6	0		0.000
Lime	lim	av	0.6			0.061
Lime	lim	1	1	0		0.000
Lime	lim	2	1	0		0.000
Lime	lim	3	1	0.04		0.200
Lime	lim	4	1	0.1		0.316
Lime	lim	5	1	0.02		0.141
Lime	lim	6	1	0		0.000
Lime	lim	7	1	0.01		0.100
Lime	lim	8	1	0.01		0.100
Lime	lim	9	1	0.01		0.100
Lime	lim	av	1			0.106
Lime	lim	1	1.5	0.02		0.115
Lime	lim	2	1.5	0.02		0.115
Lime	lim	3	1.5	0.02		0.115
Lime	lim	4	1.5	0.03		0.141
Lime	lim	5	1.5	0.03		0.141
Lime	lim	6	1.5	0.01		0.082
Lime	lim	7	1.5	0.02		0.115
Lime	lim	8	1.5	0.02		0.115
Lime	lim	9	1.5	0.03		0.141
Lime	lim	10	1.5	0		0.000
Lime	lim	11	1.5	0.02		0.115
Lime	lim	12	1.5	0.02		0.115
Lime	lim	13	1.5	0.02		0.115
Lime	lim	14	1.5	0.03		0.141
Lime	lim	av	1.5			0.112
Lime	lim	1	2	0.11		0.235
Lime	lim	2	2	0.03		0.122
Lime	lim	3	2	0.03		0.122
Lime	lim	4	2	0.02		0.100
Lime	lim	5	2	0.15		0.274

Table B 2-1 continued

Slope	Rock	No. drop	Drop H (m)	Bounce h (m)	Frames (1/200 s)	R
Lime	lim	6	2	0.04		0.141
Lime	lim	7	2	0.13		0.255
Lime	lim	8	2	0.04		0.141
Lime	lim	9	2	0.12		0.245
Lime	lim	10	2	0.13		0.255
Lime	lim	11	2	0.05		0.158
Lime	lim	12	2	0.03		0.122
Lime	lim	13	2	0.06		0.173
Lime	lim	av	2			0.180
Lime	lim	1	2.5	0.09		0.190
Lime	lim	2	2.5	0.04		0.126
Lime	lim	3	2.5	0.02		0.089
Lime	lim	4	2.5	0.01		0.063
Lime	lim	5	2.5	0.09		0.190
Lime	lim	6	2.5	0.03		0.110
Lime	lim	7	2.5	0.03		0.110
Lime	lim	8	2.5	0.32		0.358
Lime	lim	9	2.5	0.33		0.363
Lime	lim	10	2.5	0.02		0.089
Lime	lim	11	2.5	0.04		0.126
Lime	lim	12	2.5	0.01		0.063
Lime	lim	Av	2.5			0.157
Lime	lim	1	3	0.03		0.100
Lime	lim	2	3	0.12		0.200
Lime	lim	3	3	0.02		0.082
Lime	lim	4	3	0.02		0.082
Lime	lim	5	3	0.1		0.183
Lime	lim	6	3	0.06		0.141
Lime	lim	7	3	0.01		0.058
Lime	lim	8	3	0.02		0.082
Lime	lim	9	3	0.02		0.082
Lime	lim	10	3	0.03		0.100
Lime	lim	av	3			0.111
grey	bast1-3	1	0.65	0.43		0.813
grey	bast1-3	2	0.65	0.18		0.526
grey	bast1-3	3	0.65	0.38		0.765
grey	bast1-3	4	0.65	0.3		0.679
grey	bast1-3	5	0.65	0.34		0.723
grey	bast1-3	6	0.65	0.4		0.784
grey	bast1-3	7	0.65	0.36		0.744
grey	bast1-3	8	0.65	0.36		0.744
grey	bast1-3	av				0.722
grey	bast1-3	1	1	0.61		0.781
grey	bast1-3	2	1	0.7		0.837
grey	bast1-3	3	1	0.42		0.648
grey	bast1-3	4	1	0.51		0.714

Table B 2-1 continued

Slope	Rock	No. drop	Drop H (m)	Bounce h (m)	Frames (1/200 s)	R
grey	bast1-3	5	1	0.43		0.656
grey	bast1-3	6	1	0.58		0.762
grey	bast1-3	7	1	0.48		0.693
grey	bast1-3	8	1	0.56		0.748
grey	bast1-3	9	1	0.67		0.819
grey	bast1-3	av	1			0.740
grey	bast1-3	1	1.5	0.76		0.712
grey	bast1-3	2	1.5	0.7		0.683
grey	bast1-3	3	1.5	0.75		0.707
grey	bast1-3	4	1.5	1.01		0.821
grey	bast1-3	5	1.5	0.92		0.783
grey	bast1-3	6	1.5	0.72		0.693
grey	bast1-3	7	1.5	0.96		0.800
grey	bast1-3	8	1.5	0.68		0.673
grey	bast1-3	9	1.5	0.82		0.739
grey	bast1-3	10	1.5	0.96		0.800
grey	bast1-3	11	1.5	0.78		0.721
grey	bast1-3	12	1.5	0.86		0.757
grey	bast1-3	13	1.5	0.82		0.739
grey	bast1-3	av	1.5			0.741
grey	bast1-3	1	2	0.89		0.667
grey	bast1-3	2	2	0.96		0.693
grey	bast1-3	3	2	1.16		0.762
grey	bast1-3	4	2	1.07		0.731
grey	bast1-3	5	2	1.1		0.742
grey	bast1-3	6	2	1.25		0.791
grey	bast1-3	7	2	1.06		0.728
grey	bast1-3	8	2	1.09		0.738
grey	bast1-3	av	2			0.731
grey	bast1-3	1	2.5	1.15		0.678
grey	bast1-3	2	2.5	1.48		0.769
grey	bast1-3	3	2.5	1.38		0.743
grey	bast1-3	4	2.5	1.36		0.738
grey	bast1-3	5	2.5	1.5		0.775
		av	2.5			0.741
grey	grey	1	0.65	0.01		0.124
grey	grey	2	0.65	0.04		0.248
grey	grey	3	0.65	0.02		0.175
grey	grey	4	0.65	0.01		0.124
grey	grey	5	0.65	0.04		0.248
grey	grey	6	0.65	0.04		0.248
grey	grey	7	0.65	0.025		0.196
grey	grey	8	0.65	0.015		0.152
grey	grey	9	0.65	0.02		0.175
grey	grey	10	0.65	0.01		0.124
grey	grey	11	0.65	0.02		0.175

Table B 2-1 continued

Slope	Rock	No. drop	Drop H (m)	Bounce h (m)	Frames (1/200 s)	R
grey	grey	av	0.65			0.181
grey	grey	1	1	0.03		0.173
grey	grey	2	1	0.01		0.100
grey	grey	3	1	0.04		0.200
grey	grey	4	1	0.06		0.245
grey	grey	5	1	0.025		0.158
grey	grey	6	1	0.03		0.173
grey	grey	7	1	0.01		0.100
grey	grey	av	1			0.164
grey	grey	1	1.5	0.13		0.294
grey	grey	2	1.5	0.03		0.141
grey	grey	3	1.5	0.06		0.200
grey	grey	4	1.5	0.03		0.141
grey	grey	5	1.5	0.02		0.115
grey	grey	6	1.5	0.02		0.115
grey	grey	7	1.5	0.025		0.129
grey	grey	8	1.5	0.06		0.200
grey	grey	9	1.5	0.05		0.183
grey	grey	10	1.5	0.12		0.283
grey	grey	av	1.5			0.180
grey	grey	1	2	0.12		0.245
grey	grey	2	2	0.05		0.158
grey	grey	3	2	0.03		0.122
grey	grey	4	2	0.04		0.141
grey	grey	5	2	0.04		0.141
grey	grey	6	2	0.045		0.150
grey	grey	7	2	0.02		0.100
grey	grey	8	2	0.1		0.224
grey	grey	9	2	0.11		0.235
grey	grey	av	2			0.169
grey	grey	1	2.5	0.17		0.261
grey	grey	2	2.5	0.075		0.173
grey	grey	3	2.5	0.05		0.141
grey	grey	4	2.5	0.06		0.155
grey	grey	5	2.5	0.3		0.346
grey	grey	6	2.5	0.09		0.190
grey	grey	7	2.5	0.05		0.141
grey	grey	av	2.5			0.201
grey	grey	1	3	0.43		0.379
grey	grey	2	3	0.15		0.224
grey	grey	3	3	0.06		0.141
grey	grey	4	3	0.07		0.153
grey	grey	5	3	0.18		0.245
grey	grey	6	3	0.02		0.082
grey	grey	7	3	0.15		0.224

Table B 2-1 continued

Slope	Rock	No. drop	Drop H (m)	Bounce h (m)	Frames (1/200 s)	R
		av	3			0.207
frag	bast1-3	1	1.5	0.015		0.1
frag	bast1-3	2	1.5	0.01		0.082
frag	bast1-3	3	1.5	0.015		0.100
frag	bast1-3	4	1.5	0		0.000
frag	bast1-3	5	1.5	0.01		0.082
frag	bast1-3	6	1.5	0.04		0.163
frag	bast1-3	7	1.5	0		0.000
frag	bast1-3	8	1.5	0.03		0.141
frag	bast1-3	9	1.5	0.04		0.163
frag	bast1-3	10	1.5	0.02		0.115
frag	bast1-3	11	1.5	0.01		0.082
frag	bast1-3	12	1.5	0.01		0.082
frag	bast1-3	13	1.5	0.02		0.115
frag	bast1-3	14	1.5	0.015		0.100
frag	bast1-3	15	1.5	0.01		0.082
frag	bast1-3	16	1.5	0.02		0.115
frag	bast1-3	17	1.5	0		0.000
frag	bast1-3	18	1.5	0.01		0.082
frag	bast1-3	Av	1.5			0.089
gravel	bast1-3	1	1.5	0.01		0.082
gravel	bast1-3	2	1.5	0		0.000
gravel	bast1-3	3	1.5	0.015		0.100
gravel	bast1-3	4	1.5	0.005		0.058
gravel	bast1-3	5	1.5	0.02		0.115
gravel	bast1-3	6	1.5	0		0.000
gravel	bast1-3	7	1.5	0		0.000
gravel	bast1-3	8	1.5	0.01		0.082
gravel	bast1-3	9	1.5	0.005		0.058
gravel	bast1-3	av	1.5			0.055
sand	bast1-3	av	1.5	0		0.000
loess	bast1-3	1	1.5	0.01		0.082
loess	bast1-3	2	1.5	0.015		0.100
loess	bast1-3	3	1.5	0.015		0.100
loess	bast1-3	4	1.5	0.01		0.082
loess	bast1-3	5	1.5	0.015		0.100
loess	bast1-3	6	1.5	0.02		0.115
loess	bast1-3	7	1.5	0.015		0.100
loess	bast1-3	8	1.5	0.01		0.082
loess	bast1-3	9	1.5	0.02		0.115
loess	bast1-3	10	1.5	0.015		0.100
loess	bast1-3	av	1.5			0.098
loess	bs	1	1.5	0.02		0.115
loess	bs	2	1.5	0.025		0.129
loess	bs	3	1.5	0.025		0.129

Table B 2-1 continued

Slope	Rock	No. drop	Drop H (m)	Bounce h (m)	Frames (1/200 s)	R
loess	bs	4	1.5	0.015		0.100
loess	bs	5	1.5	0.05		0.183
loess	bs	6	1.5	0.02		0.115
loess	bs	7	1.5	0.02		0.115
loess	bs	8	1.5	0.01		0.082
loess	bs	9	1.5	0.015		0.100
loess	bs	av	1.5			0.119
frag#	bast1-3	1	1.5	0.01		0.082
frag#	bast1-3	2	1.5	0		0.000
frag#	bast1-3	3	1.5	0.01		0.082
frag#	bast1-3	4	1.5	0.01		0.082
frag#	bast1-3	5	1.5	0.01		0.082
frag#	bast1-3	6	1.5	0.01		0.082
frag#	bast1-3	7	1.5	0.005		0.058
frag#	bast1-3	8	1.5	0.01		0.082
frag#	bast1-3	9	1.5	0.015		0.100
frag#	bast1-3	av	1.5			0.072
frag#	bs	1	1.5	0.03		0.141
frag#	bs	2	1.5	0.005		0.058
frag#	bs	3	1.5	0.01		0.082
frag#	bs	4	1.5	0.02		0.115
frag#	bs	5	1.5	0.01		0.082
frag#	bs	6	1.5	0.02		0.115
frag#	bs	7	1.5	0.03		0.141
frag#	bs	8	1.5	0.01		0.082
frag#	bs	av	1.5			0.102
paving#	bast1-3	1	1.5	0.01		0.082
paving#	bast1-3	2	1.5	0.015		0.100
paving#	bast1-3	3	1.5	0.01		0.082
paving#	bast1-3	4	1.5	0.005		0.058
paving#	bast1-3	5	1.5	0.015		0.100
paving#	bast1-3	6	1.5	0.02		0.115
paving#	bast1-3	7	1.5	0.01		0.082
paving#	bast1-3	8	1.5	0.015		0.100
paving#	bast1-3	av	1.5			0.090
paving#	bs	1	1.5	0.005		0.058
paving#	bs	2	1.5	0.01		0.082
paving#	bs	3	1.5	0.005		0.058
paving#	bs	4	1.5	0.005		0.058
paving#	bs	5	1.5	0.02		0.115
paving#	bs	6	1.5	0.01		0.082
paving#	bs	7	1.5	0.005		0.058
paving#	bs	8	1.5	0.005		0.058
paving#	bs	9	1.5	0.015		0.100
paving#	bs	10	1.5	0.01		0.082

Table B 2-1 continued

Slope	Rock	No. drop	Drop H (m)	Bounce h (m)	Frames (1/200 s)	R
paving#	bs	11	1.5	0.01		0.082
paving#	bs	12	1.5	0.03		0.141
paving#	bs	av	1.5			0.081

The calculations of coefficients of restitution of inclined bounce on rough rocks, debris and soil materials are shown in table B 2-2. Equations and meaning of symbols are the same as those in table B 1-2.

Table B 2-2: Coefficient of restitution calculation (inclined bounce on rough rocks, debris and soil materials)

Slab Label	Slab A	Ball Label	No. drop	Drop H H'(m)	Drop H H(m)	Bounce h h' (m)	Bounce h h (m)	Frames (1/200 s)	Horiz. distance S'(m)	Horiz. distance S (m)	S1 (m)	S2 (m)	Vi (m/s)	Vrx (m/s)	Vry (m/s)	Vin (m/s)	Vit (m/s)	Vrn (m/s)	Vrt (m/s)	Rn	Rt
basalt	40	bast1-3	1	0.6	0.62	0.02	0.04	20	0.13	0.23	-0.1	0.02	3.488	2.300	0.891	2.672	2.242	2.161	1.189	0.809	0.531
basalt	40	bast1-3	2	0.6	0.64	0.04	0.08	27	0.25	0.35	-0.1	0.04	3.544	2.593	1.255	2.715	2.278	2.628	1.179	0.968	0.518
basalt	40	bast1-3	3	0.6	0.65	0.03	0.08	28	0.26	0.34	-0.08	0.05	3.571	2.429	1.258	2.736	2.295	2.525	1.052	0.923	0.458
basalt	40	bast1-3	4	0.6	0.62	0.02	0.04	25	0.15	0.28	-0.13	0.02	3.488	2.240	0.933	2.672	2.242	2.155	1.116	0.806	0.498
basalt	40	bast1-3	av	0.6	0.6															0.877	0.501
basalt	40	bast1-3	1	1	1.04	0.11	0.15	34	0.36	0.46	-0.1	0.04	4.517	2.706	1.716	3.460	2.904	3.054	0.970	0.883	0.334
basalt	40	bast1-3	2	1	1	0.03	0.03	18	0.09	0.26	-0.17	0	4.429	2.889	0.775	3.393	2.847	2.450	1.715	0.722	0.602
basalt	40	bast1-3	3	1	1	0.12	0.12	30	0.25	0.41	-0.16	0	4.429	2.733	1.536	3.393	2.847	2.933	1.107	0.865	0.389
basalt	40	bast1-3	4	1	1.06	0.05	0.11	32	0.43	0.49	-0.06	0.06	4.560	3.063	1.472	3.493	2.931	3.096	1.400	0.886	0.477
basalt	40	bast1-3	av	1	1															0.839	0.451
basalt	40	bast1-3	1	1.5	1.56	0	0.06	22	0.39	0.41	-0.02	0.06	5.532	3.727	1.085	4.238	3.556	3.227	2.158	0.761	0.607
basalt	40	bast1-3	2	1.5	1.52	0.02	0.04	30	0.52	0.56	-0.04	0.02	5.461	3.733	1.002	4.183	3.510	3.168	2.216	0.757	0.631
basalt	40	bast1-3	3	1.5	1.59	0	0.09	21	0.41	0.41	0	0.09	5.585	3.905	1.372	4.279	3.590	3.561	2.109	0.832	0.587
basalt	40	bast1-3	4	1.5	1.54	0.05	0.09	31	0.53	0.6	-0.07	0.04	5.497	3.871	1.341	4.211	3.533	3.515	2.103	0.835	0.595
basalt	40	bast1-3	5	1.5	1.55	0.06	0.11	30	0.51	0.54	-0.03	0.05	5.515	3.600	1.469	4.224	3.545	3.439	1.813	0.814	0.512
basalt	40	bast1-3	av	1.5	1.5															0.800	0.586
basalt	40	bast1-3	1	2	2	0.02	0.02	15	0.23	0.32	-0.09	0	6.264	4.267	0.635	4.799	4.027	3.229	2.861	0.673	0.710
basalt	40	bast1-3	2	2	1.98	0.1	0.08	22	0.35	0.48	-0.13	-0.02	6.233	4.364	1.267	4.775	4.006	3.775	2.528	0.791	0.631
basalt	40	bast1-3	3	2	2.04	0.21	0.25	45	0.88	0.93	-0.05	0.04	6.327	4.133	2.215	4.846	4.067	4.353	1.743	0.898	0.429
basalt	40	bast1-3	4	2	2	0.22	0.22	40	0.74	0.84	-0.1	0	6.264	4.200	2.081	4.799	4.027	4.294	1.880	0.895	0.467
basalt	40	bast1-3	av	2	2															0.814	0.559
basalt	40	bast1-3	1	2.5	2.56	0.02	0.08	30	0.75	0.78	-0.03	0.06	7.087	5.200	1.269	5.429	4.556	4.315	3.168	0.795	0.695
basalt	40	bast1-3	2	2.5	2.57	0.12	0.19	37	0.87	0.87	0	0.07	7.101	4.703	1.934	5.440	4.564	4.505	2.359	0.828	0.517

Table B 2-2 continued

Slab Label	Slab A	Ball Label	No. drop	Drop H H'(m)	Drop H H(m)	Bounce h h' (m)	Bounce h h (m)	Frames (1/200 s)	Horiz. distance S'(m)	Horiz. distance S (m)	S1 (m)	S2 (m)	Vi (m/s)	Vrx (m/s)	Vry (m/s)	Vin (m/s)	Vit (m/s)	Vrn (m/s)	Vrt (m/s)	Rn	Rt
basalt	40	bast1-3	3	2.5	2.56	0.04	0.1	32	0.74	0.76	-0.02	0.06	7.087	4.750	1.410	5.429	4.556	4.133	2.733	0.761	0.600
basalt	40	bast1-3	4	2.5	2.59	0.02	0.11	35	0.79	0.79	0	0.09	7.129	4.514	1.487	5.461	4.582	4.041	2.502	0.740	0.546
basalt	40	bast1-3	5	2.5	2.58	0.07	0.15	30	0.74	0.77	-0.03	0.08	7.115	5.133	1.736	5.450	4.573	4.629	2.817	0.849	0.616
basalt	40	bast1-3	av	2.5	2.5															0.795	0.595
basalt	40	bs	1	0.6	0.64	-0.34	-0.3	41	0.33	0.38	-0.05	0.04	3.544	1.854	0.458	2.715	2.278	0.841	1.714	0.310	0.753
basalt	40	bs	2	0.6	0.62	-0.34	-0.32	46	0.28	0.38	-0.1	0.02	3.488	1.652	0.263	2.672	2.242	0.860	1.435	0.322	0.640
basalt	40	bs	3	0.6	0.6	-0.14	-0.14	18	0.03	0.11	-0.08	0	3.431	1.222	1.114	2.628	2.205	-0.068	1.652	-0.026	0.749
basalt	40	bs	4	0.6	0.6	-0.08	-0.08	12	-0.02	0.15	-0.17	0	3.431	2.500	1.039	2.628	2.205	0.811	2.583	0.309	1.171
basalt	40	bs	5	0.6	0.63	-0.34	-0.31	44	0.22	0.29	-0.07	0.03	3.516	1.318	0.330	2.693	2.260	0.595	1.222	0.221	0.541
basalt	40	bs	6	0.6	0.67	-0.34	-0.27	37	0.25	0.27	-0.02	0.07	3.626	1.459	0.552	2.777	2.331	0.515	1.473	0.186	0.632
basalt	40	bs	av	0.6	0.6															0.260	0.641
basalt	40	bs	1	1	1.06	-0.12	-0.06	6	0.05	0.09	-0.04	0.06	4.560	3.000	1.853	3.493	2.931	0.509	3.489	0.146	1.190
basalt	40	bs	2	1	1.12	-0.34	-0.22	26	0.31	0.26	0.05	0.12	4.688	2.000	1.055	3.591	3.013	0.478	2.210	0.133	0.733
basalt	40	bs	3	1	1.04	-0.34	-0.3	49	0.4	0.44	-0.04	0.04	4.517	1.796	0.023	3.460	2.904	1.137	1.390	0.329	0.479
basalt	40	bs	4	1	1.04	-0.09	-0.05	4	0	0.04	-0.04	0.04	4.517	2.000	2.402	3.460	2.904	-0.554	3.076	-0.160	1.059
basalt	40	bs	5	1	1.01	-0.34	-0.33	48	0.44	0.53	-0.09	0.01	4.452	2.208	0.198	3.410	2.861	1.268	1.819	0.372	0.636
basalt	40	bs	6	1	1.06	-0.31	-0.25	44	0.49	0.52	-0.03	0.06	4.560	2.364	0.057	3.493	2.931	1.475	1.847	0.422	0.630
basalt	40	bs	7	1	1.05	-0.15	-0.1	11	0.08	0.14	-0.06	0.05	4.539	2.545	1.548	3.477	2.918	0.450	2.945	0.129	1.010
basalt	40	bs	8	1	1.04	-0.33	-0.29	35	0.38	0.43	-0.05	0.04	4.517	2.457	0.799	3.460	2.904	0.968	2.396	0.280	0.825
basalt	40	bs	av	1	1															0.307	0.661
basalt	40	bs	1	1.5	1.62	-0.34	-0.22	28	0.33	0.3	0.03	0.12	5.638	2.143	0.885	4.319	3.624	0.700	2.210	0.162	0.610
basalt	40	bs	2	1.5	1.54	-0.13	-0.09	5	0.07	0.11	-0.04	0.04	5.497	4.400	3.477	4.211	3.533	0.164	5.606	0.039	1.587
basalt	40	bs	3	1.5	1.57	-0.34	-0.27	32	0.38	0.42	-0.04	0.07	5.550	2.625	0.903	4.252	3.568	0.996	2.591	0.234	0.726
basalt	40	bs	4	1.5	1.53	-0.34	-0.31	50	0.92	0.97	-0.05	0.03	5.479	3.880	0.014	4.197	3.522	2.483	2.981	0.592	0.846
basalt	40	bs	5	1.5	1.59	-0.34	-0.25	42	0.65	0.67	-0.02	0.09	5.585	3.190	0.160	4.279	3.590	1.928	2.547	0.451	0.709
basalt	40	bs	6	1.5	1.58	-0.34	-0.26	28	0.39	0.35	0.04	0.08	5.568	2.500	1.170	4.265	3.579	0.710	2.667	0.167	0.745

Table B 2-2 continued

Slab Label	Slab A	Ball Label	No. drop	Drop H H'(m)	Drop H H(m)	Bounce h h' (m)	Bounce h h (m)	Frames (1/200 s)	Horiz. distance S'(m)	Horiz. distance S (m)	S1 (m)	S2 (m)	Vi (m/s)	Vrx (m/s)	Vry (m/s)	Vin (m/s)	Vit (m/s)	Vrn (m/s)	Vrt (m/s)	Rn	Rt
basalt	40	bs	7	1.5	1.54	-0.34	-0.3	27	0.38	0.4	-0.02	0.04	5.497	2.963	1.560	4.211	3.533	0.709	3.273	0.168	0.926
basalt	40	bs	8	1.5	1.57	-0.34	-0.27	30	0.42	0.38	0.04	0.07	5.550	2.533	1.064	4.252	3.568	0.813	2.625	0.191	0.736
basalt	40	bs	av	1.5	1.5															0.281	0.757
basalt	40	bs	1	2	2.05	-0.34	-0.29	38	0.65	0.69	-0.04	0.05	6.342	3.632	0.594	4.858	4.077	1.879	3.164	0.387	0.776
basalt	40	bs	2	2	2.04	-0.3	-0.26	45	0.88	0.94	-0.06	0.04	6.327	4.178	0.052	4.846	4.067	2.646	3.234	0.546	0.795
basalt	40	bs	3	2	2.06	-0.34	-0.28	38	0.55	0.6	-0.05	0.06	6.357	3.158	0.542	4.870	4.086	1.615	2.767	0.332	0.677
basalt	40	bs	4	2	2.05	-0.34	-0.29	34	0.51	0.54	-0.03	0.05	6.342	3.176	0.872	4.858	4.077	1.374	2.994	0.283	0.734
basalt	40	bs	5	2	2.06	-0.34	-0.28	28	0.45	0.48	-0.03	0.06	6.357	3.429	1.313	4.870	4.086	1.198	3.471	0.246	0.849
basalt	40	bs	6	2	2	-0.15	-0.15	9	0.11	0.19	-0.08	0	6.264	4.222	3.113	4.799	4.027	0.330	5.235	0.069	1.300
basalt	40	bs	7	2	2.02	-0.34	-0.32	36	0.53	0.61	-0.08	0.02	6.295	3.389	0.895	4.823	4.047	1.493	3.171	0.310	0.784
basalt	40	bs	8	2	2.06	-0.34	-0.28	30	0.49	0.51	-0.02	0.06	6.357	3.400	1.131	4.870	4.086	1.319	3.331	0.271	0.815
basalt	40	bs	9	2	2.04	-0.3	-0.26	36	0.51	0.57	-0.06	0.04	6.327	3.167	0.562	4.846	4.067	1.605	2.787	0.331	0.685
basalt	40	bs	av	2	2															0.338	0.765
basalt	40	bs	1	2.5	2.54	-0.32	-0.28	42	0.9	0.96	-0.06	0.04	7.059	4.571	0.303	5.408	4.538	2.706	3.697	0.500	0.815
basalt	40	bs	2	2.5	2.57	-0.34	-0.27	30	0.51	0.54	-0.03	0.07	7.101	3.600	1.064	5.440	4.564	1.499	3.442	0.276	0.754
basalt	40	bs	3	2.5	2.56	-0.34	-0.28	27	0.48	0.51	-0.03	0.06	7.087	3.778	1.412	5.429	4.556	1.347	3.801	0.248	0.834
basalt	40	bs	4	2.5	2.58	-0.34	-0.26	45	0.84	0.84	0	0.08	7.115	3.733	0.052	5.450	4.573	2.360	2.893	0.433	0.633
basalt	40	bs	5	2.5	2.5	-0.34	-0.34	24	0.37	0.45	-0.08	0	7.004	3.750	2.245	5.365	4.502	0.691	4.316	0.129	0.959
basalt	40	bs	6	2.5	2.54	-0.34	-0.3	29	0.53	0.56	-0.03	0.04	7.059	3.862	1.358	5.408	4.538	1.442	3.831	0.267	0.844
basalt	40	bs	7	2.5	2.53	-0.34	-0.31	32	0.45	0.49	-0.04	0.03	7.045	3.063	1.153	5.397	4.529	1.086	3.087	0.201	0.682
basalt	40	bs	8	2.5	2.6	-0.34	-0.24	29	0.47	0.45	0.02	0.1	7.142	3.103	0.944	5.471	4.591	1.272	2.984	0.232	0.650
basalt	40	bs	9	2.5	2.6	-0.34	-0.24	26	0.44	0.42	0.02	0.1	7.142	3.231	1.209	5.471	4.591	1.151	3.252	0.210	0.708
basalt	40	bs	av	2.5	2.5															0.277	0.764
basalt	40	bs	1	3	3.1	-0.34	-0.24	24	0.48	0.48	0	0.1	7.799	4.000	1.411	5.974	5.013	1.490	3.971	0.249	0.792
basalt	40	bs	2	3	3.04	-0.34	-0.3	25	0.4	0.43	-0.03	0.04	7.723	3.440	1.787	5.916	4.964	0.842	3.784	0.142	0.762
basalt	40	bs	3	3	3.06	-0.34	-0.28	28	0.52	0.55	-0.03	0.06	7.748	3.929	1.313	5.936	4.981	1.519	3.854	0.256	0.774

Table B 2-2 continued

Slab Label	Slab A	Ball Label	No. drop	Drop H H'(m)	Drop H H(m)	Bounce h h' (m)	Bounce h h (m)	Frames (1/200 s)	Horiz. distance S'(m)	Horiz. distance S (m)	S1 (m)	S2 (m)	Vi (m/s)	Vrx (m/s)	Vry (m/s)	Vin (m/s)	Vit (m/s)	Vrn (m/s)	Vrt (m/s)	Rn	Rt
basalt	40	bs	4	3	3.07	-0.34	-0.27	30	0.59	0.61	-0.02	0.07	7.761	4.067	1.064	5.945	4.989	1.799	3.799	0.303	0.762
basalt	40	bs	5	3	3.1	-0.34	-0.24	18	0.31	0.31	0	0.1	7.799	3.444	2.225	5.974	5.013	0.509	4.069	0.085	0.812
basalt	40	bs	6	3	3.12	-0.29	-0.17	41	0.86	0.81	0.05	0.12	7.824	3.951	-0.176	5.994	5.029	2.675	2.914	0.446	0.579
basalt	40	bs	7	3	3.1	-0.34	-0.24	18	0.33	0.31	0.02	0.1	7.799	3.444	2.225	5.974	5.013	0.509	4.069	0.085	0.812
basalt	40	bs	8	3	3.03	-0.34	-0.31	24	0.39	0.51	-0.12	0.03	7.710	4.250	1.995	5.906	4.956	1.204	4.538	0.204	0.916
basalt	40	bs	9	3	3.12	-0.34	-0.22	27	0.65	0.6	0.05	0.12	7.824	4.444	0.967	5.994	5.029	2.116	4.027	0.353	0.801
basalt	40	bs	10	3	3.04	-0.34	-0.3	32	0.85	0.88	-0.03	0.04	7.723	5.500	1.090	5.916	4.964	2.700	4.914	0.456	0.990
basalt	40	bs	Av	3	3															0.258	0.800
Lime	40	lim		0.6		no bounce															
Lime	40	lim	1	1	1.04	-0.23	-0.19	30	0.22	0.25	-0.03	0.04	4.517	1.667	0.531	3.460	2.904	0.665	1.618	0.192	0.557
Lime	40	lim	2	1	1.03	-0.05	-0.02	8	0.04	0.07	-0.03	0.03	4.495	1.750	0.304	3.444	2.890	0.892	1.536	0.259	0.532
Lime	40	lim	3	1	1.05	-0.1	-0.05	5	0.06	0.06	0	0.05	4.539	2.400	1.877	3.477	2.918	0.105	3.045	0.030	1.044
Lime	40	lim	4	1	1.04	-0.23	-0.19	37	0.13	0.11	0.02	0.04	4.517	0.595	0.120	3.460	2.904	0.291	0.532	0.084	0.183
Lime	40	lim	5	1	1.02	-0.23	-0.21	36	0.28	0.3	-0.02	0.02	4.474	1.667	0.284	3.427	2.876	0.854	1.459	0.249	0.507
Lime	40	lim	6	1	1.05	-0.23	-0.18	29	0.22	0.25	-0.03	0.05	4.539	1.724	0.530	3.477	2.918	0.702	1.662	0.202	0.570
Lime	40	lim	7	1	1	-0.2	-0.2	30	0.3	0.37	-0.07	0	4.429	2.467	0.598	3.393	2.847	1.128	2.274	0.332	0.799
Lime	40	lim	8	1	0.97	-0.03	-0.06	14	0.03	0.11	-0.08	-0.03	4.362	1.571	0.514	3.342	2.804	0.617	1.534	0.184	0.547
Lime	40	lim	9	1	1	-0.04	-0.04	11	0.02	0.07	-0.05	0	4.429	1.273	0.457	3.393	2.847	0.468	1.269	0.138	0.446
Lime	40	lim	10	1	1	-0.08	-0.08	12	0.05	0.09	-0.04	0	4.429	1.500	1.039	3.393	2.847	0.168	1.817	0.050	0.638
Lime	40	lim	11	1	1.03	-0.23	-0.2	49	0.21	0.19	0.02	0.03	4.495	0.776	-0.385	3.444	2.890	0.794	0.346	0.230	0.120
Lime	40	lim	av	1	1															0.192	0.490
Lime	40	lim	1	1.5	1.53	-0.23	-0.2	22	0.24	0.22	0.02	0.03	5.479	2.000	1.279	4.197	3.522	0.306	2.354	0.073	0.668
Lime	40	lim	2	1.5	1.52	-0.23	-0.21	26	0.35	0.38	-0.03	0.02	5.461	2.923	0.978	4.183	3.510	1.130	2.868	0.270	0.817
Lime	40	lim	3	1.5	1.56	-0.23	-0.17	23	0.33	0.29	0.04	0.06	5.532	2.522	0.914	4.238	3.556	0.921	2.519	0.217	0.708
Lime	40	lim	4	1.5	1.55	-0.23	-0.18	32	0.38	0.36	0.02	0.05	5.515	2.250	0.340	4.224	3.545	1.186	1.942	0.281	0.548
Lime	40	lim	5	1.5	1.54	-0.23	-0.19	30	0.26	0.26	0	0.04	5.497	1.733	0.531	4.211	3.533	0.707	1.669	0.168	0.472

Table B 2-2 continued

Slab Label	Slab A	Ball Label	No. drop	Drop H H'(m)	Drop H H(m)	Bounce h h' (m)	Bounce h h (m)	Frames (1/200 s)	Horiz. distance S'(m)	Horiz. distance S (m)	S1 (m)	S2 (m)	Vi (m/s)	Vrx (m/s)	Vry (m/s)	Vin (m/s)	Vit (m/s)	Vrn (m/s)	Vrt (m/s)	Rn	Rt
Lime	40	lim	6	1.5	1.5	-0.23	-0.23	26	0.27	0.3	-0.03	0	5.425	2.308	1.132	4.156	3.487	0.617	2.495	0.148	0.716
Lime	40	lim	7	1.5	1.56	-0.23	-0.17	22	0.32	0.28	0.04	0.06	5.532	2.545	1.006	4.238	3.556	0.866	2.597	0.204	0.730
Lime	40	lim	8	1.5	1.55	-0.23	-0.18	27	0.35	0.33	0.02	0.05	5.515	2.444	0.671	4.224	3.545	1.057	2.304	0.250	0.650
Lime	40	lim	9	1.5	1.58	-0.23	-0.15	22	0.27	0.23	0.04	0.08	5.568	2.091	0.824	4.265	3.579	0.713	2.131	0.167	0.596
Lime	40	lim	av	1.5	1.5															0.198	0.656
Lime	40	lim	1	2	2.04	-0.23	-0.19	34	0.32	0.3	0.02	0.04	6.327	1.765	0.284	4.846	4.067	0.917	1.534	0.189	0.377
Lime	40	lim	2	2	1.98	-0.23	-0.25	28	0.35	0.4	-0.05	-0.02	6.233	2.857	1.099	4.775	4.006	0.995	2.895	0.208	0.723
Lime	40	lim	3	2	2.02	-0.23	-0.21	31	0.45	0.45	0	0.02	6.295	2.903	0.595	4.823	4.047	1.411	2.606	0.293	0.644
Lime	40	lim	4	2	2.02	-0.23	-0.21	25	0.31	0.34	-0.03	0.02	6.295	2.720	1.067	4.823	4.047	0.931	2.769	0.193	0.684
Lime	40	lim	5	2	2.01	-0.23	-0.22	30	0.38	0.38	0	0.01	6.280	2.533	0.731	4.811	4.037	1.068	2.410	0.222	0.597
Lime	40	lim	6	2	1.94	-0.23	-0.29	37	0.3	0.4	-0.1	-0.06	6.170	2.162	0.660	4.726	3.966	0.884	2.081	0.187	0.525
Lime	40	lim	av	2	2															0.215	0.592
Lime	40	lim	1	2.5	2.58	-0.23	-0.15	22	0.33	0.3	0.03	0.08	7.115	2.727	0.824	5.450	4.573	1.122	2.619	0.206	0.573
Lime	40	lim	2	2.5	2.52	-0.23	-0.21	21	0.28	0.28	0	0.02	7.032	2.667	1.485	5.386	4.520	0.577	2.997	0.107	0.663
Lime	40	lim	3	2.5	2.58	-0.23	-0.15	24	0.38	0.35	0.03	0.08	7.115	2.917	0.661	5.450	4.573	1.368	2.659	0.251	0.582
Lime	40	lim	4	2.5	2.47	-0.21	-0.24	28	0.48	0.53	-0.05	-0.03	6.961	3.786	1.028	5.333	4.475	1.646	3.561	0.309	0.796
Lime	40	lim	5	2.5	2.52	-0.22	-0.2	26	0.44	0.44	0	0.02	7.032	3.385	0.901	5.386	4.520	1.486	3.172	0.276	0.702
Lime	40	lim	6	2.5	2.52	-0.2	-0.18	33	0.5	0.5	0	0.02	7.032	3.030	0.282	5.386	4.520	1.732	2.502	0.322	0.554
Lime	40	lim	7	2.5	2.52	-0.18	-0.16	29	0.43	0.43	0	0.02	7.032	2.966	0.392	5.386	4.520	1.606	2.524	0.298	0.558
Lime	40	lim	av	2.5	2.5															0.253	0.632
Lime	40	lim	1	3	3.02	-0.23	-0.21	13	0.24	0.24	0	0.02	7.698	3.692	2.912	5.897	4.948	0.143	4.700	0.024	0.950
Lime	40	lim	2	3	3.04	-0.23	-0.19	24	0.43	0.43	0	0.04	7.723	3.583	0.995	5.916	4.964	1.541	3.384	0.261	0.682
Lime	40	lim	3	3	3.08	-0.23	-0.15	28	0.45	0.42	0.03	0.08	7.774	3.000	0.385	5.955	4.997	1.634	2.545	0.274	0.509
Lime	40	lim	4	3	3.03	-0.23	-0.2	28	0.58	0.63	-0.05	0.03	7.710	4.500	0.742	5.906	4.956	2.324	3.924	0.394	0.792
Lime	40	lim	5	3	3.1	-0.23	-0.13	14	0.27	0.22	0.05	0.1	7.799	3.143	1.514	5.974	5.013	0.861	3.381	0.144	0.674
Lime	40	lim	6	3	3	-0.22	-0.22	18	0.25	0.28	-0.03	0	7.672	3.111	2.003	5.877	4.931	0.465	3.671	0.079	0.744

Table B 2-2 continued

Slab Label	Slab A	Ball Label	No. drop	Drop H H'(m)	Drop H H(m)	Bounce h h' (m)	Bounce h h (m)	Frames (1/200 s)	Horiz. distance S'(m)	Horiz. distance S (m)	S1 (m)	S2 (m)	Vi (m/s)	Vrx (m/s)	Vry (m/s)	Vin (m/s)	Vit (m/s)	Vrn (m/s)	Vrt (m/s)	Rn	Rt
Lime	40	lim	7	3	3.02	-0.23	-0.21	22	0.52	0.52	0	0.02	7.698	4.727	1.370	5.897	4.948	1.990	4.502	0.337	0.910
Lime	40	lim	8	3	2.98	-0.23	-0.25	24	0.3	0.34	-0.04	-0.02	7.646	2.833	1.495	5.857	4.915	0.676	3.131	0.115	0.637
Lime	40	lim	av	3	3															0.204	0.737
grey	40	bast1-3	1	0.6	0.66	-0.03	0.03	17	0.22	0.21	0.01	0.06	3.598	2.471	0.770	2.757	2.313	2.178	1.398	0.790	0.604
grey	40	bast1-3	2	0.6	0.63	0.04	0.07	23	0.28	0.28	0	0.03	3.516	2.435	1.173	2.693	2.260	2.463	1.111	0.915	0.492
grey	40	bast1-3	3	0.6	0.63	0	0.03	18	0.23	0.23	0	0.03	3.516	2.556	0.775	2.693	2.260	2.236	1.460	0.830	0.646
grey	40	bast1-3	4	0.6	0.655	-0.03	0.025	16	0.21	0.2	0.01	0.055	3.585	2.500	0.705	2.746	2.304	2.147	1.462	0.782	0.634
grey	40	bast1-3	5	0.6	0.62	0.01	0.03	20	0.23	0.23	0	0.02	3.488	2.300	0.791	2.672	2.242	2.084	1.254	0.780	0.559
grey	40	bast1-3	6	0.6	0.6	0.02	0.02	20	0.25	0.27	-0.02	0	3.431	2.700	0.691	2.628	2.205	2.264	1.624	0.862	0.737
grey	40	bast1-3	7	0.6	0.63	0.05	0.08	26	0.31	0.3	0.01	0.03	3.516	2.308	1.253	2.693	2.260	2.443	0.962	0.907	0.426
grey	40	bast1-3	av	0.6																0.838	0.585
grey	40	bast1-3	1	1	1.01	-0.35	-0.34	47	0.78	0.78	0	0.01	4.452	3.319	0.294	3.410	2.861	1.908	2.732	0.560	0.955
grey	40	bast1-3	2	1	0.95	0.14	0.09	25	0.37	0.37	0	-0.05	4.317	2.960	1.333	3.307	2.775	2.924	1.411	0.884	0.508
grey	40	bast1-3	3	1	0.97	-0.35	-0.38	42	0.53	0.53	0	-0.03	4.362	2.524	0.779	3.342	2.804	1.025	2.434	0.307	0.868
grey	40	bast1-3	4	1	1.04	0	0.04	13	0.22	0.2	0.02	0.04	4.517	3.077	0.934	3.460	2.904	2.693	1.757	0.778	0.605
grey	40	bast1-3	5	1	0.99	0.04	0.03	20	0.33	0.32	0.01	-0.01	4.407	3.200	0.791	3.376	2.833	2.662	1.943	0.789	0.686
grey	40	bast1-3	6	1	1	0.03	0.03	16	0.26	0.24	0.02	0	4.429	3.000	0.767	3.393	2.847	2.516	1.805	0.742	0.634
grey	40	bast1-3	7	1	1.06	-0.3	-0.24	50	1.05	0.94	0.11	0.06	4.560	3.760	-0.266	3.493	2.931	2.621	2.709	0.750	0.924
grey	40	bast1-3	8	1	1.01	0.02	0.03	18	0.27	0.27	0	0.01	4.452	3.000	0.775	3.410	2.861	2.522	1.800	0.740	0.629
grey	40	bast1-3	9	1	0.99	0.03	0.02	21	0.35	0.34	0.01	-0.01	4.407	3.238	0.706	3.376	2.833	2.622	2.027	0.777	0.716
grey	40	bast1-3	av	1																0.703	0.725
grey	40	bast1-3	1	1.5	1.5	0.1	0.1	29	0.56	0.53	0.03	0	5.425	3.655	1.401	4.156	3.487	3.423	1.900	0.824	0.545
grey	40	bast1-3	2	1.5	1.51	0.05	0.06	20	0.46	0.43	0.03	0.01	5.443	4.300	1.091	4.170	3.499	3.599	2.593	0.863	0.741
grey	40	bast1-3	3	1.5	1.52	0.1	0.12	28	0.58	0.54	0.04	0.02	5.461	3.857	1.544	4.183	3.510	3.662	1.962	0.875	0.559
grey	40	bast1-3	4	1.5	1.47	0.08	0.05	22	0.4	0.4	0	-0.03	5.370	3.636	0.994	4.114	3.452	3.099	2.147	0.753	0.622
grey	40	bast1-3	5	1.5	1.54	0	0.04	20	0.45	0.43	0.02	0.04	5.497	4.300	0.891	4.211	3.533	3.446	2.722	0.818	0.770

Table B 2-2 continued

Slab Label	Slab A	Ball Label	No. drop	Drop H H'(m)	Drop H H(m)	Bounce h h' (m)	Bounce h h (m)	Frames (1/200 s)	Horiz. distance S'(m)	Horiz. distance S (m)	S1 (m)	S2 (m)	Vi (m/s)	Vrx (m/s)	Vry (m/s)	Vin (m/s)	Vit (m/s)	Vrn (m/s)	Vrt (m/s)	Rn	Rt
grey	40	bast1-3	6	1.5	1.55	-0.04	0.01	16	0.34	0.31	0.03	0.05	5.515	3.875	0.517	4.224	3.545	2.887	2.636	0.683	0.744
grey	40	bast1-3	7	1.5	1.54	-0.01	0.03	19	0.43	0.43	0	0.04	5.497	4.526	0.782	4.211	3.533	3.508	2.965	0.833	0.839
grey	40	bast1-3	8	1.5	1.55	0	0.05	22	0.39	0.36	0.03	0.05	5.515	3.273	0.994	4.224	3.545	2.865	1.868	0.678	0.527
grey	40	bast1-3	av	1.5																0.791	0.668
grey	40	bast1-3	1	2	1.95	-0.33	-0.38	45	1.05	1.05	0	-0.05	6.185	4.667	0.585	4.738	3.976	2.551	3.951	0.538	0.994
grey	40	bast1-3	2	2	2.05	-0.24	-0.19	39	0.99	0.91	0.08	0.05	6.342	4.667	0.018	4.858	4.077	2.986	3.586	0.615	0.880
grey	40	bast1-3	3	2	2.14	-0.35	-0.21	25	0.73	0.6	0.13	0.14	6.480	4.800	1.067	4.964	4.165	2.268	4.363	0.457	1.047
grey	40	bast1-3	4	2	2.01	0.04	0.05	16	0.38	0.37	0.01	0.01	6.280	4.625	1.017	4.811	4.037	3.752	2.889	0.780	0.716
grey	40	bast1-3	5	2	1.98	0.04	0.02	14	0.32	0.3	0.02	-0.02	6.233	4.286	0.629	4.775	4.006	3.237	2.879	0.678	0.719
grey	40	bast1-3	6	2	2.03	-0.32	-0.29	42	0.98	0.92	0.06	0.03	6.311	4.381	0.351	4.835	4.057	2.547	3.582	0.527	0.883
grey	40	bast1-3	av	2																0.628	0.838
grey	40	bast1-3	1	2.5	2.51	0	0.01	10	0.21	0.21	0	0.01	7.018	4.200	0.445	5.376	4.511	3.041	2.931	0.566	0.650
grey	40	bast1-3	2	2.5	2.5	-0.35	-0.35	33	0.96	0.95	0.01	0	7.004	5.758	1.312	5.365	4.502	2.696	5.254	0.503	1.167
grey	40	bast1-3	3	2.5	2.55	-0.21	-0.16	36	1.01	0.95	0.06	0.05	7.073	5.278	0.006	5.418	4.547	3.388	4.047	0.625	0.890
grey	40	bast1-3	4	2.5	2.6	-0.35	-0.25	25	0.85	0.75	0.1	0.1	7.142	6.000	1.387	5.471	4.591	2.794	5.488	0.511	1.195
grey	40	bast1-3	5	2.5	2.5	0.07	0.07	26	0.64	0.64	0	0	7.004	4.923	1.176	5.365	4.502	4.065	3.015	0.758	0.670
grey	40	bast1-3	av	2.5																0.650	0.737
grey	40	grey	1	0.6	0.67	-0.35	-0.28	37	0.4	0.33	0.07	0.07	3.626	1.784	0.606	2.777	2.331	0.682	1.756	0.246	0.753
grey	40	grey	2	0.6	0.65	-0.35	-0.3	45	0.68	0.62	0.06	0.05	3.571	2.756	0.230	2.736	2.295	1.595	2.259	0.583	0.984
grey	40	grey	3	0.6	0.65	-0.35	-0.3	34	0.46	0.39	0.07	0.05	3.571	2.294	0.931	2.736	2.295	0.762	2.356	0.278	1.026
grey	40	grey	4	0.6	0.63	-0.35	-0.32	53	0.49	0.44	0.05	0.03	3.516	1.660	-0.092	2.693	2.260	1.138	1.213	0.423	0.537
grey	40	grey	5	0.6	0.64	-0.35	-0.31	36	0.36	0.31	0.05	0.04	3.544	1.722	0.839	2.715	2.278	0.464	1.859	0.171	0.816
grey	40	grey	6	0.6	0.63	-0.35	-0.32	43	0.42	0.37	0.05	0.03	3.516	1.721	0.434	2.693	2.260	0.774	1.597	0.287	0.707
grey	40	grey	7	0.6	0.63	-0.35	-0.32	39	0.42	0.37	0.05	0.03	3.516	1.897	0.685	2.693	2.260	0.695	1.894	0.258	0.838
grey	40	grey	8	0.6	0.62	-0.35	-0.33	41	0.32	0.3	0.02	0.02	3.488	1.463	0.604	2.672	2.242	0.478	1.509	0.179	0.673
grey	40	grey	9	0.6	0.61	-0.35	-0.34	37	0.35	0.31	0.04	0.01	3.460	1.676	0.930	2.650	2.224	0.364	1.882	0.137	0.846

Table B 2-2 continued

Slab Label	Slab A	Ball Label	No. drop	Drop H H'(m)	Drop H H(m)	Bounce h h' (m)	Bounce h h (m)	Frames (1/200 s)	Horiz. distance S'(m)	Horiz. distance S (m)	S1 (m)	S2 (m)	Vi (m/s)	Vrx (m/s)	Vry (m/s)	Vin (m/s)	Vit (m/s)	Vrm (m/s)	Vrt (m/s)	Rn	Rt
grey	40	grey	10	0.6	0.63	-0.35	-0.32	39	0.37	0.33	0.04	0.03	3.516	1.692	0.685	2.693	2.260	0.563	1.736	0.209	0.768
grey	40	grey	av	0.6																0.277	0.769
grey	40	grey	1	1	1.03	-0.35	-0.32	37	0.53	0.52	0.01	0.03	4.495	2.811	0.822	3.444	2.890	1.177	2.682	0.342	0.928
grey	40	grey	2	1	1.04	-0.35	-0.31	40	0.51	0.46	0.05	0.04	4.517	2.300	0.569	3.460	2.904	1.043	2.128	0.301	0.733
grey	40	grey	3	1	1.02	-0.35	-0.33	34	0.36	0.36	0	0.02	4.474	2.118	1.107	3.427	2.876	0.513	2.334	0.150	0.812
grey	40	grey	4	1	1.04	-0.35	-0.31	29	0.42	0.37	0.05	0.04	4.517	2.552	1.427	3.460	2.904	0.547	2.872	0.158	0.989
grey	40	grey	5	.1	1.03	-0.35	-0.32	38	0.55	0.52	0.03	0.03	4.495	2.737	0.752	3.444	2.890	1.183	2.580	0.344	0.893
grey	40	grey	6	1	1.05	-0.35	-0.3	47	0.67	0.62	0.05	0.05	4.539	2.638	0.124	3.477	2.918	1.601	2.101	0.460	0.720
grey	40	grey	7	1	1.02	-0.35	-0.33	42	0.44	0.41	0.03	0.02	4.474	1.952	0.541	3.427	2.876	0.840	1.844	0.245	0.641
grey	40	grey	8	1	1.01	-0.35	-0.34	40	0.53	0.53	0	0.01	4.452	2.650	0.719	3.410	2.861	1.153	2.492	0.338	0.871
grey	40	grey	av	1																0.292	0.823
grey	40	grey	1	1.5	1.53	-0.35	-0.32	58	0.96	0.95	0.01	0.03	5.479	3.276	-0.319	4.197	3.522	2.350	2.304	0.560	0.654
grey	40	grey	2	1.5	1.53	-0.35	-0.32	36	0.57	0.54	0.03	0.03	5.479	3.000	0.895	4.197	3.522	1.243	2.873	0.296	0.816
grey	40	grey	3	1.5	1.56	-0.35	-0.29	28	0.49	0.42	0.07	0.06	5.532	3.000	1.385	4.238	3.556	0.868	3.188	0.205	0.897
grey	40	grey	4	1.5	1.51	-0.35	-0.34	35	0.56	0.56	0	0.01	5.443	3.200	1.084	4.170	3.499	1.226	3.148	0.294	0.900
grey	40	grey	5	1.5	1.58	-0.35	-0.27	31	0.68	0.58	0.1	0.08	5.568	3.742	0.982	4.265	3.579	1.653	3.497	0.388	0.977
grey	40	grey	6	1.5	1.54	-0.35	-0.31	38	0.58	0.51	0.07	0.04	5.497	2.684	0.700	4.211	3.533	1.189	2.506	0.282	0.709
grey	40	grey	7	1.5	1.5	-0.35	-0.35	35	0.54	0.56	-0.02	0	5.425	3.200	1.142	4.156	3.487	1.182	3.185	0.285	0.913
grey	40	grey	av	1.5																0.330	0.838
grey	40	grey	1	2	2.03	-0.35	-0.32	33	0.49	0.49	0	0.03	6.311	2.970	1.130	4.835	4.057	1.043	3.001	0.216	0.740
grey	40	grey	2	2	2.01	-0.35	-0.34	30	0.56	0.55	0.01	0.01	6.280	3.667	1.531	4.811	4.037	1.184	3.793	0.246	0.940
grey	40	grey	3	2	2.02	-0.35	-0.33	30	0.57	0.54	0.03	0.02	6.295	3.600	1.464	4.823	4.047	1.192	3.699	0.247	0.914
grey	40	grey	4	2	2.03	-0.35	-0.32	32	0.49	0.46	0.03	0.03	6.311	2.875	1.215	4.835	4.057	0.917	2.983	0.190	0.735
grey	40	grey	5	2	2.04	-0.35	-0.31	44	0.58	0.54	0.04	0.04	6.327	2.455	0.330	4.846	4.067	1.325	2.092	0.273	0.515
grey	40	grey	6	2	2.02	-0.35	-0.33	48	0.93	0.93	0	0.02	6.295	3.875	0.198	4.823	4.047	2.339	3.096	0.485	0.765
grey	40	grey	7	2	2.02	-0.35	-0.33	25	0.4	0.37	0.03	0.02	6.295	2.960	2.027	4.823	4.047	0.350	3.570	0.073	0.882

Table B 2-2 continued

Slab Label	Slab A	Ball Label	No. drop	Drop H H'(m)	Drop H H(m)	Bounce h h' (m)	Bounce h h (m)	Frames (1/200 s)	Horiz. distance S'(m)	Horiz. distance S (m)	S1 (m)	S2 (m)	Vi (m/s)	Vrx (m/s)	Vry (m/s)	Vin (m/s)	Vit (m/s)	Vrn (m/s)	Vrt (m/s)	Rn	Rt
grey	40	grey	8	2	2.07	-0.35	-0.28	32	0.75	0.66	0.09	0.07	6.373	4.125	0.965	4.882	4.096	1.912	3.780	0.392	0.923
grey	40	grey	9	2	2.08	-0.33	-0.25	31	0.81	0.71	0.1	0.08	6.388	4.581	0.853	4.894	4.106	2.291	4.057	0.468	0.988
grey	40	grey	10	2	2.04	-0.35	-0.31	29	0.62	0.57	0.05	0.04	6.327	3.931	1.427	4.846	4.067	1.434	3.928	0.296	0.966
grey	40	grey	Av	2																0.289	0.837
grey	40	grey	1	2.5	2.56	-0.35	-0.29	22	0.53	0.45	0.08	0.06	7.087	4.091	2.097	5.429	4.556	1.023	4.482	0.188	0.984
grey	40	grey	2	2.5	2.55	-0.35	-0.3	35	0.56	0.5	0.06	0.05	7.073	2.857	0.856	5.418	4.547	1.181	2.739	0.218	0.602
grey	40	grey	3	2.5	2.59	-0.35	-0.26	17	0.43	0.31	0.12	0.09	7.129	3.647	2.642	5.461	4.582	0.320	4.492	0.059	0.980
grey	40	grey	4	2.5	2.59	-0.35	-0.26	23	0.58	0.46	0.12	0.09	7.129	4.000	1.697	5.461	4.582	1.271	4.155	0.233	0.907
grey	40	grey	5	2.5	2.55	-0.35	-0.3	22	0.4	0.34	0.06	0.05	7.073	3.091	2.188	5.418	4.547	0.311	3.774	0.057	0.830
grey	40	grey	6	2.5	2.63	-0.35	-0.22	14	0.46	0.31	0.15	0.13	7.183	4.429	2.800	5.503	4.617	0.702	5.192	0.128	1.124
grey	40	grey	7	2.5	2.58	-0.35	-0.27	23	0.46	0.37	0.09	0.08	7.115	3.217	1.784	5.450	4.573	0.702	3.611	0.129	0.790
grey	40	grey	av	2.5																0.145	0.849
grey	40	grey	1	3	3.01	-0.35	-0.34	35	0.47	0.44	0.03	0.01	7.685	2.514	1.084	5.887	4.940	0.785	2.623	0.133	0.531
grey	40	grey	2	3	3.12	-0.35	-0.23	18	0.51	0.38	0.13	0.12	7.824	4.222	2.114	5.994	5.029	1.095	4.593	0.183	0.913
grey	40	grey	3	3	3.02	-0.35	-0.33	28	0.53	0.51	0.02	0.02	7.698	3.643	1.670	5.897	4.948	1.062	3.864	0.180	0.781
grey	40	grey	4	3	3	-0.35	-0.35	25	0.49	0.49	0	0	7.672	3.920	2.187	5.877	4.931	0.844	4.409	0.144	0.894
grey	40	grey	5	3	3.01	-0.35	-0.34	23	0.45	0.43	0.02	0.01	7.685	3.739	2.392	5.887	4.940	0.571	4.402	0.097	0.891
grey	40	grey	6	3	3.08	-0.35	-0.27	20	0.56	0.44	0.12	0.08	7.774	4.400	2.210	5.955	4.997	1.136	4.791	0.191	0.959
grey	40	grey	7	3	3.06	-0.35	-0.29	21	0.53	0.45	0.08	0.06	7.748	4.286	2.247	5.936	4.981	1.034	4.727	0.174	0.949
grey	40	grey	8	3	3	-0.35	-0.35	27	0.57	0.55	0.02	0	7.672	4.074	1.930	5.877	4.931	1.140	4.362	0.194	0.884
grey	40	grey	9	3	3.03	-0.35	-0.32	40	1.02	0.98	0.04	0.03	7.710	4.900	0.619	5.906	4.956	2.675	4.151	0.453	0.838
grey	40	grey	10	3	3.05	-0.35	-0.3	34	0.65	0.56	0.09	0.05	7.736	3.294	0.931	5.926	4.972	1.404	3.122	0.237	0.628
grey	40	grey	av	3																0.199	0.827
frag	40	bast1-3	1	1.5	1.55	-0.27	-0.22	28	0.27	0.32	-0.05	0.05	5.515	2.286	0.885	4.224	3.545	0.791	2.320	0.187	0.654
frag	40	bast1-3	2	1.5	1.5	-0.26	-0.26	51	0.23	0.37	-0.14	0	5.425	1.451	-0.231	4.156	3.487	1.110	0.963	0.267	0.276
frag	40	bast1-3	3	1.5	1.57	-0.17	-0.1	28	0.08	0.16	-0.08	0.07	5.550	1.143	0.028	4.252	3.568	0.713	0.893	0.168	0.250

Table B 2-2 continued

Slab Label	Slab A	Ball Label	No. drop	Drop H H'(m)	Drop H H(m)	Bounce h h' (m)	Bounce h h (m)	Frames (1/200 s)	Horiz. distance S'(m)	Horiz. distance S (m)	S1 (m)	S2 (m)	Vi (m/s)	Vrx (m/s)	Vry (m/s)	Vin (m/s)	Vit (m/s)	Vrn (m/s)	Vrt (m/s)	Rn	Rt
frag	40	bast1-3	4	1.5	1.56	-0.26	-0.2	35	0.24	0.32	-0.08	0.06	5.532	1.829	0.284	4.238	3.556	0.957	1.584	0.226	0.445
frag	40	bast1-3	5	1.5	1.51	0.08	0.09	18	-0.05	0.1	-0.15	0.01	5.443	1.111	1.329	4.170	3.499	1.732	-0.003	0.415	-0.001
frag	40	bast1-3	6	1.5	1.52	-0.26	-0.24	45	0.2	0.33	-0.13	0.02	5.461	1.467	-0.037	4.183	3.510	0.971	1.100	0.232	0.313
frag	40	bast1-3	av	1.5	1.5															0.216	0.388
frag	20	bast1-3	1	1.5	1.5	0.02	0.02	15	0.07	0.04	0.03	0	5.425	0.533	0.635	5.098	1.855	0.779	0.284	0.153	0.153
frag	20	bast1-3	2	1.5	1.5	0.02	0.02	18	0.13	0.08	0.05	0	5.425	0.889	0.664	5.098	1.855	0.928	0.608	0.182	0.328
frag	20	bast1-3	3	1.5	1.5	0.01	0.01	5	0.03	0.03	0	0	5.425	1.200	0.523	5.098	1.855	0.902	0.949	0.177	0.511
frag	20	bast1-3	av	1.5	1.5								5.425			5.098	1.855	0.000		0.171	0.331
gravel	20	bast1-3	1	1.5	1.5	0.01	0.01	20	0.03	0.03	0	0	5.425	0.300	0.591	5.098	1.855	0.657	0.080	0.129	0.043
gravel	20	bast1-3	2	1.5	1.51	-0.02	-0.01	29	0.1	0.15	-0.05	0.01	5.443	1.034	-0.642	5.115	1.862	0.957	0.752	0.187	0.404
gravel	20	bast1-3	3	1.5	1.5	-0.01	-0.01	12	0.06	0.06	0	0	5.425	1.000	-0.128	5.098	1.855	0.462	0.896	0.091	0.483
gravel	20	bast1-3	av	1.5	1.5															0.136	0.310
sand	20	bast1-3	1	1.5	1.5	0.03	0.03	40	0.05	0.05	0	0	5.425	0.250	0.767	5.098	1.855	1.148	-0.027	0.225	-0.015
sand	20	bast1-3	2	1.5	1.5	0.02	0.02	26	0.03	0.03	0	0	5.425	0.231	0.626	5.098	1.855	0.823	0.003	0.161	0.001
sand	20	bast1-3	av																	0.193	-0.007
soil	20	bast1-3	1	1.5	1.52	0.02	0.04	20	0.08	0.12	-0.04	0.02	5.461	1.200	0.891	5.132	1.868	1.247	0.823	0.243	0.441
soil	20	bast1-3	2	1.5	1.52	0	0.02	12	0.03	0.08	-0.05	0.02	5.461	1.333	0.628	5.132	1.868	1.046	1.038	0.204	0.556
soil	20	bast1-3	3	1.5	1.5	0.015	0.015	16	-0.01	0.07	-0.08	0	5.425	0.875	0.580	5.098	1.855	0.844	0.624	0.166	0.336
soil	20	bast1-3	4	1.5	1.5	0.015	0.015	13	-0.04	0.04	-0.08	0	5.425	0.615	0.550	5.098	1.855	0.727	0.390	0.143	0.210
soil	20	bast1-3	5	1.5	1.5	0.015	0.015	16	-0.03	0.05	-0.08	0	5.425	0.625	0.580	5.098	1.855	0.759	0.389	0.149	0.210
soil	20	bast1-3	6	1.5	1.5	0.015	0.015	13	-0.04	0.04	-0.08	0	5.425	0.615	0.550	5.098	1.855	0.727	0.390	0.143	0.210
soil	20	bast1-3	7	1.5	1.51	0	0.01	12	0.02	0.07	-0.05	0.01	5.443	1.167	0.461	5.115	1.862	0.832	0.939	0.163	0.504
soil	20	bast1-3	av	1.5	1.5															0.173	0.352
soil	20	bs	1	1.5	1.5	0.02	0.02	14	0.06	0.12	-0.06	0	5.425	1.714	0.629	5.098	1.855	1.177	1.396	0.231	0.752
soil	20	bs	2	1.5	1.51	0.015	0.025	11	0.13	0.13	0	0.01	5.443	2.364	0.724	5.115	1.862	1.489	1.973	0.291	1.060

Table B 2-2 continued

Slab Label	Slab A	Ball Label	No. drop	Drop H H'(m)	Drop H H(m)	Bounce h h' (m)	Bounce h h (m)	Frames (1/200 s)	Horiz. distance S'(m)	Horiz. distance S (m)	S1 (m)	S2 (m)	Vi (m/s)	Vrx (m/s)	Vry (m/s)	Vin (m/s)	Vit (m/s)	Vrn (m/s)	Vrt (m/s)	Rn	Rt
soil	20	bs	3	1.5	1.52	0	0.02	14	0.06	0.06	0	0.02	5.461	0.857	0.629	5.132	1.868	0.884	0.590	0.172	0.316
soil	20	bs	4	1.5	1.52	0	0.02	8	0.06	0.05	0.01	0.02	5.461	1.250	0.696	5.132	1.868	1.082	0.937	0.211	0.501
soil	20	bs	5	1.5	1.52	0	0.02	14	0.1	0.11	-0.01	0.02	5.461	1.571	0.629	5.132	1.868	1.129	1.262	0.220	0.675
soil	20	bs	6	1.5	1.52	0.03	0.05	19	0.08	0.08	0	0.02	5.461	0.842	0.992	5.132	1.868	1.220	0.452	0.238	0.242
soil	20	bs	7	1.5	1.51	0	0.01	15	0.11	0.12	-0.01	0.01	5.443	1.600	0.501	5.115	1.862	1.018	1.332	0.199	0.716
soil	20	bs	8	1.5	1.5	0.05	0.05	22	0.15	0.18	-0.03	0	5.425	1.636	0.994	5.098	1.855	1.494	1.198	0.293	0.645
soil	20	bs	9	1.5	1.52	0	0.02	9	0.06	0.06	0	0.02	5.461	1.333	0.665	5.132	1.868	1.081	1.025	0.211	0.549
soil	20	bs	av	1.5	1.5								5.425			5.098	1.855			0.230	0.606
frag#	20	bast1-3	1	1.5	1.53	-0.1	-0.07	31	0.24	0.24	0	0.03	5.479	1.548	-0.309	5.149	1.874	0.820	1.349	0.159	0.720
frag#	20	bast1-3	2	1.5	1.52	-0.1	-0.08	35	0.25	0.25	0	0.02	5.461	1.429	-0.401	5.132	1.868	0.866	1.205	0.169	0.645
frag#	20	bast1-3	3	1.5	1.52	0	0.02	11	0.05	0.07	-0.02	0.02	5.461	1.273	0.633	5.132	1.868	1.031	0.979	0.201	0.524
frag#	20	bast1-3	4	1.5	1.53	-0.06	-0.03	23	0.13	0.12	0.01	0.03	5.479	1.043	-0.303	5.149	1.874	0.642	0.877	0.125	0.468
frag#	20	bast1-3	5	1.5	1.5	-0.06	-0.06	21	0.15	0.2	-0.05	0	5.425	1.905	0.056	5.098	1.855	0.598	1.809	0.117	0.975
frag#	20	bast1-3	6	1.5	1.5	0.01	0.01	11	0.01	0.06	-0.05	0	5.425	1.091	0.452	5.098	1.855	0.797	0.871	0.156	0.469
frag#	20	bast1-3	7	1.5	1.53	-0.01	0.02	10	0.09	0.06	0.03	0.03	5.479	1.200	0.645	5.149	1.874	1.017	0.907	0.197	0.484
frag#	20	bast1-3	av	1.5	1.5															0.161	0.612
frag#	20	bs	1	1.5	1.51	0	0.01	17	0.1	0.1	0	0.01	5.443	1.176	0.535	5.115	1.862	0.905	0.923	0.177	0.496
frag#	20	bs	2	1.5	1.51	-0.02	-0.01	18	0.15	0.15	0	0.01	5.443	1.667	-0.330	5.115	1.862	0.880	1.453	0.172	0.781
frag#	20	bs	3	1.5	1.5	-0.02	-0.02	15	0.1	0.18	-0.08	0	5.425	2.400	-0.101	5.098	1.855	0.726	2.221	0.142	1.197
frag#	20	bs	4	1.5	1.55	-0.03	0.02	18	0.18	0.06	0.12	0.05	5.515	0.667	0.664	5.182	1.886	0.852	0.399	0.164	0.212
frag#	20	bs	av	1.5	1.5															0.164	0.671
paving#	20	bast1-3	1	1.5	1.5	0.01	0.01	18	0.02	0.03	-0.01	0	5.425	0.333	0.553	5.098	1.855	0.633	0.124	0.124	0.067
paving#	20	bast1-3	2	1.5	1.5	0.02	0.02	15	0.07	0.11	-0.04	0	5.425	1.467	0.635	5.098	1.855	1.098	1.161	0.215	0.626
paving#	20	bast1-3	3	1.5	1.5	0.02	0.02	10	0.18	0.09	0.09	0	5.425	1.800	0.645	5.098	1.855	1.222	1.471	0.240	0.793
paving#	20	bast1-3	4	1.5	1.5	0.02	0.02	13	0.1	0.1	0	0	5.425	1.538	0.627	5.098	1.855	1.115	1.231	0.219	0.664
paving#	20	bast1-3	5	1.5	1.5	0.01	0.01	9	0.06	0.06	0	0	5.425	1.333	0.443	5.098	1.855	0.872	1.101	0.171	0.594

Table B 2-2 continued

Slab Label	Slab A	Ball Label	No. drop	Drop H H'(m)	Drop H H(m)	Bounce h h' (m)	Bounce h h (m)	Frames (1/200 s)	Horiz. distance S'(m)	Horiz. distance S (m)	S1 (m)	S2 (m)	Vi (m/s)	Vrx (m/s)	Vry (m/s)	Vin (m/s)	Vit (m/s)	Vrn (m/s)	Vrt (m/s)	Rn	Rt
paving#	20	bast1-3	6	1.5	1.5	0.015	0.015	12	0.08	0.08	0	0	5.425	1.333	0.544	5.098	1.855	0.968	1.067	0.190	0.575
paving#	20	bast1-3	7	1.5	1.5	0.005	0.005	9	0.05	0.05	0	0	5.425	1.111	0.332	5.098	1.855	0.692	0.931	0.136	0.502
paving#	20	bast1-3	8	1.5	1.5	0.005	0.005	8	0.03	0.03	0	0	5.425	0.750	0.321	5.098	1.855	0.558	0.595	0.110	0.321
paving#	20	bast1-3	9	1.5	1.5	-0.06	-0.06	28	0.26	0.26	0	0	5.425	1.857	-0.258	5.098	1.855	0.393	1.657	0.077	0.893
paving#	20	bast1-3	10	1.5	1.5	0.005	0.005	12	0.05	0.05	0	0	5.425	0.833	0.378	5.098	1.855	0.640	0.654	0.126	0.352
paving#	20	bast1-3	1	1.5	1.5	0.01	0.01	15	0.12	0.12	0	0	5.425	1.600	0.501	5.098	1.855	1.018	1.332	0.200	0.718
paving#	20	bast1-3	2	1.5	1.52	-0.08	-0.06	22	0.29	0.19	0.1	0.02	5.461	1.727	0.006	5.132	1.868	0.596	1.625	0.116	0.870
paving#	20	bast1-3	3	1.5	1.5	0.01	0.01	10	0.05	0.05	0	0	5.425	1.000	0.445	5.098	1.855	0.760	0.787	0.149	0.424
paving#	20	bast1-3	4	1.5	1.53	-0.09	-0.06	30	0.3	0.25	0.05	0.03	5.479	1.667	-0.336	5.149	1.874	0.255	1.451	0.049	0.774
paving#	20	bast1-3	5	1.5	1.53	-0.03	0	11	0.18	0.06	0.12	0.03	5.479	1.091	0.270	5.149	1.874	0.627	0.933	0.122	0.498
paving#	20	bast1-3	av	1.5																0.150	0.578
paving#	20	bs	1	1.5	1.5	0.005	0.005	11	0.23	0.1	0.13	0	5.425	1.818	0.361	5.098	1.855	0.961	1.585	0.188	0.854
paving#	20	bs	2	1.5	1.5	0	0	34	0.26	0.16	0.1	0	5.425	0.941	0.834	5.098	1.855	1.105	0.599	0.217	0.323
paving#	20	bs	3	1.5	1.54	-0.08	-0.04	30	0.3	0.26	0.04	0.04	5.497	1.733	-0.469	5.165	1.880	0.152	1.468	0.029	0.781
paving#	20	bs	4	1.5	1.5	0.005	0.005	10	0.29	0.09	0.2	0	5.425	1.800	0.345	5.098	1.855	0.940	1.573	0.184	0.848
paving#	20	bs	5	1.5	1.53	-0.01	0.02	23	0.21	0.11	0.1	0.03	5.479	0.957	0.738	5.149	1.874	1.021	0.646	0.198	0.345
paving#	20	bs	6	1.5	1.5	0.015	0.015	14	0.17	0.08	0.09	0	5.425	1.143	0.558	5.098	1.855	0.915	0.883	0.179	0.476
paving#	20	bs	7	1.5	1.53	-0.02	0.01	15	0.15	0.07	0.08	0.03	5.479	0.933	0.501	5.149	1.874	0.790	0.706	0.153	0.377
paving#	20	bs	8	1.5	1.5	-0.03	-0.03	20	0.26	0.13	0.13	0	5.425	1.300	-0.191	5.098	1.855	0.266	1.156	0.052	0.623
paving#	20	bs	9	1.5	1.5	0.015	0.015	14	0.14	0.08	0.06	0	5.425	1.143	0.558	5.098	1.855	0.915	0.883	0.179	0.476
paving#	20	bs	av	1.5																0.154	0.567

B.3 Rockfall field tests for the Coefficient of Restitution

Field tests for the coefficients of restitution have been carried out on massive basalt (basalt1), rubbly basalt (basalt2) and scree slopes. The calculations of restitution coefficients are shown in table B3 -1. Equations for the calculation are shown in chapter 3. Meanings of symbols are the same as those in table B1-2.

Table B3-1 Coefficient of restitution calculation (field test in Lyttelton)

Slope	No.	Slope	Drop			bounce	Horizon.	frames	time	Vi	Vrx	Vry	Vin	Vit	Vrn	Vrt	Rn	Rt
type	drop	Angle	S1	H' (m)	H (m)	H(m)	S (m)	(1/200 s)	(s)	(m/s)	(m/s)	(m/s)	(m/s)	(m/s)	(m/s)	(m/s)		
basalt1	1	12	0.7	4.5	3.8	0.05	0.35	20	0.100	8.635	3.500	0.991	8.446	1.795	1.697	3.218	0.201	1.792
basalt1	2	12	0.8	4.5	3.7	0.15	0.4	24	0.120	8.520	3.333	1.839	8.334	1.771	2.491	2.878	0.299	1.625
basalt1	3	12	1	4.5	3.5	0.2	0.5	30	0.150	8.287	3.333	2.069	8.106	1.723	2.717	2.830	0.335	1.643
basalt1	4	12	0.75	4.5	3.75	0.05	0.2	20	0.100	8.578	2.000	0.991	8.390	1.783	1.385	1.750	0.165	0.981
basalt1	5	12	1	4.5	3.5	0.1	0.3	25	0.125	8.287	2.400	1.413	8.106	1.723	1.881	2.054	0.232	1.192
basalt1	6	12	0.9	4.5	3.6	0	0.15	10	0.050	8.404	3.000	0.245	8.221	1.747	0.864	2.883	0.105	1.650
basalt1	7	12	1	4.5	3.5	0.25	0.8	26	0.130	8.287	6.154	2.561	8.106	1.723	3.784	5.487	0.467	3.185
basalt1	8	12	0.9	4.5	3.6	0.05	0.15	12	0.060	8.404	2.500	1.128	8.221	1.747	1.623	2.211	0.197	1.265
basalt1	9	12	1	4.5	3.5	0.75	0.65	56	0.280	8.287	2.321	4.052	8.106	1.723	4.446	1.428	0.549	0.829
basalt1	10	0	0.9	4.5	3.6	0.5	0	38	0.190	8.404	0.000	3.564	8.404	0.000	3.564	0.000	0.373	
basalt1	11	12	0.8	4.5	3.7	0.05	0.25	14	0.070	8.520	3.571	1.058	8.334	1.771	1.777	3.273	0.213	1.848
basalt1	12	5	0.75	4.5	3.75	0.05	0.05	16	0.080	8.578	0.625	1.017	8.545	0.748	1.068	0.534	0.125	0.714
basalt1	13	0	0.75	4.5	3.75	0.03	0	15	0.075	8.578	0.000	0.768	8.578	0.000	0.768	0.000	0.089	
basalt1	14	0	0.8	4.5	3.7	0.03	0	16	0.080	8.520	0.000	0.767	8.520	0.000	0.767	0.000	0.090	
basalt1	av																0.246	0.772
basalt2	1	28	1	4.5	3.5	-0.8	1.6	71	0.355	8.287	4.507	-0.512	7.317	3.890	1.664	4.220	0.227	1.085
basalt2	2	28	0.75	4.5	3.75	-0.5	1.25	62	0.310	8.578	4.032	-0.092	7.574	4.027	1.811	3.604	0.239	0.895
basalt2	3	28	0.7	4.5	3.8	-0.5	0.8	68	0.340	8.635	2.353	0.197	7.624	4.054	1.279	1.985	0.168	0.490

Table B 3-1 continued

Slope type	No. drop	Slope Angle	Drop			bounce H(m)	Horizon. S (m)	frames (1/200 s)	time (s)	Vi (m/s)	Vrx (m/s)	Vry (m/s)	Vin (m/s)	Vit (m/s)	Vrn (m/s)	Vrt (m/s)	Rn	Rt
			S1	H' (m)	H (m)													
basalt2	4	28	0.9	4.5	3.6	0.05	0.25	13	0.065	8.404	3.846	1.088	7.421	3.946	2.766	2.885	0.373	0.731
basalt2	5	28	0.9	4.5	3.6	0.03	0.3	16	0.080	8.404	3.750	0.767	7.421	3.946	2.438	2.951	0.329	0.748
basalt2	6	28	1.1	4.5	3.4	0.05	0.3	20	0.100	8.167	3.000	0.991	7.211	3.834	2.283	2.184	0.317	0.570
basalt2	7	10	1.1	4.5	3.4	0.3	0.2	38	0.190	8.167	1.053	2.511	8.043	1.418	2.656	0.601	0.330	0.423
basalt2	8	28	0.75	4.5	3.75	-0.5	0.65	55	0.275	8.578	2.364	-0.469	7.574	4.027	0.695	2.307	0.092	0.573
basalt2	9	10	1.1	4.5	3.4	0.03	0.25	16	0.080	8.167	3.125	0.767	8.043	1.418	1.298	2.944	0.161	2.076
basalt2	10	28	0.9	4.5	3.6	-0.75	1.2	59	0.295	8.404	4.068	-1.095	7.421	3.946	0.943	4.106	0.127	1.041
basalt2	11	28	0.75	4.5	3.75	0	0.25	13	0.065	8.578	3.846	0.319	7.574	4.027	2.087	3.246	0.276	0.806
basalt2	12	28	1	4.5	3.5	-0.6	0.75	56	0.280	8.287	2.679	-0.769	7.317	3.890	0.578	2.726	0.079	0.701
basalt2	av																0.226	0.660
scree	1	20	0.5	4	3.5	-0.25	0.7	65	0.325	8.287	2.154	0.825	7.787	2.834	1.512	1.742	0.194	0.615
scree	2	0	0	4	4	0.05	0										0.112	
scree	3	20	0.2	4	3.8	0.1	0.25	30	0.150	8.635	1.667	1.402	8.114	2.953	1.888	1.086	0.233	0.368
scree	4	20	0.2	4	3.8	0.05	0.1	24	0.120	8.635	0.833	1.005	8.114	2.953	1.230	0.439	0.152	0.149
scree	5	10	0.15	4	3.85	0.1	0.2	32	0.160	8.691	1.250	1.410	8.559	1.509	1.605	0.986	0.188	0.653
scree	6	10	0.1	4	3.9	0.05	0.2	20	0.100	8.747	2.000	0.991	8.615	1.519	1.323	1.798	0.154	1.183
scree	7	10	0.2	4	3.8	0.15	0.25	32	0.160	8.635	1.563	1.722	8.503	1.499	1.967	1.240	0.231	0.827
scree	8	10	0.25	4	3.75	0.1	0.25	30	0.150	8.578	1.667	1.402	8.447	1.489	1.671	1.398	0.198	0.938
scree	9	5	0	4	4	0.15	0.2	22	0.110	8.859	1.818	1.903	8.825	0.772	2.054	1.645	0.233	2.131
scree	10	10	0.2	4	3.8	0.05	0.15	23	0.115	8.635	1.304	0.999	8.503	1.499	1.210	1.111	0.142	0.741
scree	11	5	0	4	4	0.05	0.08	30	0.150	8.859	0.533	1.069	8.825	0.772	1.111	0.438	0.126	0.567
scree	12	20	0.6	4	3.4	-0.25	0.52	44	0.220	8.167	2.364	-0.057	7.675	2.793	0.755	2.241	0.098	0.802
scree	13	10	0.2	4	3.8	0.08	0.2	18	0.090	8.635	2.222	1.330	8.503	1.499	1.696	1.957	0.199	1.306
scree	14	10	0.2	4	3.8	0.08	0.25	23	0.115	8.635	2.174	1.260	8.503	1.499	1.618	1.922	0.190	1.282
scree	15	20	0.7	4	3.3	-0.2	0.4	45	0.225	8.046	1.778	0.215	7.561	2.752	0.810	1.597	0.107	0.580
scree	av																0.170	0.677

Appendix C

Site Investigation and Field Trial Records

This appendix gives records of site investigation, profile survey and field tests at Lyttelton quarry and Marine Tavern site.

C1 Field trial in Lyttelton Quarry

C1.1 Profile survey

EDM survey data of the profile for rockfall field trial at Lyttelton are shown in table C1-1.

Site: Lyttelton quarry Date: 10/30, 4/11, 1999.

Height of instrument (m) 1.542 1.551

Height of staff (m) 1.5 1.551

Table C1-1: Profile survey data at Lyttelton Quarry

Point	Vertical Reading (m)	Height Difference (m)	Reduced Height (m)	Horizontal Distance (m)	Notes
1	-0.068	-0.042	-0.11	9.153	Measured in 30/10
2	-0.065	-0.042	-0.107	11.202	
3	-0.074	-0.042	-0.116	13.194	
4	-0.135	-0.042	-0.177	14.792	
5	-0.021	-0.042	-0.063	15.962	
6	0.084	-0.042	0.042	16.868	
7	0.56	-0.042	0.518	17.933	
8	1.195	-0.042	1.153	18.647	
9	1.401	-0.042	1.359	19.01	
10	1.556	-0.042	1.514	19.87	
11	2.083	-0.042	2.041	20.527	
12	2.674	-0.042	2.632	21.129	
13	3.245	-0.042	3.203	21.58	
#25	3.479	0	3.479	21.866	Bottom of paint mark
14	3.427	-0.042	3.385	21.876	Bottom of paint mark
#24	4.092	0	4.092	21.877	#: Measured in 4/11, 1999
#23	4.483	0	4.483	22.18	
#22	5.085	0	5.085	22.338	
#21	5.58	0	5.58	22.556	
#20	5.911	0	5.911	22.819	
#19	6.359	0	6.359	23.111	
#18	6.843	0	6.843	23.334	
#17	7.281	0	7.281	23.655	
#16	7.631	0	7.631	23.912	bottom of lahar layer
#15	8.229	0	8.229	23.982	

Table C1-1 continued

Point	Vertical Reading (m)	Height Difference (m)	Reduced Height (m)	Horizontal Distance (m)	Notes
#14	8.696	0	8.696	24.162	
#13	9.186	0	9.186	24.189	
#12	9.786	0	9.786	24.36	top of lahar layer
#8	11.419	0	11.419	24.428	
#9	11.102	0	11.102	24.444	
#11	10.1	0	10.1	24.46	
#10	10.738	0	10.738	24.518	
#7	12.119	0	12.119	24.555	
#6	12.588	0	12.588	24.769	
#5	13.111	0	13.111	24.985	
#4	13.721	0	13.721	25.01	
#3	14.063	0	14.063	25.257	top of paint mark
#2	14.611	0	14.611	25.388	
#1	15.017	0	15.017	25.732	measured 4/11
16	14.97	-0.042	14.928	25.907	
15	15.65	-0.042	15.608	26.755	

C1-2 Schmidt hammer measurement

Schmidt hammer tests have been done on both rock slopes in the field and smooth surface of rock samples taken from the field. Results of the upper 50% measurement are shown in table C1-2.

C1.3 Surface roughness measurement

Surface roughness is measured by compass (point 1-21) and by profile survey (point 21-39). Standard deviation (Stdev.) and the roughness value for CRSP simulation (S) are also calculated (table C1-3).

Table C1-2 Schmidt number measurement of rocks in Lyttelton Quarry

Rock type		Schmidt numbers											
		1	2	3	4	5	6	7	8	9	10	Mean	Stdev
Massive basalt	in situ	61	55.2	55	54.2	51.5	52.5	51	50.5	49.5	50.5	53.1	3.4
	sample	55	52	52.5	54.5	54	54.5	52.5	55	53.2	53.5	53.7	1.1
Rubbly basalt	in situ	43	42	33	32	37	31	36	35	32.5	34.5	35.6	4.1
	sample	47.4	48.5	51	48.5	49	45.5	49.2	46.8	45.5	47.5	47.9	1.7
lahar	in situ	18.5	22	22.5	20.5	21	20.8	19	20.5	19.5	18.5	20.3	1.4

Table C1-3: Surface roughness measurement (Lyttelton Quarry)

Survey point	Cell No.	Angles (degree)	Mean	Stdev.	S
1-4	21	-2 4 -8 -2 4 4 2 -4 4 -1 0 -8 -7 -4 4 -4 -8 7 8	-0.58	5.21	0.018
4-5	20	5 20 16 14	13.75	6.34	0.022
5-6	19	10 4 5 4 6 3 1 4 2	4.33	2.60	0.009
6-7	18	22 37 4 12 23 14 30 20	20.25	10.40	0.037
7-8	17	14 18 22 36 32 42 44 36	30.50	11.20	0.040
8-9	16	24 50 30 42 38 34 40 22 38 26	34.40	8.88	0.031
9-10	15	10 16 17 12 25 20 22 18 28	18.67	5.81	0.020
10-14	14	32 30 22 34 35 32 35 38 32 42 58 56 46 36	37.71	9.88	0.035
14-15	13	58 60 50 80 60 48 60 70 58 72 62 80 64 72 64 58 60 70 58 74 70	64.19	8.69	0.031
15-16	12	50 44 54 42 45 40	45.83	5.23	0.018
16-21	11	48 42 40 42 52 52 52 48 56 52 48 56 75 62 57 59 63	53.18	8.75	0.031
21-23	10	54 49	51.50	3.54	0.012
23-26	9	83 72 91	82.00	9.54	0.034
26-27	8	65		9.54	0.034
27-32	7	74 92 88 105 77	87.20	12.44	0.044
32-33	6	59		8.00	0.028
33-35	5	73 90	81.50	12.02	0.043
35-36	4	52		8.00	0.028
36-37	3	74		8.00	0.028
37-38	2	50		8.00	0.028
38-39	1	29		8.00	0.028

Table C1-4: Boulder size and rest position

Boulder No.	Position (m)		Size (cm)		
	X	Y	Length	Width	Height
1	21.755	0.5	35	25	18
2	16.755	-3.3	40	30	22
3	15.755	2.8	30	20	20
4	15.555	2.2	30	30	20
5	15.355	-2.4	40	30	18
6	14.655	-2.7	30	26	20
7	14.555	-2.6	40	35	18
8	14.455	-1.6	35	22	20
9	14.255	-0.5	25	25	22
10	14.255	0.4	32	22	17
11	14.155	0.2	30	20	20
12	13.955	0.5	30	25	20
13	13.655	-1.8	35	28	20
14	13.655	-4.7	25	25	18
15	13.355	-2	30	25	20
16	13.255	-1	30	28	22
17	13.255	0.9	36	30	18

Table C1-4 continued

Boulder No.	Position (m)		Size (cm)		
	X	Y	Length	Width	Height
18	13.155	0.2	36	35	25
19	12.755	-1	30	30	22
20	12.755	-0.3	30	30	20
21	12.755	0.2	25	25	20
22	12.655	-1.8	45	32	25
23	12.555	-1.2	33	32	30
24	12.555	-2	30	28	22
25	12.555	0	40	30	30
26	12.555	0.5	35	25	18
27	12.455	-1.5	40	30	28
28	12.455	0.7	48	30	20
29	12.255	0	40	35	22
30	12.255	2	40	30	22
31	12.155	1.5	30	25	22
32	12.055	-1	30	25	20
33	11.855	-1.2	25	22	20
34	11.755	-1.7	30	22	20
35	11.755	0	28	25	25
36	11.655	1	30	22	20
37	11.255	-1.5	28	25	18
38	11.155	-0.5	30	30	18
39	11.155	0.9	35	20	20
40	10.955	0.6			
41	10.655	0.7			
42	7.835	0.5	30	22	18

C1.4 Boulder measurement

The rest positions (X: distance from top of slope, Y: distance from the section line) and size of the boulders rolled in the field trial are shown in table C1-4.

C1.5 Field trial results

Bounce height and velocity of each boulder at the base of rock slope section (point1) and the toe of slope (point2) was recorded by the high-speed camera. Boulder velocity is calculated by the travelled distance within a few frames while the boulder is passing the analysis point. The results are shown in table C1-5.

Table C1-5: Field trial result (bounce height and velocity at two analysis points)

Boulder No.	Point 1				Point2			
	h1(m)	S1 (m)	Frames	V1 (m/s)	h2 (m)	S2 (m)	Frames	V2 (m/s)
1	0.1	0.25	4	12.5	0.1	0.15	4	7.5
2	2.5				0.6	0.3	4	15
3	0.25	0.28	4	14	0.1	0.25	5	10
4	0.3	0.27	4	13.5	1.3	0.25	5	10
5	0.2	0.25	5	10	0.1	0.25	8	6.25
6	1.2	0.25	5	10	0.2	0.25	6	8.333
7	1.5	0.25	5	10	0.25	0.25	5	10
8	0.4	0.25	4	12.5	0.7	0.25	6	8.333
9	2.5	0.25	4	12.5	0.2	0.25	3.5	14.29
10	2.2	0.25	4.5	11.11	0.25	0.25	6	8.333
11	3.2	0.25	4	12.5	1.51	0.25	3	16.67
12	0.5	0.25	4	12.5	0.2	0.25	4	12.5
13	1.3	0.25	4.5	11.11	0.25	0.25	5.5	9.091
14	0.5	0.25	5	10	0.1	0.25	6	8.333
15	1.25	0.25	5.5	9.091	0.2	0.25	10	5
16	0.5	0.25	4	12.5	Does not reach this point			
17	2.2	0.25	4	12.5	0.2	0.25	5	10
18	0.3	0.25	4.5	11.11	0.3	0.25	4.5	11.11
19	0.5	0.25	4	12.5	0.1	0.25	10	5
20	0.7	0.25	6	8.333	0.2	0.25	5	10
21	1.7	0.25	4	12.5	0.15	0.25	3.5	14.29
22	0.2	0.25	3.5	14.29	0.3	0.25	4	12.5
23	0.7	0.25	4	12.5	0.1	0.25	4	12.5
24	2.2	0.25	4	12.5	0.3	0.25	5	10
25	1.2	0.25	3	16.67	0.25	0.25	5	10
26	1.5	0.25	3	16.67	0.1	0.25	4	12.5
27	0.5	0.25	3	16.67	0.2	0.25	6	8.333
28	0.8	0.25	4	12.5	0.1	0.25	6	8.333
29	0.5	0.25	4	12.5	0.2	0.25	10	5
30	2.5	0.25	4	12.5	0.5	0.25	8	6.25
31	0.5	0.25	4	12.5	0.3	0.25	5	10
32	2.1	0.25	3.5	14.29	0.25	0.25	4.5	11.11
33	0.25	0.25	4	12.5	0.1	0.25	7	7.143
34	2.25	0.25	4	12.5	0.2	0.25	6	8.333
35	2	0.25	5	10	0.25	0.25	8	6.25
36	1	0.25	6	8.333	0.35	0.25	5	10
37	3	0.25	5	10	0.45	0.25	4	12.5
38	2.2	0.25	4	12.5	0.3	0.25	3	16.67
39	0.8	0.25	5	10	0.1	0.25	10	5
40	2.5	0.25	4	12.5	0.2	0.25	6	8.333

C.2 Site investigation at Marine Apartments, Sumner

C2-1 Profile survey data

Profile survey data for the 15 sections used in rockfall simulations in chapter 5 are shown in table C2-1 (from Eliot Sinclair and Partners Ltd.).

Table C2-1: Survey data of sections, Marine Apartments

Section No	0		6		12		78		84		18		24	
	x	z	x	z	x	z	x	z	x	z	x	z	x	z
1	0	37.9	0	42.8	0	47.6	0	43.6	0	43.4	0	49.2	0	57.7
2	2.7	35	1.3	41.7	-1	45.8	1.1	42.7	1.3	41.6	-0.8	47.9	0.5	56.9
3	3	31.3	5.4	34.7	-0.6	45.5	2	40.5	2.5	40.5	0.1	45.9	1	54.9
4	7.6	13.5	5.4	34.1	-1	44.5	2.6	39.5	3.2	39.5	-0.5	45.1	0.5	53.2
5	11.4	12.4	5.2	33.9	-0.6	43.4	3.6	38.8	3.7	39.1	-0.8	44.2	0.6	52.7
6	16.8	12.2	6.9	29.7	-0.7	42.1	3.3	38.4	4	38.4	-0.5	43.2	0.2	50.9
7			4.8	29	3.1	38.6	4.2	37	3.7	37.6	-0.6	41.8	2.1	48.7
8			4.4	28.6	4.2	37.2	4.6	36	15.2	13.9	-1	39.6	1.8	48
9			3.5	27.9	4.5	35.4	5.4	34.8	17.2	13.2	0	38	4.7	44.9
10			13.1	12.6	2.1	32.6	5.2	33.7	22.9	12	0.4	37.5	3.6	43.4
11			18.2	12.1	1.8	30.8	10	23.6			1.9	32.6	4.9	43
12					2.1	29.9	13	16.4			1.9	32	5.5	42
13					1.8	28.3	16.6	15.5			3	29.5	5.3	40.9
14					10.4	13.4	17.6	14.8			5.1	18.7	5.8	39.4
15					13.5	13	23.2	13			9.2	16.4	5.7	39.1
16					16.2	12.8	26.6	12.2			10.5	15.2	6.3	18.6
17											14.2	14.2	7	18.1
18											16.8	13.8	12.8	16.3
19													14	15.7
20													22	13.6
21													23.3	13.2
30			36		42		48		54		60		66		72	
x	z	x	z	x	z	x	z	x	z	x	z	x	z	x	z
0	55.8	0	55	0	52.5	0	55.2	0	52.9	0	58.5	0	49.6	0	44.9
0	54.9	-0.2	52.6	-0.5	50.6	2.7	51.7	1.6	51.1	0.7	57.8	2.7	46.2	2.5	41.6
0.8	54.1	3.5	47.2	3.6	44.8	2.6	50.6	1.7	50	0.6	56.6	2.2	45.6	1.7	39.2
0.7	53.2	3.9	47.1	2.6	43.8	2.2	49.4	1.6	49.3	0.9	56.1	3.5	41.6	2	38
0.2	52	4.1	46.1	2.2	40.6	1.6	47.7	2	48.4	0.8	54.8	3.5	40.5	0.8	37.3
1	50.6	4.2	45.5	2.8	38.2	1.7	47.2	-0.2	45.9	1.3	53.3	4.4	39.1	0.9	35.8
3.6	48	3.1	44.7	1.2	35.7	1.4	46.7	-1.8	44.2	0.9	52.2	4.2	38.6	3.7	33.3
4.2	46.1	4.8	43.6	2.7	33.2	1.8	44.8	-0.6	44	1.1	51.3	5.9	36	4.8	30.3
4.7	45	8.7	38.9	3.5	32.3	2	44.5	1.6	39.7	0.4	49.6	5.6	35.5	5.3	27.6
4.6	44	6.7	36.8	3.1	30.8	1.5	43.3	2	37.6	1.8	49.6	5.8	35	5.8	26.4
4.4	42.8	6.2	34.5	2.8	29.1	1.5	41.9	4.1	34.5	3	43.7	5.6	31.6	6	25.1
5.2	40.9	5.4	32.6	3	28.6	1.8	41.1	6.3	33.6	4.3	41.1	6.2	30.8	6.5	24
5.2	40.2	5.6	31.1	2.8	27.2	0.8	38.9	6	32.8	4.2	39.2	5.8	28.9	6.6	22.8

Table C2-1 continued

30		36		42		48		54		60		66		72	
x	z	x	z	x	z	x	z	x	z	x	z	x	z	x	z
5.2	39.7	5.4	30.4	2.4	26.7	1.8	37.8	6.3	32.2	4.9	36.3	6.4	25.8	6.7	22.5
5.5	39.1	5.3	29.1	3.2	25.9	2.2	36.5	4.7	29.2	4.4	34.8	6.2	23.2	6.6	21.7
5.3	38.3	5.2	27.6	1.9	22.8	1.8	35.2	5.3	28.2	6	32.7	10.4	15.9	9.6	17.6
5.8	37.2	5.6	27	2.9	22.5	2.5	34.8	5.2	27.2	5.5	32.5	13.7	14.2	16.4	14
5.2	36.4	5.6	25.7	3	21	4.7	31.8	6.5	21.7	6.2	31.2	20	13.7	18.1	13.6
4.8	33.8	6	25.4	9.6	17.3	4.8	30.4	5.8	21.1	6.5	30.5	22.2	13.2	22.7	12.5
4.3	33.2	6.1	24.4	11	16.3	5.3	27.1	5.6	23.4	6.1	28.7				
5	32.8	4.2	23.8	18	13.5	4.8	24.3	3.3	15.2	5.3	26.9				
5.1	31.9	4.2	20	21.4	13.1	4.6	24	9.1	15.4	5.4	25.7				
5.6	31.7	11.2	17.2			4.8	22.7	10.7	15	7.5	15.8				
5.4	30.9	13	15.9			4.8	18.3	16.5	13.9	21.2	13.9				
6.4	29.2	21.6	13.5			8.7	17.9	22.4	13.2						
6.4	28.3					20	13.5								
5.8	27.7					23.2	13.1								
6.2	25.9														
6.6	24.4														
6.4	23.5														
6	20.2														
7.3	18.9														
14.1	16														
22.2	13.5														
27	13.2														

C2-2 Schmidt hammer and surface roughness measurement

Schmidt numbers of the agglomerate (upper 50%) and surface roughness for some segments of the agglomerate and debris slope of the Marine site are shown in table C2-2.

Table C2-2: Schmidt hammer and surface roughness measurements

No			1	2	3	4	5	6	7	8	9	10	11	Mean	Std.
Schmidt number			30	31	31	31	32	33	34	37	38	38		38.1	5.9
			38	40	41	41	42	44	46	47	49				
Slope roughness	Rock		70	85	90	74	60	78	60	60	60	68		70.5	11.1
			50	58	70	59	88	72	90	62	70	64	58	67.4	12.5
	Debris	1	90	78	78	66	68	72	60					73.1	9.86
		2	62	58	50	60								57.5	5.26
		3	0	2	-1	8	10	6	5	-9	-1			1.53	6.69
			8	9	-2	-8	-10	6							